Verónica María Corrales Carvajal
BSc Biological Engineering

Tracking nutrient decisions in *Drosophila melanogaster*

A thesis submitted in fulfilment of the requirements for the degree of
Doctor of Philosophy in
Bioengineering Systems

Supervisor: Dr. Carlos Vidal Ribeiro, Principal Investigator, Champalimaud Centre for the Unknown
Co-supervisors: Dr. Ahmed Aldo Faisal, Principal Investigator, Imperial College London
Dr. Manuel Nunes da Ponte, Full Professor, Universidade Nova de Lisboa.

Jury:

President: Dr. Ana Isabel Nobre Martins Aguiar de Oliveira Ricardo
External examiners: Dr. Giorgio Francesco Gilestro
Dr. Alisson Marques de Miranda Cabral Gontijo
Internal examiners: Dr. Gonzalo García de Polavieja
Dr. Margarida Casa Ribeiro Castro Caldas Braga

FACULDADE DE CIÊNCIAS E TECNOLOGIA
UNIVERSIDADE NOVA DE LISBOA

September 2016

Copyright statement

Tracking nutrient decisions in *Drosophila melanogaster* © Copyright by Verónica M Corrales Carvajal, Faculdade de Ciências e Tecnologia and Universidade Nova de Lisboa, 2016.

This copyright applies to all chapters except Chapter 2 which has been published in the scientific journal *eLife* and is therefore subjected to the terms of the Creative Commons Attribution license, which permits unrestricted use and redistribution provided that the original author and source are credited.

A Faculdade de Ciências e Tecnologia e a Universidade Nova de Lisboa têm o direito, perpétuo e sem limites geográficos, de arquivar e publicar esta dissertação através de exemplares impressos reproduzidos em papel ou de forma digital, ou por qualquer outro meio conhecido ou que venha a ser inventado, e de a divulgar através de repositórios científicos e de admitir a sua cópia e distribuição com objetivos educacionais ou de investigação, não comerciais, desde que seja dado crédito ao autor e editor.

Dedication and acknowledgements

I dedicate this work to the people that stood by my side and gave me a reason to move forward: my parents, my partner in life and my lab colleagues.

I'd like to specifically thank the fly community for the long conversations about babies and cats and the crazy Fridays at the fly room. I would also like to thank the INDP students for being inspiring in every way, because being surrounded by smarter people was a powerful reason to improve myself.

Special thanks to, Gonçalo Lopes, Alex Gomez-Marin, Ricardo Ribeiro, Eric DeWitt, Scott Rennie and Vivek Athalye for helping me with technical, scientific and philosophical questions that raised during this journey. To Gabriela Fioreze, João Marques, Patricia Francisco, Samantha Herbert and Samuel Walker for all the fun, hugs and tears.

I'm grateful for the enriching experience I had when interacting with the students and postdocs from the Faisal Lab during my time in London. They were kind, warm and incredibly smart. A piece of my heart stayed with them.

I'd like to thank the CNP community for providing a great environment for personal and professional growth, and my thesis committee: Adam Kampff, Christian Machens and Gonzalo de Polavieja for their support and wise advice.

More specifically, I would like to acknowledge the people that helped me creating and optimizing the tracking algorithm: Teresa Montez wrote the tracking algorithm in the initial stages of the project; José Cruz and Ricardo Ribeiro introduced the multiple frame loading in memory which was a crucial step in optimizing the speed of the algorithm; Gonçalo Lopes helped me with the implementation of the algorithm in Bonsai and Alex Gomez-Marin gave me useful technical advice in the implementation of the heading algorithm.

I also want to thank the MIT-Portugal program for giving me the opportunity to do research in Portugal and London. I'd like to give special thanks to Dr. José Silva Lopes and Isabel Carvalho, for all the administrative support provided during these years.

Finally, I'd like to thank my supervisors for their guidance ad mentoring and for making this project possible.

Resumo

Os animais adaptam o seu comportamento integrando informação sensorial externa e as necessidades metabólicas internas. Em conformidade, muitos organismos conseguem detetar desequilíbrios metabólicos e ajustam as suas escolhas nutricionais para restabelecer a homeostasia. Uma questão essencial em neurobiologia é de que forma os circuitos neuronais integram a informação sobre o estado interno do individuo e coordenam os comportamentos adequados para ultrapassar dificuldades metabólicas. É necessário desenvolver métodos que permitam uma análise quantitativa detalhada de como os animais se comportam quando tomam determinadas decisões nutricionais. No decorrer deste projeto, desenvolvemos um setup de captura de imagens que permite filmar os movimentos da mosca da fruta, *Drosophila melanogaster*, enquanto esta toma determinadas escolhas nutricionais. Este setup permitiu-nos estudar de que forma o estado metabólico e reprodutivo da mosca influenciam na sua decisão de explorar o ambiente ou utilizar os recursos alimentares de forma a manter a homeostasia nutricional. Descobrimos que o balanço entre estes comportamentos é definido pelo estado nutricional interno: moscas privadas de aminoácidos focam-se em pontos de comida ricos em proteína enquanto que as moscas não-privadas preferem explorar o ambiente mais globalmente. Demonstramos ainda que este setup e análise podem ser utilizados para dissecar os circuitos neurais e genéticos que comandam as decisões nutricionais: primeiro, mostramos que os recetores olfativos da mosca são necessários para que ela reconheça eficientemente a levadura como sendo um alimento; segundo, demostramos que a octopamina é necessária para mediar as alterações de comportamento devido à copulação mas não para detetar os níveis internos de nutrientes; terceiro, mostramos que os recetores gustativos são fundamentais para manter o interesse nas fontes ricas em proteína após a privação de aminoácidos. Os nossos resultados fornecem uma descrição quantitativa das mudanças comportamentais necessárias para atingir o equilíbrio nutricional, fornecendo um modelo para o estudo dos mecanismos responsáveis por estes comportamentos.

Palavras chave: Análise computacional do comportamento, estado metabólico, nutrição, homeostasia, neurogenética.

Summary

Animals integrate external sensory information and current metabolic needs to adapt their behavior in order to survive. Accordingly, many organisms can detect an internal nutritional imbalance and adjust their nutritional choices to restore homeostasis. Detailed quantitative analyses of nutrient-choice behaviors are needed to deepen our understanding of how neural circuits integrate internal state information and drive compensatory behavior when facing metabolic challenges. During this project, we developed an automated video tracking setup to characterize how metabolic and reproductive states interact to shape exploitation and exploration decisions taken by the adult fruit fly *Drosophila melanogaster*, to achieve nutritional homeostasis. We find that these two states have specific effects on the decisions to stop on and leave proteinaceous food patches. Furthermore, the internal nutrient state defines the exploration-exploitation trade-off: nutrient deprived flies focus on specific patches while satiated flies explore more globally. We provide few examples of how our paradigm could be used in the dissection of the genetic and neuronal pathways underlying nutrient decisions: First, we show that olfaction is not required for the compensatory high yeast feeding after amino acid deprivation, but that it mediates the efficient recognition of yeast as an appropriate food source in mated females. Second, we show that octopamine is required to mediate homeostatic postmating responses without affecting internal nutrient sensing. Third, we show how gustation is required to sustain interest for protein-rich resources upon amino acid deprivation. Our results provide a quantitative description of how the fly changes behavioral decisions to achieve homeostatic nutrient balancing and provide a framework for future detailed mechanistic dissection of such decisions.

Keywords: computational analysis of behavior, internal states, nutrition, neurogenetics, homeostasis.

Table of contents

Figures index

Tables index

Overview

The first chapter is a brief literature review of important topics relevant to this thesis, including general and recent research in advanced methods to quantify and study animal behavior and a brief overview of recent findings in the area of nutrition. Chapter 2 is the manuscript submitted for publication to the *eLife* journal, the central and most important chapter of this dissertation as it comprises the most relevant findings of my research. Chapter 3 describes in detail the design and manufacturing of foraging setup and some algorithms that were developed to pre-process the data before its analysis. Chapter 4 describes analyses and experiments that were not included in the submitted manuscript but from which we gained partial but important insight on the locomotor patterns of flies in the presence and absence of food patches in a foraging arena, the application of multiple tools for the analysis of behavior, nutritional geometry and the role of olfaction, gustation and octopamine in yeast-related decisions that can set the stage for future work in uncovering the molecular mechanisms underlying foraging decisions in *Drosophila.* All these findings are discussed in Chapter 5. Finally, in the appendix I include detailed steps on how to use the tracking setup described in Chapter 3 and the exact configuration of the cameras I used for all the recordings performed during this project.

Chapter 1. General introduction

The main function of the brain is to process incoming information from the environment and coordinate, in accordance with the internal state, a series of responses oriented to achieve a certain objective. The collection of these responses constitutes the *behavior* of the animal. How is behavior encoded in the genome? In other words how do neuronal circuits and the molecular machineries in them control and shape behavior? What are the general principles that govern behavior? Tackling these questions is challenging and requires the combination of advanced computational analysis techniques and powerful genetic tools, like those developed for model organisms such as the fruit fly *Drosophila melanogaster* and the nematode *Caenorhabditis elegans.*

In the first half of this review, I describe some properties observed in the organization of behavior and some of the latest methods used in its quantification and analysis. In the second half, I give a short overview of what is known about nutrition in *Drosophila* and some of the complex features of behavior that are observed in fruit flies and that allow researchers to use *Drosophila* as a model system to explore the neural circuits and molecular mechanisms underlying behavioral outputs.

1.1 Behavior organization and modulation

Although a short and simple definition of behavior was given in the very first sentences of this introduction, having a complete and exact definition for this term is not trivial. There is debate about what does and what does not constitute behavior, if non-animals or those lacking a nervous system can behave or if intentional lack of movement is also behavior (Levitis, Lidicker, and Freund 2009). In this review, we refer to behavior as “the macroscopic expression of neural activity, implemented by muscular and glandular contractions acting on the body, and resulting in egocentric and allocentric changes in an organized temporal sequence” (Gomez-Marin et al. 2014).

Some behaviors can be subdivided in smaller behaviors, or sub-behaviors (Sokolowski 2001). For example, during foraging, an animal explores the environment in search for food, once encountered, it proceeds to capture it and then to consume it. In this way, behaviors can span on multiple time scales that can vary by several orders of magnitude (Egnor and Branson 2016). The transition between behaviors can be sharp (Seeds et al. 2014) or unfold in a continuous gradient (Gomez-Marin et al. 2016). Behaviour can be innate or learned, and it can be spontaneous or triggered by external or internal signals (Tinbergen 1951).

In this section, I describe in more detail some of the properties of behavior organization and give some examples of how context (internal or external factors) can modulate different behaviors.

1.1.1 Variability

Many behaviors such as scape responses (Domenici et al. 2008) or direction of turning during flight (Maye et al. 2007) are variable and unpredictable. The same animal will not show exactly the same behavioral output when exposed to exactly the same stimuli if tested multiple times (Briggman and Abarbanel 2005). In fact, even in the absence of external stimuli, an organism will still show some behavioral variability (Maye et al. 2007), a challenge that has been graciously captured by the Harvard Law of Animal Behavior: "*Under carefully controlled experimental circumstances, an animal will behave as it damned well pleases*".

From an evolutionary point of view, it is clear why animals must behave in a variable manner. By behaving in an unpredictable way they can evade predators, surprise preys. It is exploring their environment that they increase the chance of finding mates or better sources of food. It is exploring their own actions that they can find solutions to unseen problems (Brembs 2011; Renart and Machens 2014).

The sources of this variability are usually attributed to neural noise (de Ruyter van Steveninck et al. 1997; Faisal, Selen, and Wolpert 2008). Introducing random fluctuations, or noise, on simulations of neural network activity and behavioral output successfully recreates the behavioral variability observed in the laboratory (Maesani et al. 2015; Jin and Kozhevnikov 2011). However, animals seem to intentionally increase their behavioral variability when faced with challenging tasks (Tervo et al. 2014) or novel situations (Roberts and Gharib 2006). Animals can also decrease the variability in their behavioral output during learning to avoid a punishing stimulus (Wolf and Heisenberg 1991) or to earn a reward (Santos et al. 2015). A detailed and quantitative analysis of the courtship song pattern in *Drosophila,* demonstrated that the variation in song structure previously believed to come from neural noise was actually tightly regulated according to the dynamic sensory experience of the courting male (Coen et al. 2014). Behavioral variability can therefore originate from different sources: intrinsic noise coming from the biochemical limitations of interacting molecules in ion channels and synapses; the deterministic but suboptimal probabilistic computations of the brain when, for example, integrating distinct sensory cues (Beck et al. 2012; Renart and Machens 2014), this "intentional" modulation of variability by other brain areas can in turn can be modulated by internal state or external factors (J. Martin, Faure, and Ernst 2001; Tervo et al. 2014; London et al. 2010); and external noise coming from the stochasticity of the environment and therefore variable sensory input. Many of these external and internal factors are not fully observable by the experimenter due to technical limitations in the measuring equipment, which makes the pinning down of the specific causes of neural and therefore behavioral variability a challenge that is still under intense study (Renart and Machens 2014).

1.1.2 Behavioral building blocks

Despite all the variability observed in behavior, stereotyped patterns still arise. During courtship, most *Drosophila* males chase the female and generate a "courtship song" by vibrating one of their extended wings. Other behaviors commonly observed during this ritual are licking, tapping and mounting the female (Sokolowski 2001). Although these sub-behaviors inside the broader courtship bout vary in

duration, frequency and order of presentation, an observer can easily recognize that a courtship bout is taking place by observing the display of one or more of these sub-behaviors.

Given that behaviors can in turn brake down into even smaller behaviors such as grasp, step, reorient, biologists have asked whether behavior can be decomposed in individual and stereotyped basic units, defined either by the control of dedicated neural circuits, biophysics, or both. Because what a human defines as a unit might not be what is relevant for the animal or its nervous system, unsupervised methods for the analysis of behavioral structure are taking the lead on approaching the challenge of finding such units.

An elegant study in that direction using the model organism *Caenorhabditis elegans* has extracted four basic shapes that account for 95% of the variance in the shape space of the worm's locomotion (Stephens et al. 2008). The usefulness of this low-dimensional description in uncovering the link between the molecular mechanisms and behavior was demonstrated by Brown and colleagues when they found that the same four eigenworms could capture 92% of the variance observed in a set of 307 mutant strains (Brown et al. 2013). Using this basis, they created a dictionary of behavioral motifs that was used to cluster gene mutations leading to similar motor phenotypes. An analogous dimensionality reduction approach was used to extract 50 postural modes of *D. melanogaster* from which an unsupervised behavioral space can be derived and where widely recognized behaviors such as gaits and wing movements have dedicated regions and could therefore be used to organize and classify other unsupervised behaviors (Berman et al. 2014). In mice, modules extracted from 3D body motion have also been identified (Wiltschko et al. 2015).

Although it is not yet clear if there is a unit of behavior, the discovery of neurons that can could switch on and off specific motor programs (Wiersma and Ikeda 1964) suggested the existence of behavioral modules defined by neural control. Today, there are many examples in *Drosophila* in which the activation of a specific subset of neurons causes the execution of a sub-behavior such as abdominal bending and courtship song (von Philipsborn et al. 2011), backward walking (Bidaye et al. 2014) or the discrete grooming of a specific body part (Seeds et al. 2014). In fact, by being able to activate distinct cleaning modules, Seeds and colleagues not only proved that grooming behavior is modular but also proposed a model of how the brain would coordinate the sequential activation of such modules. They called it "suppression hierarchy": discrete cleaning modules were activated in parallel but with a different level of activation (due to either more dust or different sensory gain in that part of the body) and the winner module would be selected based on a winner-take-all mechanism inhibiting all other modules. The consequent cleaning of the winner body part would decrease the level of activation of that module causing another module to win the next round and therefore generating a sequential activation of behaviors that matched the structure of the grooming observed in the laboratory (Seeds et al. 2014).

In a beautiful study of sequential behavior in *C. elegans*, Kato and colleagues used brain-wide calcium imaging to show how the direction of neural population dynamic state corresponds to the order of presentation of specific behavioral sequences, providing insight in our understanding of how the brain coordinates long-lasting sequences of sub-behaviors (Kato et al. 2015).

1.1.3 Hierarchy

The notion of a hierarchical organization in the neural control of behavior dates from more than 50 years ago, when Tinbergen proposed his hierarchical model of behavioral decisions (Tinbergen 1951). From his observations in the wild, he proposed that an animal first takes the decision to enter into a broader behavioral category, such as mating or fighting, and only then decides which sub-behavior to implement, such as biting, chasing or threatening. He also proposed a corresponding hierarchical organization of the neural circuits, where the activation of higher nodes or "centers" would lead to the implementation of a specific behavioral program. Nodes at the same level would mutually inhibit each other and would have feedforward connections with nodes at lower levels, driving the sub-behaviors. Interestingly, a recent study in the Anderson laboratory, showed that a cluster of P1 neurons in *Drosophila* promoted both courtship or aggression depending on the level of activation (Hoopfer et al. 2015). Suggesting that there could be indeed higher circuit nodes in charge of deciding what behavioral program to activate in a lower level of the hierarchy.

While Tinbergen's hierarchy of circuit nodes refers to how different elements are controlled or connected with each other, there is another type of hierarchy that can be observed in the organization of behavior, the one that refers to classification or embedment where bigger elements are composed of smaller elements (Hogan 2015; Dawkins 1976). Gomez-Marin and colleagues investigated if this type of hierarchy could reveal the structure of the crawling behavior of *C. elegans* by testing data compression algorithms to find "patterns and patterns of patterns" of behavioral sequences (Gomez-Marin, Stephens, and Brown 2016). They found that the resulting motifs were infrequent but provided a new way of comparing behaviours across different strains. They also propose to use the level of compressibility as measure of a behavioral complexity. In another study, Berman and colleagues applied methods from information theory to show that a hierarchical organization of the behavioral repertoire of single flies walking on a shallow arena (2 mm high) could predict the future actions of the fly (Berman, Bialek, and Shaevitz 2016). These results add evidence to the long ago predicted hierarchical organization of animal's actions, using unsupervised techniques to define behavioral modules or motifs.

1.1.4 Burstiness

The onset of spontaneous behaviors might seem to be randomly distributed in time to a human observer, however, once quantified, many of these behaviors have been reported as following a power-law or a heavy tail distribution. Reports of fractality (the pattern of events is self-similar across different scales of measurement) exist for fly's feeding (Shimada, Kawazoe, and Hara 1993), foraging (Koganezawa et al. 2009), flight maneuvers (Maye et al. 2007) and locomotor behavior (J.-R. Martin 2004). In general, a "bursty" dynamics, characterized as many frequent events separated by long periods of inactivity, has been described for a wide range of behaviors going from foraging in mice (Jung et al. 2014) to human dynamics (Barabási 2005). Observations of Lévy-like patterns across multiple species suggest that there must be non-linear endogenous mechanisms underlying spontaneous behavior (Maye et al. 2007). In *Drosophila*, two important structures in the central brain,

the mushroom body and the ellipsoid body, have been shown to affect or modulate the degree of burstiness observed in the pattern of locomotor activity of walking fruit flies (J. Martin, Faure, and Ernst 2001; Sorribes et al. 2011). Barabási had proposed a model in which the heavy-tailed distribution observed in human dynamics originates from a decision process in which individuals performed tasks following a self-defined priority causing most tasks to happen in a short period of time while few others would only happen after long periods of time (Barabási 2005). Interestingly, the fact that the mushroom body affects burstiness provides experimental evidence for Barabási's model, as this brain structure has also been shown to be required for decision-making tasks in *Drosophila* (Tang and Guo 2001), suggesting a link between decision-making and behavioral bursts.

1.1.5 Homology

As the wings of bats and the arms of primates, despite their external differences, share a similar structure that led zoologists to conclude they derived from a common ancestor, a long-standing aim of ethology has been to look for behavioral primitives that allow ethologists to investigate the evolution of behavior (Lorenz 1958). Until now, only few studies have quantified the similarity between behavioral programs across species. One of them found surprising similarities in the stepping patterns of human toddlers with those shown by cats, rats, macaques and guineafowls, suggesting the existence of common motor primitives that might derive from a common ancestral neural network (Dominici et al. 2011). Another study described a "mobility gradient" across several vertebrate species including rodents and carnivores. Examining the orientation of the trunk with respect to the base of the body, Golani observed that the transition out of immobility unfolded gradually during which the types of movements performed by the animal went from stereotyped to variable and complex, starting usually by movement in the horizontal plane, then forward displacement and ending in the vertical plane. This structure appeared during locomotor development, aggressive and exploratory behavior (Golani 1992). Notably, a similar mobility gradient was also found in fruit flies under the influence of cocaine, where a gradual increase of degrees of freedom was observed in the transition out of immobility and back (Gomez-Marin et al. 2016), opening the possibility to explore behavioral homology using this genetically tractable organism.

1.1.6 Modulation of behavior by external and internal factors

Behavior can be modulated by multiple factors (reviewed in (Palmer and Kristan 2011)). External factors include visual, auditory and chemosensory cues or punishing cues coming from the surrounding environment, social context, availability of food and environmental conditions. Internal factors include genetic background, past experiences (learning), the current behavioral state (for example, if the animal is walking or inactive), arousal state, fear, mating status and metabolic state (hungry or deprived of a particular nutrient). Few detailed examples are shown below:

External sensory cues: A beautiful example of how the integration of multiple sensory cues can shape the behavior of an animal, is that of the female mosquito when it searches for hosts (Gibson and Torr 1999). CO_2 is used as a long-range cue that gates the responses to other sensory stimuli

(McMeniman et al. 2014). After the detection of CO_2 the mosquitos follow the odor plume to approach the hosts and become strongly attracted to visual features and once close enough to a host, the decision to land is made based on heat, humidity and host-specific odors (van Breugel et al. 2015).

Genetic background: Using isogenic lines of *Drosophila* (individuals with the same genotype), Ayroles and colleagues found that different genetic backgrounds have different degrees of behavioral variability, that phenotypic variability, as a trait, is heritable and the loci affecting for such variability can be mapped (Ayroles et al. 2015).

Current behavioral state: The execution of a present behavioral program might inhibit the execution of other behaviors. For example, feeding renders the leech largely insensitive to mechano-sensory stimuli and inhibits the execution of other behaviors such as swimming, crawling and bending (Gaudry and Kristan 2009). Other behavioral states alter subsequent behavioral choice through the modulation of the sensitivity of sensory neurons. Flying in locusts and flies (Maimon, Straw, and Dickinson 2010; Rind, Santer, and Wright 2008) and walking in flies (Chiappe et al. 2010) increase the responsiveness in neurons of the visual system.

Learned contingencies: A very elegant study that brought important insight into our understanding of how different contextual information is integrated in the brain to elicit a specific behavioral response was performed by the Ruta laboratory using *Drosophila* (Cohn, Morantte, and Ruta 2015). They found out that the mushroom body, known to bias odor responses based on a learned contingency (Keene and Waddell 2007), does so by having discrete anatomic compartments, each of these innervated by sub-sets of dopaminergic neurons and sending information to output neurons thought to then drive behavioral responses. Different appetitive or punishing stimuli, as well as different behavioral states, would cause different patterns of synaptic activity with dopaminergic neurons on each of these compartments, which happen to be functionally connected. These patterns of dopaminergic activity are also shaped by the feedback from the output neurons, revealing a dynamic and highly interconnected network that integrates both behavioral state and learned associations with environmental cues to drive behavior accordingly.

Internal states: Recent mating has been shown to decrease attraction to other potential mates in several species, ranging from flies (Kubli 2003) and moths (Barrozo, Gadenne, and Anton 2010), to frogs (Miranda and Wilczynski 2009) and mice (Serguera et al. 2008).

1.2 Advanced tools for the quantification of *Drosophila* behavior

Despite the highly dynamic nature of behavioral processes most behavioral readouts used to be static and scored manually in very labor intense steps. Among the draw-backs of this approach were the subjective bias introduced by the scoring scientist, the lack of access to patterns happening at timescales that the naked-eye could not uncover and the low throughput that made it difficult to take advantage of the neurogenetic tools available in *Drosophila* which are most powerful if applied in a high throughput manner.

In the last few years, there has been an outbreak of automated technologies to quantify and analyze behavior (Anderson and Perona 2014; Egnor and Branson 2016; Dell et al. 2014). Image-based tracking in combination with a detailed and careful computational analysis has been used to discover several interesting behavioral strategies implemented by *Drosophila,* among which we have the discovery that these animals are capable of visual place learning (Ofstad, Zuker, and Reiser 2011), that collective odor avoidance is mediated by mechanosensory sensilla in their legs (Ramdya et al. 2014), that larvae approach appetitive odors by combining stereo-olfaction with active sampling (Gomez-Marin, Stephens, and Louis 2011) and that the presence of an attractive odor gates the interest to high contrast visual features (van Breugel and Dickinson 2014), which led to a similar finding in female mosquitos when searching to blood-feed from a human host (van Breugel et al. 2015).

With the advent of new technologies will come the era of big behavioral data which poses big promises as well as challenges for both behaviorists and neuroscientists. As Gomez-Marin and colleagues mention in their review, behavior should not be seen as the mere output of the nervous system but as the very foundation of neuroscience (Gomez-Marin et al. 2014). Big and rich behavioral datasets will hopefully come coupled with the corresponding neurological recordings or manipulations, allowing scientists to build causal links between neural circuits and very detailed features of behavior. On the other hand, big data comes with big responsibility. To give meaning to large amounts of data we need good theoretical frameworks, carefully planned experimental designs and a universal language that allow us to extract the principles governing behavior. Some other technical challenges such as data sharing, storage and management, data segmentation and control of environmental richness to explore the full behavioral repertoire of the animal, will also have to be addressed.

1.2.1 Data acquisition

Sophisticated equipment to acquire the behavior in different species of animals is becoming more and more available. The miniaturization and cost reduction of data acquisition equipment such as cameras, accelerometers, global position systems and sensors in general are allowing scientists to study migration patterns, foraging, pollination strategies and group dynamics in most animals irrespective of their size (Wilmers et al. 2015). Just to have an idea of the tool accessibility: with a cheap webcam and a low resolution video with lossy but good-enough compression, it is now possible to record the full lifespan (~24 months) of a rodent (Gomez-Marin et al. 2014). All these technological advances open an exciting new era for the analysis of behavior.

In the laboratory, a great variety of techniques to quantify the behavior of *Drosophila melanogaster* are being continuously developed and improved. Due to their general-purpose and high spatiotemporal resolution, video cameras are the most widely used tools to record the behavior of single or multiple animals. Features of the desired behavior can be extracted online or offline using machine-vision techniques. See Dell et al. 2014 (Table S1) for a detailed description of the strengths and limitations of the main tracking systems available. Worth highlighting is the tracking system called *idTracker*, freely available at http://www.idtracker.es/. This system uses a fingerprinting technique to recognize the

identity of each individual in a group and maintains such identity even after several unmarked individuals have overlapped. It has proved successful when tracking groups of flies, fishes, mice and ants (Pérez-Escudero et al. 2014). Another useful tracking system is *CTRAX* (Branson et al. 2009), also freely available at http://ctrax.sourceforge.net, although not as successful at maintaining the identity of multiple individuals, it offers an extensive set of post-analysis tools focused on extracting multiple features of the individual and social behavior of *Drosophila* (Kabra et al. 2013). Some specialized tracking systems focus on extracting the pose and orientation of particular body parts. *CADABRA* (Dankert et al. 2009), for example, was designed to capture the wing orientation with respect to the body and the body orientation of one individual with respect a conspecific, aiming at a detailed quantitative description of courtship and aggression in *Drosophila*. Mendes et al. and J. Kain et al. (2013) used light reflection techniques or dyes, respectively, to track the leg movements and quantify gait parameters of the fruit fly. For a review of the current difficulties in extracting relevant behavioral features from video and the state of the art techniques to do so, see Egnor and Branson (2016) and Dell et al. 2014. Some of those challenges are: the limitation of fingerprinting to relatively low (< 20) number of individuals and very specific background settings, the trade-off between spatiotemporal resolution and the detailed knowledge of the position and orientation of different body parts, and the difficulty of differentiating individuals from a complex and natural background. There have been reports of online tracking of multiple freely flying flies with multiple cameras (Straw et al. 2011), but taking these systems into the field remains a challenge.

Besides the use of cameras, multiple sensors have been used to quantify specific behavioral variables such as infrared detectors to monitor sleep and locomotor activity (Pfeiffenberger et al. 2010); microphones to detect courtship song patterning (Coen et al. 2014); the movements of an air-floating ball in a head-fixed preparation to couple fly's movements to neural activity (Seelig et al. 2010); torque meters to measure turns during tethered flight (Wolf and Heisenberg 1991); frustrated Total Internal Reflection to measure the footprints and gate parameters of the fly walking on a flat surface (Mendes et al. 2013); capacitance and electronic sensors to measure the contact of the fly with the food (Ro, Harvanek, and Pletcher 2014; Itskov et al. 2014) and photodiodes to measure the amount of liquid ingested (Yapici et al. 2016), all allowing for the monitoring of the feeding motor program.

1.2.2 Data Analysis

After acquiring the videos and tracking data it is often useful to classify the behaviors performed by the animal. The researcher might be interested in understanding how a given neuronal or genetic manipulation affects the performance of a specific behavior. In these cases, supervised methods, in which the user defines the behavior of interest, come handy. In other cases, in which the researcher does not want to define the behavior but rather explore the type of clusters that arise from the raw data, unsupervised machine learning methods should be used.

1.2.2.1 Supervised methods

A given behavior can be classified by manually defining a set of rules on different measured parameters. For example, setting a threshold on the linear speed can help us distinguish between

walking and staying in place (Robie, Straw, and Dickinson 2010; J.-R. Martin 2004). After the animal has stopped, the amount of pixel change or the micromovements of the centroid, can determine if the animal is completely still or actively performing an action such as grooming or feeding. Although manually set, these set of rules are often inspired on the shape of the distributions of the kinematic parameters: the distribution of speed is often binomial (Benjamini et al. 2010), and therefore, a threshold can be manually set between the two peaks of the distribution. The shape or slope of the distribution can change at a given point, which can also be used to define the threshold (Gomez-Marin, Stephens, and Louis 2011). The main limitation of this implementation is that in many cases it is not clear what should be the rule that defines the behavior and the rules might change across different groups of individuals.

These problems can be overcome using machine learning techniques to train a classifier based on a relatively small user-labeled instances of the behavior of interest. A very useful open-source tool that does exactly this is called *JAABA* (http://jaaba.sourceforge.net/). *JAABA* provides an interactive and relatively easy-to-use interface in which non-experts in machine learning can still apply it to automate the classification of the behaviors they study (Kabra et al. 2013).

The combination of manually defined rules and machine learning classification has already proved useful in finding correlations between neuronal circuits and male-specific aggression (Asahina et al. 2014; Dankert et al. 2009).

1.2.2.2 Unsupervised methods

Dimensionality reduction techniques can be used to reduce the space of postures of an animal to few basic shapes or modes that can then be used to look for systematic phenotypic differences or similarities across diverse genetic backgrounds and therefore contribute to the mapping of molecular mechanisms (and potentially neural circuits) to behavior (Vogelstein et al. 2014; Brown et al. 2013).

Berman et al. (2014) extracted clusters that correspond to discrete behavioral states from basic postures obtained directly from the images using PCA. The dynamics of postural changes are then captured in wavelet spectrograms that are then mapped to a two-dimensional representation using a visualization technique called t-SNE (t-distributed stochastic neighbor embedding) (Van Der Maaten and Hinton 2008).

Although unsupervised methods to map behavior structure are just gaining strength, they promise to offer important insight on the real behavioral repertoire and variability present in animals (Todd, Kain, and de Bivort 2016).

1.3 Impact of nutrients on dietary balancing in *Drosophila*

Recent advances in molecular, genetic and imaging technologies in model organisms have led to an appreciation that the moment has come in which we might get the opportunity to mechanistically understand how the brain perceives and processes information to guide behaviors (Vosshall 2007). Model organisms have played a pivotal role in allowing us to gain a mechanistic understanding of how

the nervous system controls behavior, including feeding behavior. The fruit fly, *Drosophila melanogaster*, represents an ideal model organism to dissect the molecular and cellular basis of behavior (Vosshall 2007). In fact, the tiny fruit fly brain is currently being used to understand the building blocks of cognition (Haberkern and Jayaraman 2016). For example, abstract internal representation of self-motion and spatial orientation in this small insect were found to be similar to that of mammals (Seelig and Jayaraman 2015). This finding provides a simpler system in which to test computational models that were otherwise very challenging at the complex scale of the vertebrate brain. Research using *Drosophila* has made seminal contributions to our understanding of the genetic basis of behavior due to the availability of sophisticated genetic tools (Luo, Callaway, and Svoboda 2008; Olsen and Wilson 2008), a numerically simple nervous system, and the advent of methods to quantitatively characterize behavior.

1.3.1 Nutrient sensing

1.3.1.1 Smell and taste

All olfactory sensory neurons (OSNs) in the fly are located in the antennae and the maxillary palps. One to four OSNs are housed in each sensory hair called sensilla. Each OSN expresses one of three known types of chemosensory receptor genes: odorant receptor (OR) genes, gustatory receptor (GR) genes and ionotropic receptor (IR) genes (Vosshall and Stocker 2007; Rytz, Croset, and Benton 2013). OSNs that express the same receptor type project to the same glomerulus in the antennae lobe, the functional homologue of the olfactory bulb in rodents. OR and GR receptors have seven transmembrane domains, but are distantly related (Clyne et al. 1999; Scott et al. 2001). Most GRs are known as taste receptors and are found in gustatory organs except for a number of them that are found in the antennae and might have the function of odorant receptors, such as GR21a and GR63a, which together confer CO_2 sensitivity to the fly (Jones et al. 2007). The great majority of IR agonists are amines and carboxylic acids (Silbering et al. 2011).

Most of the gustatory receptor neurons (GRNs) are located in taste bristles present in the labellum, legs, wings and female ovipositor (Vosshall and Stocker 2007). Few other gustatory receptor neurons are not associated to taste bristles and are located in the taste pegs in the labial palps and in the internal sense organs in the pharynx (Thorne et al. 2004). Sensory neurons in the labellum and in the pharynx project their axons to the subesophageal zone (SEZ) (Ito et al. 2014), the taste center in the fly brain (Marella et al. 2006). Similar to olfactory sensilla, each taste bristle in the labellum houses between two and four GRNs, while the taste pegs house one GRN each (Vosshall and Stocker 2007). While the taste neurons situated in the labellum and legs mediate the proboscis extension reflex and initiation of feeding, the gustatory neurons at the pharynx mediate the sustained consumption of sugars (LeDue et al. 2015; Yapici et al. 2016; Thoma et al. 2016).

1.3.1.2 Smelling yeast

Yeast is a complex food source composed by multiple metabolites. In nature, yeast also generates multiple fermentation sub-products when growing on fruit. *Drosophila* is strongly attracted to mixtures

of fermentation-associated volatiles (Becher et al. 2012; Scheidler et al. 2015), which are primarily detected through olfactory receptors (ORs) (Stökl et al. 2010). Some examples are: OR9a and OR92a detect acetoin, OR42b detects ethyl acetate, OrR67a detects phenyl ethanol and OR85d detects phenyl-ethyl acetate (Dweck, Knaden, and Hansson 2015). In fact, some plants emit a mixture of some of these odors as a deceptive pollination strategy to attract drosophilids (Stökl et al. 2010) and yeast itself uses some of these volatile acetate esters to promote dispersal of its cells (Christiaens et al. 2014). In some cases, *Drosophila* even uses the smell of yeast-derived metabolites that are generated only in the presence of certain antioxidants, to detect the presence of such antioxidants on the food given that it cannot smell them directly (Dweck et al. 2015).

Several ionotropic receptors have recently been associated to the recognition of fermentation-related odours. A recent study found that virgin flies use both the smell of acetic acid, mediated by the ionotropic receptor IR75a, and the presence of amino acids in the food, to increase their receptivity to courting males (Gorter et al. 2016). Other ionotropic receptors, IR76b and IR41a, are known to mediate *Drosophila* attraction to polyamines, which are also present in fermenting fruit and promote reproductive output (Hussain, Zhang, et al. 2016).

1.3.2 *Nutrient decisions*

How is value-based decision making implemented in the brain? More specifically, how nutritional needs lead animals to take specific feeding decisions? Previous studies have described that in different decision making situations *Drosophila melanogaster* is able to asses and compare several factors before taking a decision. Examples of studied *Drosophila* decision making paradigms are egg-laying site selection (C.-H. Yang et al. 2008; Miller et al. 2011; Joseph et al. 2009), chemotaxis (Gomez-Marin, Stephens, and Louis 2011) and avoidance of danger, based on olfactory and visual memories (Yin et al. 2009; Zhang et al. 2007).

Value based decision making is a more complex type of behavior which requires the animal to decide between alternative actions according to their current needs, and hence the value they assign to each of the competing options (Gold and Shadlen 2007). Ribeiro and Dickson developed a simple two-choice feeding preference assay where flies are allowed to decide between sucrose, as a carbohydrate source, and yeast, as a protein source (Ribeiro and Dickson 2010). The food sources are mixed with either a red or blue dye which after ingestion remains visible through their abdomen, affording an easy identification of their choice. Animals fed *ad libitum* prefer the carbohydrate rich food. Appropriately protein-deprived flies switch their preference from sucrose to yeast. These feeding decisions are modulated by their mating status, relying on the action of the sex peptide receptor (SPR) in internal *ppk*$^{+}$ sensory neurons and the neuronal nutrient sensing TOR/S6K pathway as a possible internal sensor of the current nutritional state. This internal information in combination with the external sensory information from the food sources is used to instruct a value-based decision in order to achieve metabolic homeostasis.

A recent study found that flies' nutritional decisions do not necessarily match their egg laying decisions (Lihoreau et al. 2016), suggesting an extra level of complexity in Drosophila's nutrient decisions.

A great body of work led by Stephen Simpson and co-workers, using a nutritional geometry framework, has shed light in our understanding of the rules of compromise that animals follow when a particular intake target cannot be reached (Simpson and Raubenheimer 2012). They demonstrated in their protein leverage theory that animals prefer to prioritize protein at the expense of overconsuming fat and carbohydrates; a decision that might lead to obesity (Simpson and Raubenheimer 2005).

It has been demonstrated that when given the choice, flies select to consume 1-to-4 Protein-to-Carbohydrate ratio, which maximizes lifetime egg production, a measure close to fitness (Lee et al. 2008). As demonstrated by studies in many other species besides *Drosophila*, there seems to be a trade-off between reproductive output and lifespan, where a high-protein ratio promotes the former, while a low protein ratio promotes the later (Fontana and Partridge 2015; Grandison, Piper, and Partridge 2009; Skorupa et al. 2008; Solon-Biet et al. 2014; Solon-Biet et al. 2015; Levine et al. 2014). The mechanisms by which the brain shapes behavioral output during dietary balancing to solve this ethologically relevant trade-off are still largely unknown.

Chapter 2. Internal states drive nutrient homeostasis by modulating exploration-exploitation trade-off

2.1 Abstract

Internal states can deeply alter the behavior of animals. Which aspects of behavior change upon metabolic challenges and how these allow the animal to achieve nutrient homeostasis is poorly understood. We used an automated video tracking setup to characterize how amino acid and reproductive states interact to shape exploitation and exploration decisions taken by adult *Drosophila melanogaster,* to achieve nutritional homeostasis. We find that these two states have specific effects on the decisions to engage and leave proteinaceous food patches. Furthermore, the internal nutrient state defines the exploration-exploitation trade-off: nutrient deprived flies focus on specific patches while satiated flies explore more globally. Finally, we show that olfaction mediates the efficient recognition of yeast as an appropriate protein source and that octopamine is specifically required to mediate homeostatic postmating responses without affecting internal nutrient sensing. Internal states therefore modulate specific aspects of exploitation and exploration to change nutrient selection.

2.2 Introduction

Nutrition is key for optimizing the evolutionary fitness of animals. Accordingly, many organisms are able to select the nutrients that fulfill their current needs. Recent work has highlighted the importance of the balance of dietary carbohydrates and proteins/amino acids (AAs) for overall mortality, fecundity and lifespan in most species (Fontana and Partridge 2015) ranging from *Drosophila* (Grandison, Piper, and Partridge 2009; Lee et al. 2008; Skorupa et al. 2008) to rodents (Solon-Biet et al. 2014; Solon-Biet et al. 2015) and humans (Levine et al. 2014). The emerging picture is that there is a trade-off between reproduction and longevity driven by the protein-to-carbohydrate ratio in the diet: a low ratio extends lifespan but reduces reproductive output, while a high ratio reduces lifespan but promotes offspring production (Simpson, Le Couteur, and Raubenheimer 2015). The mechanisms by which the brain shapes behavioral output during dietary balancing to solve this ethologically relevant trade-off are still largely unknown.

Significant advances have been made in our understanding of the neural circuitry underlying decision-making (Barron et al. 2015; Lisman 2015). But we are only beginning to understand how the internal state of an animal dictates the selection of specific actions (Krashes et al. 2009; Sternson 2013; Mahler et al. 2014; Cohn, Morantte, and Ruta 2015). This question becomes particularly relevant in value-based decision making, such as nutrient balancing, where the value of the available options is dependent on the current needs of the animal (Vargas et al. 2010; Ribeiro and Dickson 2010; Itskov and Ribeiro 2013; Simpson and Raubenheimer 2012). Thus, the behavioral strategies animals use to

This chapter has been published in the eLife journal (http://dx.doi.org/10.7554/eLife.19920) and is therefore subjected to Creative Commons Attribution license, which permits unrestricted use and redistribution provided that the original author and source are credited.

adapt nutrient decisions to their internal states provide an ethologically relevant framework to understand how internal states change behavior to mediate value-based decisions.

The fly has emerged as an important model to study complex computational tasks due to the availability of sophisticated genetic tools (Luo, Callaway, and Svoboda 2008; Olsen and Wilson 2008), a numerically simple nervous system, and the advent of methods to quantitatively characterize behavior. Advanced computational tools have been applied successfully in *Drosophila* to study for example chemotaxis (Gomez-Marin, Stephens, and Louis 2011; van Breugel and Dickinson 2014), action mapping (Berman et al. 2014), aggression and courtship (Dankert et al. 2009; Coen et al. 2016), fly-fly interactions (Branson et al. 2009; Schneider, Dickinson, and Levine 2012; Ramdya et al. 2014), and predator avoidance (Muijres et al. 2014). This recent quantitative approach to behavioral analysis has given rise to the field of computational ethology: the use of computerized tools to measure behavior automatically, to characterize and describe it quantitatively, and to explore patterns which can explain the principles governing it (Anderson and Perona 2014). When combined with powerful genetic approaches (Bath et al. 2014; Ohyama et al. 2015) the fine description of behavior afforded by these methods will allow us to make significant steps forward in our understanding of the neuronal circuits and molecular pathways that mediate behavior.

Flies can detect and behaviorally compensate for the lack or imbalance of proteins and amino acids in the food (Vargas et al. 2010; Ribeiro and Dickson 2010; Bjordal et al. 2014) and adapt their salt and protein intake to their current mating state (Walker, Corrales-Carvajal, and Ribeiro 2015). The current nutrient state is thought to be read out directly by the nervous system through the action of nutrient-sensitive mechanisms such as the TOR and GCN2 pathways (Bjordal et al. 2014; Chantranupong, Wolfson, and Sabatini 2015; Ribeiro and Dickson 2010). Mating acts on salt and yeast appetite via the action of male-derived Sex Peptide acting on the Sex Peptide Receptor in female reproductive tract neurons, and the resultant silencing of downstream SAG neurons (Feng et al. 2014; Walker, Corrales-Carvajal, and Ribeiro 2015; Ribeiro and Dickson 2010). SAG neurons have been proposed to then change chemosensory processing to modify nutrient intake (Walker, Corrales-Carvajal, and Ribeiro 2015). The recent development of technologies that can measure the flies' feeding behavior quantitatively (Itskov et al. 2014; Ro, Harvanek, and Pletcher 2014; Yapici et al. 2016) gives access to the fine structure of the feeding program, and how flies homeostatically modulate this program according to their internal state. However, the further structure of foraging decisions, such as arriving at or leaving a specific food patch, and how flies balance the trade-off between exploiting a needed nutrient resource and exploring the surrounding environment to discover new resources, is still poorly understood. Understanding how internal states change the behavioral strategies of an animal should allow us to understand how the animal manages to maintain nutrient homeostasis.

Here, we developed a quantitative value-based decision making paradigm to study the foraging strategies implemented by adult *Drosophila melanogaster* to reach protein homeostasis. We use a semi-automated video tracking setup to characterize the exploitation and exploration of sucrose and yeast patches by flies in different dietary amino acid and mating states. We found that metabolic state and mating modulate the decisions to engage and leave a yeast patch. Furthermore, we describe how

the lack of dietary amino acids increases patch exploitation and restricts global exploration and how these behaviors dynamically shift towards increasing exploration as the fly reaches satiation. Importantly, we found that olfaction is not required to reach protein homeostasis, but that it mediates the efficient recognition of yeast as an appropriate food source. Finally, we show that octopamine mediates homeostatic postmating responses, but not the effects of internal sensing of amino acid deprivation state. Our results provide a quantitative and mechanistic description of how the fly changes behavioral decisions to achieve homeostatic nutrient balancing.

2.3 Results

2.3.1 Automated monitoring of nutrient choices using image-based tracking

Animals are able to adapt their feeding preference towards a particular food in response to their current needs (Sørensen et al. 2008; Ribeiro and Dickson 2010; Vargas et al. 2010; Simpson and Raubenheimer 2012; Griffioen-Roose et al. 2012; Dethier 1976). However, the behavioral strategies used by animals to make feeding decisions according to their internal state are currently largely unknown. To capture how flies decide what food to eat, we built an automated image-based tracking setup (Figure 2.1A) that captures the position of a single *Drosophila melanogaster* in a foraging arena (Figure 2.1B) containing 9 yeast patches (amino acid source) and 9 sucrose patches (carbohydrate source). The distribution of the food patches was designed to promote frequent encounters with food sources, such that nutritional decisions, rather than food detection, determine the fly's food exploitation strategies.

We recorded the behavior of the fly over two hours during these nutritional decisions, and developed custom software to track the position of the fly's body and head centroids. We then extracted multiple kinematic parameters (see Materials and Methods for detailed list) and computed the locomotor activity and the distance of the fly from each food patch during the whole duration of the assay (Figure 2.1C and D and Video 1). Upon a detailed analysis of the distribution of head speeds when the flies were inside or outside food patches (Figure 2.11A) we decided to use two speed thresholds to split the locomotor activity of the flies into three types: *resting* (speed ≤ 0.2 mm/s), *micromovement* (0.2 mm/s < speed ≤ 2 mm/s) and *walking* (speed > 2 mm/s). Furthermore, slow walking bouts (2 mm/s < speed < 4 mm/s) that were coupled with a rapid change in angular speed were defined as *sharp turns* (2 mm/s < speed < 4 mm/s and |angular speed| ≥ 125º/s) (Figure 2.1C and D). To characterize the behaviors that occur during these defined locomotor activity types, we manually annotated resting, feeding, grooming and walking events and assigned them to the corresponding speed profiles. In agreement with previous studies (J.-R. Martin 2004; Robie, Straw, and Dickinson 2010; Zou et al. 2011), we found that more than 80% of the speeds displayed during manually annotated resting or walking periods were below 0.2 mm/s or above 2 mm/s, respectively (Figure 2.11B). Furthermore, we reasoned that micromovements could correspond to either grooming or feeding. Indeed, 70% of grooming fell in the micromovement category; while for manually-annotated feeding bouts, half of these periods were categorized as micromovements, and the other half occurred at low speeds and

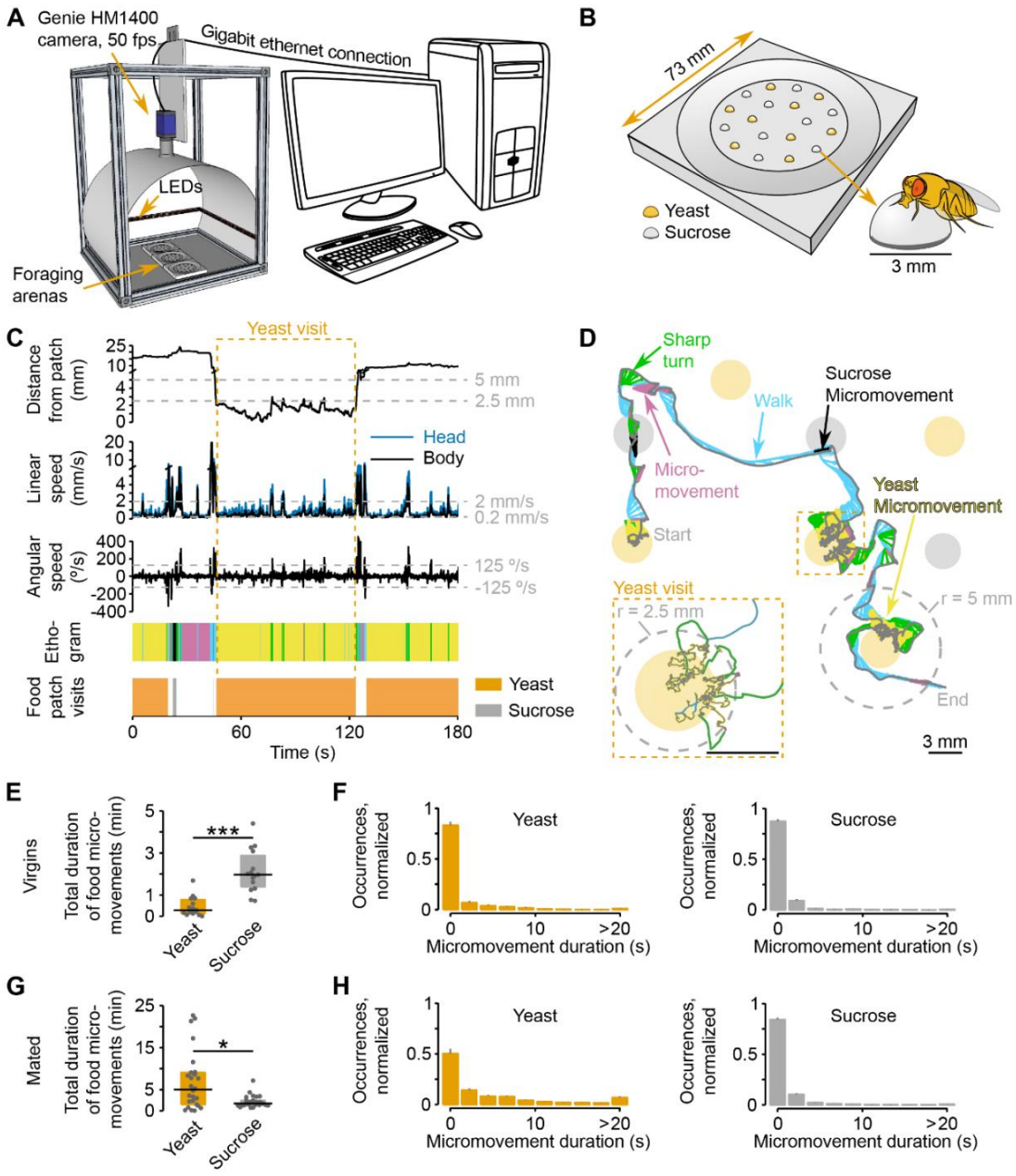

Figure 2.1 – Automated monitoring of nutrient choices using image-based tracking

(A) Schematic of the image-based tracking setup. (B) Schematic of the foraging arena, containing an inner flat circular area with 9 sucrose (carbohydrate source) and 9 yeast (amino acid source) patches. Each food patch has an approximate diameter of 3 mm which is approximately the body length of the experimental flies. (C) Example of the kinematic parameters and behavior classification associated to the representative trajectory shown in (D). Dashed gray horizontal lines indicate the thresholds used for behavior classification, definition of yeast and sucrose micromovements and food patch visits (see materials and methods). Dashed orange rectangle marks the beginning and end of the yeast visit (see inset in D). The different colors in the ethogram correspond to the behaviors labeled with the same color in (D). (D) Representative trajectory of a fly walking in the arena. Filled circles represent food patches. Gray and colored trajectories correspond to head and body centroid position, respectively. Small arrows in between both trajectories indicate body orientation. The color code for the different behaviors is indicated by the colored labels. Inset: a yeast visit is defined as a group of consecutive yeast micromovements, in which the head distance to the center of the food patch was never >5 mm (gray dashed line in the main trajectory). (E, G) Total duration of yeast and sucrose micromovements for virgin, n = 15 (E) and mated, n = 26 (G) female flies fed with the AA+ rich diet. (F, H) Distribution of yeast and sucrose micromovement durations for virgin (F) and mated (H) female flies fed with the rich diet. Bin size: 2.2 seconds. *$p < 0.05$, ***$p < 0.001$, significance was tested by Wilcoxon rank-sum test. In panels E and G and in the following figures in which boxplots are used, the black line represents the median, colored boxes represent inter-quartile range (IQR) and gray dots represent the value of the y-axis parameter for single flies.

were thus classified as resting. However, flies showed a very low rate of proboscis extension during feeding bouts at < 0.2 mm/s (data not shown) and we therefore reasoned that these slow bouts had little contribution to the amount of food ingested. For this reason, we decided to use the time the fly was performing micromovements when its head was in contact with the food patch as a proxy for the time the fly spent feeding (henceforth termed *yeast micromovements* or *sucrose micromovements*). To strengthen the argument that these micromovement periods within a food patch represented mostly feeding bouts and not grooming, we used the annotated video segments to quantify the percentage of feeding and grooming during a food micromovement bout. Indeed, we observed that 92.2% of the yeast micromovements and 70.6% of the sucrose micromovements corresponded to feeding bouts (Figure 2.11C). Hence *sucrose* and *yeast micromovements* are a good way to capture the periods the fly spends feeding on a food patch.

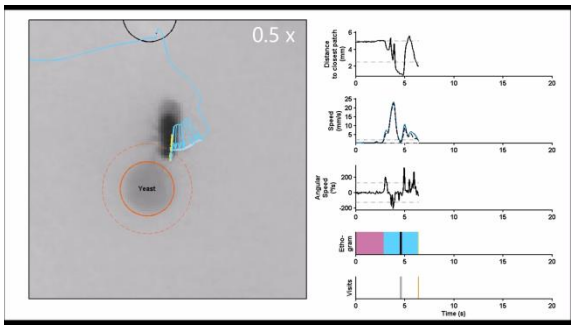

Video 1. Behavior classification during nutrient decisions.

A 20-second-segment of the trajectory depicted in Figure 2.1C-D, starting on second 40 and following the same color code. During the first 7 seconds of this segment, the video is slowed-down 0.5x and from there on, it is shown in real life speed, as indicated by the white label at the top right corner of the video frame with the fly.

To start exploring how flies with different internal states react to the different foods, we used this metric to characterize the behavior of virgin and mated females that were previously fed a rich diet. Virgin flies displayed a preference for sucrose over yeast over the total time of the assay, while the opposite was observed in mated females (E and G). A closer look at the duration of micromovements on the two food sources, revealed very similar duration profiles between yeast and sucrose for virgin females, while a higher prevalence of long events (≥ 20 s) on yeast when compared to sucrose was observed in mated flies (Figure 2.1F and H). These results suggest that for mated females, yeast has a higher salience as food source, even in fully-fed conditions. These observations are in accord with previous reports showing that mating leads to a switch in yeast preference in flies (Ribeiro and Dickson 2010; Vargas et al. 2010; Walker, Corrales-Carvajal, and Ribeiro 2015). Thus, the analysis of food micromovements allows us to capture previously-described changes in food preference elicited by mating. Furthermore, these results demonstrate that one way in which mating increases yeast preference is by inducing long feeding bouts, allowing us to make first conclusions about the mechanisms behind changes in food choice.

2.3.2 Flies increase yeast feeding and micromovements in response to amino acid challenges and mating

A key question in nutritional neuroscience is how animals homeostatically compensate for the lack of specific nutrients (Simpson and Raubenheimer 2012; Itskov and Ribeiro 2013; Morrison and Laeger 2015; Dethier 1976). A concrete example of this homeostatic regulation of feeding behavior is the

robust increase in preference for yeast when flies are deprived of proteinaceous food (Ribeiro and Dickson 2010; Vargas et al. 2010). To study the behavioral strategies underlying nutritional homeostasis, we decided to use a chemically defined (holidic) medium (Piper et al. 2014) to specifically manipulate amino acids (AA) in the diet, leaving the other macronutrients and micronutrients intact. Previous work has identified three different AA compositions having different impacts on reproduction in mated females: *AA+ rich* (supporting a high rate of egg laying), *AA+ suboptimal* (supporting a lower rate of egg laying) and *AA-* (leading to a dramatic reduction in egg laying) (Piper et al. 2014) (Figure 2.2A). Furthermore, to better understand how internal metabolic state and mating state interact at the behavioral level we also analyzed virgin females pre-fed these different diets.

To precisely measure the feeding behavior of flies with different internal states, we used the flyPAD technology (Figure 2.12A), which allowed us to decompose the feeding motor pattern into "sips" (Itskov et al. 2014). As the number of sips correlates strongly with food intake, this method enabled us to precisely measure the impact of internal states on feeding decisions. Consistent with previous observations (Walker, Corrales-Carvajal, and Ribeiro 2015; Ribeiro and Dickson 2010; Vargas et al. 2010) (Figure 2.1E), virgin flies showed very little interest in yeast during the whole assay, as measured by the total number of yeast sips (Figure 2.2Bi). Yeast feeding increased with AA deprivation (Figure 2.2Bii), and mating (Figure 2.2Biii). Notably, AA-challenged mated females showed a strong increase in the number of yeast sips (Figure 2.2Biv and v) with the highest rate of yeast feeding in mated flies completely deprived of AAs (Figure 2.2Bv). We next asked whether these differences in feeding behavior could be captured using the yeast and sucrose micromovements measured using the tracking setup. Indeed, we observed that the yeast micromovements increased in the same way as the yeast sips after AA challenges in virgin and mated females (Figure 2.2C). Importantly none of these internal state changes led to an increase in the total number of sucrose sips (Figure 2.12B) or in the total duration of sucrose micromovements (Figure 2.13), highlighting the dietary specificity of the manipulation and allowing us to focus our subsequent analysis on the fly's behavior towards yeast patches. Flies are therefore capable of sensing deficits in AAs and of compensating by specifically increasing feeding and micromovements on yeast, an AA-rich substrate. Furthermore, this homeostatic response is modulated by the mating state of the fly. Our tracking approach is therefore now a validated strategy to uncover the changes in behavioral strategies elicited by different internal states and how these changes allow the animal to reach homeostasis.

2.3.3 Flies show high inter-individual variability in the response to yeast

We investigated the dynamics of yeast micromovements by comparing the ethogram of each individual fly along the two hours of the assay and across all the internal state conditions tested (Figure 2.2D, yeast micromovements are shown in yellow). This type of visualization revealed that the behavior towards yeast was highly variable. The observed increase in the total duration of yeast micromovements across the different internal state conditions seems to come from the combination of two factors: on one hand, the proportion of flies that showed any interest in yeast at all (Figure 2.14A) and on the other hand, the strength of the interest displayed by these flies, measured by the total

duration of yeast micromovements. The behavior towards yeast was also highly variable across individuals of the same condition, increasing as a function of deprivation (Figure 2.14B). For example, the total duration of yeast micromovements displayed by AA-deprived flies ranged from 5 to 59 minutes. Still, the initial steep increase in yeast micromovements during the first 30 minutes of the assay was very consistent (Figure 2.2Ev and Figure 2.12C). The reaction to internal state changes is

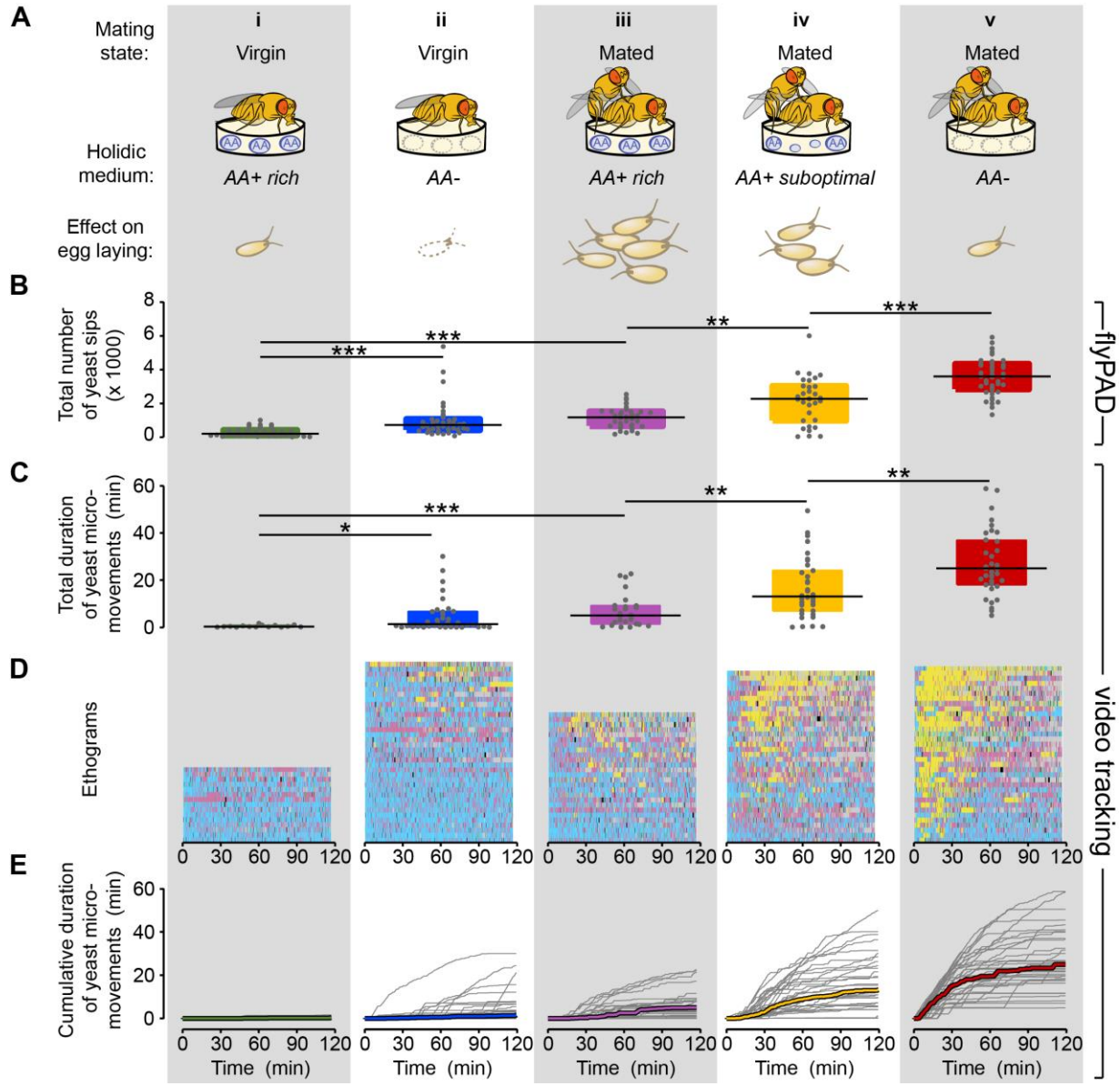

Figure 2.2 – Flies increase yeast feeding and micromovements in response to amino acid challenges and mating

(A) Graphical representation of the five internal states tested and the resulting reproductive output as reported by (Piper et al. 2014), all flies were pre-fed during 3 days with the holidic medium indicated in parenthesis: i) Virgin AA+ rich, ii) Virgin AA-, iii) Mated AA+ rich, iv) Mated AA+ suboptimal, v) Mated AA-. (B) Effect of internal states on the total number of yeast sips obtained using flyPAD assay (n = 32-43). (C) Effect of internal states on the total duration of yeast micromovements obtained from the video tracking assay (n = 15-35). (D) Behaviors displayed by single flies in the five internal states indicated in (A), during the video tracking assay. Each row represents the ethogram a single fly, following the same color code shown in Figure 2.1D. Yellow: yeast micromovements. Black: sucrose micromovements. Pink: micromovements outside the food patches. Blue: walking bouts. Gray: resting bouts. Green: sharp turns. (E) Dynamics of yeast micromovements quantified as the cumulative duration of yeast micromovements. Gray lines correspond to single flies. Thick colored lines indicate median. *$p < 0.05$, **$p < 0.01$, ***$p < 0.001$, significance was tested by Wilcoxon rank-sum test with Bonferroni correction.

therefore highly variable across individuals. However, full AA deprivation in mated females leads to a robust population-wide effect, highlighting the importance of AAs for the animal.

2.3.4 Metabolic state and mating modulate the probability of engaging and leaving a yeast patch

To feed, flies need to stay on food patches. We decided to call these events *visits* (Figure 2.1C and inset in Figure 2.1D). A *visit* is defined as all consecutive bouts of micromovements on the same patch, for as long as the fly stayed in close proximity to the patch. As we observed in the total duration of yeast micromovements, the total duration of yeast visits increased as a result of mating and AA deprivation (Figure 2.3A). Therefore, we hypothesized that the fly increases yeast intake by changing different aspects of its foraging decisions, such as *approaching* a patch more often, *engaging* it more and/or *leaving* it less often. We measured approaching, engaging and leaving decisions by quantifying the number of encounters, the fraction of encounters in which the fly stops on a spot (*visits*) and the duration of visits, respectively. One easy way to increase the duration of yeast visits would be to approach yeast patches more often. However, none of the internal state modifications leading to an increase in yeast intake caused an increase in the total number of yeast encounters (Figure 2.15A). Furthermore, the rate of encounters remains constant across internal states, with the exception of the mated fully AA-deprived females, which had a low absolute number of encounters (Figure 2.3B). To explain the behavioral changes underlying homeostasis, we focused on the decision to engage (Figure 2.3C) and leave (Figure 2.3D and Figure 2.15B) a yeast patch.

We found that in virgins, AA deprivation had a specific effect as it only modulated the decision to leave a patch, with deprived virgins showing longer visits (Figure 2.3D and Figure 2.15B). Mating also modulated the decision to leave, as fully-fed mated females took longer to leave a yeast patch than virgins (Figure 2.3D and Figure 2.15B), and, to a smaller degree, had a higher probability of engaging a proteinaceous food patch upon encounter (Figure 2.3C). Surprisingly, pre-feeding mated flies with the suboptimal diet caused a dramatic increase in the probability of engagement (Figure 2.3C). The strong effect on the decision to engage shows that flies are able to homeostatically modify their behavior in response to even subtle dietary differences that have a negative impact on their fitness (Piper et al. 2014). This is even more striking considering that the removal of all AAs does not lead to further changes in the engagement and leaving decisions, despite its drastic impact on egg production and yeast feeding (Figure 2.2).

We showed above that there is considerable variability across individuals in their behavioral response towards yeast. Interestingly, this was also the case for the strategies each mated fly chose to compensate for both AA challenges. We observed that these flies reached the same total times on yeast by mixing strategies in different ways: some flies had fewer but longer visits, while others had a higher number of visits, but each visit was shorter (Figure 2.3E). Taken together, these data show that both metabolic and mating states significantly change the decisions to engage and leave a yeast patch. Furthermore, the strongest effect is observed when both states act together, as seen in AA

challenged mated females. The specific behavioral strategy each fly employs to reach homeostasis, however, varies widely.

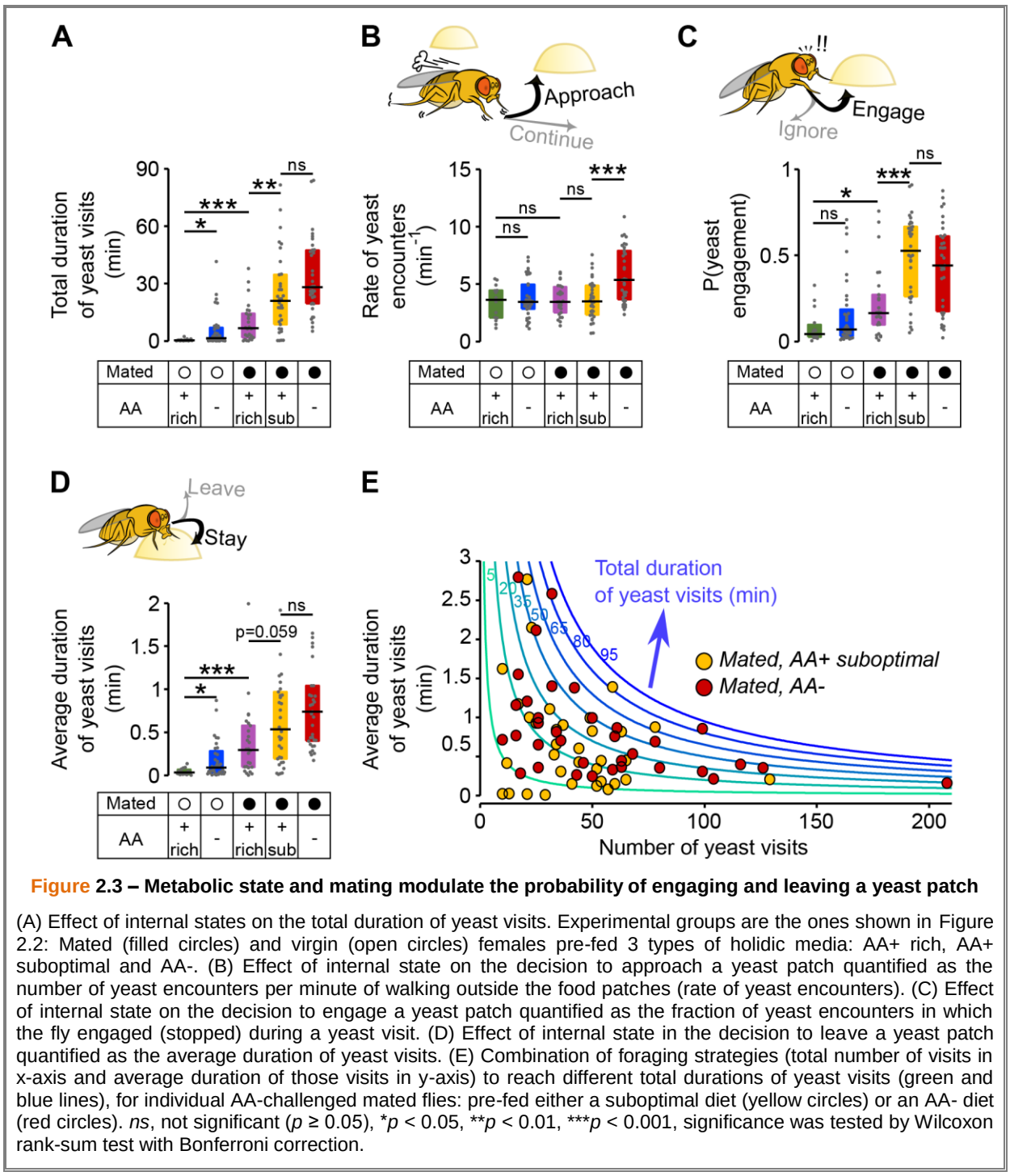

Figure 2.3 – Metabolic state and mating modulate the probability of engaging and leaving a yeast patch

(A) Effect of internal states on the total duration of yeast visits. Experimental groups are the ones shown in Figure 2.2: Mated (filled circles) and virgin (open circles) females pre-fed 3 types of holidic media: AA+ rich, AA+ suboptimal and AA-. (B) Effect of internal state on the decision to approach a yeast patch quantified as the number of yeast encounters per minute of walking outside the food patches (rate of yeast encounters). (C) Effect of internal state on the decision to engage a yeast patch quantified as the fraction of yeast encounters in which the fly engaged (stopped) during a yeast visit. (D) Effect of internal state in the decision to leave a yeast patch quantified as the average duration of yeast visits. (E) Combination of foraging strategies (total number of visits in x-axis and average duration of those visits in y-axis) to reach different total durations of yeast visits (green and blue lines), for individual AA-challenged mated flies: pre-fed either a suboptimal diet (yellow circles) or an AA- diet (red circles). *ns*, not significant ($p \geq 0.05$), *$p < 0.05$, **$p < 0.01$, ***$p < 0.001$, significance was tested by Wilcoxon rank-sum test with Bonferroni correction.

2.3.5 The lack of dietary AAs increases exploitation and local exploration of yeast patches

We have shown that AA deprivation leads to a 1.6-fold increase in yeast feeding when compared to the suboptimal diet treatment (Figure 2.2B). Surprisingly, however, a change of this order of magnitude is not visible in the total duration of the yeast visits (Figure 2.3A), nor is this homeostatic effect recapitulated in changes in specific foraging decisions (Figure 2.3). We therefore speculated

that instead of modulating exploratory decisions, a lack of AAs could increase the eagerness of the flies to exploit the yeast spot. Indeed, the time course of yeast visits (Figure 2.4A and Figure 2.16A) shows that AA-deprived flies displayed a sharp increase in the total duration of yeast visits during the first minutes, while flies pre-fed a suboptimal AA diet displayed a much more delayed and shallower increase in this parameter. As these early visits were also longer (Figure 2.16B), we measured the time it took each fly to engage in its first "long" (≥ 30s) visit (Figure 2.16C and D), and found that AA-deprived flies indeed attained their first long yeast visit much sooner than flies fed a suboptimal diet (Figure 2.4B): the median latency for AA-deprived flies was just 4.38 min (IQR = 2.08 – 7.7), which was three times shorter than the 12.37 min (IQR = 19.87 – 9.86) observed in flies fed with the suboptimal diet. These results therefore suggest that AA-deprived flies are indeed more motivated to exploit yeast spots.

We next asked if AA deprivation could also induce differences in the way flies behaved on the yeast patches. When we plotted the distribution of the positions of the flies on the proteinaceous food patches, we observed that AA-deprived flies covered the patches more homogeneously than flies kept on a suboptimal diet, which preferred to stay at the edge of the patch Figure 2.4C). In fact, deprived flies ventured much more into the food patch as quantified by the fact that during a visit, their average minimum distance from the patch center was much smaller (Figure 2.4D) and that they covered a larger area of the resource (Figure 2.4E). These data suggest that AA-deprived flies are not only more motivated to start exploiting a yeast patch but are also more active while on the food patch. This was further supported when we quantified locomotor activity during each visit to yeast. As visible in the two example trajectories displayed in Figure 2.4F, we observed that deprived flies were more active, displaying higher linear (Figure 2.4G and H) and angular speeds (Figure 2.4I). Accordingly, these flies had fewer resting bouts and more sharp turns (Figure 2.4J). These changes in behavior observed on the food patch were only induced by a complete lack of AAs, as there was no difference in these parameters between mated females pre-fed the rich diet versus those pre-fed the suboptimal diet (Figure 2.17). All these data are in agreement with an increase in yeast exploitation upon full AA deprivation. Flies lacking AAs would be more "eager" to exploit and therefore ingest yeast, leading to a strong increase in yeast feeding as observed using the flyPAD (Figure 2.2B).

Animals homeostatically increase food intake upon food deprivation, by changing the micro-structure of their feeding motor pattern (Itskov et al. 2014; Davis and Smith 1992) (Figure 2.18A). As video tracking does not give us access to the fine structure of the proboscis motor program, we used the flyPAD technology to characterize the changes in the microstructure of feeding upon AA deprivation. Pre-feeding flies a suboptimal diet led to a decrease only in the inter-burst-interval (IBI) when compared to flies kept on a rich diet (Figure 2.18B) while the number of sips in each feeding burst did not change (Figure 2.18C). Full AA deprivation, however, led to a strong increase in the number of sips per burst with only a mild further decrease in the IBI. It is interesting to note that these effects are very similar to those observed upon mating in yeast-deprived females, which leads to both a decrease in the inter-burst interval and an increase in the number of yeast sips per burst (Walker, Corrales-Carvajal, and Ribeiro 2015). Taken together, while AA deprivation has minimal effects on the decision to engage and leave a proteinaceous food patch, this metabolic manipulation leads to drastic changes

in its exploitation. The described changes in activity are likely to support an increased use of the yeast resource, which is further promoted by a change in the feeding motor pattern of the fly. The increase

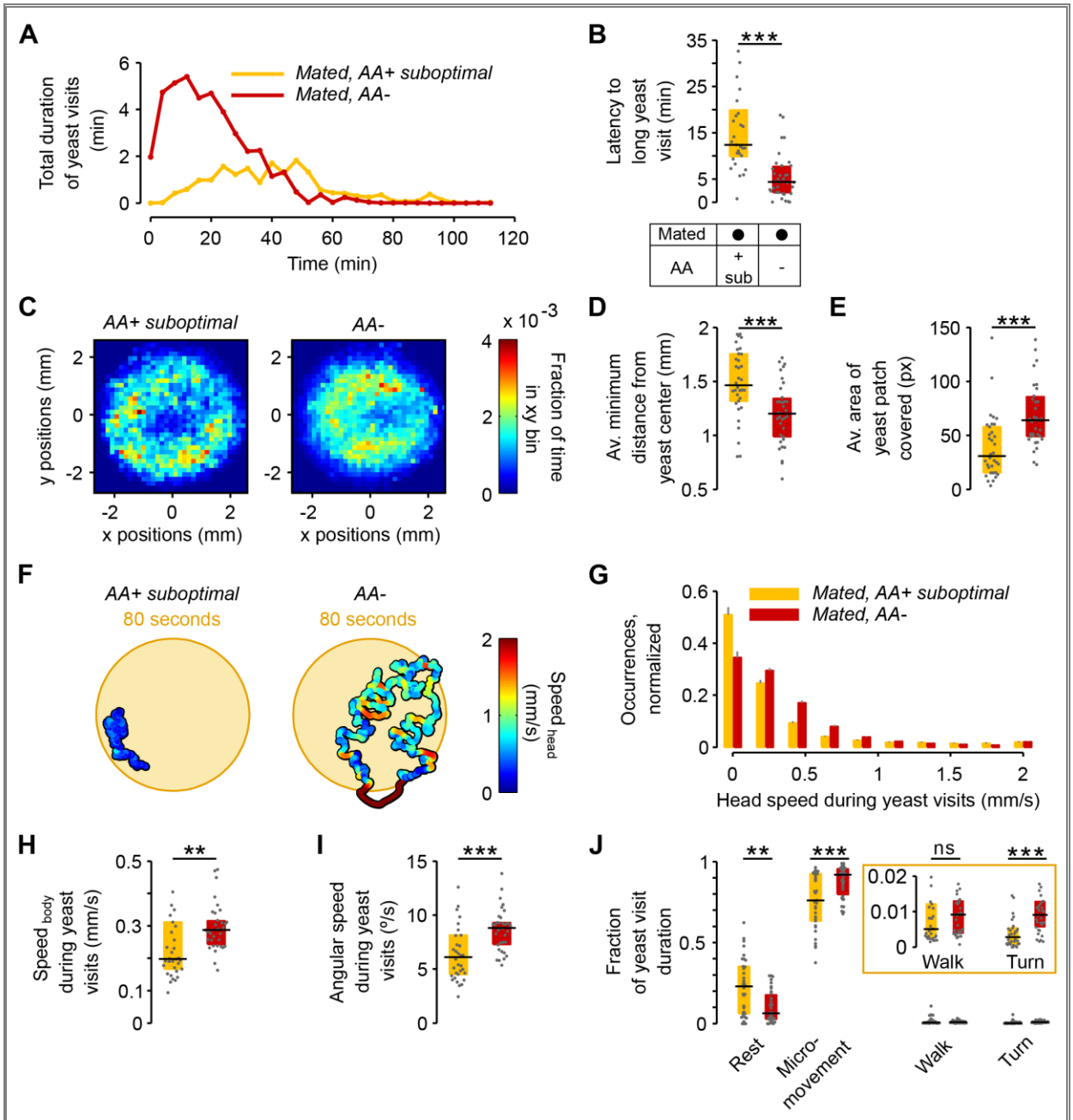

Figure 2.4 – The lack of dietary AAs increases exploitation and local exploration of yeast patches

(A) Rolling median of the total duration of yeast visits using a 5 minute window and a step of 4 minutes for flies pre-fed a suboptimal diet (yellow) and AA- diet (red). (B) Effect of AA deprivation on the time elapsed until the fly engages in the first "long" (≥ 30 s) yeast visit. (C) Histogram of the x-y relative position of all mated flies pre-fed a suboptimal diet (left) or a AA- diet (right) with respect to the center of the yeast patch (0,0). The pixel color indicates the fraction of time that flies in the indicated condition spent in the corresponding location bin. (D) Effect of AA deprivation on the average minimum distance to the center of the yeast patch, during a yeast visit. (E) Effect of AA deprivation in the average area covered during a yeast visit. (F) Example trajectories of head position during a yeast visit for a fly of the indicated condition. Hot colors indicate higher head speeds. (G-J) Effect of AA deprivation on the locomotor activity of mated flies during yeast visits: (G) average histogram of head speeds, (H) body centroid speed, (I) angular speed and (J) proportion of the indicted behaviors during yeast visits. *ns*, not significant ($p \geq 0.05$), ** $p < 0.01$, *** $p < 0.001$, significance was tested by Wilcoxon rank-sum test with Bonferroni correction. Panels B, D, E, H-J compare the indicated parameters between mated flies pre-fed a suboptimal diet (yellow) and mated flies pre-fed an AA- diet (red).

In exploitation can also be interpreted as an increase in local, resource-directed exploration which could aid the micro-optimization of food intake within non-homogenous natural food patches.

2.3.6 Amino acid challenges reduce global exploration and increase revisits to the same yeast patch

The data presented above clearly demonstrate that different internal states interact to modulate food exploitation. But what could be the effects of internal states on the exploratory behaviors of flies? In order to capture how far the fly would forage to reach the next yeast patch, we calculated three types of transition probabilities: transitions to the same yeast patch, transitions to adjacent yeast patches, and transitions to distant yeast patches. We found that mated flies fed the rich diet had a high probability of transitioning to distant yeast patches (75%) (Figure 2.5A and D), and a lower probability of transitioning to adjacent food patches (25%) (Figure 2.5A and E). Strikingly, these flies almost never returned to the yeast patch they had just visited (Figure 2.5A and F). Fully-fed flies therefore display a high rate of global exploratory activity, traveling larger distances during their transitions (Figure 2.5G) and mainly choosing to visit distant food patches (as in the example trace). Challenging flies with a suboptimal diet (Figure 2.5B) or one lacking all AAs (Figure 2.5C) significantly altered their exploratory behavior: they strongly reduced their probability of transitioning to distant yeast patches (Figure 2.5D) and increased the probability of transitioning to adjacent yeast patches (Figure 2.5E). Further, in contrast to the fully-fed flies, AA-challenged flies showed a strong increase in their probability of returning to the same yeast patch (Figure 2.5F and Figure 2.19). As one would expect, these changes in behavior are also seen as a decrease in the average distance traveled by animals during transitions to yeast (Figure 2.5G). Dietary AA challenges therefore lead to a switch from global to local exploration (see example traces in Figure 2.5A-C). One of the most striking changes is the strong increase in returns to the same yeast patch upon AA deprivation. This change in exploratory strategy leads to an effective additional increase in the time on the same yeast patch without requiring a change in the decision to leave it (Figure 2.3D and Figure 2.15B). Taken together, these changes in exploratory strategy should enable the fly to efficiently increase the intake of yeast while minimizing the distance traveled to the next spot. It also allows the fly to focus on a resource whose quality she knows while avoiding testing food patches of unknown qualities, thereby reducing exploratory risk.

2.3.7 Flies dynamically adapt their exploitatory and exploratory behavior to their internal AA state

If yeast exploitation and exploration are indeed regulated by the internal AA state of the fly, we hypothesized that flies should dynamically adapt their behavior as their internal state changes over the course of the assay due to satiation. To capture this effect independently from the varying yeast intake dynamics displayed by each fly, we divided the total duration of yeast micromovements of each fly into four periods, which we called “yeast quartiles” (Figure 2.6A). Each *yeast quartile* consists of 25% of the time that the fly spent in yeast micromovements, but covers a different amount of absolute time in the assay for each fly.

As hypothesized, the flies displayed clear differences in their foraging behavior across the four analyzed quartiles. The effect on exploration was clearly visible in the raw tracking traces for the four quartiles (Figure 2.6B). As the time spent on yeast increased, the average distance traveled to the next yeast patch (Figure 2.6C) and the probability of visiting a distant yeast patch increased (Figure 2.6D), while the probability of revisiting the same yeast patch decreased (Figure 2.6E). Accordingly, parameters related to patch exploitation such as the average minimum distance from the center of the spot (Figure 2.6F), the angular speed on the yeast patch (Figure 2.6G), and the average duration of the yeast visit (Figure 2.6H) reverted to the values observed in fully-fed females (Figure 2.20A-C).

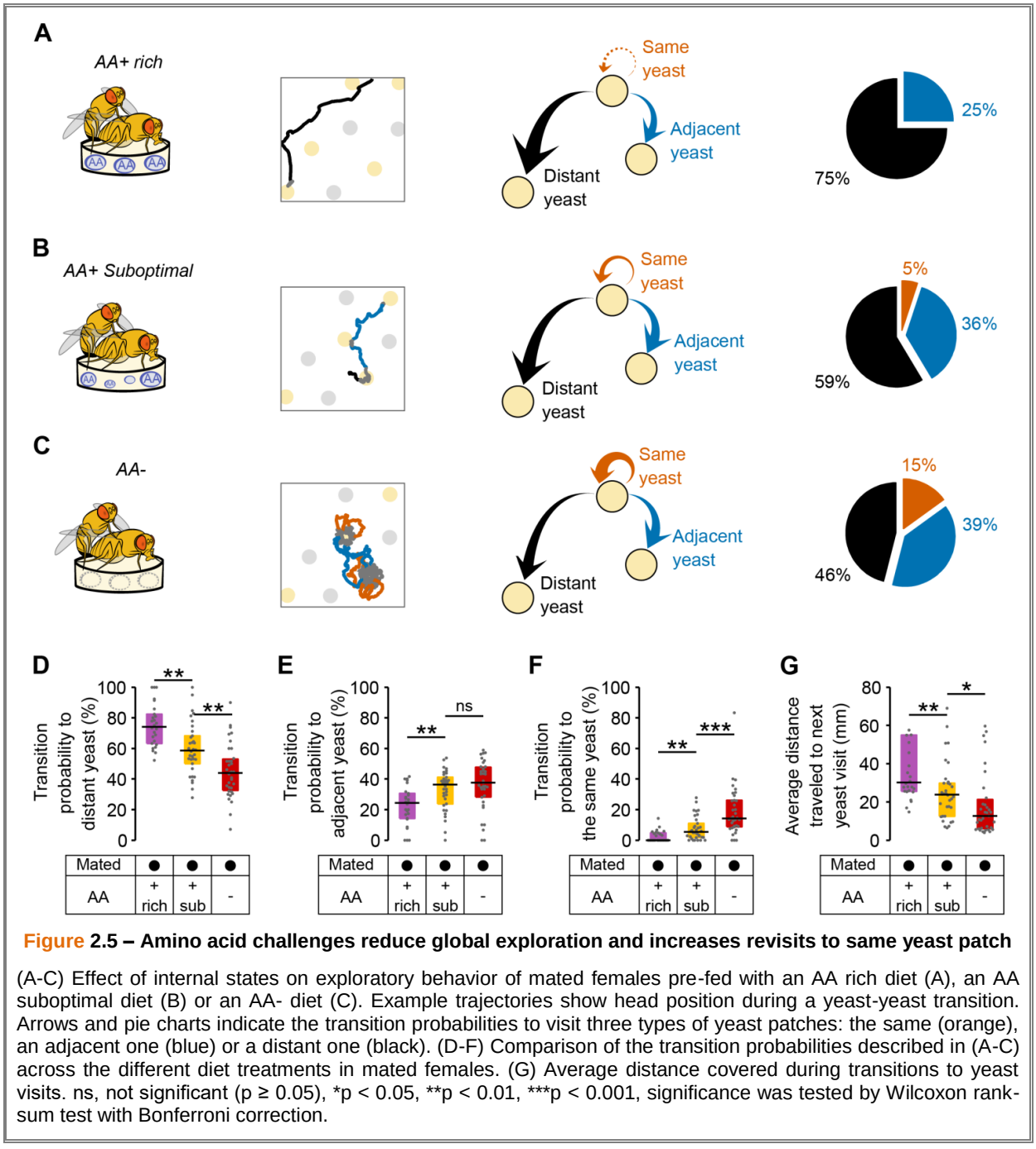

Figure 2.5 – Amino acid challenges reduce global exploration and increases revisits to same yeast patch

(A-C) Effect of internal states on exploratory behavior of mated females pre-fed with an AA rich diet (A), an AA suboptimal diet (B) or an AA- diet (C). Example trajectories show head position during a yeast-yeast transition. Arrows and pie charts indicate the transition probabilities to visit three types of yeast patches: the same (orange), an adjacent one (blue) or a distant one (black). (D-F) Comparison of the transition probabilities described in (A-C) across the different diet treatments in mated females. (G) Average distance covered during transitions to yeast visits. ns, not significant ($p \geq 0.05$), *$p < 0.05$, **$p < 0.01$, ***$p < 0.001$, significance was tested by Wilcoxon rank-sum test with Bonferroni correction.

These results show that flies are capable of dynamically adapting their behavioral strategies according to their current internal state and strengthen the notion that foraging strategies are modified by the AA state of the animal to homeostatically balance the intake of AA-rich foods.

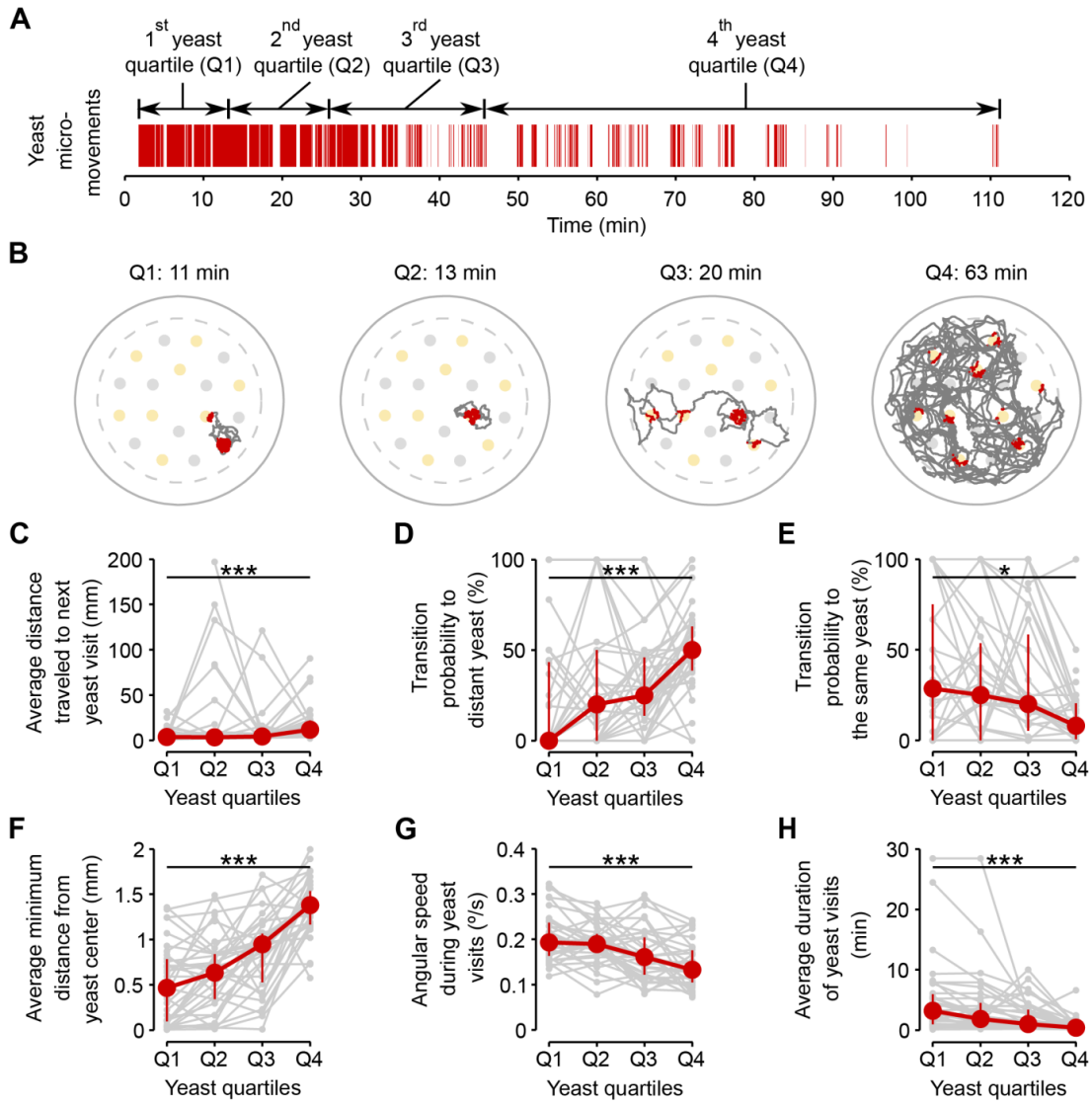

Figure 2.6 – Flies dynamically adapt their exploitatory and exploratory behavior as their internal AA satiation changes

(A) Definition of yeast quartiles based on the total duration of yeast micromovements along the two hours of the video tracking assay for an example fly. Arrows indicate start and end points of each yeast quartile. Each yeast quartile consists of 25% of the time that the fly spent in yeast micromovements, but covers a different amount of absolute time in the assay for each fly, as shown in (B). (B) Example trajectories of head positions during each yeast quartile defined in (A). Red indicates the occurrence of a yeast micromovement. (C-H) Effect of yeast satiation on exploration (C-E) and exploitation (F-H) parameters, for mated AA-deprived flies, quantified during the four yeast quartiles of each fly. As the flies spend more time on yeast, the values of these parameters change towards the values of flies fed with a rich diet. *$p < 0.05$, ***$p < 0.001$, significance was tested by Wilcoxon rank-sum test.

2.3.8 *ORs mediate efficient recognition of yeast as an appropriate food source*

Starvation changes olfactory representations of food odors and these changes are thought to be required to find food efficiently (Root et al. 2011; Beshel and Zhong 2013). To begin to uncover the neuronal mechanisms underlying foraging decisions, we decided to analyze the role of olfaction in nutrient homeostasis. The OR type of olfactory receptors have been shown to significantly contribute to the olfactory detection of yeast over large distances (Becher et al. 2010; Christiaens et al. 2014; Dweck et al. 2015) and are known to mediate physiological responses to yeast odors (Libert et al. 2007). We therefore focused on the function of these receptors in homeostatic yeast feeding by tracking the foraging behavior of flies lacking *Orco*, a co-receptor essential for OR function (Larsson et al. 2004). Unexpectedly, we observed that in general upon AA deprivation, *Orco* mutants showed a similar total duration of yeast visits as controls (Figure 2.7A). However, upon closer inspection of the time course of yeast visits, we observed that flies with impaired olfaction had a very long latency to engage in a long yeast visit when compared to the genetic controls (Figure 2.7B-D, see also Figure 2.4A and Figure 2.21). While *Orco* mutants needed around 25 minutes to enter into a high yeast exploitation "mode" (median = 25.58 min, IQR = 15.05 – 30.06) the genetic controls required only 5-8 minutes to do so (Figure 2.7C).

Olfaction has been proposed to be important for the fly to locate food sources (Root et al. 2011). *Orco* mutants, however, have plenty of encounters with yeast during the latency period. This is clearly visible in the example trace (Figure 2.7E) where pink dots mark encounters with yeast patches. In fact, the number of encounters of *Orco* mutant flies with yeast patches was similar to, or even higher than, that of controls (Figure 2.7F). The increased latency also seems not to be due to an impairment in locomotion, as mutant flies walked as fast when outside the food patches as genetic controls (Figure 2.7G). These data indicate that in our assay, *Orco* mutant flies easily find yeast spots but fail to efficiently engage into long yeast visits.

If *Orco* mutant flies are inefficient in engaging yeast spots, how do they manage to homeostatically compensate for the AA challenge? We observed that the duration of the first long visit (Figure 2.7H) and the probability of revisiting the same yeast patch (Figure 2.7I) were greater for the *Orco* mutants than for the controls. These results indicate that mutant flies were either more AA deprived than controls or compensated for their sensory deficit by displaying a generally higher exploitatory motivation. Taken together these results show that OR-mediated olfaction is necessary for efficient recognition of yeast as an appropriate resource but is not required to locate food patches at a short range or to achieve nutritional homeostasis.

2.3.9 *Octopamine mediates homeostatic postmating responses but not internal sensing of AA deprivation state*

Neuromodulators are thought to be important in translating internal states into behavioral output (Taghert and Nitabach 2012). While octopamine has been shown to mediate the postmating increase in yeast feeding (Walker, Corrales-Carvajal, and Ribeiro 2015), it has been proposed that octopamine does not contribute to homeostatic changes in feeding behavior (Z. Yang et al. 2015). We therefore

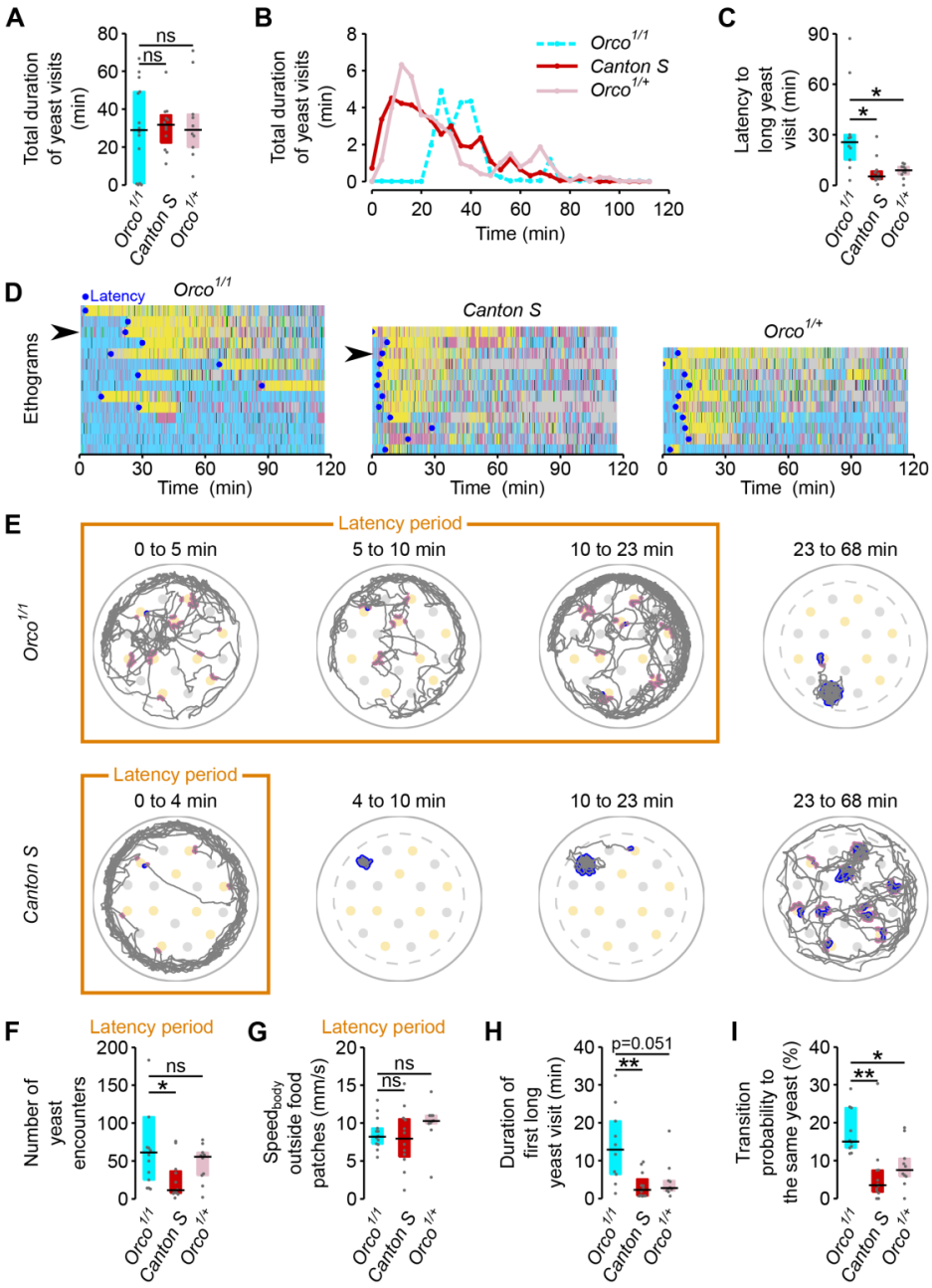

Figure 2.7 – ORs mediate efficient recognition of yeast as an appropriate food source

(A) *Orco*$^{1/1}$ AA-deprived flies spend as much total time visiting yeast as AA-deprived control flies (n = 10-14). (B) Rolling median of the total duration of yeast visits using a 5 minute window and a step of 4 minutes. (C) Effect of *Orco* mutation on the latency to engage in the first "long" (≥ 30s) yeast visit. (D) Behaviors displayed by *Orco* and control flies, along the 120 minutes of the assay. Each row represents the ethogram a single fly, following the same color code shown in Figure 2.1D. Yellow: yeast micromovements. Black: sucrose micromovements. Pink: micromovements outside the food patches. Blue: walking bouts. Gray: resting bouts. Green: sharp turns. Blue circles indicate the latency (see C) of each fly. Arrows indicate example flies shown in (E). (E) Top: Example trajectory of head positions of an *Orco*$^{1/1}$ AA-deprived fly during the 23-minute-long latency period (first three panels on the left) and during 45 minutes after the latency period (fourth panel). Bottom: Example trajectory of head positions of a Canton S AA-deprived fly during the 4-minute-long latency period (first panel on the left) and from the latency point up to minute 68 (three panels on the right). Highlighted trajectory segments represent yeast encounters (pink) and yeast visits (blue). (F-G) Exploration and locomotor activity during latency period is not affected in *Orco*$^{1/1}$ flies as indicated by the number of yeast encounters (F) and the body centroid speed outside food patches (G). (H) The first long yeast visit is longer in *Orco*$^{1/1}$ flies than in control flies. (I) Probability of transition to same yeast patch is higher in *Orco*$^{1/1}$ flies than in control flies. ns, not significant ($p \geq 0.05$), *$p < 0.05$, **$p < 0.01$, significance was tested by Wilcoxon rank-sum test with Bonferroni correction.

decided to test possible neuromodulatory effects of octopamine on yeast foraging, using mutants for the gene encoding Tyramine β-hydroxylase (TβH), an enzyme required for the biosynthesis of octopamine. As expected, we observed that in AA-deprived females, the drastic increase in the total duration of yeast visits after mating was greatly reduced in *TβH*^{nM18} flies (Figure 2.8A and Figure 2.22A). Likewise, octopamine also seems to be required to elicit the full increase in the probability of engagement on yeast (Figure 2.8B and Figure 2.22B) and the full increase in the duration of yeast visits (Figure 2.8C and Figure 2.22C), reiterating our previous observation that these two parameters are modulated by mating (Figure 2.3). To test whether octopamine was also required for mediating changes in yeast feeding behavior upon AA deprivation, we used the flyPAD technology. *TβH*^{nM18} virgin flies were able to increase the number of sips after AA deprivation to a similar extent as control flies (Figure 2.8D and Figure 2.22D) showing that octopamine is not involved in translating the internal state of AA deprivation into increased yeast intake. Overall, these results confirm that the decisions to engage and leave a yeast spot are strongly modulated by mating. They also show that octopamine mediates these postmating responses towards yeast, but is not required to sense the internal AA deprivation state.

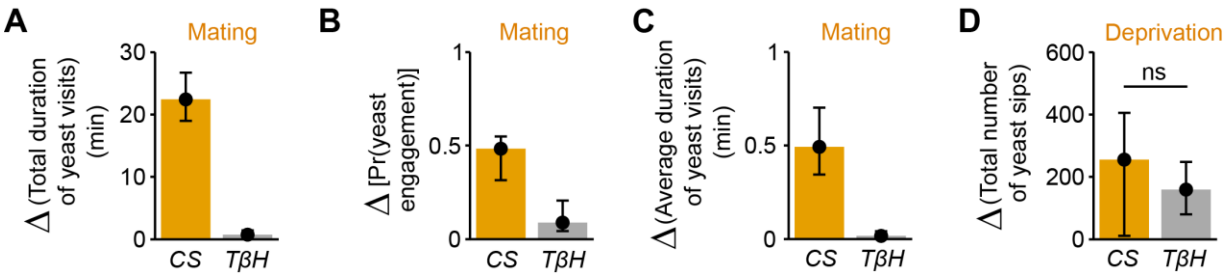

Figure 2.8 – Octopamine mediates postmating response towards yeast but not internal sensing of AA deprivation state

(A-C) Effect of *TβH* mutation on the postmating change in foraging parameters, obtained from the video tracking assay after 1 hour: total duration of yeast visits (A), probability of engaging a yeast patch (B) and average duration of yeast visits (C) for *Canton S* and *Tβh*^{nM18} females, both AA-deprived. Bars depict difference between median value of mated minus virgin groups for the correspondent parameter. Error bars show 5% and 95% bootstrap confidence intervals (n = 25-33). (D) Effect of *TβH* mutation on the increase of yeast sips after AA deprivation in virgin females, quantified using the flyPAD setup. Bars depict difference between median values of AA+ (suboptimal) minus AA-deprived groups. Error bars show 5% and 95% bootstrap confidence intervals (n = 26-34). *ns*, not significant. (A-C) Show statistically significant differences between *Canton S* and *Tβh*^{nM18} females, as the confidence intervals do not overlap.

2.4 Discussion

In order to maintain nutrient homeostasis animals need to be able to adapt their nutrient preferences to their current state. But which behavioral alterations underlie such changes in preference? Here we use an automated video tracking setup to quantitatively capture the behavioral adaptations to AA and mating state changes that allow the animal to maintain nutrient homeostasis. We started by separating the behaviors flies display towards food into discrete decisions: the decision to approach a food patch, the decision to engage it, and the decision to leave it (Figure 2.9). Strikingly, mating and AA challenges induced compensatory behaviors towards yeast patches but not sucrose patches,

indicating that the fly changes its exploitation decisions in a resource specific way. Furthermore, internal state modifications impact specific decisions to a different extent. While mating had a major effect on the probability of a fly leaving a yeast spot, AA challenges strongly increased the probability of engaging a food patch. Nevertheless, the effect of AA deprivation on the decision to engage a food patch was strongly dependent on mating suggesting that both internal states act synergistically to increase yeast intake. Furthermore, while full AA deprivation leads to a strong increase in yeast feeding when compared to flies kept on a suboptimal diet, the described decisions were not altered by this drastic nutritional manipulation. There was, however, a considerable decrease in the latency to engage yeast spots for a long time and a general increase in parameters related to the "eagerness" of the fly to exploit the resource (latency to engage, locomotor activity on the patch and area of patch covered). Internal states, therefore, alter feeding in specific ways, allowing the fly either to spend more time on the food through the modulation of patch decisions, or to increase resource exploitation through the modulation of motivation without changing patch decisions. These discrete changes allow the animal to dose its exploitatory behavior and hence the intake of nutrients over a large range (~17 fold) to match its current needs.

The specific changes observed in the behavior upon alterations of internal state are in agreement with

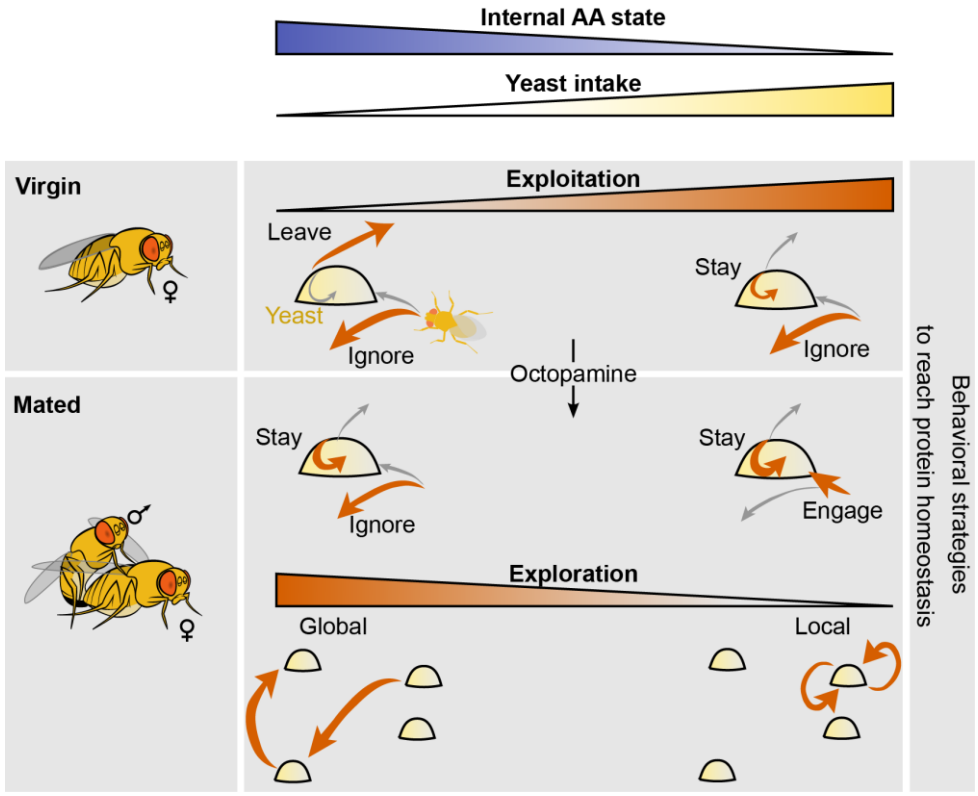

Figure 2.9 – Model of behavioral strategies modulated by internal AA state

We propose a model in which virgin flies with high internal levels of AAs display low intake mostly ignore yeast patches upon encounter and have a high probability of leaving the yeast patch upon engagement. Internal AA levels decrease as a consequence of poor diets which induce a change in the leaving decision, inducing increased yeast intake. Octopamine mediates the postmating changes in the foraging decisions of engaging and leaving the yeast patch upon encounter. As the internal AA levels decrease in mated females, their exploration patterns switch from global exploration to local exploration and multiple returns to the same yeast patch.

a modular organization of behavioral control. Such modularity has been previously described in the organization of motor output, such as locomotion (Kiehn 2016), swimming (Huang et al. 2013), grooming (Seeds et al. 2014), and feeding (Itskov et al. 2014; Walker, Corrales-Carvajal, and Ribeiro 2015). This suggests that the brain uses different mechanisms and hence circuits to change specific aspects of behavioral outcomes or decisions and that these changes add up to reach a specific goal. In agreement with this model, it has been shown that the impact of different starvation times on gustatory input relies on different mechanisms (Inagaki, Panse, and Anderson 2014). Similarly, our data show that octopamine is specifically required for mediating the changes in yeast decisions observed upon mating but not upon AA deprivation (Figure 2.9). Nevertheless, some decisions, such as the decision to engage a yeast spot, seem to be synergistically gated by both the mating and the AA state of the fly. It will be interesting to dissect how different internal states act at the circuit level to change behavioral decisions: do they act differentially on specific neuronal populations, or is the observed synergism a reflection of the different internal states acting on the same set of neurons?

While at the population level the effect of internal state manipulations led to stereotypical changes in behavior, the effect of internal state on the decisions implemented varied greatly at the individual level. This effect is reminiscent of the large individual differences observed in human physiology in response to identical diets (Zeevi et al. 2015). While such behavioral differences can stem from different metabolic states prior to the experiment, transgenerational effects in metabolism (Öst et al. 2014), or differences in the microbiota of the flies (Broderick and Lemaitre 2012), there is a real possibility that they also reflect idiosyncrasies in behavior and metabolic susceptibilities to internal state changes at the individual level. Indeed, upon AA challenges, we observed that some flies increased their total time on yeast by having many short yeast visits, while some flies had fewer but longer visits. It will be interesting to investigate if these differences reflect behavioral idiosyncrasies, as observed before in many animals including *Drosophila* (Dingemanse et al. 2010; J. S. Kain, Stokes, and de Bivort 2012; Buchanan et al. 2015). Differentiating between these two possibilities and identifying the physiological and circuit mechanisms leading to idiosyncrasies will be key to a better understanding of behavior. This is especially relevant for understanding metabolic conditions related to nutrition such as obesity.

In order to balance the intake of specific nutrients the animal should be able to specifically change its decisions towards the food source which contains the nutrient it needs. Our data show that this is indeed the case, pointing to a possible important contribution of chemosensory systems to nutrient decisions. Indeed, taste processing has been shown to be changed by the mating state of the animal and to contribute to the adaptation of behavioral decisions such as food choice (Walker, Corrales-Carvajal, and Ribeiro 2015) and egg laying site selection (Hussain, Üçpunar, et al. 2016). The contribution of olfaction to nutrient selection is less well understood. The sense of smell is thought to be mostly important for food search behavior (Semmelhack and Wang 2009; Becher et al. 2010), with starvation changing olfactory sensitivity to improve the finding of a food source (Root et al. 2011). Our data suggest that while olfactory-impaired flies are able to homeostatically increase yeast intake upon AA deprivation, OR-mediated olfaction still plays an important role in their capacity to do so. Interestingly, olfaction does not seem to be important for locating the food but for identifying yeast as an appropriate food source. These data suggest that flies use multimodal integration to decide which

food to ingest. In humans, flavor, the integration of different sensory modalities such as taste and smell, is key to the perception of food (Verhagen and Engelen 2006). Similarly, in mosquitoes olfaction acts together with other sensory cues to initiate a meal (McMeniman et al. 2014). Identifying the chemosensory basis for yeast feeding decisions might therefore be a powerful way to investigate the neuronal basis of flavor perception.

While one would expect that internal states increase food intake by changing exploitation decisions, their effects on exploratory behaviors in our paradigm are not trivial. Exploration is key for animals to find the resources they require and to acquire information about their surrounding environment (Calhoun, Chalasani, and Sharpee 2014; Hassell and Shouthwood 1978; Hills et al. 2015). In our paradigm, however, animals do not need to search for resources as they are readily available. A key question then becomes why animals leave a food patch at all, especially when they are deprived of AAs. The fact that they still do so means that there is a value in leaving the current food patch, even if that one provides the urgently required nutrients to produce offspring and has not been depleted yet. We can only speculate that there must be an advantage in taking the "risk" of exploring unknown options and maybe identifying a better resource. Animals might often require other resources and leaving the current food patch might allow them to also explore the availability of these. Flies seem to nevertheless manage their exposure to uncertainty by tuning the spatial properties of their exploration. Their internal states not only define the probability to leave a food patch, they also define if they will explore locally or more globally. The more deprived they are, the more local their exploratory pattern will be (Figure 2.9). Remarkably, while the leaving probability of flies pre-exposed to a suboptimal AA diet and a diet lacking AAs looks identical, their exploratory patterns are very different. For example, AA-deprived flies display a higher rate of returns to the same patch right after leaving it. Therefore, while the neuronal processes determining staying decisions seem not to be altered between both AA-challenged states, full AA deprivation must act on the circuits controlling explorations to strongly increases the probability of revisiting the spot the fly just left. This allows the fly to de facto stay longer on the same food patch without changing its leaving decisions. We would like to propose that the apparent separate regulation of these two aspects of the fly behavior suggests that there are two separate internal state sensing processes regulating exploitation and exploration decisions. The combination of both behavioral and circuit modules would allow the fly to trade off the requirement to exploit specific resources and the "risk" of exposing itself to resources of unknown or lower quality. Furthermore, it is interesting to note the similarity between the revisits to the same food patch we observed upon strong AA deprivation and the "dances" observed by Vincent Dethier in the blowfly (Dethier 1976). Both phenomena are examples of how animals regulate their search behavior and exposure to uncertainty by modulating the local dynamics of their exploratory behavior, in a state-dependent manner. While the budget theory is a classic aspect of foraging theory, it has recently started to be reassessed. It is mainly controversial if energy-deprived animals, including humans, are more or less risk-prone (Kacelnik and El Mouden 2013). Our data suggest that the exploratory behavior of AA-deprived animals minimizes their exposure to uncertainty. The description of how different aspects of risk management are implemented at the behavioral level opens up the

opportunity to identify the circuit mechanisms by which internal states control exploration-exploitation trade-offs and therefore how animals decide how much to expose themselves to the unknown.

The success of neurogenetics has relied to a large extent on the use of simple binary end-point behavioral assays to perform large-scale unbiased screens (Leitão-gonçalves and Ribeiro 2014; Vosshall 2007; Ugur, Chen, and Bellen 2016). This approach has allowed the field to make important contributions to the molecular and circuit basis of innumerable phenomena, including learning and memory (Heisenberg 2015), chronobiology (Konopka and Benzer 1971), innate behaviors (Yapici et al. 2008; Demir and Dickson 2005), and sensory physiology (Larsson et al. 2004). While identifying these cornerstones of neuroscience was crucial, we are now in a position to start understanding how these mechanisms act at the circuit level to perform more complex computations such as the ones used during decision-making and exploration. This endeavor requires the use of a richer and dynamic description and analysis of behavior (Gomez-Marin et al. 2014). We used a combination of computer vision (Anderson and Perona 2014) and other quantitative, automated systems such as capacitance-based behavioral assays (Itskov et al. 2014) with internal state and genetic manipulations to characterize and identify the behavioral changes allowing the animal to achieve homeostasis. It is interesting to consider that while we identify an important role of OR-mediated olfaction in nutrient decision-making, this would not have been possible using end-point analyses, as the animal manages to compensate for its sensory challenge using alternative means. The use of dynamic, quantitative descriptions of complex behavior therefore enables neuroscientists to decompose these into discrete processes, opening up the possibility to go beyond assigning circuits and molecules to general behaviors to start explaining how they act to control the generation of complex cognitive processes.

2.5 Materials and Methods

2.5.1 Drosophila *stocks, genetics and rearing conditions*

Unless stated otherwise all experiments were performed with *Canton S* female flies. *Canton S* flies were obtained from the Bloomington stock center. $Orco^{1/1}$ flies were a kind gift of Sofia Lavista-Llanos from the Hansson laboratory (Larsson et al. 2004). $Orco^{1/+}$ flies were obtained by crossing *Canton* S virgins with $Orco^{1/1}$ males. $T\beta h^{nM18}$ flies were a kind gift of Scott Waddell (M Monastirioti, Linn, and White 1996). Fly rearing, maintenance, and behavioral testing were performed at 25°C in climate-controlled chambers at 70% relative humidity in a 12-hr-light-dark cycle. All experimental and control groups were matched for age and husbandry conditions.

2.5.2 Media compositions

The standard yeast-based medium (YBM) contained, per liter, 80 g cane molasses, 22 g sugar beet syrup, 8 g agar, 80 g corn flour, 10 g soya flour, 18 g yeast extract, 8 ml propionic acid, and 12 ml nipagin (15% in ethanol) supplemented with instant yeast granules on surface. To ensure a homogenous density of offspring among experiments, fly cultures were always set with 5 females and

3 males per vial and left to lay eggs for 3 days. Flies were reared in YBM until adulthood. Three different types of holidic medium were used as described previously (Piper et al. 2014) using the following formulations: 50S200NYaa (*AA+ rich*), 50S200NHUNTaa (*AA+ suboptimal*) and 50S0N (*AA-)*. Composition of the media are as described in table 1 and supplementary table 1 of (Piper et al. 2014), without food preservatives and only differ in amino acids composition. The proportion of amino acids in 50S200NYaa diet is adjusted to match that in yeast and was considered a rich diet maximizing egg laying (Piper et al. 2014). The detailed holidic media compositions can be found in Table 2.1.

Table 2.1 - Composition of holidic medium

	Ingredient	Stock	Amount per liter
Gelling agent	Agar		20 g
Sugar	Sucrose		17.12 g
Amino acids for 50S200NHUNTaa*	L-isoleucine		1.82 g
	L-leucine		1.21 g
	L-tyrosine		0.42 g
Amino acids for 50S200NYaa*	L-isoleucine		1.16 g
	L-leucine		1.64 g
	L-tyrosine		0.84 g
Metal ions	$CaCl_2.6H_2O$	1000x: 250 g/l	1 ml
	$CuSO_4.5H_2O$	1000x: 2.5 g/l	1 ml
	$FeSO_4.7H_2O$	1000x: 25 g/l	1 ml
	$MgSO_4$ (anhydrous)	1000x: 250 g/l	1 ml
	$MnCl_2.4H_2O$	1000x:1 g/l	1 ml
	$ZnSO_4.7H_2O$	1000x: 25 g/l	1 ml
Cholesterol	Cholesterol	20 mg/ml in EtOH	15 ml
Water	Water (milliQ)	1 liter minus combined volume to be added after autoclaving	
Autoclave 15 min at 120ºC. All additions below should be performed using sterile technique			
Amino acids for 50S200NHUNTaa*	Essential amino acid stock solution	8 g/l L-arginine monohydrochloride 10 g/l L-histidine 19 g/l L-lysine monohydrochloride 8 g/l L-methionine 13 g/l L-phenylalanine 20 g/l L-threonine 5 g/l L-tryptophan 28 g/l L-valine	60.51 ml
	Non-essential amino acid stock solution	35 g/l L-alanine 17 g/l L-asparagine 17 g/l L-aspartic acid sodium salt monohydrate 0.5 g/l L-cysteine hydrochloride 25 g/l L-glutamine 32 g/l glycine 15 g/l L-proline 19 g/l L-serine	60.51 ml
	Sodium glutamate stock solution	100 g/l L-glutamic acid monosodium salt hydrate	15.13 ml
Amino acids for 50S200NYaa*	Essential amino acid stock solution	23.51 g/l L-arginine monohydrochloride 11.21 g/l L-histidine 28.70 g/l L-lysine monohydrochloride 5.62 g/l L-methionine 15.14 g/l L-phenylalanine	60.51 ml

		21.39 g/l L-threonine 7.27 g/l L-tryptophan 22.12 g/l L-valine	
	Non-essential amino acid stock solution	26.25 g/l L-alanine 13.89 g/l L-asparagine 13.89 g/l L-aspartic acid sodium salt monohydrate 30.09 g/l L-glutamine 17.89 g/l glycine 9.32 g/l L-proline 12.56 g/l L-serine	60.51 ml
	Sodium glutamate stock solution	100 g/l L-glutamic acid monosodium salt hydrate	18.21 ml
	Cysteine stock solution	50 g/l L-cysteine hydrochloride	5.28 ml
Base	Buffer	10x: 30 ml/l glacial acetic acid 30 g/l KH_2PO_4 10 g/l $NaHCO_3$	100 ml
Vitamins	Vitamin solution	125x: 0.1 g/l thiamine hydrochloride 0.05 g/l riboflavin 0.6 g/l nicotinic acid 0.775 g/l Ca pantothenate 0.125 g/l pyridoxine hydrochloride 0.01 g/l biotin	14 ml
	Sodium folate	1000x: 0.5 g/l	1 ml
Other nutrients		125x: 6.25 g/l choline chloride 0.63 g/l myo-inositol 8.13 g/l inosine 7.5 g/l uridine	8 ml

* To prepare the 50S200NHUNTaa diet, use the values shaded in blue. To prepare the 50S200NYaa diet, use the values shaded in orange.

2.5.3 Behavioral assays

Groups of 9 to 11 newly hatched (0 – 6 hours old) female flies of the indicated genotypes were transferred to vials containing fresh standard medium (Figure 2.10). Three days after, all vials were transferred to fresh standard medium and 4 males were added to half of the vials to obtain mated female flies. After two more days, all vials were transferred once again to fresh standard YBM. On the sixth day, all vials were transferred to fresh holidic media. Flies were left to feed *ad-libitum* for three days on the holidic media and then tested in the video tracking or flyPAD setups. Single flies were tested in individual arenas that contained two food sources: 18% yeast and 18% sucrose, each in 0.75% (tracking) or 1% (flyPAD) agarose. Flies were individually transferred to the arenas by mouth aspiration and allowed to feed for 1 (flyPAD) or 2 (tracking) hours, except for the tracking experiment with $T\beta h^{nM18}$ flies, which lasted 1 hour. flyPAD data were acquired using the Bonsai framework (Lopes et al. 2015) and analyzed in MATLAB (MathWorks) using custom-written software, as described (Itskov et al. 2014). To avoid patch exhaustion before the end of the tracking assays, each circular patch contained 5 μL of food with a diameter of approximately 3 mm. After each assay, the tracking arenas were washed with soap, rinsed with 70% ethanol, and finally with distilled water.

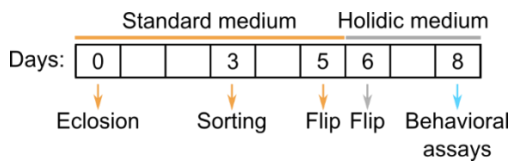

Figure 2.10 – Pre-feeding protocol

Videos that had more than 10% of lost frames (due to technical problems during acquisition) were excluded from the analysis. No further data was excluded. The experiment that compares the conditions *AA+ suboptimal* and *AA-* (results shown in Figures 1-6) was performed 3 times independently, which means that an independent set of individuals (n=15-35, shown in the corresponding figure legend) was reared and tested under the corresponding conditions. The experiment comparing *AA+ rich* vs *AA-* was performed 2 times independently. The experiments comparing $T\beta h^{nM18}$ or *Orco* mutant flies with their corresponding controls were performed once with the sample size indicated in the corresponding figure legend. We confirmed that the claims made in this manuscript held for every experimental replicate. We never tested the same individual more than once.

2.5.4 Behavioral box and arena design

The behavioral arenas for the video tracking (Figure 2.1B) were designed and manufactured in-house using a laser-cutter and a milling machine. Material used for the base was acrylic and glass for the lid. The outer diameter of the arena was 73 mm. The inner area containing food patches was flat and had a diameter of 50 mm and a distance to the lid of 2.1 mm. To allow a top-view of the fly throughout the whole experiment, the outer area of the arena had 10º of inclination (Simon and Dickinson 2010) and the glass lid was coated 10 μL of SigmaCote® the night before the assays. Food patches were distributed in two concentric circles equidistantly from the edge. Furthermore, sucrose and yeast patches were alternated such that from a given food patch, there was at least one adjacent yeast and one adjacent sucrose patch. The radius of each food patch was approximately 1.5 mm. The minimum distance between the centers of two adjacent food patches is 10 mm. White LEDs 12V DC (4.8 watt/meter), were used for illumination of the arenas. They were placed under the arenas, as backlight illumination and on the walls of the behavioral box, surrounding the arenas, as shown in Figure 2.1A. A white cardboard arch was used to improve illumination to reflect light towards the arenas (Figure 2.1A). Three fly arenas were recorded simultaneously from the top using a video camera (Genie HM1400 camera, Teledyne DALSA; frame acquisition rate: 50 fps) connected to a desktop computer using a Gigabit Ethernet connection.

2.5.5 Tracking algorithm

Body centroid positions and major axis of the fly body in each frame were extracted using custom off-line tracking algorithms written in Bonsai (Lopes et al. 2015) and Matlab (Mathworks). The arena diameter in the video was measured to find the correspondence between pixels in the video and mm in the real world (1 pixel = 0.155 mm). The typical length of the major axis of the fly body in a video was 19 pixels (~3mm). Video acquisition was made with slight overexposure to obtain a strong contrast between the fly and the arena. Since the fly body was the darkest object in the arena, a pixel intensity threshold was used to obtain the centroid and orientation of the fly blob. The head position was extracted using custom MATLAB (Mathworks) software. Head position in the first frame was manually selected. From there on, the head position is automatically propagated to the consecutive

frames using a proximity rule (Gomez-Marin, Stephens, and Louis 2011). This rule, however, does not hold during a jump of the fly. Therefore, in addition to the proximity rule, for the intervals in-between jumps, the head position was automatically corrected using the fact that flies walk forward most of the time. Manual annotation of 510 inter-jump-intervals revealed that 98% were correctly classified.

2.5.6 Behavioral classification

Raw trajectories of head and body centroids were smoothed using a Gaussian filter of 16 frames (0.32 s) width. The width was chosen empirically by comparing the raw and smoothed tracks. The speed was measured from the smoothed coordinates by calculating the distance covered from the current frame and the next frame, divided by the time between them (0.02 s). Similarly, the angular speed was measured by calculating the difference between the heading angle from the current frame and the next frame, divided by the time between them. The heading angle for this calculation was obtained from the head and tail smoothed centroids. Walking and non-walking instances were classified applying a 2 mm/s threshold in the head speed, based on the distribution of head speed for AA-deprived flies in Figure 2.11A and previous studies (J.-R. Martin 2004; Robie, Straw, and Dickinson 2010). The head speed used was also smoothed using a Gaussian filter of 60 frames (1.2 s) to avoid rapid changes in classification around the thresholds. Sharp turns were classified when a local maximum in the angular speed exceeded a 125º/s threshold, as long as the body centroid speed was below 4 mm/s. A wider Gaussian filter (width of 2.4 s) was applied to the head speed to classify resting bouts, using a threshold of 0.2 mm/s. The remaining events during the non-walking segments that were not classified as resting were classified as micromovements.

2.5.7 Food encounters, micromovements, and visits

Manual annotation of 107 feeding events showed that when the head position was at 3 mm or less from the center of the food patch, flies were already close enough to have leg contact. Initially, *encounters* with a food patch were defined as the moments in which the fly crossed this 3 mm distance threshold. To avoid misclassifying the transient head movement associated with grooming or feeding around this threshold as new encounters, consecutive encounters were merged when the total displacement of the head in any direction was lower or equal than to 2 pixels (0.31 mm) during the time elapsed in-between the encounters. From each feeding event, the distance from the head of the fly to the center of the patch was also captured. Since 95% of the first proboscis extensions happened below 2.5 mm, this was the selected distance threshold to define *yeast* and *sucrose micromovements* (Figure 2.11D). In this way, food micromovements were defined as the time in which flies were classified in a micromovement (see definition in previous section) and their head was simultaneously inside a circle of 2.5 mm around the food patch (see gray dashed line in Figure 2.1D inset). The 2 pixels displacement rule used in the definition of encounters was also applied here to avoid definitions of false new micromovements. A *visit* was defined as a series of consecutive food micromovements (already corrected for small displacements) in which the head distance to the center of the food patch was never larger than 5 mm during the time elapsed in-between the food micromovements (Figure

2.1D inset). 5 mm is the maximum radius of non-overlapping circles around the food patches (see gray dashed line in main trajectory of Figure 2.1D). This 5 mm threshold was also used to merge consecutive encounters (consecutive encounters were merged if the head distance to the center of the food patch was never larger than 5 mm during the time in-between encounters). In this way, for every visit there is an encounter, but there can be an encounter and no visit if the fly does not stop at the food patch (food micromovement).

2.5.8 Exploitation, exploration and locomotor activity parameters

All of these parameters, unless specified otherwise, were calculated for each fly and for the whole duration of the assay.

1. **Yeast** (or sucrose) **micromovements**: Events in which the fly was micromoving (0.2 mm/s < head speed < 2 mm/s, see *Behavioral classification* section for details) on the food patch (head position ≤ 2.5 mm).
2. **Total duration of yeast** (or sucrose) **micromovements (min)**: Sum of the durations of all yeast (or sucrose) micromovements. Initially calculated in frames and converted to minutes by dividing by the frame rate (50 frames per second) and dividing by 60.
3. **Fraction of yeast non-eaters**: Number of flies with a total duration of yeast visits lower than 1 minute divided by the total number of flies in that internal state condition.
4. **Coefficient of variation:** Standard deviation divided by the mean of the total duration of yeast micromovements for each internal state condition.
5. **Cumulative time of yeast micromovements (min)**: Cumulative sum of frames in which the fly was in a yeast micromovement, converted to minutes as described for parameter 2.
6. **Yeast** (or sucrose) **visits:** Series of consecutive food micromovements in which the head distance to the center of the food patch was never larger than 5 mm during the time elapsed in-between the food micromovements.
7. **Total duration of yeast visits (min)**: Sum of the durations of all yeast visits. Durations of visits were calculated similarly to parameter 2.
8. **Number of yeast encounters**: Sum of all yeast encounters.
9. **Rate of yeast encounters**: Sum of all yeast encounters divided by the time spent walking outside the food patches.
10. **Probability to engage a yeast patch**: Number of encounters with yeast that contained at least one yeast micromovement, divided by the total number of yeast encounters.
11. **Average duration of yeast visits (min)**: Sum of all the durations of yeast visits divided by the total number of yeast visits.
12. **Number of yeast visits**: Sum of all yeast visits.
13. **Rolling median of total duration of yeast visits (min):** Sum of the duration of all yeast visits that occurred within a 5 minute sliding window with a step of 4 minutes.
14. **Latency to long yeast visit (min)**: Time elapsed from the beginning of the assay until the fly engages in a visit which is at least 30 seconds long.

15. **Average minimum distance from yeast (mm)**: Average of the minimum head distance to the center of the yeast patch for each visit, across all yeast visits.
16. **Average area covered during yeast visits (pixels):** Average across all yeast visits of the number of different pixels covered by the head of the fly during each yeast visit.
17. **Speed$_{body}$ during yeast visits (mm/s)**: Average of body centroid speed across all frames in which the fly was inside a yeast visit. Calculation of speed was as described in the *behavioral classification* section and then smoothed using a Gaussian filter of 60 frames (1.2 s).
18. **Angular speed during yeast visits (º/s)**: Average of angular speed across all frames in which the fly was inside a yeast visit. Calculation of angular speed was as described in the *behavioral classification* section.
19. **Transition probability to a distant yeast patch**: Number of visits to a distant yeast patch divided by the total number of yeast visits. Visits to distant yeast patches were of two kinds: either the distance between the previous and current patch centers was > 16 mm or the distance from the fly head to the center of the previous patch was > 16 mm at any point during the inter-visit-interval. Only transitions between *visited* yeast patches were considered.
20. **Transition probability to an adjacent yeast patch**: Number of visits to an adjacent yeast patch divided by the total number of yeast visits. Two patches were defined as adjacent if the distance between their centers was ≤ 16 mm. Only transitions in which the distance from the fly head to the center of the previous patch was ≤ 16 mm during the whole inter-visit-interval were considered. Otherwise, the transition was classified as to a distant yeast patch (see parameter 19). Only transitions between *visited* yeast patches were considered.
21. **Transition probability to the same yeast patch**: Number of visits to the same yeast patch divided by the total number of yeast visits. Visits to the same yeast patch were those in which the previous visit happened in the same patch as the current visit. Only transitions in which the distance from the fly head to the center of the previous patch was ≤ 16 mm during the whole inter-visit-interval were considered. Otherwise, the transition was classified as to a distant yeast patch (see parameter 19). Only transitions between *visited* yeast patches were considered. The values of the transition probabilities depicted as pie charts in Figure 2.5A-C are the medians shown in panels D-F scaled so they sum to 100%.
22. **Distance traveled to next yeast visit (mm)**: Average distance covered from the end of a visit to any food patch (yeast or sucrose) to the beginning of the next visit to a yeast patch.
23. **Yeast quartiles**: The sum of the durations of all the yeast micromovements from the latency point (see parameter 14) onwards, was considered as 100% of yeast time, for a given fly. First yeast quartile (Q1) was the time elapsed between the latency point and the 25% of yeast time for that fly. Q2 was the time elapsed between 25% and 50% of yeast time for that fly. In the same way, Q3 went from 50% to 75% and Q4 from 75% to 100% of yeast time for that fly.
24. **Speed outside food patches (mm/s)**: Similar to parameter 17, but for all frames in which the fly was not engaged in a food visit. In Figure 2.7G, this parameter was calculated only for the latency period (parameter 14).

2.6 Acknowledgements

We thank Sofia Lavista-Llanos (Hansson Lab), Scott Waddell and Carolina Rezával (Goodwin Lab) for sharing fly stocks. Stocks obtained from the Bloomington Drosophila Stock Center (NIH P40OD018537) were used in this study. We thank Célia Baltazar for technical assistance in running some of the tracking and flyPAD experiments; Pavel Itskov for assistance with analysis code for flyPAD data; Ana Machado for contributions to early phases of this project; Alex Gomez-Marin, Gonçalo Lopes, José Cruz and Ricardo Ribeiro for help in improving the tracking algorithms; and FABLAB-EDP (http://fablabedp.edp.pt) for kindly providing access to the milling machine used for the arenas manufacturing. We also thank Christian K. Machens, Gonzalo G. de Polavieja, Samuel SJ Walker and members of the Behavior and Metabolism laboratory for helpful discussions and comments on the manuscript, as well as Gil Costa for his help with illustrations.

2.7 Additional information

2.7.1 Funding

This project was supported by the Portuguese Foundation for Science and Technology (FCT) grant PTDC/BIA-BCM/118684/2010 and the Human Frontier Science Program Project Grant RGP0022/2012 to C.R. and A.A.F., V.M.C.-C. was supported by the MIT-Portugal Program, FCT fellowship SFRH/BD/51113/2010. The Champalimaud Neuroscience Programme is supported by the Champalimaud Foundation.

2.7.2 Author contributions

Initial conceptual and technical development of the project: VMC, AAF and CR; Supervision of the project: CR; Performed experiments: VMC; Performed data analysis and interpretation: VMC and CR; Wrote the manuscript: VMC and CR.

2.8 Supplementary figures

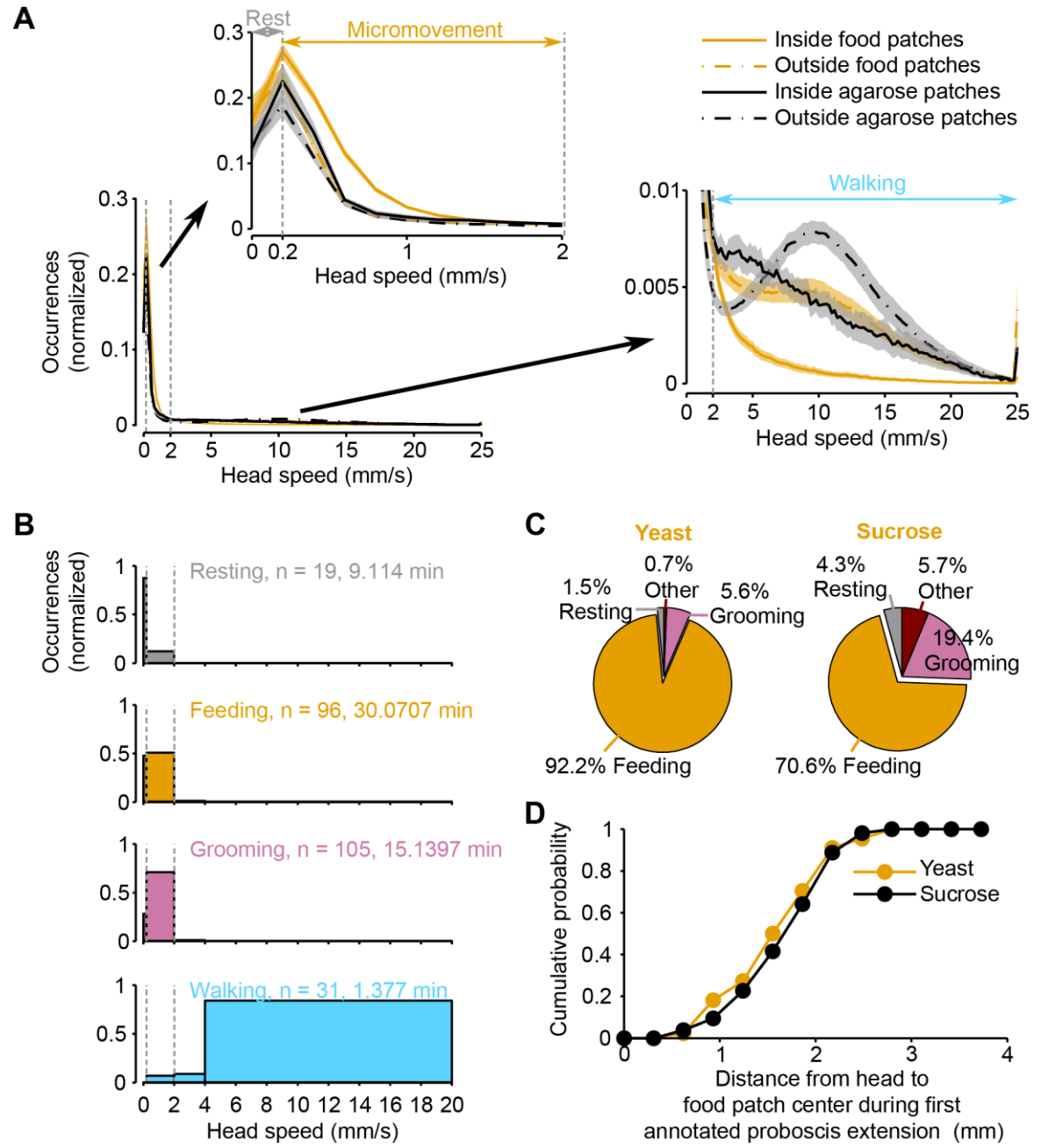

Figure 2.11 – Ground truthing of behavior

(A) Normalized histogram of head speed of amino acid-deprived mated females (AA- diet) from two independent video tracking experiments: orange lines represent data obtained from an assay in which the arena contained 9 yeast and 9 sucrose patches; black lines represent data obtained from an assay in which the arena contained 18 agarose patches (no food). For each experiment, the speed was calculated for periods inside and outside food patches. Vertical dashed gray lines in main panel and insets indicate the speed thresholds used to classify resting (0-0.2 mm/s), micromovement (0.2 - 2 mm/s) and walking (> 2mm/s). Insets are a zoom-in of the indicated regions of the main histogram. Black and orange lines indicate mean and shaded area s.e.m. (B) Normalized histogram of the head speed displayed during manually annotated behaviors. (C) Proportion of manually annotated behaviors observed during yeast (left) or sucrose (right) micromovements. (D) Cumulative histogram of head positions during the first annotated proboscis extension in a yeast patch.

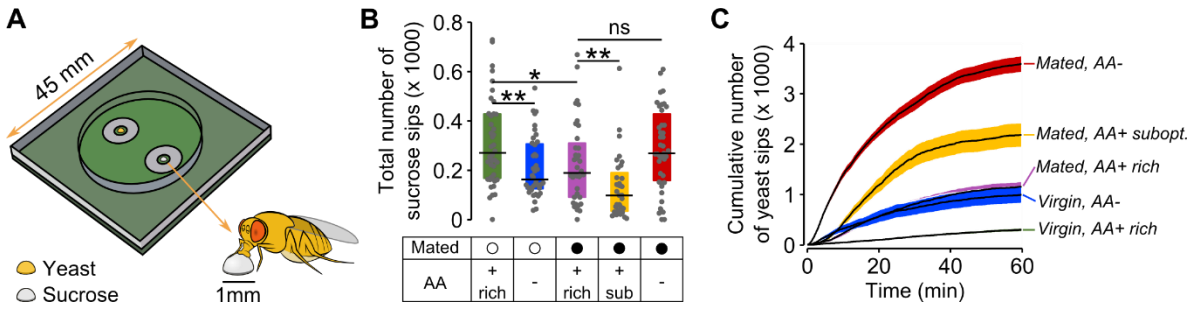

Figure 2.12 – flyPAD setup, sucrose sips and yeast sips dynamics

(A) Schematic of flyPAD arena, adapted from (Itskov et al. 2014). (B) Effect of internal states on the number of sucrose sips. Experimental groups are: Mated (filled circles) and virgin (open circles) females pre-fed 3 types of holidic media: AA+ rich, AA+ suboptimal and AA-. The concentration of yeast and sucrose in the food patches was the same used in the video tracking assay. (C) Cumulative number of yeast sips of flies in the five internal state conditions indicated. Line represents the mean and the shading the s.e.m.

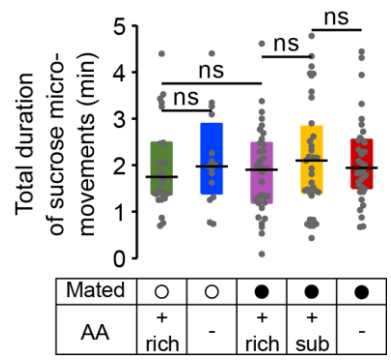

Figure 2.13 – Sucrose micromovements

Effect of internal state on the total duration of sucrose micromovements obtained from the video tracking assay.

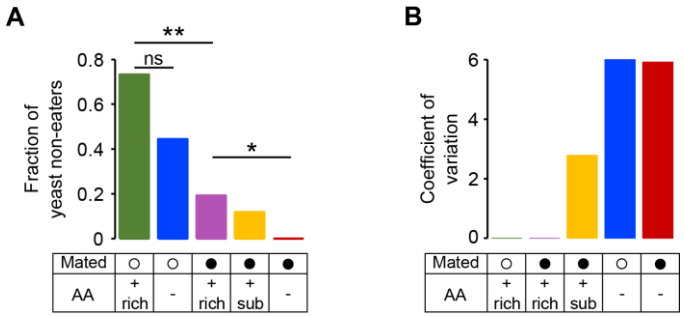

Figure 2.14 – Fraction of yeast non-eaters and coefficient of variation for yeast micromovements

(A) Effect of internal states on the proportion of yeast non-eaters. A yeast non-eater is a fly for which the total duration of yeast visits was lower than 1 minute. Significance was tested by a 2 x 2 Fischer's exact test using the modified Wald method (Agresti and Coull 1998) with Bonferroni correction. (B) Effect of internal states on the coefficient of variation for yeast micromovements (CV = SD/mean).

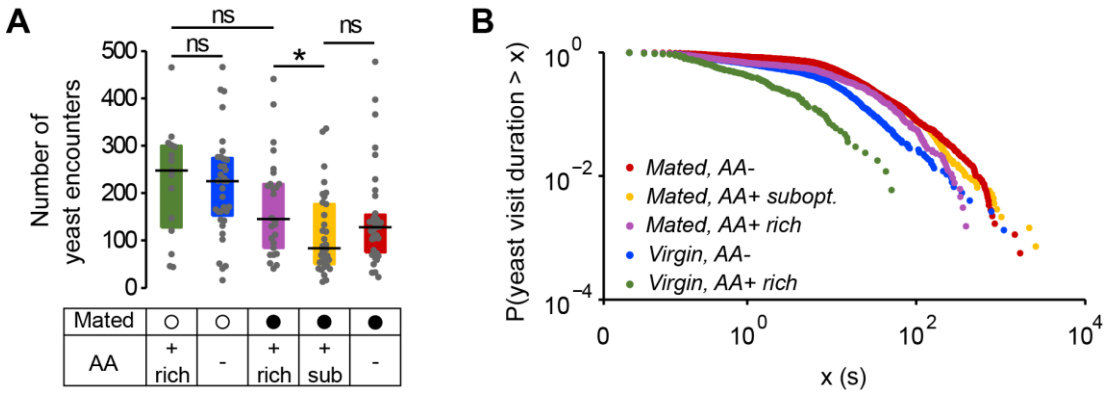

Figure 2.15 – Yeast encounters and probability of leaving

(A) Effect of internal state on the absolute number of yeast encounters. (B) Complementary cumulative distribution function for yeast visit duration. Single dots represent one yeast visit. All yeast visits belonging to all animals of the same internal state condition were pooled, ranked and plotted in the same color as indicated in (Clauset, Shalizi, and Newman 2009).

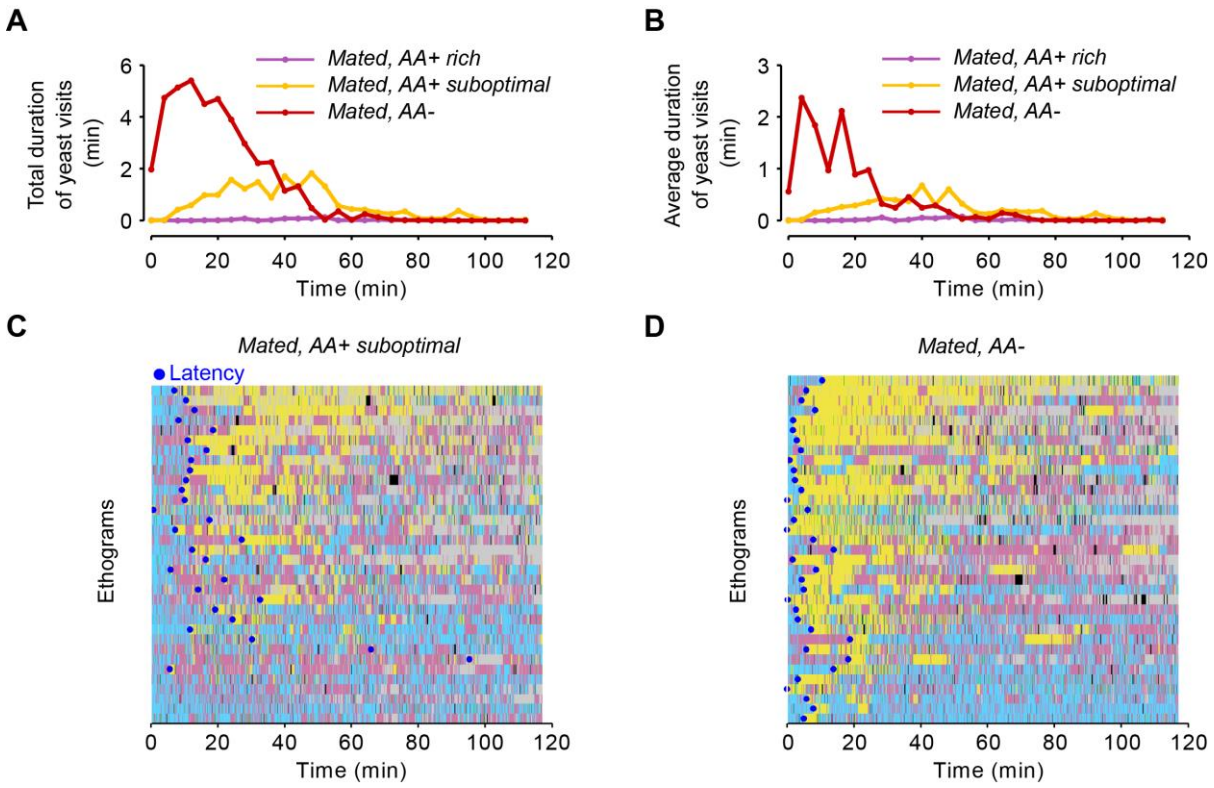

Figure 2.16 – Yeast visits dynamics and latency

(A, B) Rolling median of the total duration of yeast visits (A) and average duration of yeast visits (B) using a 5 minute window and a step of 4 minutes for flies fed a rich diet (purple), suboptimal diet (yellow), and AA-deprived flies (red). (C, D) Ethograms from Figure 2.2D showing the latency to engage in the first "long" (≥ 30s) yeast visit for each fly of the indicated condition as a blue dot.

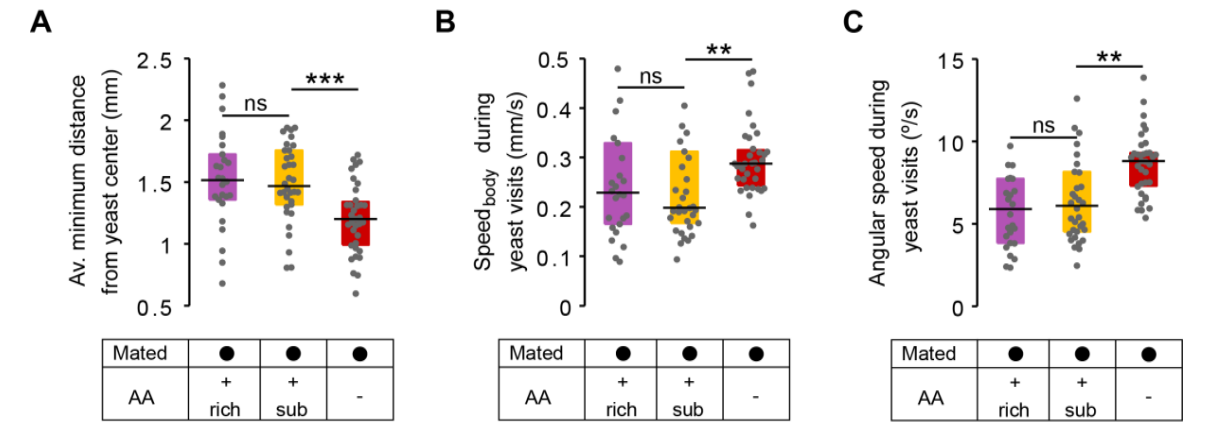

Figure 2.17 – No effect on local exploration of yeast patches for flies pre-fed a suboptimal diet

(A) Effect of AA challenges on the average minimum distance to the center of yeast patches, during a yeast visit. (B) Effect of AA challenges on the body centroid speed, during a yeast visit. (C) Effect of AA challenges on the angular speed, during a yeast visit.

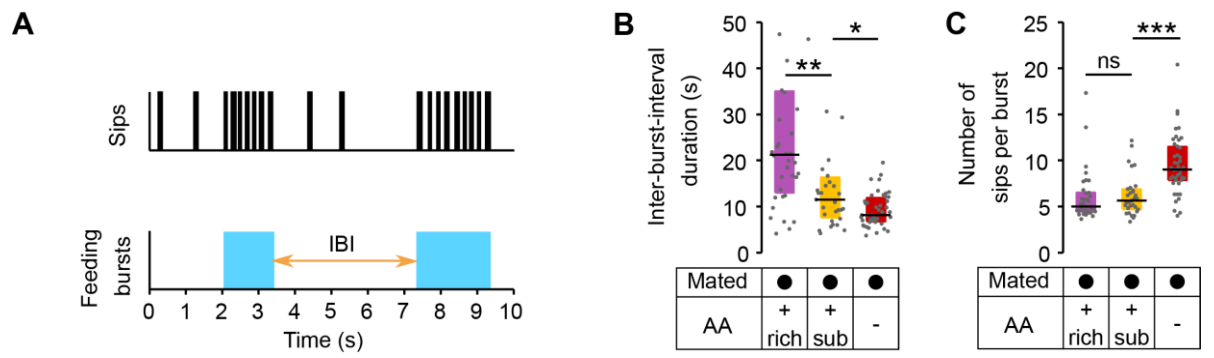

Figure 2.18 – Modulation of yeast feeding program microstructure by AA challenges

(A) Schematic of feeding program microstructure. Two components of the feeding microstructure can be modulated to reach protein homeostasis: the number of sips inside each feeding burst (blue shading) and the inter-burst interval (IBI). (B) Mean inter-burst-interval duration. (C) Mean number of yeast sips inside a feeding burst.

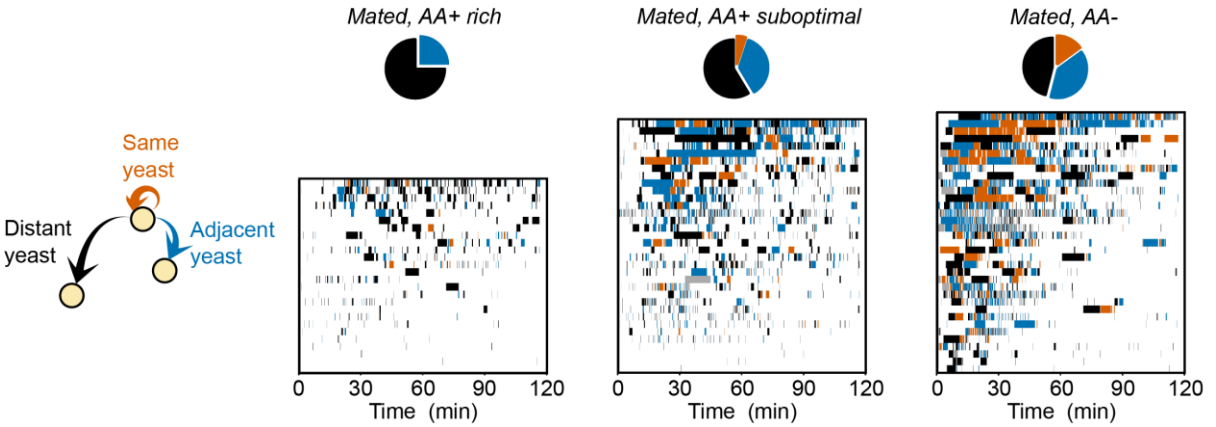

Figure 2.19 – Dynamics of yeast-yeast transitions in single flies

Ethograms showing the yeast visits for each fly (each row is a single fly) along the 120 min of the video tracking assay, for the indicated condition. Colors indicate if the food patch previous to every yeast visit was the same (orange), an adjacent (blue) or a distant one (black). Pie charts indicate the accumulated median transition probabilities by the end of the assay, for the indicated condition (same as Figure 2.5A-C).

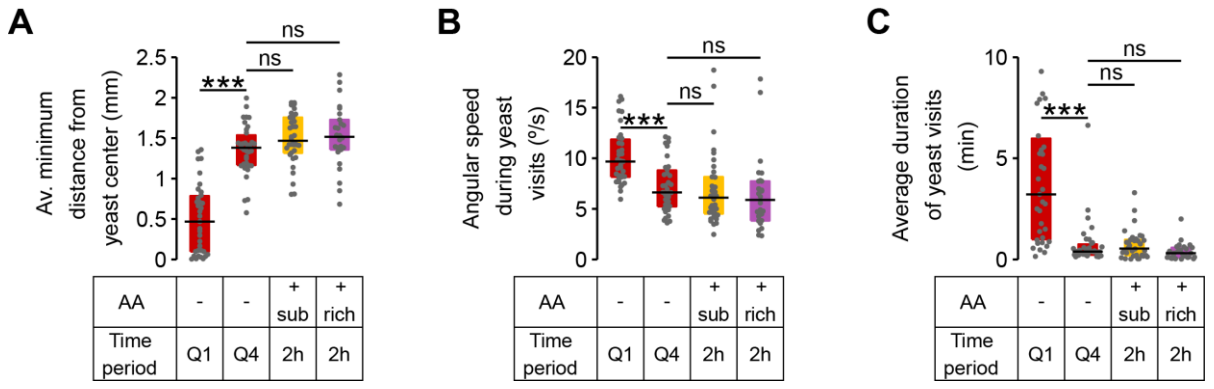

Figure 2.20 – Exploitation parameters in AA-deprived flies revert back to fully-fed values

(A-C) Exploitation parameters from first yeast quartile (Q1) and fourth yeast quartile (Q4) of AA-deprived mated females compared to the values observed in flies pre-fed a rich and a suboptimal diet along the 2 hours of the video tracking assay. (A) Average minimum distance of the head to the center of the yeast patch, (B) angular speed, during yeast visits. (C) Average duration of yeast visits. *ns*, not significant ($p \geq 0.05$), ***$p < 0.001$, significance was tested by Wilcoxon rank-sum test with Bonferroni correction.

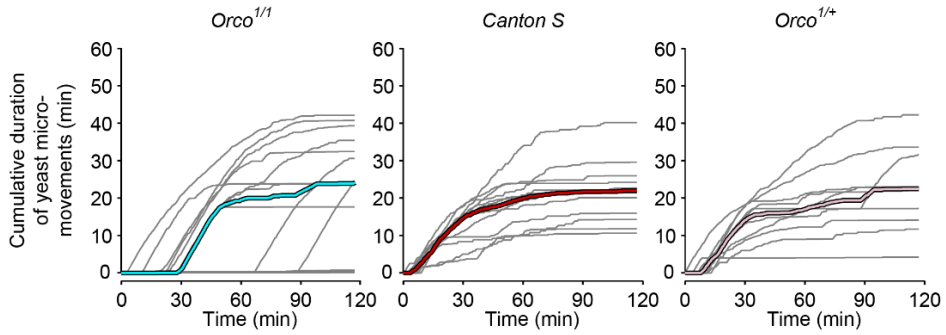

Figure 2.21 – Yeast dynamics of Orco mutant flies

Cumulative duration of yeast micromovements. Gray lines correspond to single flies. Thick colored lines indicate median.

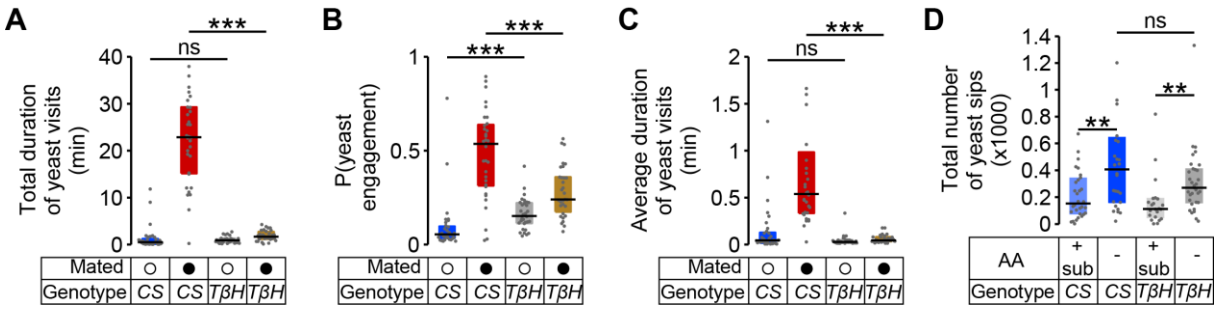

Figure 2.22 – Octopamine mediates postmating response to yeast

(A-C) Effect of *TβH* mutation on the postmating change in foraging parameters, obtained using the video tracking setup: (A) total duration of yeast visits, (B) probability of engaging a yeast patch and (C) average duration of yeast visits for AA-deprived *Canton S* and $T\beta h^{nM18}$ females. (D) Effect of *TβH* mutation on the increase of yeast sips after AA deprivation in virgin females, using the flyPAD assay. *ns*, not significant ($p \geq 0.05$), *$p < 0.05$, **$p < 0.01$, ***$p < 0.001$, significance was tested by Wilcoxon rank-sum test with Bonferroni correction.

Chapter 3. Behavioral setup and pre-analysis algorithms

In this chapter, I describe in further detail the design and characteristics of the tracking setup and the behavioral arenas; I also describe the logic behind the algorithms used to acquire the information about the fly's position and orientation, as well as other important algorithms for the automatic detection of food patches in the arena and for handling the information about the different experimental conditions of each individual fly such that data retrieval during the data analysis phase was easy and practical.

3.1 Behavioral setup

Four independent tracking setups containing 3 behavioral arenas each were built using the tools provided in the workshop of the Champalimaud Center for the Unknown and the prototyping machines in FABLAB EDP (http://fablabedp.edp.pt). For the box, I used 2 mm x 2 mm aluminum rails (Figure 3.1A). The video cameras used were Genie HM1400 series, resolution: 1400 x 1024, maximum framerate at full resolution: 75 fps, pixel size: 7.4 μm x 7.4 μm, CMOS sensor with size 10.40 mm x 7.60 mm (12.88 mm diag.), output: gigabit Ethernet. Lens: Óptica Cinegon 1.9/10 mm 1", Serie compact 400-1000nm. The videos captured the behavior of the flies at a frame rate of 50 Hz with a resolution of 1400 x 478.

The arenas were designed in Google SketchUp (Figure 3.1B) and had a modular design, such that the inner area could easily be removed and replaced with different designs of the food patch distribution (Figure 3.1B and Figure 3.1C inset). The outer area was designed with a slope of 10º to prevent the flies from walking on the ceiling and thus to allow for a top-view of the fly throughout the whole experiment (Simon and Dickinson 2010). In order to keep the arenas in a fixed position with respect to the cameras and to facilitate the insertion of the flies at the beginning of the experiment, I designed a support where all the arenas and the glass lid could slide in (Figure 3.1C, piece in gray). However, bringing this design to real life proved to be difficult and expensive, so instead, I used the FABLAB EDP facility to create 3D-printed corners that fulfilled the same purpose and were both cheap and easy to manufacture (Figure 3.1D). The outer piece or base of the arenas was created in the milling machine, also in FABLAB EDP (Figure 3.1E). After this, it was necessary to polish them carefully using a file and sandpaper. The final product is shown in Figure 3.1F and the final assembly in Figure 3.1G. The details of the food patch distribution used in the experiments are shown in Figure 3.2.

To provide illumination I added two sets of white LEDs: one below the arenas, covered by a white acrylic sheet (backlight illumination) and one on all four walls of the box (Figure 3.1A). A white cardboard arch was used to improve illumination to reflect light towards the arenas.

The videos were acquired with high overexposure to reduce the size of the video file and facilitate the detection of the fly as the blob with highest contrast against the white background.

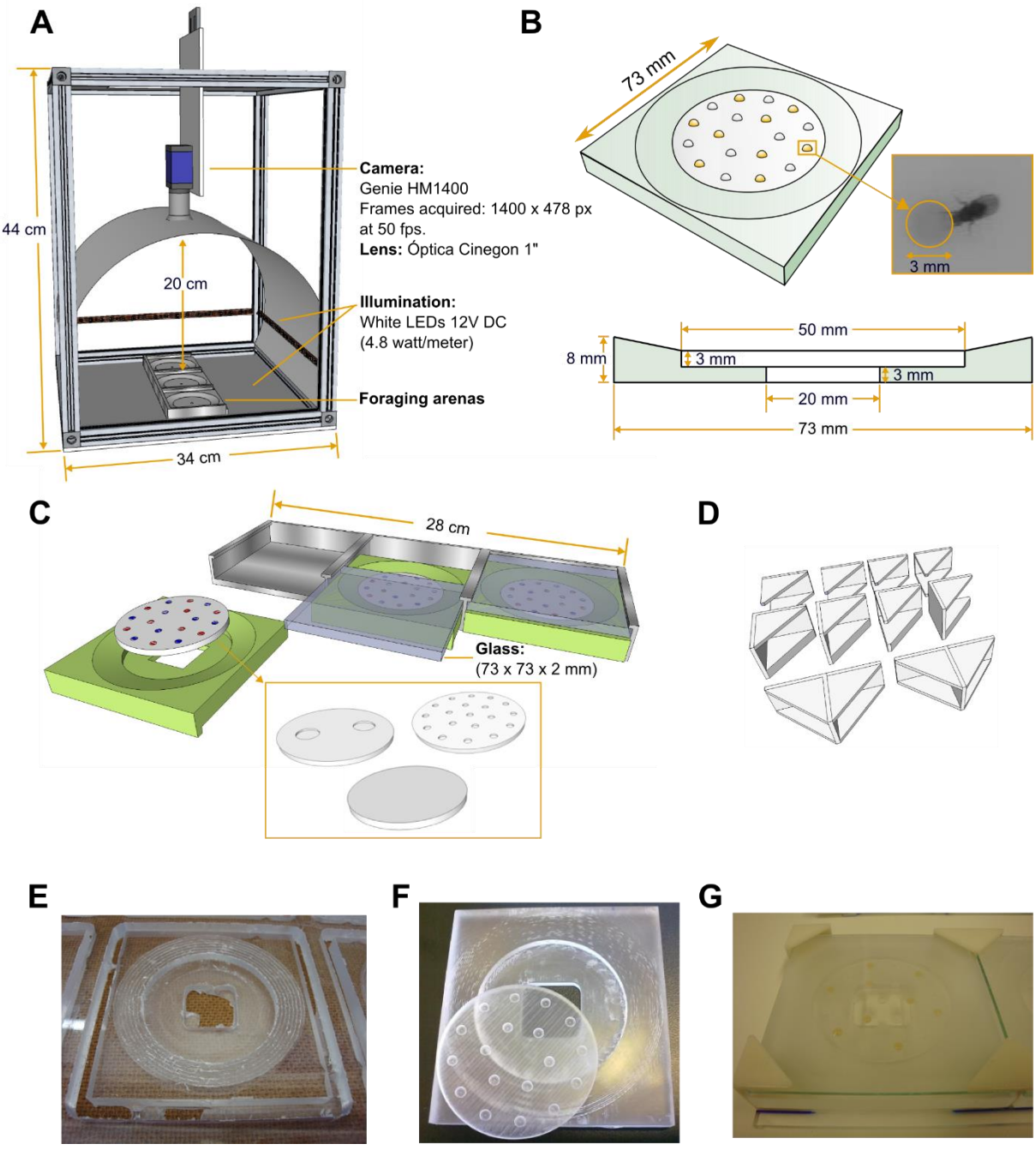

Figure 3.1 – Foraging setup and arenas manufacturing

(A) Schematic of the image-based tracking setup. A video camera is placed on top of three foraging arenas that contain a single fly each. (B) Foraging arena with 9 sucrose and 9 yeast food patches (top). Side view and dimensions of the foraging arenas (bottom). (C) Three arenas fit in one support to maintain a fix position with respect to the camera. Each arena is composed by two pieces: a base and an inner dish that can have different distribution of locations for the food patches. All arenas are covered with glass lids. (D) 3D-printed corners that act as support instead of the one depicted in C (gray). (E) Arenas as they come out of the milling machine. (F) Arenas after polishing. (G) Final arena assembled into the support and covered with the glass lid.

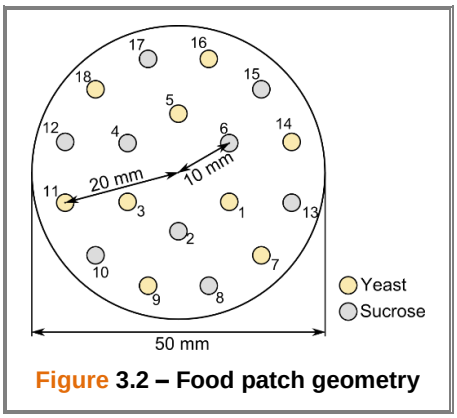

Figure 3.2 – Food patch geometry

3.2 Automatic detection of food patch positions

Monitoring the activity of the fly with respect to the food requires that the position of each one of the 18 spots is determined accurately. Therefore, I developed a food patch detection algorithm that uses the information of a predefined geometry template and built-in machine-vision algorithms to obtain the position of the spots in the arena in an automated way.

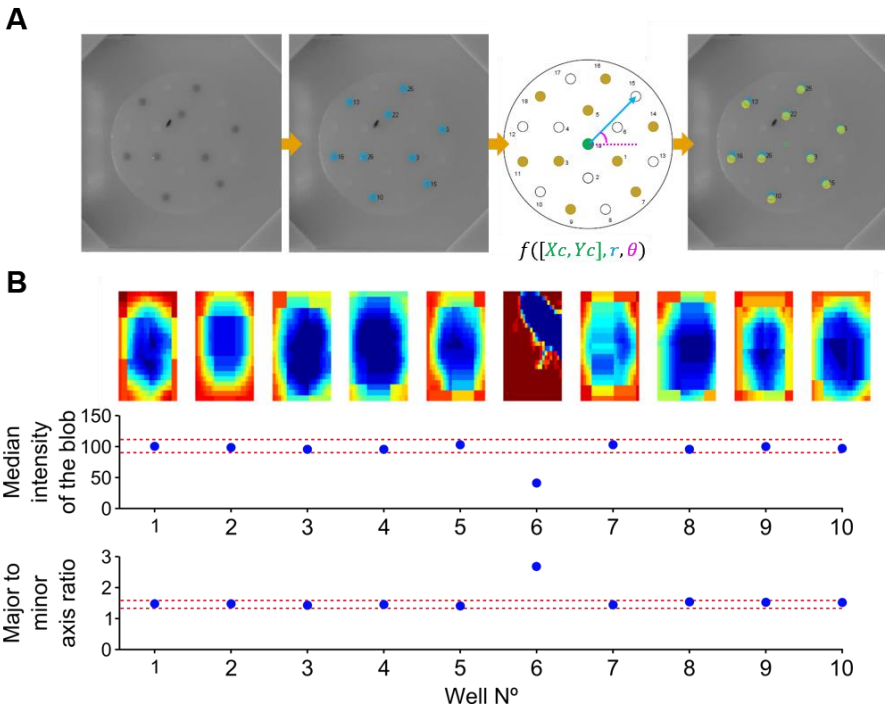

Figure 3.3 – Automatic detection of food patch position

(A) From left to right: Raw image from the arena with the food patches and the fly; automatic detection of yeast spots based on contrast and circular shape using circular Hough transform (blue circles); predefined spot positions template is a function of the center of the arena *[Xc,Yc]*, the distance from the center to the outer patches *r*, and the rotation angle θ; superposition of the predefined template (in yellow circles) over the detected yeast spots (blue circles). (B) Close up to detected yeast spots. Hot colors indicate low pixel intensity. In this particular example, the fly erroneously detected as a food patch, but both its median intensity and its ellipsoid shape are outliers and are used to distinguish it from the yeast patches.

Figure 3.3A displays the main sequence of steps in this algorithm: first, high-contrast circular shapes are automatically detected using the circular Hough transform (built-in MATLAB function *imfindcircles*), then, the geometry template is superimposed to the detected circles and the parameters and 3 parameters are iterated to reach the smallest distance between corresponding patch centers: the center of the arena, the outer radius and the rotation angle. In some occasions, the fly was detected as a high-contrast circular shape as well, or the fly was on top of one of the spots. These cases were identified by detecting a simultaneous outlier in both the median intensity of the objects detected and the major-to-minor axis ratio, as shown in Figure 3.3B.

3.3 Tracking algorithm

We developed a simple tracking algorithm in MATLAB (Mathworks) that generated as output the body centroid, the major axis length and the orientation of the fly blob (Figure 3.4). To focus the analysis on the region of interest, we applied a mask to the raw image; then, a simple threshold was enough to isolate the fly as the blob of interest since there was only one fly per arena. Once isolated, a set of features characterizing that blob such as centroid, orientation, area, major and minor axis length were obtained using MATLAB's built-in function *regionprops*.

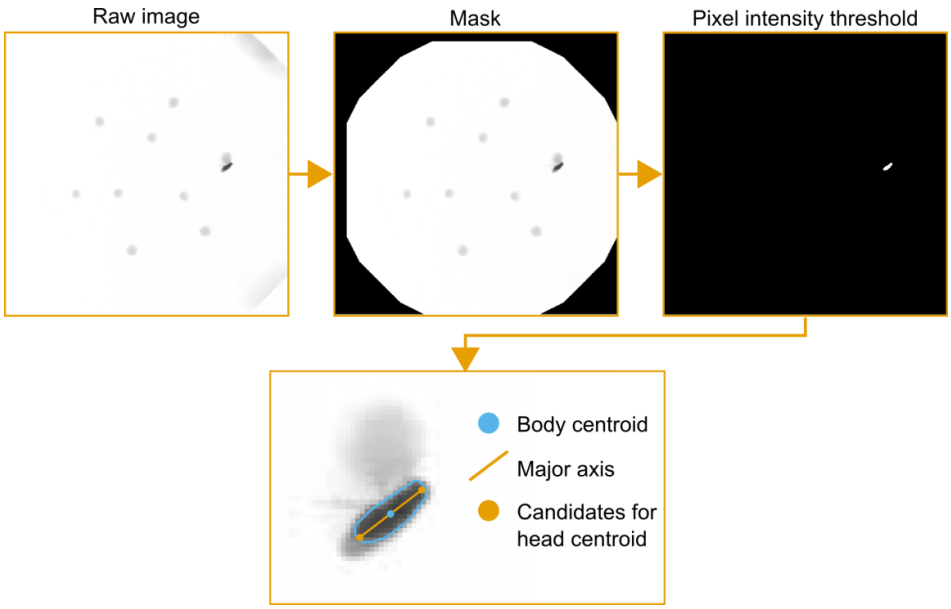

Figure 3.4 – Main steps of tracking algorithm

The main steps of the tracking algorithm are: 1) a mask is applied to the raw image of the arena and the fly to limit the analysis on the region of interest. 2) A pixel intensity threshold isolates the fly as the darkest object on the arena. 3) A blob analysis using the MATLAB's built-in function *regionprops* provides the centroid, orientation and major axis length of the identified blob.

To avoid confusing small dirt as flies, we also set a minimum threshold on the blob area of 20 pixels and selected the largest blob after the threshold was applied. Since the most time-consuming step of the tracking algorithm was the frame reading step, we added a line of code to load 500 frames simultaneously into memory, such that the subsequent processing of those frames was much faster.

3.3.1 *Implementation of tracking algorithm in MATLAB*

Table 3.1 shows the tracking code written in MATLAB for the left arena.

Table 3.1 – Tracking algorithm in MATLAB (example for left arena)

```
% ------------------------------------------------------------------------
% Code to track a single fly (in multiple arenas) body position to have
% kinematic quantification of 2D-translation
% in the 2-choice multiple-spot feeding assay of Veronica (Ribeiro lab)
% by Veronica Corrales-Carvajal, Teresa Montez, José Cruz and
% Alex Gomez-Marin, Nov 2013
% ------------------------------------------------------------------------

clear
close all
format compact

videoPath = 'C:\Users\Public\Videos\Recordings Fly Tracker Prject\Exp 3\';
param.arenaThreshold=130;

Filenames={...
'0003A03R05Cam03P0WT-CantonS.avi';...
'0003A03R05Cam04P0WT-CantonS.avi';...
};

for lfilename=1:length(Filenames)
    filename = Filenames{lfilename};
    param.filename=filename;

    % data file (directly from video)
    VideoRaw=VideoReader([videoPath filename], 'Tag', 'My reader object');
    load('mask.mat');

    fps=VideoRaw.FrameRate;
    maxFrame=VideoRaw.NumberOfFrames;

    % select initial and final frames (and time coarsening, if necessary)
    iniFrame=1; %
    finalFrame=maxFrame;
    cgTime=1; % we do not skip frames
    param.Finalframe=finalFrame;
    param.cgTime=cgTime;

    param.frameH=VideoRaw.Height-15;
    param.frameWL=floor(VideoRaw.Width/3)-10;%Width of left arena

    % and where I will save all the position data
    frames2analyse=iniFrame:cgTime:finalFrame;
    FlytracksL=nan(length(frames2analyse),6);

    % JAC's code
    MAX_FRAME = 500;
    count = MAX_FRAME;
    % ----
    frameCount=0;
    for lframe=frames2analyse
        frameCount=frameCount+1;
        %% Reading frame %% --> JAC's code.
        if( count == MAX_FRAME )
            if (lframe+count-1)<finalFrame
                flymoviedataBatch = read(VideoRaw,...
                    [lframe lframe+count-1]);
                count = 1;
            else
                flymoviedataBatch=read(VideoRaw,[lframe finalFrame]);
                count=1;
            end

        end
        i500 = flymoviedataBatch(:,:,1,count);
        count = count + 1;

        %% Thresholding Fly %%
        clear flyData flyshape
```

```
        flyData = not(im2bw(i500, param.arenaThreshold/255)) * 255;
        flyshape=uint8(flyData).*mask;

        for arena=1%:3
            if arena==1
               yCrop=1; yCrop2=param.frameH; xCrop=1;xCrop2=param.frameWL;
            % write here the cropping values for the other arenas
            end
            %% crop it to the arena-of-interest reference frame
            i=flyshape(yCrop:yCrop2,xCrop:xCrop2);

            %% Extracting Blob properties
            % count objects and properties necessary
            [L,numobj] = bwlabel(i,8);
            regprops=regionprops(L,'Centroid','Area','Orientation',...
                'MajorAxisLength','MinorAxisLength');
            % and keep the largest dark-enough object,
            % hoping in this case it is the fly
            bigobject1=find([regprops.Area]==max([regprops.Area]));
            Arees0=[regprops.Area];

            % and set a threshold in case the animal disappears,
            % not to track a small dirt
            Athr=20; % NOTE: HEURISTIC VALUE
            % (we do not need it if the fly does not ever leave the arena)
            if Arees0(bigobject1)>Athr
                bigobject=bigobject1(1);
                centr=regprops(bigobject).Centroid;
                % the lovely centroid locations
                xc=centr(1);
                yc=centr(2);
                or=regprops(bigobject).Orientation;
                MajAx=regprops(bigobject).MajorAxisLength;
                MinAx=regprops(bigobject).MinorAxisLength;
                A=regprops(bigobject).Area;
            else % we could skip if there is always a large enough fly
                xc=NaN; yc=NaN; xrh=NaN; yrh=NaN; xrt=NaN; yrt=NaN;
            end

            %% Saving all parameters in separate for each arena %%
            if arena==1
                FlytracksL(frameCount,:)=[xc yc or MajAx MinAx A];
            end
        end
    end
    save FlytracksL.mat FlytracksL param filename
end
% ------------------------------------------------------------------------
% final comments: note that the units of positions are in pixels
% ------------------------------------------------------------------------
%% To plot the fly shown in Figure 3.4 for a desired frame:
% Acquire the surrounding polygon in the desired frame using the following
% line when extracting centroid, area and other properties:
% Spolygon=regprops(bigobject).ConvexHull;
% And assuming that xc, yc, or and MajAx are the x and y positions,
% orientation and major axis length, respectively, for the desired frame:
nicebluecolor=[86 180 233]/255;
niceorangecolor=[230 159 0]/255;
flymoviedata=VideoRaw.read(desired_frame);
imshow(flymoviedata)
hold on
plot(Spolygon(:,1),Spolygon(:,2),'-','LineWidth',3,'Color',nicebluecolor)
Majoraxisbody(1,1)=xc-MajAx/2.3*cosd(or);
Majoraxisbody(2,1)=xc+MajAx/2.3*cosd(or);
Majoraxisbody(1,2)=yc+MajAx/2.3*sind(or);
Majoraxisbody(2,2)=yc-MajAx/2.3*sind(or);
plot(Majoraxisbody(:,1),Majoraxisbody(:,2),'-m','LineWidth',3,...
    'Color',niceorangecolor)
plot(Majoraxisbody(:,1),Majoraxisbody(:,2),'om','LineWidth',3,...
    'MarkerSize',7,...
    'MarkerFaceColor',niceorangecolor,'MarkerEdgeColor',niceorangecolor)
plot(xc,yc,'og','LineWidth',3,'MarkerSize',7,...
    'MarkerFaceColor',nicebluecolor,'MarkerEdgeColor',nicebluecolor)
```

3.3.2 *Implementation of tracking algorithm in Bonsai*

In order to track more videos in less time, we also implemented the described tracking algorithm in Bonsai, a visual programming framework developed by colleagues at the Champalimaud Center for the Unknown (Lopes et al. 2015). The Bonsai workflow of the tracking algorithm is shown in (Figure 3.5). This new implementation successfully yielded the same outputs as the MATLAB algorithm but much faster: while the processing of a 2-hour-long video (360x10^3 frames, 3 arenas) in MATLAB took 4 hours, Bonsai took only 30 minutes to yield the same output.

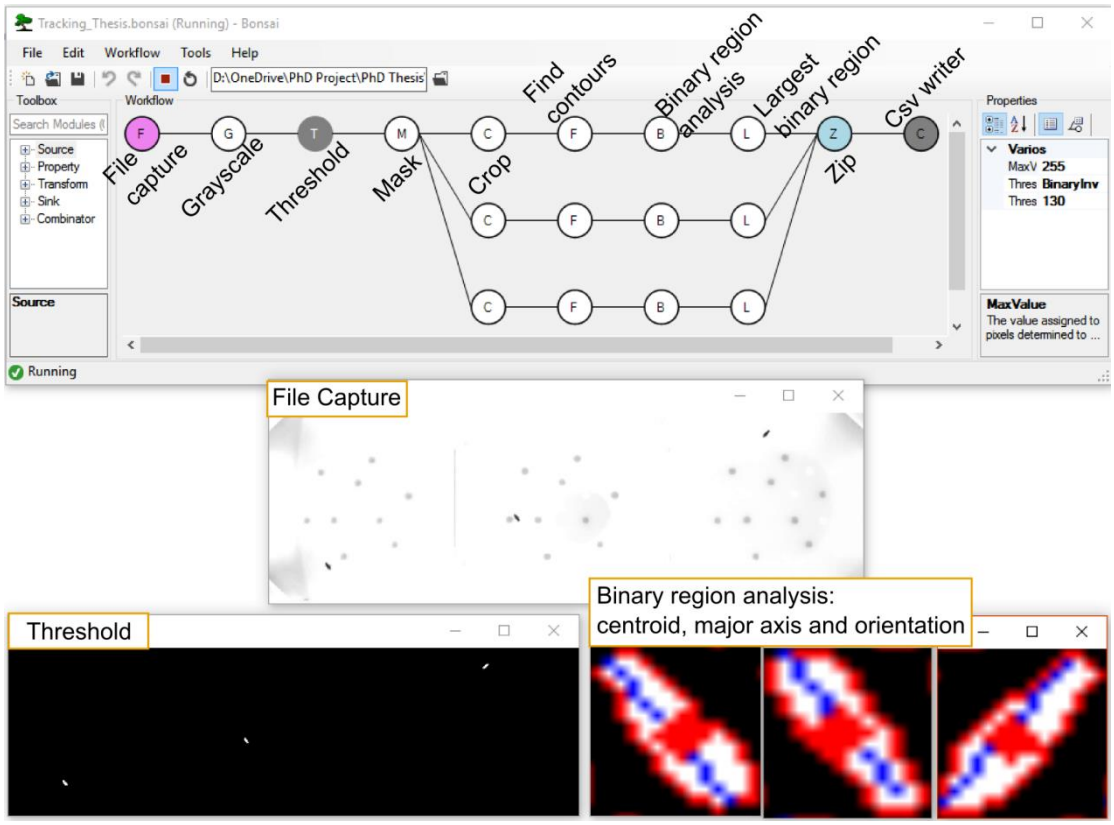

Figure 3.5 – Tracking algorithm implemented in Bonsai

The bonsai programming framework is used to extract centroid, orientation and major axis length of the fly blob (Lopes et al. 2015). Each circle is a data-processing node: the *filecapture* node loads the video (if double-clicked, Bonsai will display the video as shown under the "File Capture" label. The output of the *Threshold* node is also shown. The *crop* node divides the frame into the left, center and right arena and then the blob analysis is executed for arena independently and in parallel (output shown under the label "binary region analysis"). The *zip* node combines the output data into a single table that is then printed as a csv file using the *csvwriter* node.

Figure 3.5 also makes evident the usefulness of Bonsai in data processing: an algorithm that is written in more than 100 lines in MATLAB, can be created in Bonsai in just 1 minute by using its node structure and user-friendly visual interface that makes every step of the algorithm easy to follow and understand.

3.3.3 *Head detection algorithm*

We then developed a second algorithm, this time only in MATLAB, to extract the head position. This algorithm combined two strategies: First, we manually set the position of the head of the fly in the first video frame and used it to classify the end points of the major axis (see Figure 3.4, "candidates for head centroid") into head or tail based on a proximity rule (Gomez-Marin, Stephens, and Louis 2011): given that we have a high enough framerate (50 fps), the distance *D1* between the head position of the fly in the current frame (time *t*) and the head position in the previous frame (time *t-1*) will be smaller than *D2*, the distance to the tail position in the previous frame (Figure 3.6A), therefore, as long as there are no jumps, it is possible to propagate the assignation of head and tails from the first frame using this rule.

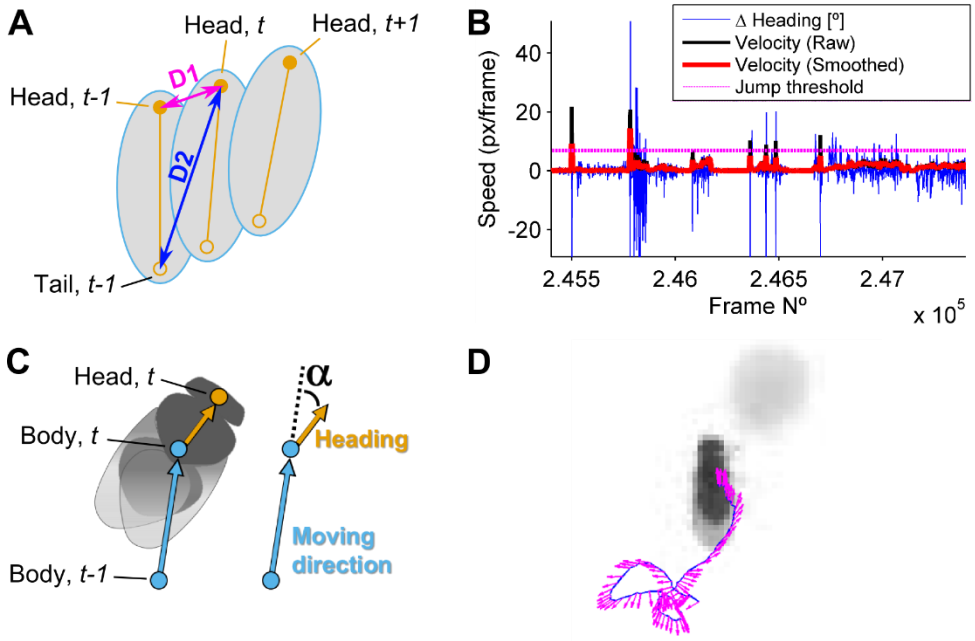

Figure 3.6 – Parameters used in the head detection algorithm

(A) Distance rule. The head position assignation is propagated as long as the fly does not jump using the distance rule: First, we manually define the head in the first frame (time *t-1*), then, given that D1 < D2, it is possible to assign the head at *t* and continue to do so on the following frames. (B) Speed threshold used to detect jumps (horizontal magenta line) applied to the smoothed speed (red). The heading (blue) and the raw speed (black) are also shown. (C) To determine the forward/not-forward walking bouts, a threshold was applied on α, the angle between the walking direction vector (vector joining body centroid in time *t* with body centroid in time *t-1*, blue arrow) and the heading vector (vector joining the head and the body centroid at time *t*, orange arrow). (D) In some exceptional occasions, flies walk backwards/sideways (not forward) for more than 2 body-lengths.

However, this proximity rule becomes invalid when the fly jumps. To detect the jumps, the raw speed was smoothed using a sliding average with a very short window of 60 ms (Figure 3.6B). Then, the threshold for a jump was set at 4*average walking speed, where the average walking speed was defined as speed > 4 mm/s. To correct the head position in the intervals between jumps, we scanned for periods in which the fly covered a distance of at least 2 body-lengths (~40 px) in which the angle between the heading and the walking direction vectors (α, Figure 3.6C) was between [-80º, 80º] for at least 75% of that time. When these criteria were met, we assumed the fly was walking forward and

therefore, the head assignment was correct. If on the contrary, 75% of the time the fly appeared to be walking backwards during that distance, then the head assignment was inverted. Finally, if none of these criteria were met (see Figure 3.6D for an example), the parameters to defined forward direction were loosened to α between [-90º, 90º] for more than 50% of the time on any distance segment. Since this last criteria was much more lose and prone to error, 510 of these problematic segments (found across 136 flies) were manually annotated and only 2% of them had an incorrect classification of head and tail positions. Therefore, combining the proximity rule with the forward walking rule produces a robust algorithm that can correctly track the head position of the fly across time.

3.4 Structure array with information about each individual fly

An important step before the analysis of the acquired data is organizing the information about each individual fly such that comparison across different type of experimental conditions is easy and fast. For this an excel table was created with all the information of the experimental conditions of the flies recorded in each video, such as genotype, metabolic state, mating state, concentration and distribution of food patches, the video filename, among others (Figure 3.7A). Since the values in this table were numerical (to facilitate posterior analysis in MATLAB), the label corresponding to each number is explained in a different tab (Figure 3.7B). The information on the first table (Figure 3.7A), was then saved in a structure array called "FlyDB" in MATLAB (Figure 3.7C), while the information about the labels that correspond to each number (Figure 3.7B) was saved in another structure array called "LabelsDB".

The filename of each recorded video was also designed to store information about the genotype, experiment Nº, the run of the day in which it was acquired, among others. The details about the specific structure of the video filenames are described in Table 3.2.

Table 3.2 – Video filename structure

Filename segment	Description	Nº of digits	Examples
1	Experiment Nº	4	"0003"
2	Experiment subdivision	1	"C"
3	Run Nº	2	"01", "02" or "03" for the corresponding run number during the day
4	Repetition day	3	"R01" (for the first day), "R02" (for the second day in which the same experiment was performed)
5	Camera Nº	7	"Cam01P0", "Cam02P0", "Cam03P0", or "Cam04P0"
6	Genotype Abbreviation	10	"WT-CantonS"

In this way, to select the data that was collected only on day 3, for example, one could use the video filename stored in the FlyDB.Filename field to create a logical vector:

```
Logical_vector=cell2mat(cellfun(@(x)~isempty(strfind(x,'R03')),...
      {FlyDB.Filename},'uniformoutput',false));
```

A

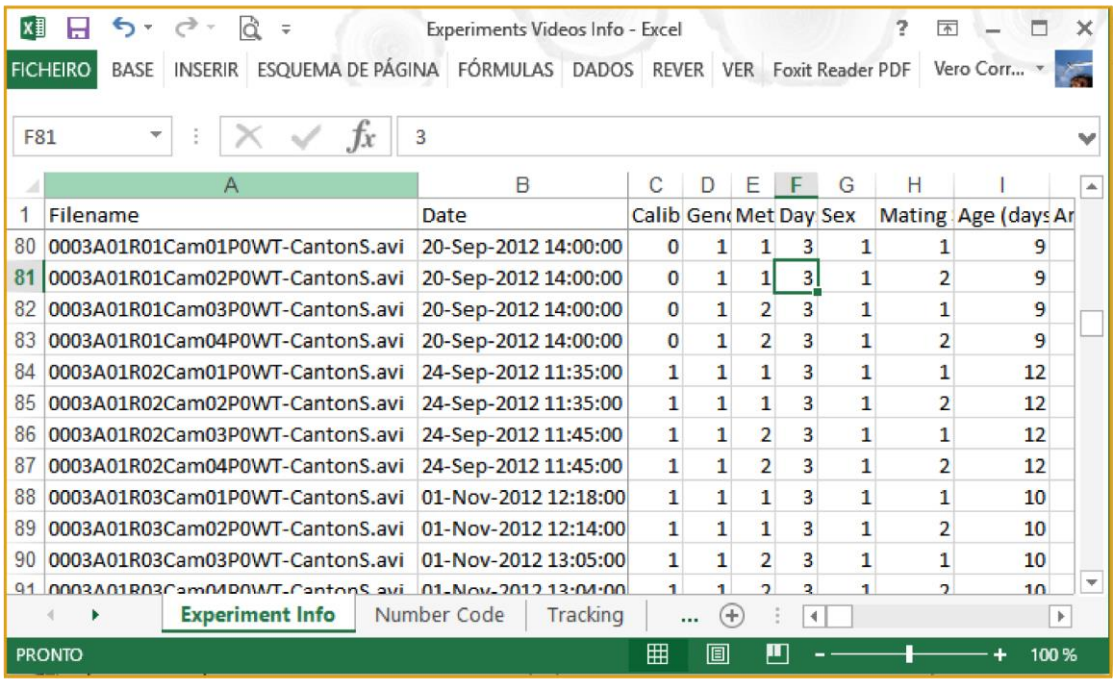

	A	B	C	D	E	F	G	H	I
1	Filename	Date	Calib	Gen	Met	Day	Sex	Mating	Age (days
80	0003A01R01Cam01P0WT-CantonS.avi	20-Sep-2012 14:00:00	0	1	1	3	1	1	9
81	0003A01R01Cam02P0WT-CantonS.avi	20-Sep-2012 14:00:00	0	1	1	3	1	2	9
82	0003A01R01Cam03P0WT-CantonS.avi	20-Sep-2012 14:00:00	0	1	2	3	1	1	9
83	0003A01R01Cam04P0WT-CantonS.avi	20-Sep-2012 14:00:00	0	1	2	3	1	2	9
84	0003A01R02Cam01P0WT-CantonS.avi	24-Sep-2012 11:35:00	1	1	1	3	1	1	12
85	0003A01R02Cam02P0WT-CantonS.avi	24-Sep-2012 11:35:00	1	1	1	3	1	2	12
86	0003A01R02Cam03P0WT-CantonS.avi	24-Sep-2012 11:45:00	1	1	2	3	1	1	12
87	0003A01R02Cam04P0WT-CantonS.avi	24-Sep-2012 11:45:00	1	1	2	3	1	2	12
88	0003A01R03Cam01P0WT-CantonS.avi	01-Nov-2012 12:18:00	1	1	1	3	1	1	10
89	0003A01R03Cam02P0WT-CantonS.avi	01-Nov-2012 12:14:00	1	1	1	3	1	2	10
90	0003A01R03Cam03P0WT-CantonS.avi	01-Nov-2012 13:05:00	1	1	2	3	1	1	10
91	0003A01R03Cam04P0WT-CantonS.avi	01-Nov-2012 13:04:00	1	1	2	3	1	2	10

B

	A	B	C	D	E	F	G
1	Number	Genotype	Metabolic Status	Sex	Mating Status	FoodType	Concentr. Units
2							
3	1	Canton S	AA+ (Hunt)	Female	Mated	Yeast	g/L
4	2	WT Dahomey	AA-	Male	Virgin	Sucrose	g/L
5	3	WT Portugal	S-		Virg x SP0	Empty	-
6	4	WT Dickinson	S- & AA-		Virg x SP ctrl	Agarose	g/L
7	5	SPR_B-/-	Wet Starved				
8	6	SPR_L-/-	Fully Fed (Vienna) w/o sprY				
9	7	FM7/SPR_B	AA+ (Yaa)				
10	8	DopR2	Fully Fed (Vienna) with sprinkledY				
11	9	Or83b-/-					
12	10	Or83b+/-					

C

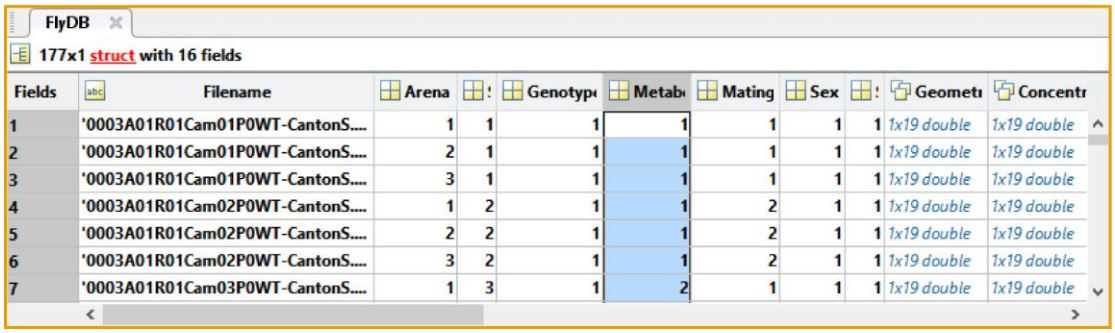

Fields	Filename	Arena		Genotyp	Metab	Mating	Sex		Geometi	Concentr
1	'0003A01R01Cam01P0WT-CantonS....	1	1	1	1	1	1	1	1x19 double	1x19 double
2	'0003A01R01Cam01P0WT-CantonS....	2	1	1	1	1	1	1	1x19 double	1x19 double
3	'0003A01R01Cam01P0WT-CantonS....	3	1	1	1	1	1	1	1x19 double	1x19 double
4	'0003A01R01Cam02P0WT-CantonS....	1	2	1	1	2	1	1	1x19 double	1x19 double
5	'0003A01R01Cam02P0WT-CantonS....	2	2	1	1	2	1	1	1x19 double	1x19 double
6	'0003A01R01Cam02P0WT-CantonS....	3	2	1	1	2	1	1	1x19 double	1x19 double
7	'0003A01R01Cam03P0WT-CantonS....	1	3	1	2	1	1	1	1x19 double	1x19 double

Figure 3.7 – Database with experiment information

(A) All the information about the experimental conditions of the flies recorded in a given video is introduced initially in excel using numerical values for each type of experimental treatment. (B) The labels that correspond to each numerical value stored in (A) are shown in a different tab “Number Code”. (C) The information in (A) is then transformed in MATLAB and saved as a structure array. Each field (row) contains the information for one single fly.

Or to select all flies of one particular condition stored in FlyDB, for example 'virgin', simply use:

```
Logical_vector=[FlyDB.Mating]==Number_Index
```

Where the `Number_Index` is the row number in `LabelsDB.(DesiredTreatmentType)` where the number corresponding to the treatment is stored. For example, for virgin flies, the `Number_Index` would be:

```
Number_Index=find(cell2mat(cellfun(@(x)~isempty(strfind(x,'Virgin')),...
    LabelsDB.Mating{2},'uniformoutput',false)));
```

Finally, a very useful application of these numbers is the creation of a *condition index*. Since each type of experimental treatment has a corresponding number, it is easy to create a simple mathematical formula that generates a different condition number for all possible combinations of treatments. For example, if we have 2 types of mating state and 3 types of metabolic states, one can have 6 possible combinations (Table 3.3) and the formula to obtain the *condition index* in function of a given mating and metabolic state is:

```
Condition_Index = Total_Metabolic*(MatingState-1) + MetabolicState
```

Where `Total_Metabolic` is the total number of metabolic states, `MatingState` is the number of the corresponding mating state and `MetabolicState` is the number of the corresponding metabolic state.

Table 3.3 – Condition index example

		Metabolic State		
		1: AA+ rich	**2**: AA+ suboptimal	**3**: AA-
Mating State	**1**: Mated	Cond 1	Cond 2	Cond 3
	2: Virgin	Cond 4	Cond 5	Cond 6

To add a third experimental treatment type, one can imagine Table 3.3 with different layers, in which each layer is a different genotype, for example. In that case, the formula to obtain the *condition index* would be:

```
Condition_Index = Total_Metabolic*(MatingState-1) + MetabolicState +...
    (Total_Metabolic*Total_Mating)*(Genotype-1)
```

3.5 Conclusion

In this chapter I've described the algorithms that were used to extract the body and head centroids of the flies, the position of the food patches in the arenas and the way in which the different experimental condition information was stored in MATLAB for further use in the data analysis.

Chapter 4. Analysis of behaviors associated with nutrient decisions

This chapter is dedicated to tell the story behind the story told in Chapter 2. I have divided this chapter in four sections. Section 4.1 shows the characterization of the locomotor activity of the flies in an arena with and without food patches. I also explore the orientation and movement patterns of the fly with respect to the food in an attempt to gain insight in how flies approach the food that can later be used to dissect the contribution of olfaction, gustation and sight in the finding and recognition of yeast at short range.

In section 4.2 I show how different analysis tools can be used to study the behavior associated with nutrient decisions. First, I describe a method that could be used to classify behaviors based on the distributions of relevant kinematic parameters for those behaviors. Then, I show how one could use a Bayesian classifier to predict the internal state of a fly based on its behavior. Next, principal component analysis was used to pinpoint the biggest behavioral differences between two close metabolic states. Bioinformatic tools were also used to create a tree of similarity between the behavioral sequences. The behavior of the flies belonging to different clusters was studied for each internal state condition.

Section 4.3 briefly shows the dynamics of yeast and sucrose decisions for each fly in belonging to 4 different internal state conditions. Then, I briefly discuss how AA-deprived flies at the end of the 2 hour-assay do not yet display the exploratory behaviors of fully fed flies.

In the last section of this chapter, I discuss some preliminary results on the modulation of olfaction by AA deprivation and on the role of taste in sustaining the interest on yeast in AA-deprived flies. I finalize by presenting results that suggest the involvement of octopamine in mediating the postmating increase of yeast feeding; findings that were published in Walker et al. 2015.

4.1 Characterization of locomotor activity and exploration patterns in the foraging arena

4.1.1 The effect of internal state on locomotor activity

In addition to the quantification of the behavior of the flies on the food patches (described in detail in Chapter 2), image-based tracking allow us to look into the behavior of the fly around and far from the food. We used 2-dimensional histograms to characterize the positional preference and locomotor activity of the flies across different internal states (Figure 4.1).

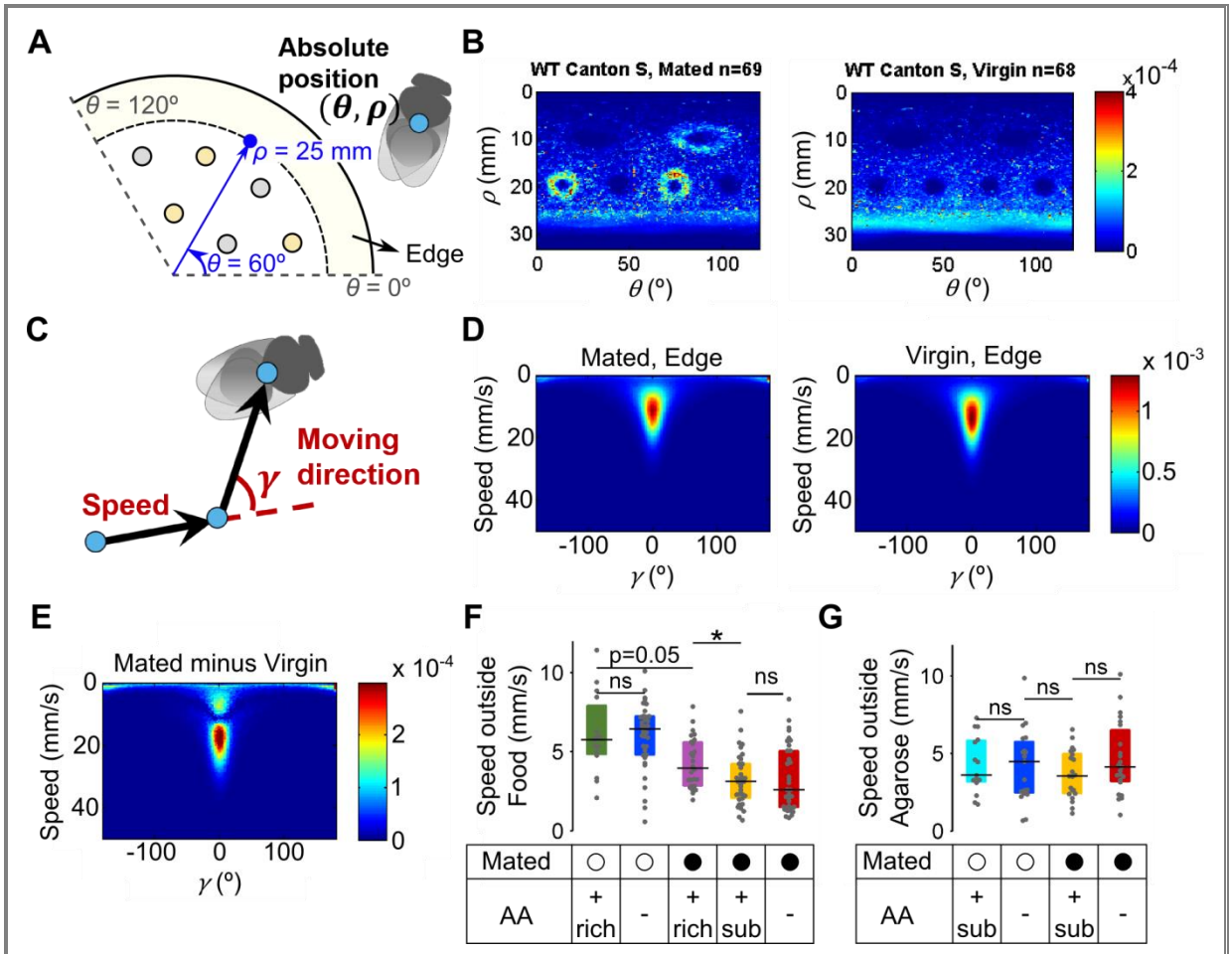

Figure 4.1 – Characterization of positional preference and locomotor activity

(A) Graphical representation of the tracking arena showing the value of the blue dot in polar coordinates. (B) Histogram of the position of all mated flies (left) and all virgin flies (right) in polar coordinates. The pixel color indicates the fraction of time that flies in the indicated condition spent in the corresponding location bin. Since the arena has three symmetric segments of 120º (as shown in A). (C) Graphical representation of the velocity and turning angle. (D) Histogram of velocity and turning angle displayed in the edge of the arena (see A) for all mated (left) and all virgin (right) flies. The pixel color indicates the fraction of time that the particular combination of speed and turning angle in that bin was observed. (E) The difference between the histograms in (D). (F) Effect of internal state on the locomotor activity of the flies measured by body centroid speed, in the presence of food. (G) Effect of internal state on body centroid speed in the absence of food (tested in an arena with agarose spots).

Since the arena contains 3 symmetrical segments of 120º (Figure 4.1A), we pooled the positions of the flies of the 3 segments into 1 to improve the resolution of the histogram. We observed that mated flies prefer to spend more time in the outer yeast patches than in the inner ones (Figure 4.1B), while virgins prefer to spend more time in the edge (ρ > 25 mm) than in any kind of food patch. We then looked at the walking behavior of mated and virgin flies by quantifying how often a given combination of speed and moving direction was observed (Figure 4.1C). Virgin flies displayed higher walking speeds than mated flies (Figure 4.1D and E). AA-challenged flies (pre-fed a suboptimal diet or a diet without AA (section 2.5.2)) display lower speeds than flies pre-fed a rich diet (Figure 4.1F). Importantly, these differences in speed were not due to the increased feeding time of mated and AA-challenged flies because we are only quantifying the speed outside the food patches. We evaluated if these differences in activity across internal states were specific to the presence of food by measuring the speed of flies in an arena containing only agarose patches (without nutritive food). Interestingly,

flies from all internal state conditions displayed very similar speeds in the absence of food (Figure 4.1G). To investigate if there were other aspects of locomotor activity modulated by internal state in the absence of food, we measured other parameters such as distance covered (Figure 4.2A), percentage of time walking (Figure 4.2B), percentage of time in the edge of the arena (Figure 4.2C), edge activity (number of visits to the edge per second of walking) (Figure 4.2D), angular speed (Figure 4.2E) and MSDR (a measure of stop and go motion) (Figure 4.2F). We found no significant differences across the internal states except in the edge activity, but that difference might be due to a technical issue with the arenas (data not shown).

We must mention the fact that we did not test flies pre-fed a rich diet in the arena without food, which means that we still do not know if challenging flies with a suboptimal AA diet has an effect on overall locomotion. We can state that AA deprived flies show similar locomotor activity than flies pre-fed a suboptimal diet, however, as we concluded in section 2.3.5, the main difference between these two conditions is the eagerness of the flies to eat yeast, while the global foraging strategies were already very similar. Therefore, as the global effects of amino acid deprivation in foraging strategies are already observed when flies are pre-fed a suboptimal diet (compared to a rich diet), there is a strong possibility that we might be missing any existing effects of this deprivation in locomotor activity by not comparing to the flies pre-fed the rich diet.

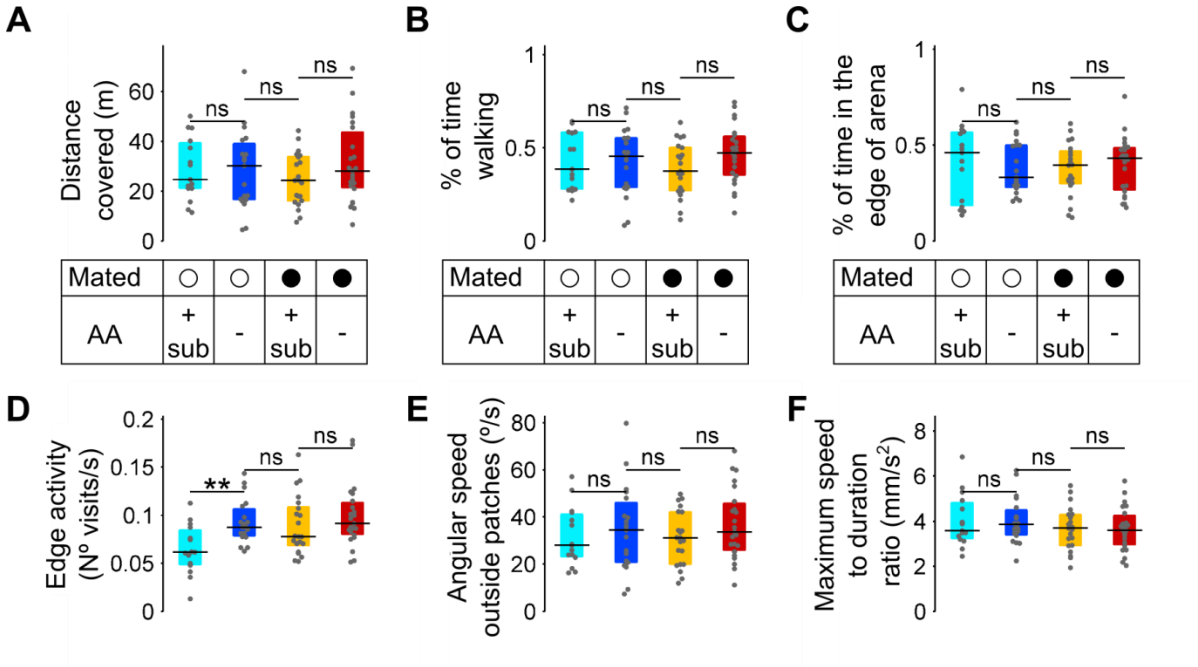

Figure 4.2 – Locomotor activity in the absence of food across different internal states

Effect of internal state on a set of locomotor activity parameters. (A) Distance covered. (B) Percentage of time walking (walking bouts were defined in section 2.5.6). (C) Percentage of time in the edge of the arena (edge bouts happened when the fly was more than 25 mm away from the center of the arena). (D) Edge activity (number of visits to the edge per second of walking. (E) Angular speed outside the agarose patches. (F) Maximum speed to duration ration, calculated as the average of maximum speed during a walking bout divided by the duration of that bout as long as the bout was longer than 1 second.

4.1.2 Characterization of fly orientation towards food patches

We then focused on characterizing the flies' movement inside and around the food patches and its modulation by internal state by quantifying the angle of the moving direction vector with respect to the food patch (Figure 4.3A). Mated females tended to spend more time inside yeast patches rather than in their vicinity (distance from body centroid to patch center < 5 mm) (Figure 4.3B) and displayed angles that were mostly distributed around 0º and 180º, which means moving towards and away of the patch (either facing or giving the back to the patch), while virgins spent more time further away and moving in a tangential manner (angles around 90º). Both virgins and mated flies had a similar distribution towards sucrose: both further away and moving tangentially (Figure 4.3C). These distributions are exactly what was expected given what we learned in Chapter 2: mated flies that are AA-challenged prefer to feed on yeast, and when they feed they display a micromovement, a back and forth displacement of the body centroid which results in higher occurrences of angles around 0º and 180º. On the other hand, virgins do not pay too much attention to the food patches at all, so they spend more time walking in between patches displaying a wider range of angles centered on 90º (tangential direction).

We then focused on what happened around the food patches (and not inside) by excluding instances where the fly was within the feeding radius and expanding the radius around the patch (distance of body centroid > 3 mm and < 10 mm, see shaded areas in Figure 4.3D,E left schemes). Since we were looking at a larger radius, we focused on the edge area around the outer patches to avoid overlapping with the feeding radius of the neighboring patches. Surprisingly, the distributions for yeast (Figure 4.3D) and for sucrose (Figure 4.3E) looked very similar, both for mated and virgin flies, with angles in the tangential direction prevailing over all others. This result might suggest that flies approach yeast and sucrose patches in a similar way and therefore that yeast olfactory cues do not play an important role in the preference flies display towards yeast.

However, one of the setbacks of this analysis is that it was performed with body centroids and moving directions rather than with head centroids and actual orientation of the fly body towards the food patch. Therefore, we further apply the same analysis but now looking at the body orientation of the fly towards the food patch (Figure 4.4A). This time we also looked at the different metabolic states in addition to the mating states. As expected, as mated flies get more deprived from AAs they spend more time inside the yeast spots and the occurrences around 180º within the patch disappeared corroborating the supposition that those occurrences were due to the back and forth micromovements of the body centroid as the fly fed (Figure 4.4B, top panels).

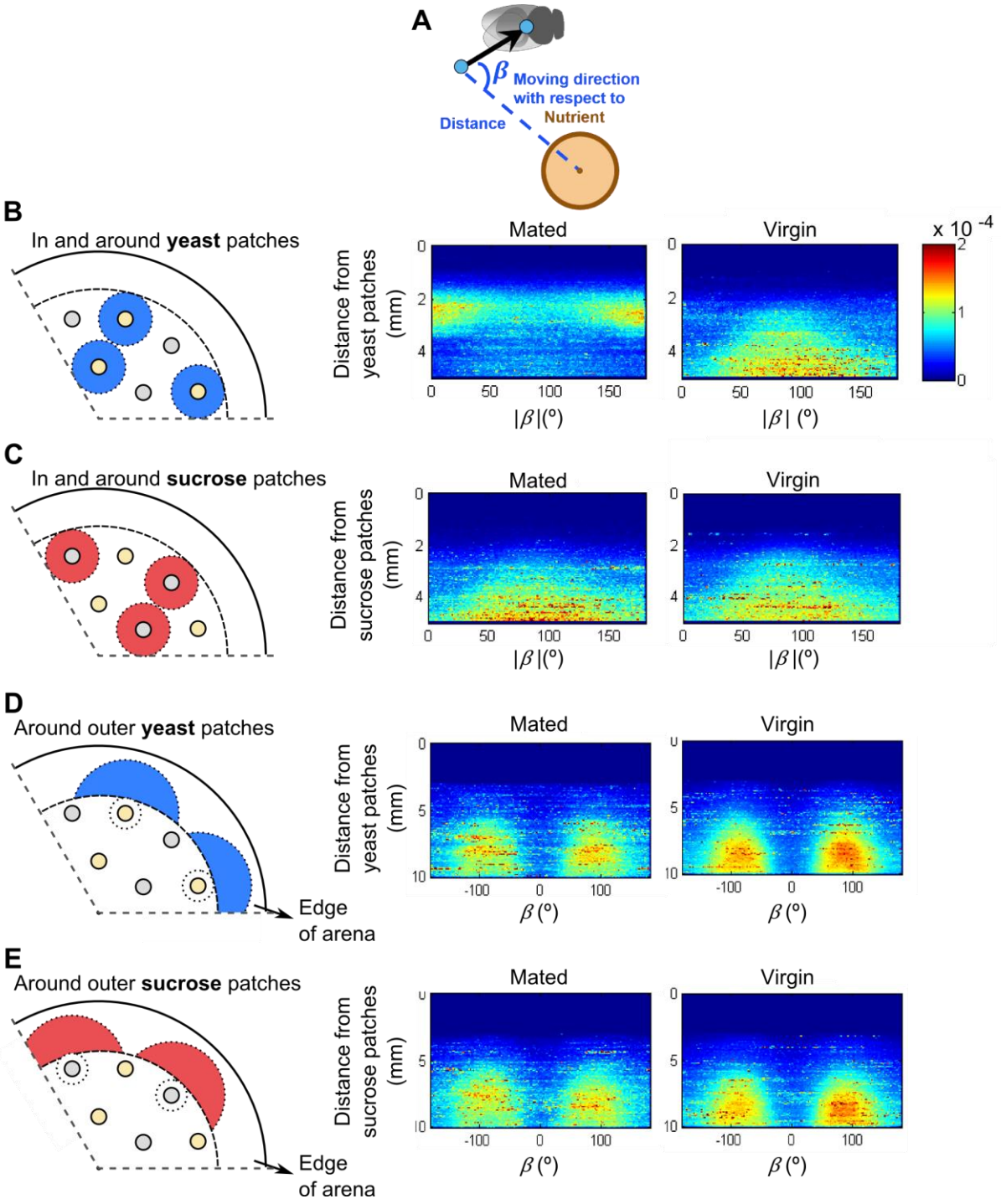

Figure 4.3 – Characterization of flies' moving direction with respect to food patches

(A) Graphical representation of parameter β, the angle between the moving direction of the body centroid (black arrow) and the vector that joins the body centroid with the center of the food patch (blue dashed line). (B and D) Histograms of β and distance from yeast patches on the blue shaded area (left panel) for mated (center panel) and virgin (right panel) flies. (C and E) Histograms of β and distance from sucrose patches on the red shaded area (left panel) for mated (center panel) and virgin (right panel) flies. The pixel color indicates the fraction of time that the particular combination of β and distance to food was observed in that bin.

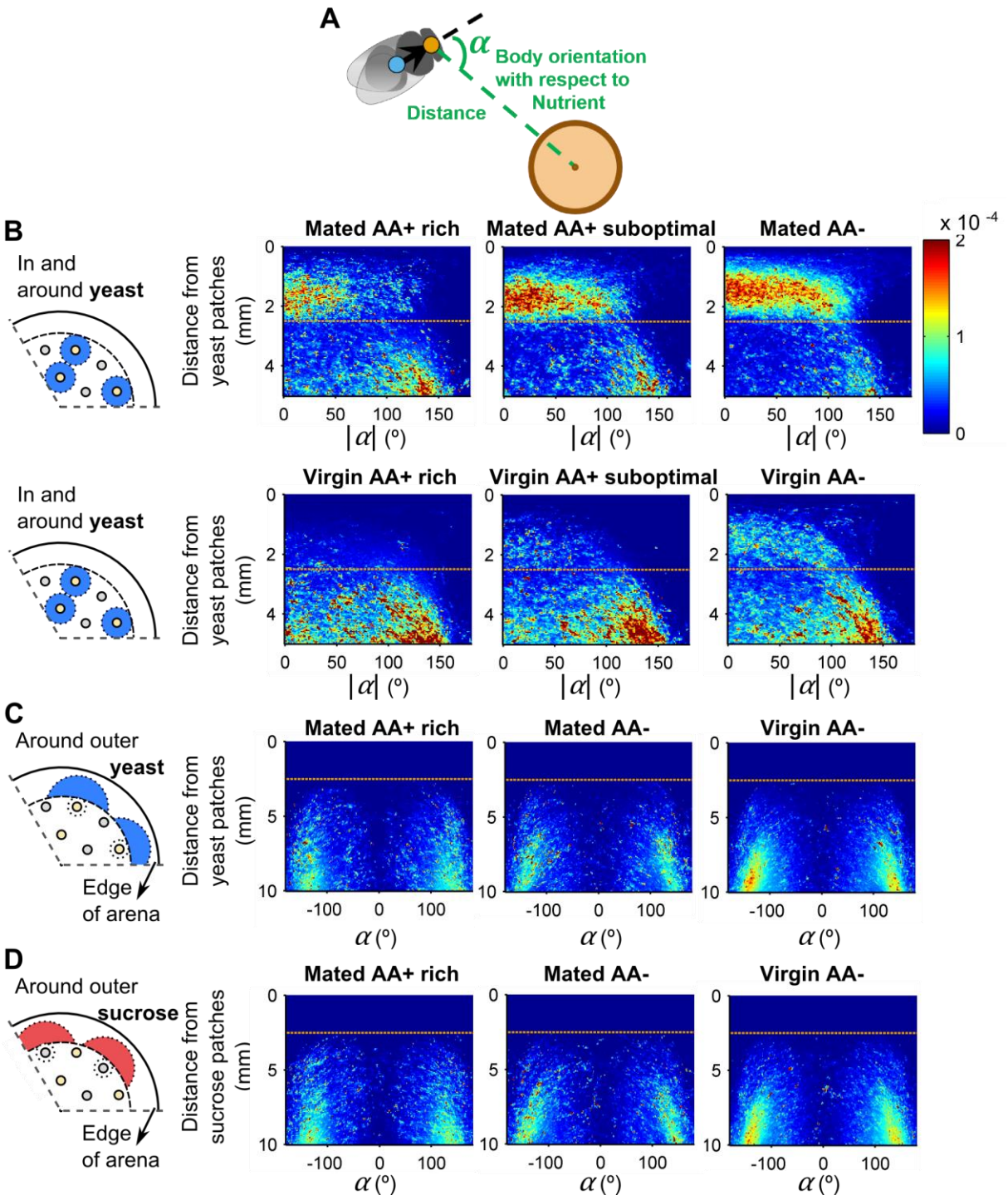

Figure 4.4 – Characterization of flies' orientation with respect to food patches

(A) Graphical representation of parameter α, the angle between the body orientation of the fly (black arrow) and the vector that joins the head centroid with the center of the food patch (green dashed line). (B and C) Histograms of α and distance from yeast patches on the blue shaded area (left panels) for the indicated internal state condition. (D) Histograms of α and distance from sucrose patches on the red shaded area (left panel) for the indicated internal state condition. The pixel color indicates the fraction of time that the particular combination of α and distance to food was observed in that bin.

The distributions of body orientation displayed by virgins are, however, very different from the ones observed in Figure 4.3B, with most of the orientations having a value around 140º with respect to the food patch. In a similar manner, the distributions of the orientation in the vicinity of outer yeast and sucrose patches show higher occurrences of 140º angles. These results indicate that we are simply looking at the distributions of the flies' walking pattern in the edge of the arena, rather than the distribution of the approach to food: when flies walk on the edge area, they maintain their body facing outside the arena, but they move sideways (Figure 4.5), which explains the observed differences between the moving direction and the body orientation with respect to the food patches.

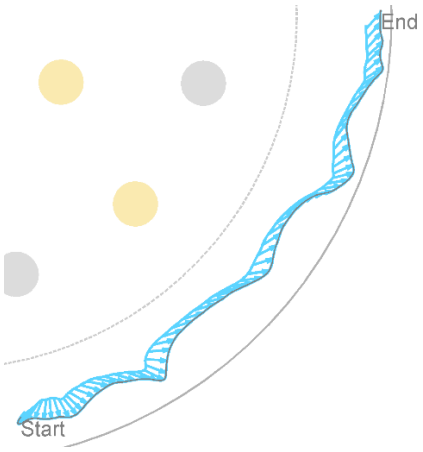

Figure 4.5 – Fly walking in the edge

Representative trajectory of a fly walking in the edge of the arena. Body centroid is shown by the blue line, head centroid by the gray line and blue arrows indicate body orientation.

There are several setbacks with this approach: it does not take into account the dynamics, there is no discrimination between an approach that ends into a feeding event and one where the fly just passes by and the occurrences are based on time, not on number of approaches, so a fly that grooms for a long time next to a spot bias the whole distribution.

There is a hypothesis we wanted to test but a good method to test it remained elusive to me: Flies decide to approach and engage (odorous) yeast patches at a distance based on olfactory and/or visual cues, while the approach to (odorless) sucrose patches could be random and the decision to engage could be taken only after leg contact (tarsal taste stimulation). There are a couple of snapshots, completely anecdotal that speak in favor of that hypothesis (Figure 4.6). To test the sucrose approach leg-contact-then-sip hypothesis, we would need to combine the flyPAD (Itskov et al. 2014) with the tracking setup to be able to distinguish between a leg contact and a sip to the spot, but quantifying the decision point at which the turn towards yeast occurs at a distance requires more thinking about it.

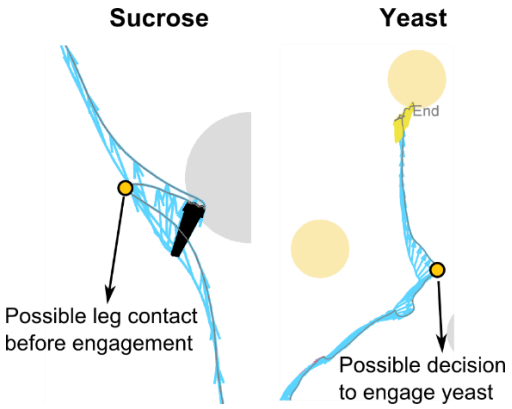

Figure 4.6 – Hypothesis about sucrose and yeast approach

Hypothesis about yeast and sucrose approach and engage decisions: Flies could decide to approach and engage yeast patches at a distance based on olfactory and/or visual cues, but the approach to sucrose patches could be random and the decision to engage is taken only after leg contact (tarsal taste stimulation).

4.1.3 Flies seem to be able to "mark the spot"

In an attempt to know if flies remembered a given food patch, I quantified all the returns of a fly to every patch in the arena, independently of the stops she made in between (Figure 4.7A-C). The distributions of durations and distances covered during those returns were very similar for all the

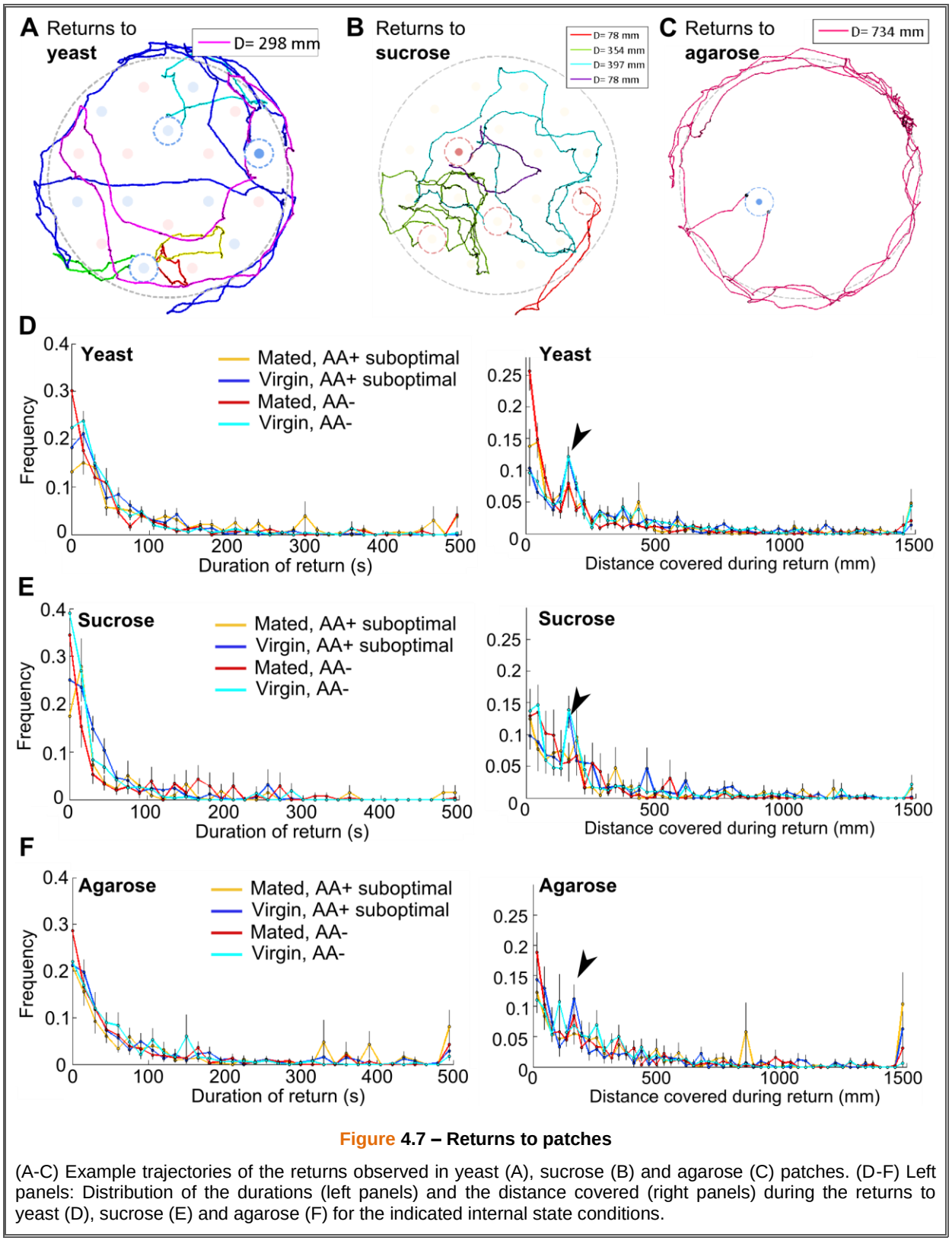

Figure 4.7 – Returns to patches

(A-C) Example trajectories of the returns observed in yeast (A), sucrose (B) and agarose (C) patches. (D-F) Left panels: Distribution of the durations (left panels) and the distance covered (right panels) during the returns to yeast (D), sucrose (E) and agarose (F) for the indicated internal state conditions.

substrates: yeast (Figure 4.7D), sucrose (Figure 4.7E) and agarose (no food) (Figure 4.7F), suggesting that the observed returns might not be elicited by any food-related component. In fact, there is a common peak in the distance distribution (Figure 4.7D-F right panel, black arrow) around 170 mm that falls between 157 mm and 188 mm, which are the values of the inner and outer perimeter of the edge ring (Perimeter of inner edge circle: π x 50 mm = 157 mm; perimeter of outer edge circle: π x 60 mm = 188.5 mm) which might be explained by flies recognizing the place where they last left the inner area and after a lap on the edge, they would return to the inner area in the same place where they left it. This is an interesting finding that inspires a set of interesting questions: How are flies able to recognize that they have given one turn on the arena's edge? Are they marking the patch to which they are returning using a pheromone or are they remembering its position and integrating their way back? This seems to be independent of the path quality as they also do it for agarose patches.

The high peak on very short distances covered during the yeast returns in the mated AA-deprived flies (Figure 4.7D right panel) is consistent with the previously described increased locomotor activity in the yeast patches (Figure 2.4F and J) and revisits (Figure 2.5F). As a matter of fact, the revisits we describe are actually **defined** as the fly staying in the vicinity (see section 2.5.8, parameter 21: transition probability to same yeast patch) and we know that if we remove this distance threshold (16 mm), the results do not change, so staying in the vicinity is the main reason for an increased revisit probability and not an increase number of returns where the fly leaves far away from the spot. Therefore, the observed revisits do not support the hypothesis of memory or path integration in flies. However, at the time I did this analysis the concept of food micromovements did not existed. Also, the current foraging arena was designed without any visual landmarks. Therefore, further analyses in an arena with visual landmarks and even obstacles hiding the yeast spots or experiments in the dark are necessary to prove or disprove the conclusions here stated.

4.2 Useful tools in the analysis of behavior

One of the first steps in exploring new behavioral data sets is to simply calculate a set of parameters that help answering concrete questions about the behavior under study. In our case, we wanted to know how flies modulated their foraging and feeding behavior to satisfy their nutritional needs. In particular, we were interested in knowing the microstructure of yeast and sucrose visits: how often did they happen, for how long, the rate of approaches and returns. We were also interested in their exploratory patterns: were they focusing the exploration to a certain area of the arena or were they exploring the whole arena? Most of these questions were answered and discussed in Chapter 2 based on 24 parameters that have been described in detail in section 2.5.8. We also investigated the effects of internal state on the locomotor activity (Figure 4.1 and Figure 4.2) and on the walking patterns of the flies (Figure 4.3 Figure 4.4). In this section I describe further insight obtained from these parameters.

4.2.1 *Defining a continuous metric to classify a specific behavior based on parameter distributions: a case example*

Studying the behavior associated to nutrient decisions requires the reliable identification of the moments in which the fly interacts with the food. Our first intuition was to simply set a threshold around each food patch and define contact or interaction every time the head of the fly crossed such threshold (Figure 4.8Ai). The speed at which the fly crosses this threshold is also important as it indicates the degree of interest towards the approached resource. We examined the joint probability distribution of these two parameters (speed and distance from patch center) for different substrates: agarose (Figure 4.8Aii), yeast (Figure 4.8Aiii) and sucrose (Figure 4.8Aiv). We observed that flies prefer to remain in the edge of sucrose spots when compared to the yeast spots where they prefer to walk all the way to the center.

We considered we could extract more information about the degree of engagement with the food if we used a probabilistic function on these parameters (speed and distance from the patch), rather than a simple threshold on them. By defining engagement with the food in terms of continuous functions of these parameters, we would have a continuous reporter of the degree of interest of the flies with the food from any position of the arena as opposed to just a binary indication of interaction. We call it "engagement" and not "feeding", because we cannot tell apart grooming from feeding on the spot at the current video resolution. We therefore defined a new parameter *Engagement Index* as $Engagement\ Index = g(d) * h(s)$, where d is distance from the head to the center of the spot in mm, s is speed of the body centroid in mm/s and $g(d)$ and $h(s)$ are functions of d and s respectively, defined as follows:

$$g(d) = \begin{cases} 1 & if \quad d \leq 1.9 \\ N(1.9,0.4) & if \quad 1.9 < d \leq 4 \\ 0 & if \quad d > 4 \end{cases} \qquad h(s) = \begin{cases} 1 & if \quad s \leq 1 \\ N(0.8,0.3) & if \quad 1 < s \leq 4 \\ 0 & if \quad s > 4 \end{cases}$$

The values used to define these functions were extracted from the observed distribution of the data (Figure 4.8B).

The engagement index was quantified during manually annotated yeast feeding events (Figure 4.8C) and we observed that it indeed increased rapidly and reached its maximum value as the flies fed.

However, one disadvantage of the current definition of engagement is that it penalized small speed bursts during a feeding event (Figure 4.8Cii lower panel), which later realized were good reporters of the eagerness to eat from the spot (Figure 2.4H). In fact, a characteristic profile of speeds over 0.5 mm/s seems to be specific to the presence of food, since it is absent around agarose-only spots (Figure 4.8Aii-iv).

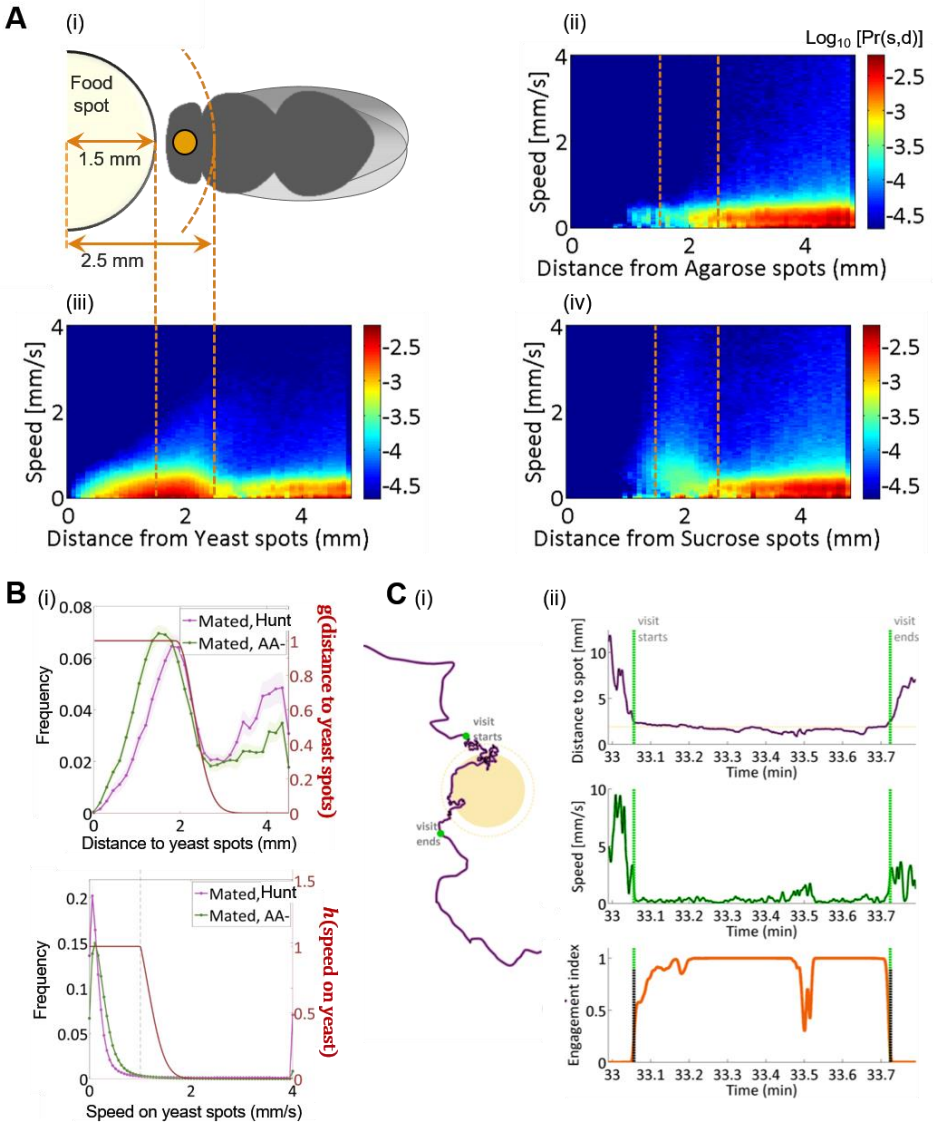

Figure 4.8 – Quantifying the activity of the flies with respect to the food patches.

(A) Distribution of two kinematic parameters around the food patches: distance of the fly head to the center of the spot and speed of the fly. (Ai) Graphical representation of a fly close to a food patch. White circle represents head position and dotted orange line marks the edge of the food patches at 1.5 mm. (Aii) – (Aiv) Joint probability distribution of distance to the spot and speed for different spot composition: (Aii) Agarose, (Aiii) Agarose + Yeast, (Aiv) Agarose + Sucrose. Hot colors indicate higher probability of finding a particular pair of these parameters within the specified ranges (axes limits). (B) Functions of distance $g(d)$, and speed $h(s)$ that define the engagement index. $Engagement\ index = g(d) * h(s)$. (Bi) The $g(d)$ function, in red, reaches a maximum value of 1 when the fly is very close or inside the spot ($d \leq 1.9$ mm) and decays progressively as the fly gets further away from the spot, reaching 0 when the fly is no longer closer to that spot, but to the neighbor spot ($d \geq 4.8$ mm). Some of the key values for this function were obtained from a fit to the observed distribution of distances of the head from the yeast spots, in green. (Bii) Similar to $g(d)$, the $h(s)$ function reaches a maximum value of 1 when the fly displays a low speed and decays progressively as the fly increases her speed. (C) Validation of the engagement index with manually annotated yeast feeding events. (Ci) Head trajectory during a representative yeast feeding event. Green dots mark the start and the end of the visit. Yellow circle represents the yeast spot. (Cii) Distance from spot, speed and engagement index during the yeast feeding event depicted in (Ci). Green dotted lines mark position in time of the start and the end of the visit.

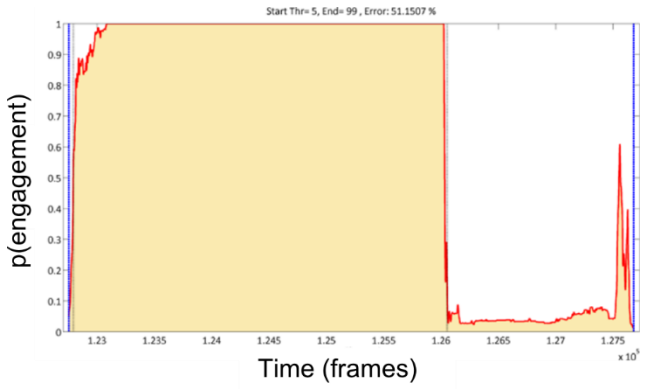

Figure 4.9 – Engagement signal of a fly in the proximity of a yeast spot

The calculation of this parameter could allow the study the fly's approach to the food patches as it assumed interesting shapes as the flies left the patch but remained in its vicinity (Figure 4.9). However, we still had to set thresholds to the start and end of every engagement bout to minimize the error in the calculation of the duration of a given feeding event.

At this point, the reader might be wondering why we use thresholds at all, if the initial idea was to avoid their use. In practice, it is much easier to have a binary description of an event to be able to characterize it: When does it happen? How often? How long does it last? A binary description of an engagement event allowed us to characterize the interaction of the fly with the spot. To do so we needed to apply a threshold on the engagement function, and I decided to apply this threshold directly to the two initial kinematic parameters that were relevant to describe the interaction of the fly with the patch: speed (the fly must be active but not displacing: 0.2 mm/s < speed < 2 mm/s) and distance from the food patch center (distance < 2.5 mm). In this way, the new parameter *food micromovement* was the definition used in the paper to describe engagement events and its definition is described in detail in sections 2.3.1 and 2.5.7.

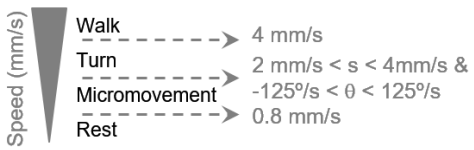

Figure 4.10 – Speed segmentation

The engagement probability function could still be useful if we had similar probability functions describing competing behaviors, such as grooming or walking. In this way, the winning probability would allow a machine to classify the most likely behavior at any time point. Although this would have been an interesting method to classify multiple behaviors, I decided to focus only on the different levels of locomotor activity of the fly, by segmenting the linear and angular speed of the flies (Figure 4.10). The details of this classification are described in sections 2.3.1 and 2.5.6.

4.2.2 A Bayesian classifier of internal state based on behavioral parameters

The Bayes' rule is a widely used method to make inferences based on previous evidence (Stone 2013):

$$P(hypotheis|data) = \frac{P(data|hypothesis) \times P(hypothesis)}{P(data)}$$

In this equation $P(data|hypothesis)$ is called *likelihood* and corresponds to the likelihood of observing the data given that the hypothesis is true. $P(hypothesis)$ is called the *prior probability* and corresponds to the probability that the hypothesis is true before observing the current evidence. $P(data)$ is called

the *marginal likelihood* and corresponds to the probability of observing the data under all possible hypotheses and its calculated as the sum of likelihoods times priors. Finally, $P(hypotheis|data)$ is called the *posterior probability* and it corresponds to our updated belief that the hypothesis is true given the new evidence or data.

We can take advantage of this simple but powerful rule to predict the internal state of an individual based on its behavior. As an example, the distributions of positional preference shown in Figure 4.1B can be used as the likelihood distributions to predict the internal state of a given fly based on a random piece of its trajectory in the arena. In that case, the *likelihood* would be $P(\theta, \rho|Condition_i)$ and it would represent how probable it is to observe a set of positions in the arena given a certain internal state. The *prior probability,* $P(Condition_i)$, could simply be 1/(number of internal states being studied). And the *posterior probability,* $P(Condition_i|\theta, \rho)$, is the probability that a test fly has a certain internal state condition given the observed trajectory. In summary:

$$P(Condition_i|\theta, \rho) = \frac{P(\theta, \rho|Condition_i) \times P(Condition_i)}{\sum_i P(\theta, \rho|Condition_i) \times P(Condition_i)}$$

Previous studies have shown that the Sex Peptide (SP), a peptide transferred from the male's seminal fluid to the female during copulation, is responsible in mediating most of the female's postmating behaviors including yeast preference and appetite (Liu and Kubli 2003; Chen et al. 1988; Ribeiro and Dickson 2010; Walker, Corrales-Carvajal, and Ribeiro 2015). In other words, females mated to SP deficient males will exhibit low yeast appetite, while females mated to SP control males will exhibit a higher yeast appetite. Therefore, these females constitute a good testbed for our Bayesian classifier.

We took trajectory segments (20 min) of the flies for classification and extracted the posterior probability for each data point in the trajectory (Figure 4.11A). For simplicity, we assumed independency and multiplied all the posterior probabilities of each point in the trajectory to obtain the final posterior probability for the whole trajectory. We calculated one posterior probability for each possible internal state condition, in this case for mated and virgin state and the fly was classified according to the internal state that presented the highest posterior probability given the trajectory observed. We used mated and virgin *Canton S* flies to generate the posterior probabilities for all possible arena locations using the Bayes' rule above (training data set) (Figure 4.11B). Virgin females mated to SP males were "correctly" classified as having a virgin phenotype in 65% of the cases already with very short input trajectories (< 2 min) (Figure 4.11C). Slightly longer trajectories (~ 8 min) were necessary to reach the same 65% of correct classifications for virgin flies mated to the SP control males.

There are many variables that can be modified to improve the classification: the binning of the posterior histogram, the number of trials, the step of the trajectory input, the time point of the assay at which the trajectory is selected, selecting consecutive trajectory points or simply random points of the trajectory. Instead of using histograms of certain parameters as the likelihoods in the Bayes' rule, one could fit a mixture of Gaussians on the distribution of the desired parameter and therefore have a likelihood function that depends on fewer variables. In this example we based our classification only in the position of the fly in the arena (θ and ρ) but the posterior probabilities can be modified to be

functions of many other parameters such as speed, time on food, number of visits to the food, transitions between food patches and so on.

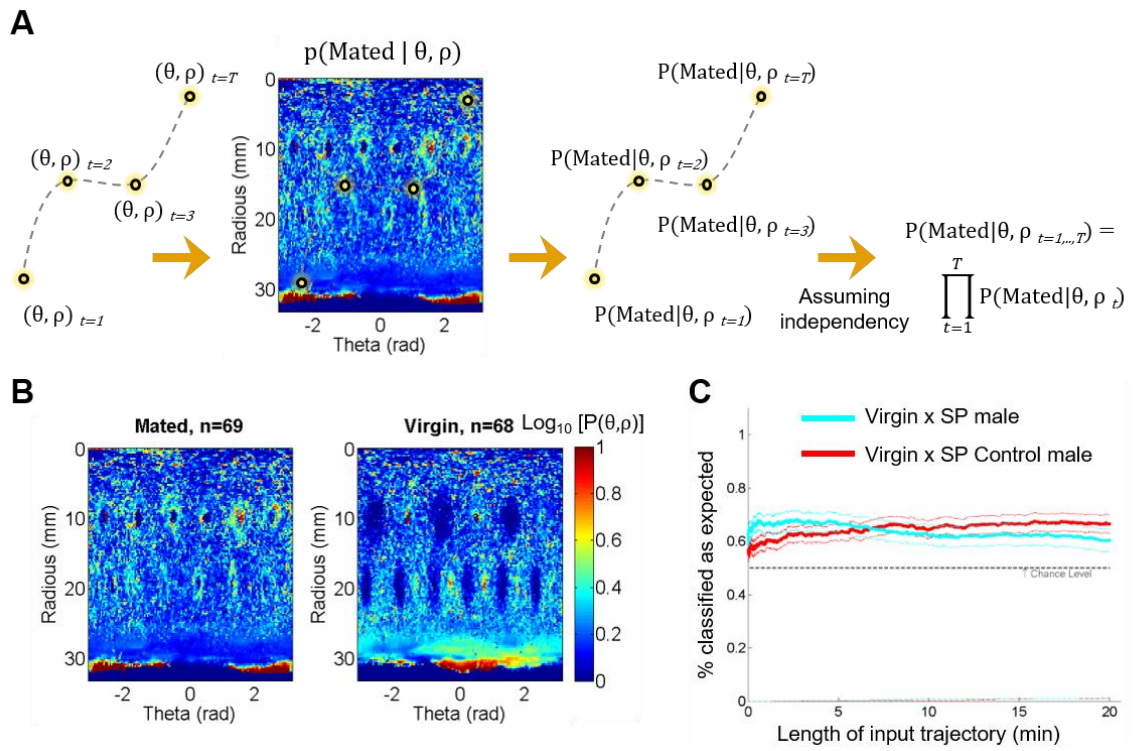

Figure 4.11 – Bayesian classifier of internal state condition based on positional preference

(A) Steps of the classification algorithm. First, we select a trajectory in the test flies and calculate the posterior probability of each point in the trajectory using the density map of posterior probabilities for each arena location. This density map was calculated using the Bayes' rule in which the likelihoods were the polar coordinate histograms of mated and virgin *Canton S* flies. Second, the posterior probabilities of each point in the trajectory are multiplied to obtain the posterior probability of that condition given the complete trajectory. The fly is classified according to the winning posterior probability. (B) Density maps of the posterior probabilities for mated and virgin flies. Colors indicate the posterior probability of the indicated condition for each location bin. 150 bins were used for each dimension. (C) Classification results for different trajectory lengths for virgins mated with SP mutant males (expected to behave like virgins) or SP control males (expected to behave like mated). Points in the input trajectories were spaced 100 ms between them. 10 trajectories of 20 min were selected for each fly at random starting points within the 120 min assay. The % of "correct" classification is the average across flies of the average of those 10 trials per fly.

Once optimized the posterior probabilities could act as descriptors of the behavioral elements that distinguish one internal state condition from another and therefore serve as a powerful phenotyping tool that would be very useful when combined with high-throughput genetic or neuronal screens.

4.2.3 Principal component analysis

The principal component analysis is a dimensionality reduction technique. Since many of the extracted parameters may be strongly correlated and therefore will not be telling us any new information about the behavior, we applied PCA to extract the principal components of variation that are linearly uncorrelated. The first principal component has the largest possible variance and from there on, each subsequent component captures as much variability as possible as long as it is orthogonal to all

previous components. A nice and clear example of the implementation of PCA using MATLAB built-in functions can be found here: http://www.mathworks.com/help/stats/quality-of-life-in-u-s-cities.html

The list of parameters we used in the PCA is shown in Table 4.1. We separated the parameters in 4 groups or classes: 1) *exploitation*: those parameters directly related with the time spent on yeast or sucrose and therefore increasing the probability to feed/exploit the resource; 2) *global exploration:* parameters related to the way the fly explore the food patches in the whole arena; 3) *patch exploration:* parameters related to the local exploration of the food patch; 4) *locomotor activity.*

Table 4.1 – List of behavioral parameters and their class

Parameter	Class
Total Y or S	Exploitation
Nº visits Y or S	Exploitation
Visit duration Y or S	Exploitation
Engagement Y or S	Exploitation
Nº encounters Y or S	Global exploration
YPI encounters	Global exploration
Y inter-visit distance	Global exploration
Transition to same, close or far yeast	Global exploration
Lag phase/Latency	Global exploration
Distance from Y or S	Patch exploration
Linear speed (in Y visits)	Patch exploration
Angular speed (in Y visits)	Patch exploration
Speed (outside visits)	Locomotor activity
% active/walking (outside visits)	Locomotor activity
% Time on edge	Locomotor activity
Edge activity	Locomotor activity

We used the PCA to compare the behavior of flies pre-fed AA+ suboptimal diet and AA- diet. The correlation matrices of these two conditions (Figure 4.12) show that the decision to engage (Engagement Y), rather than the decision to stay (Visit duration) or approach (Nº of Y encounters), has a stronger role in determining the total time spent on yeast (Total Y). In fact, the number of yeast encounters is negatively correlated with total time on yeast and positively correlated with locomotor activity parameters such as speed and percentage of time walking outside the patches. Interestingly, although the first two principal components account for 50% of the variance (Figure 4.13A), they do a very poor job separating the two internal state conditions (Figure 4.13B). As expected, the parameters with higher negative weight in the PC1 are the ones strongly correlated with the total time on yeast (Figure 4.13D); while the parameters with higher positive weight are those related to locomotor activity. This means that the difference between AA-deprived flies and suboptimally-fed flies does not lie in the global strategies that lead to higher times on yeast. Interestingly, the third principal component does a better job discriminating between these two internal state conditions (Figure 4.13C) and the parameters that have more weight in this component are those related to patch exploration, such as the speed inside the yeast patches and the global exploration parameters that directly relate to the eagerness of exploiting the yeast resource, such as the latency period (or lag phase) and the probability of returning to the same yeast patch (transition to same Y).

These results were already described and discussed in Chapter 2, but I wanted to highlight how this alternative analysis led us to the same conclusions, which is particularly important in cases where analyzing each parameter one by one is unfeasible or not practical. We also learned that multiple

parameters are necessary to describe, since we require 9 principal components to explain 90% of the variance in this data (Figure 4.13A).

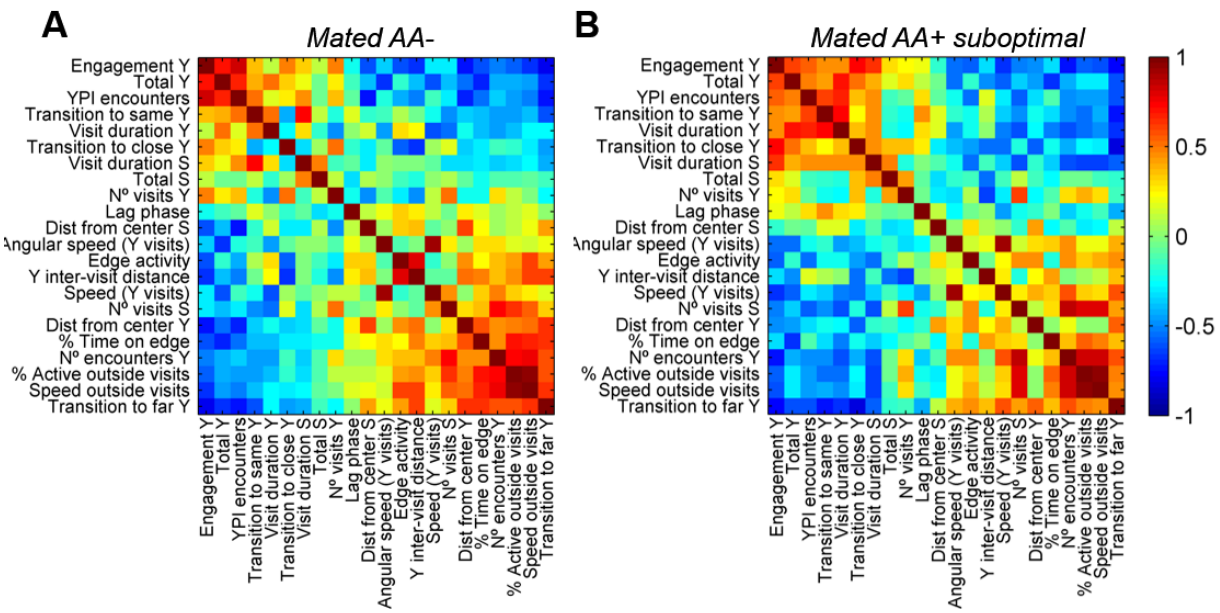

Figure 4.12 – Correlation matrix of behavioral parameters

Correlation matrix of the parameters showed in Table 4.1 for two internal state conditions: mated AA deprived flies and mated flies pre-fed suboptimal diet

4.2.4 Hierarchical clustering reveals clusters of locomotor activity

The negative correlation between the total duration of yeast micromovements (Total Y) and locomotor activity (speed outside visits) observed in the correlation matrix of AA-deprived flies (Figure 4.12A) is statistically significant and it seems to get weaker for the other internal state conditions as the flies spend less time on yeast (Figure 4.14). This negative correlation reminds me of an after-meal nap. It could be that the more they eat, the slower they get. However, from this experiment we cannot conclude if locomotor activity is a consequence or a predictor of time spent on yeast because due to the very short latency period of AA-deprived flies we do not have enough time to determine clearly the locomotor activity of these flies before they engage in the high yeast period.

It is known that flies display different levels of locomotor activity throughout the day (Gilestro 2012) and given the observed correlation between locomotor activity and time on yeast, it could be possible that the large variability observed in yeast times was partially due to the time of the day at which these experiments were performed. However, when we compared the total duration of yeast micromovements of each fly with the time of the day at which it was tested, we found no correlation (Figure 4.15).

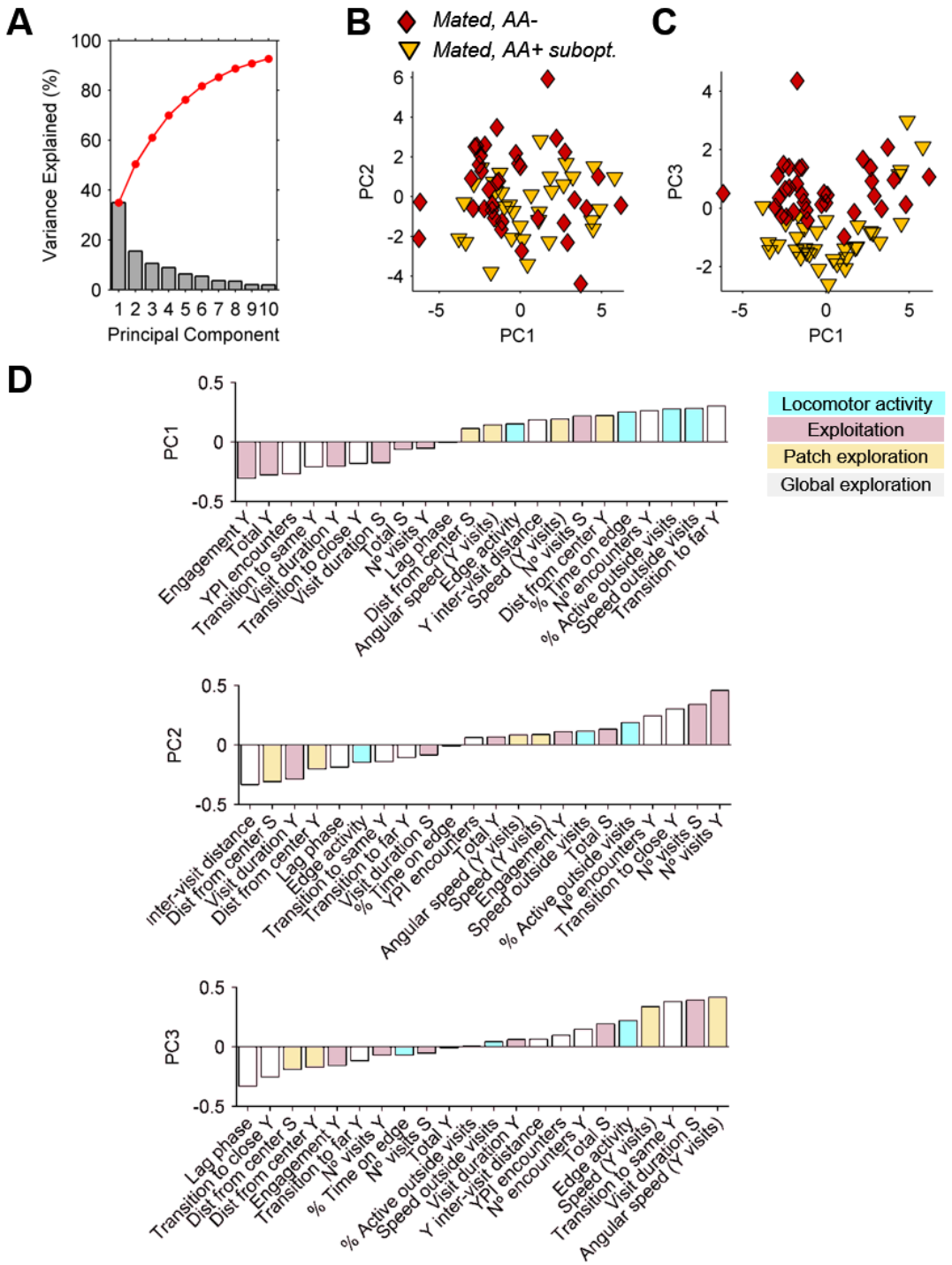

Figure 4.13 – PCA of behavioral parameters

(A) Cumulative percentage of the variance explained by the principal components. (B and C) Individual fly data points in the new parameter space defined by the PC2 vs PC1 (B) or PC3 vs PC1 (C). (D) Weight of each input parameter in the first three principal components. The colors indicate the group or class to which each parameter belongs.

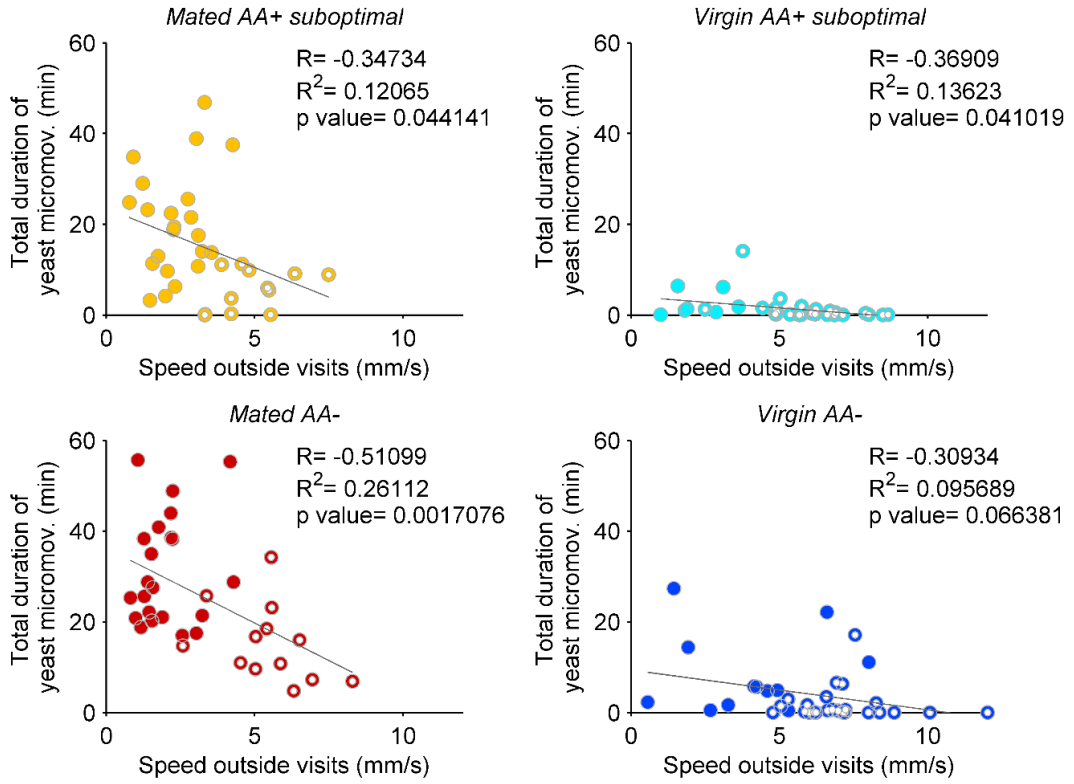

Figure 4.14 – Correlation between time on yeast and speed

Effect of internal state on the correlation between the total duration of yeast micromovements and the speed outside food patches. Each circle represents one fly. Open circles represent the flies that belonged to the "fast" cluster using the hierarchical clustering algorithm.

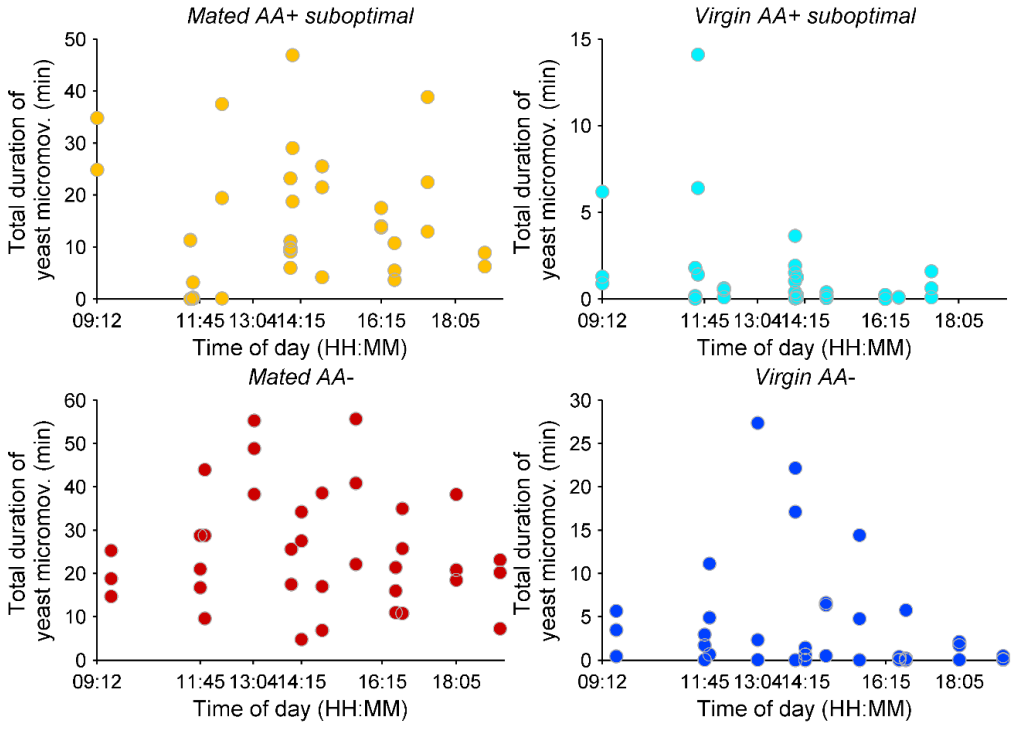

Figure 4.15 – No effect of time of day on total duration of yeast micromovements

The great variability in yeast total times and its inverse correlation with speed was also obvious in the ethograms (behavioral sequences), especially for the mated flies pre-fed suboptimal diet and for AA-deprived flies (Figure 4.16 right panels).

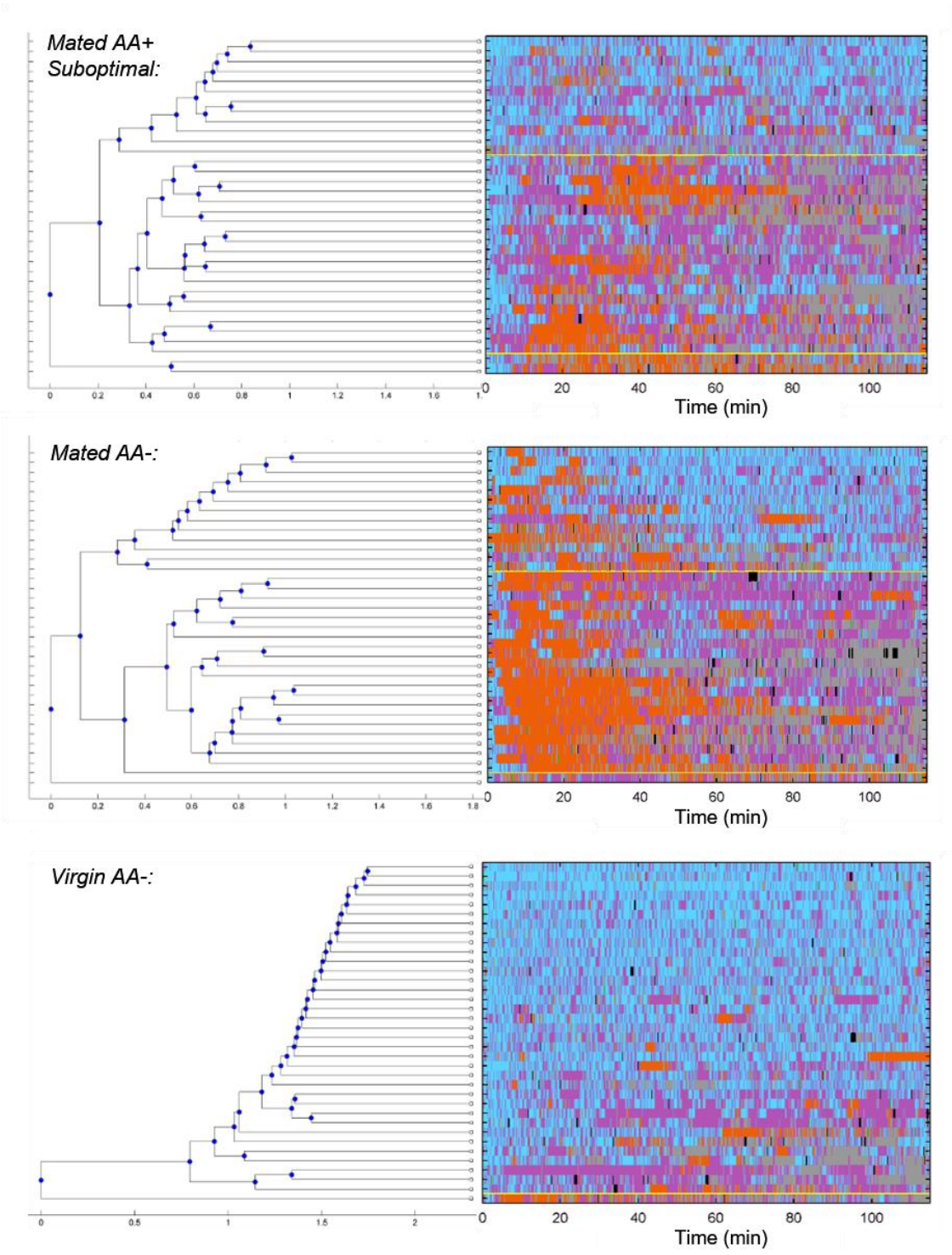

Figure 4.16 – Ethograms and "phylogenetic" tree for behaviors in the presence of food

Phylogenetic trees (left) of pairwise distances between sequences of behavior (right) in an arena with yeast and sucrose patches. Sequences were input as amino acid sequences in which each behavior was attributed one amino acid. Blue corresponds to walking, purple to micromovements outside the food, orange to yeast micromovements, black to sucrose micromovements and gray to resting.

We used bioinformatic tools to measure the distance between these behavioral sequences as if they were protein sequences: we attributed one amino acid to each behavior type e.g. walking, resting, micromovent on yeast. To measure the pairwise distance, we used MATLAB's built-in function

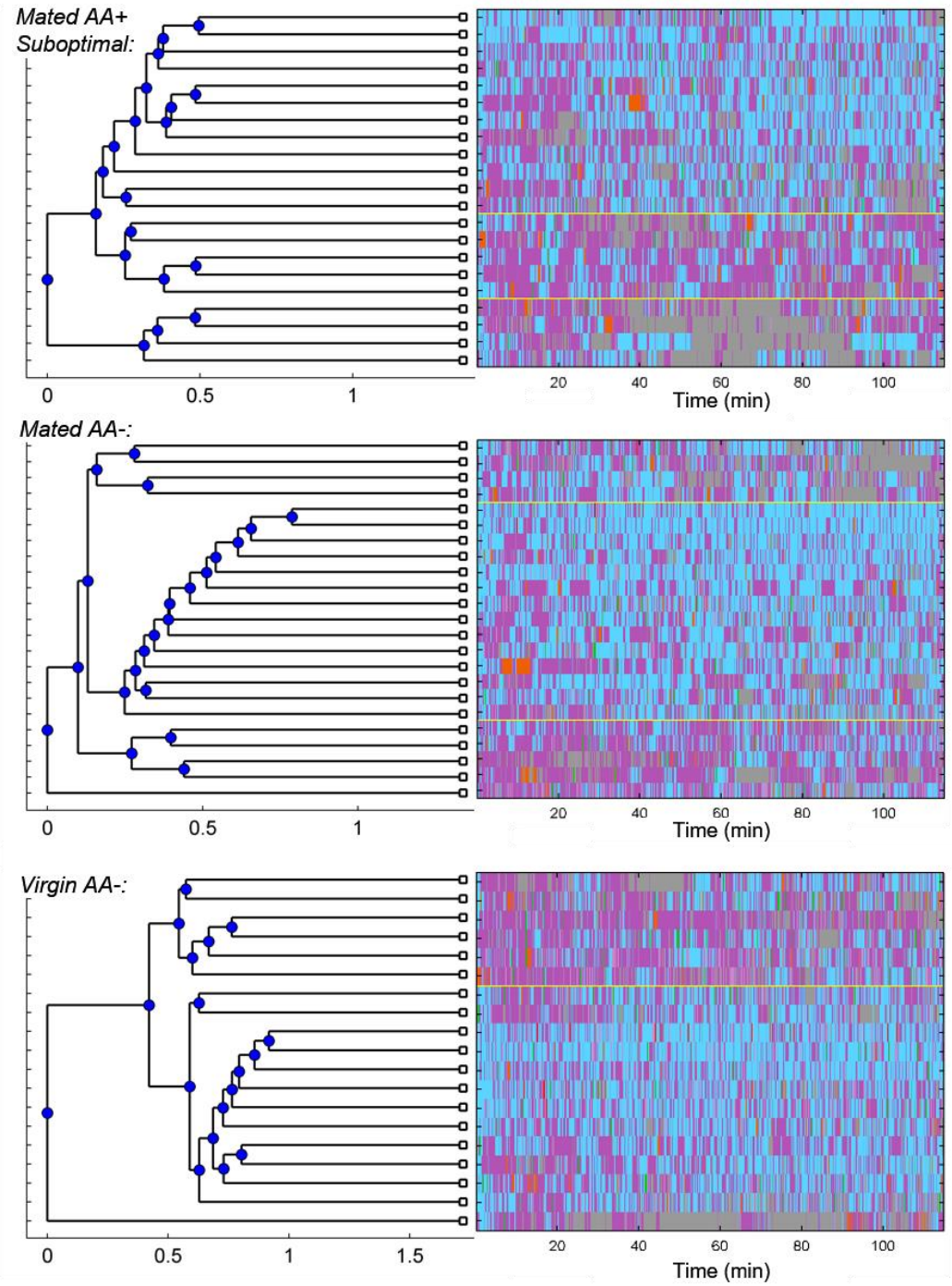

Figure 4.17 – Ethograms and "phylogenetic" tree for behaviors in the absence of food

Phylogenetic trees (left) of pairwise distances between sequences of behavior (right) in an arena with agarose patches (no food). Sequences were input as amino acid sequences in which each behavior was attributed one amino acid. Blue corresponds to walking, purple to micromovements outside the food, orange to yeast micromovements, black to sucrose micromovements and gray to resting.

seqpdist and to generate the “phylogenetic” tree or in other words, the hierarchy of similarity between the aligned sequences we used the function *seqlinkage* with the average distance (Figure 4.16 left panels).

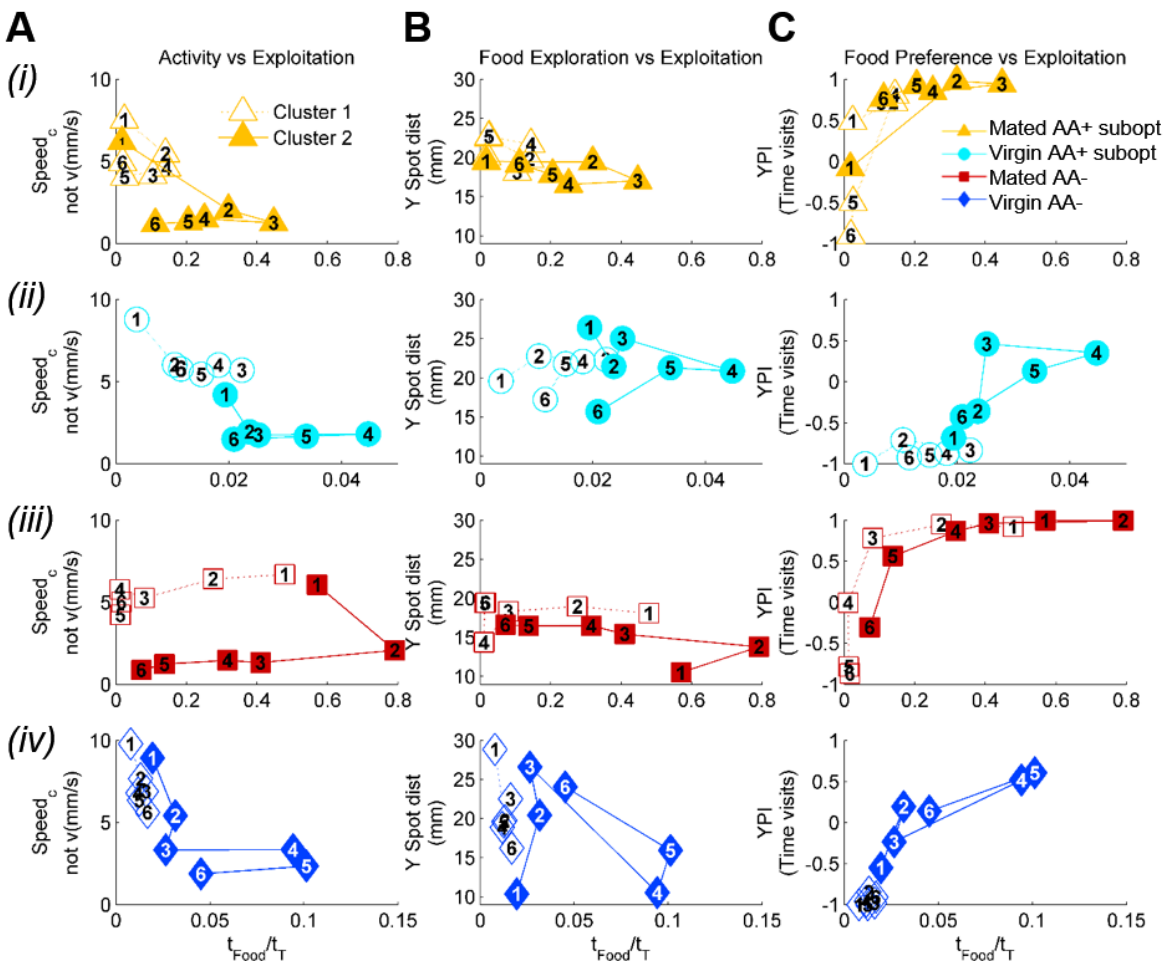

Figure 4.18 – Dynamics of exploitation and exploration parameters for each cluster

Locomotor activity, yeast exploration and yeast preference with respect to yeast exploitation for the different clusters within each internal state condition along the 2 hours of the tracking assay. Each data point shows the median value of the indicated parameters for the faster flies’ cluster (open symbols) and the slower cluster (filled symbols). The number inside the symbol indicates one of seven time segments along the two-hour-long assay as follows: 1) 0 – 5 min; 2) 5 – 15 min; 3) 15 – 35 min; 4) 35 – 55 min; 5) 55 – 75 min; 6) 75 – 95 min; 7) 95 – 115 min.

The main two clusters observed in the mated flies (Figure 4.16) corresponded mainly to flies that ate more and moved slower on one hand, and to flies that ate less and moved faster on the other hand. The same clusters shown in Figure 4.16 are shown in Figure 4.14 as open circles for the faster flies and filled circles for the slower flies. Similar fast and slow clusters are observed in the absence of food (flies tested in an arena with agarose spots) (Figure 4.17). It would be interesting to test if flies that display lower levels of locomotor activity in the absence of food correspond to those flies that present higher yeast times in the presence of food. To test how the clusters within the same internal state condition differ in their behavior along the course of the assay, we divided the 2 hours of the assay into 7 time segments and plotted the speed, the distance between visited yeast spots and the yeast

preference index against the time on food, and analyzed how the different clusters moved inside these two-dimensional spaces designed to report locomotor activity, exploration and preference with respect to yeast exploitation (Figure 4.18).

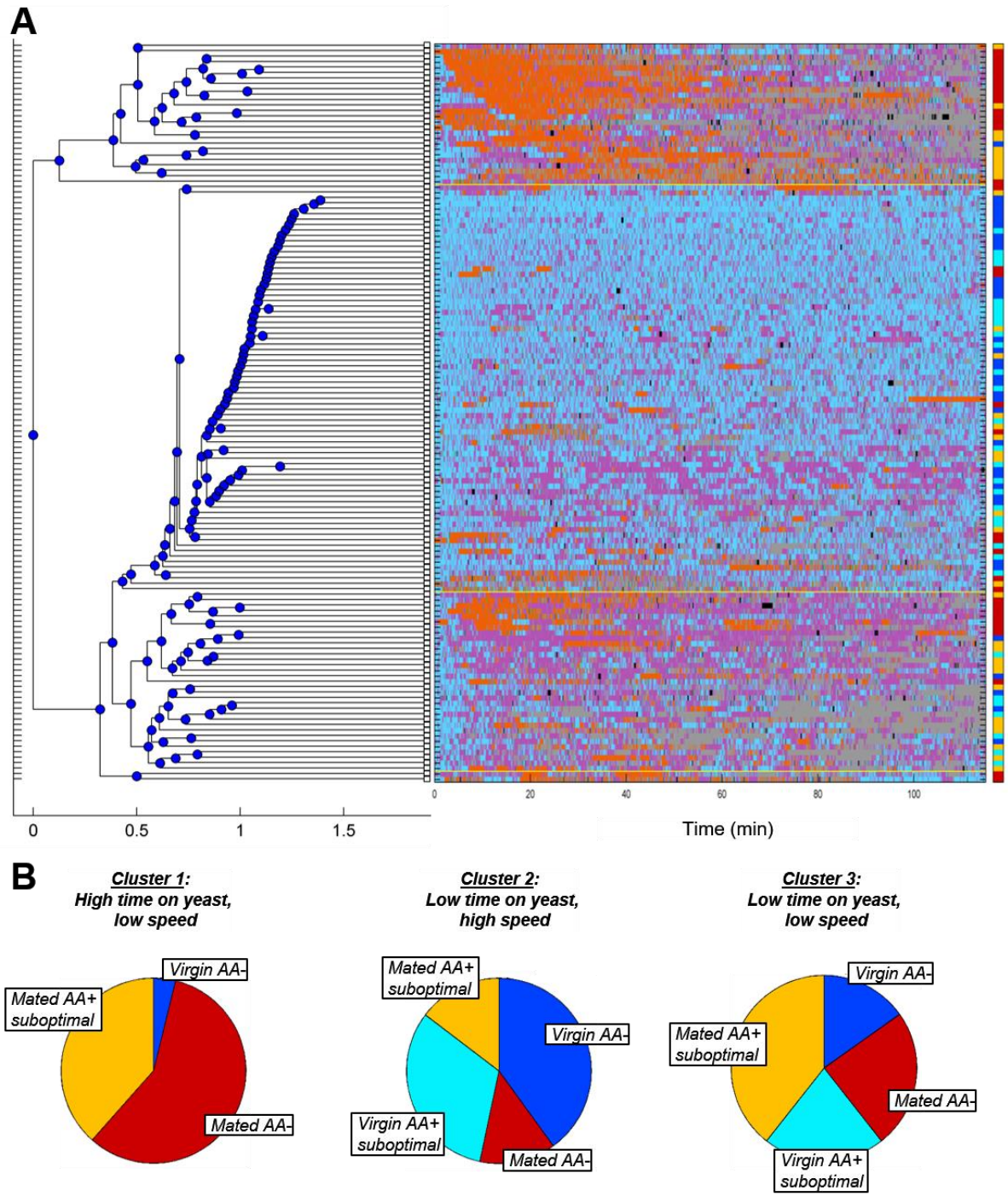

Figure 4.19 – Hierarchical clustering of ethograms of all 4 internal state conditions

Hierarchical clustering on aligned behavioral sequences of all flies belonging to 4 internal state conditions: Mated and virgin pre-fed suboptimal diet or a diet lacking AAs. (A) Left: "Phylogenetic" tree shows the distances between the behavioral sequences on the right panel. In the ethograms the color code is as indicated in Figure 4.16. The vertical bar on the right side of the ethograms indicates the internal state condition of the fly in that line. The color code for the internal states conditions is shown in B. (B) Proportion of internal state conditions in each of the clusters.

We observed that AA-challenged (AA+ suboptimal and AA-) mated flies start in the same position in the activity vs exploitation (Figure 4.18Ai and Aiii), but then move in opposite directions in the following time segments. We can also observe how the yeast preference decreases over time, in a similar way for both clusters of the AA-deprived mated flies (Figure 4.18Ciii).

Although this approach allows us to compare the behaviors of the different clusters within each internal state condition, we cannot compare across conditions, as the clusters were defined using the information for the flies of a single condition at a time. Therefore, we applied the same clustering algorithm to the pooled sequences of all 4 internal state conditions and observed 3 main clusters (Figure 4.19A): 1) High time on yeast and low speed, 2) Low time on yeast and high speed and 3) Low time on yeast and low speed. The first cluster was composed mainly by AA-challenged mated females (Figure 4.19B), while the second cluster was composed mainly by virgin females. The last cluster contained flies from all 4 internal states in similar proportions.

The fact that some of these behavioral sequences are closer across conditions than within conditions reveals another level of complexity in the analysis of behavior. How should we analyze them? Should we evaluate the effect of internal state on behavior only within clusters? In my opinion, one should do so if the clusters were clearly different from one another; however, in this case the transition across clusters is continuous. It is possible that aligning behavioral sequences on an absolute time scale is not the best input for a clustering algorithm: some flies start exploiting yeast earlier than others and they do so for very variable periods of times. We therefore decided not to use this clustering technique and simply compare all flies belonging to one internal state to all flies belonging to another internal state as we did in Chapter 2.

4.2.5 Visualizing the dynamics of a given parameter: example using the decision to stay in a yeast patch

One of the main advantages of using image-based tracking to capture the fly's behavior is the access we gain to the dynamics of any quantified parameter throughout the assay. To facilitate the visualization of the parameters we calculated (Table 4.1), I developed a flexible algorithm that plots any selected parameter during any defined set of time segments and compares it across any set of selected conditions. The output can be shown as boxplots during discrete time segments with the results of the statistical comparison across internal states (Figure 4.20A), as rolling medians to observe a more continuous behavior of the parameter (Figure 4.20B) or as distributions of two types: histograms (Figure 4.20G top panels) or complementary cumulative distributions special depicting heavy-tail distributions (Figure 4.20G bottom panels). The algorithm also allows to set different time ranges per fly which facilitates different alignments of the fly data (Figure 4.20E and F).

Interesting additional information can be obtained from analyzing the dynamics of a given parameter: a good example was shown for the *Orco* mutants in Figure 2.7B, where the total time spent on yeast was the same for the mutants and wild type control, except that there was a delay that was only observable when we plotted the behavior of this parameter over time. In a similar manner, the average duration of yeast visits is not significantly different between mated flies pre-fed suboptimal diet and

those pre-fed AA- diet when is calculated for the whole duration of the assay (Figure 2.3D). However, when we observe the dynamics of this parameter it is possible to see that they differ greatly during the first 10 minutes of the assay (Figure 4.20A and B). Nevertheless, when we looked at the ethograms of the flies for these two internal state conditions, we saw that most of that difference in the first minutes of the assay was due to a difference in the latency flies show to engage in a long (≥ 30s) yeast visit for the first time (Figure 4.20C and D). When we aligned the absolute assay time to set x = 0 when the

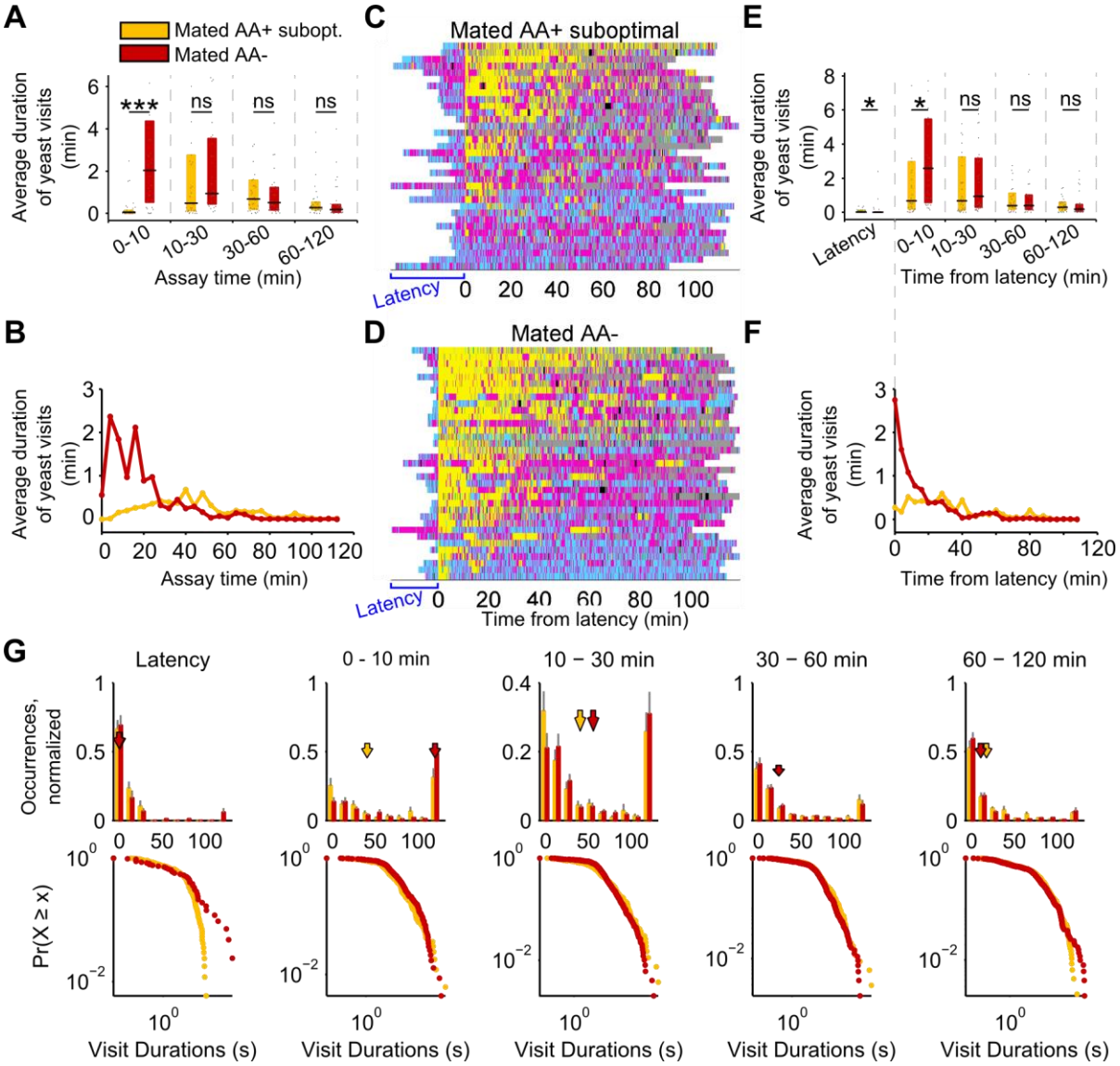

Figure 4.20 – Yeast visit duration dynamics for AA-challenged flies

(A) Average yeast visit duration for the indicated time segments of the 2-hour-long assay for flies pre-fed a suboptimal diet (yellow) and AA- diet (red). (B) Rolling median of the average duration of yeast visits using a 5 minute window and a step of 4 minutes. (C, D) Behaviors displayed by single flies pre-fed suboptimal diet (C) or AA- diet (D). Each row represents the ethogram a single fly aligned to the latency to engage in the first "long" (≥ 30s) yeast visit. Yellow: yeast micromovements. Black: sucrose micromovements. Pink: micromovements outside the food patches. Blue: walking bouts. Gray: resting bouts. Green: sharp turns. (E) Average duration of yeast visits for the indicated time segments counting from the latency onwards. (F) Rolling median of the average duration of yeast visits using a 5 minute window and a step of 4 minutes. All flies were aligned to the latency period as x = 0. (G) Average distribution (top panels) and Complementary cumulative distribution function (bottom) for yeast visit durations. Single dots represent one yeast visit. Arrows indicate median of average visit duration for flies pre-fed a suboptimal diet (yellow) and AA- diet (red).

latency period is over as shown in Figure 4.20C and D, we observed that the durations during the first 10 min after the latency period were not as different as they were in the first 10 min of the assay (Figure 4.20E and F). Although Figure 4.20E shows the median and the IQR for the average yeast visit duration, this parameter has a heavy-tailed distribution (Figure 4.20G) and therefore the "average" or the median of the average is not the most probable outcome for this parameter (see the arrows indicating the median on top of the distribution in Figure 4.20G). Even in this case, the distributions during the first ten minutes after the latency period do look different and we therefore pinpoint another subtle difference between flies pre-fed suboptimal diet vs those pre-fed AA- diet.

The definition of latency was inspired in the work of (Root et al. 2011), where they measure the time elapsed until flies spend more than 5 seconds inside the food-odor area and use this metric to quantify the modulation of olfactory perception by starvation. We selected a 30-second threshold based on the distribution of yeast visit durations (Figure 4.21): for all conditions 70% of the visits durations were below 30s (vertical lines). We also based our decision on the alignment of the ethogram plots based on the defined "long" visit threshold (Figure 4.20C and D).

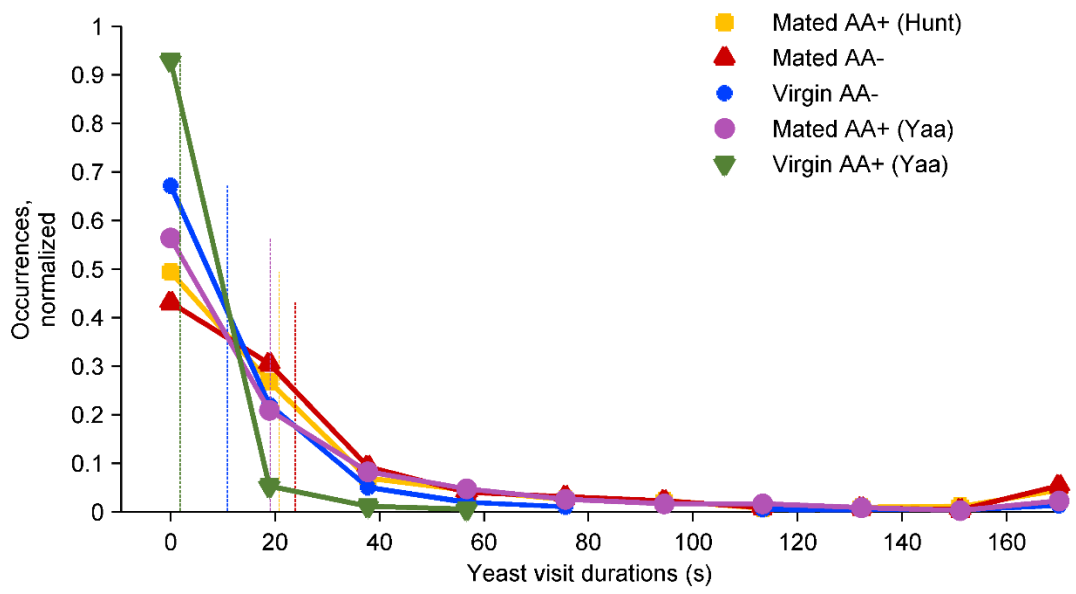

Figure 4.21 – Distribution of yeast visit durations

Distribution of yeast visit durations. The vertical dotted lines indicate the x-bin where the cumulative distribution reaches 70% for each internal state condition (shown in different colors).

4.3 Nutritional geometry

A great body of work led by Stephen Simpson and co-workers, using a nutritional geometry framework, has shed light in our understanding of the rules of compromise that animals follow when a particular intake target cannot be reached (Simpson and Raubenheimer 2012). They demonstrated in their protein leverage theory that animals prefer to prioritize protein at the expense of overconsuming fat and carbohydrates; a decision that might lead to obesity (Simpson and Raubenheimer 2005).

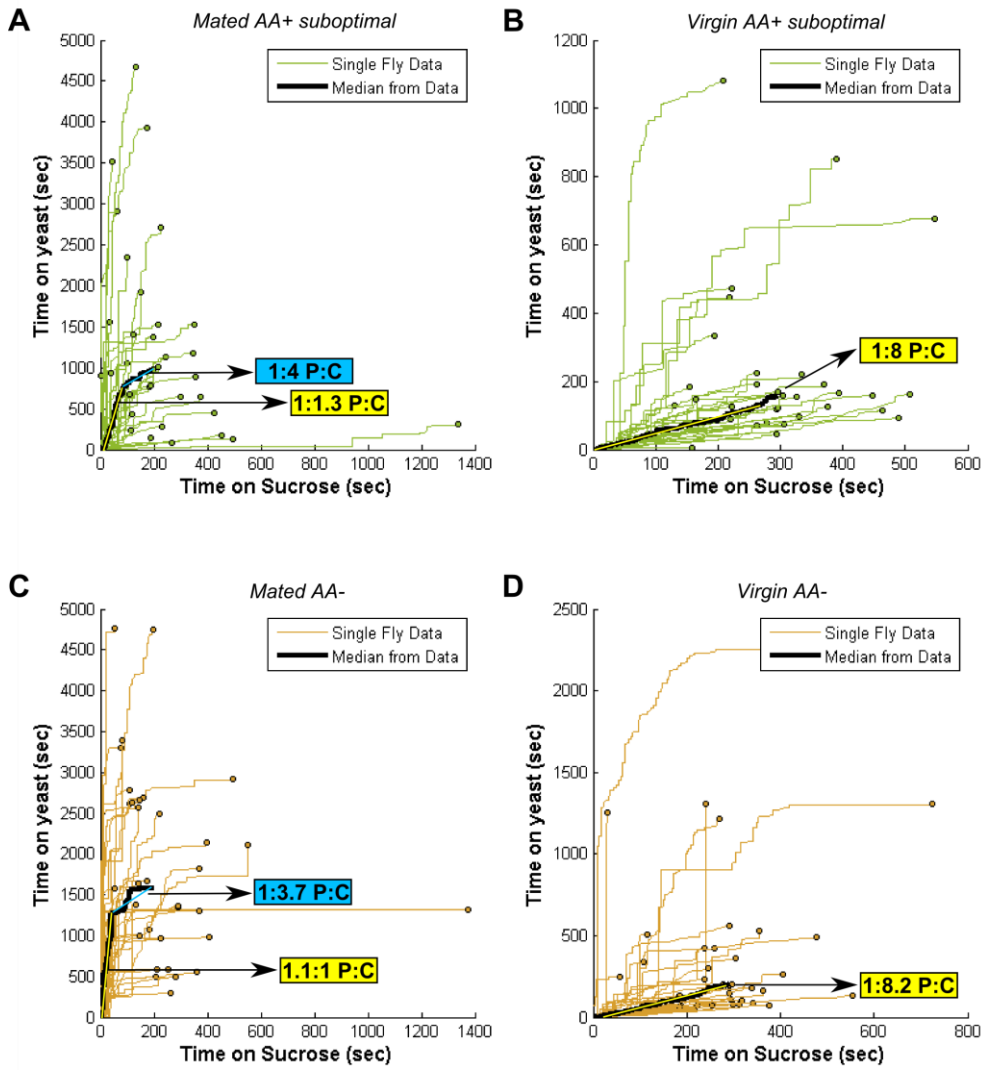

Figure 4.22 – Nutritional geometry of yeast and sucrose decisions

Nutritional geometry of yeast and sucrose decisions for (A) Mated AA+ suboptimal, (B) Virgin AA+ suboptimal, (C) Mated AA- and (D) Virgin AA-. Single lines correspond to trajectories followed by single flies. Circles at the end of the trajectories indicate the accumulated yeast and sucrose time at the end of the 2-hour-long tracking assay. Black thick line indicates the population median. The protein:carbohydrate ratios (P:C) calculated for the yellow and blue straight lines were based on the protein and carbohydrate composition found in SAF-Instant® Yeast Red Label from Lesaffre used for these experiments, per 100g of yeast: 50 g of protein and 33 g of carbohydrates.

This framework was also used to evaluate the effect of diet composition on the flies' reproductive output and lifespan (Skorupa et al. 2008; Lee et al. 2008). Lee and colleagues showed that given a choice between sugar and yeast, flies tend to balance the consumption of these two nutrients such that they consume a 1:4 Protein:Carbohydrate ratio (P:C), maximizing life time egg production a measure related to fitness. The dynamics of the nutrient decisions that lead to reach such ratio at a shorter time scale is still poorly understood. Our image-based tracking setup allows us to look at the step-by-step decision process and how it is affected by deviations from homeostasis (e.g. AA deprivation) or mating status at the individual level.

Mated flies showed very high variability in the proportion of yeast and sucrose times, leading to a wide range of accumulated P:C ratios at the end of the assay (Figure 4.22A and C). Most AA-challenged mated females showed an initial phase where they are mostly spending time on yeast and a later phase where they switch their preference towards sucrose. This population tendency is captured in the population median to which I have fitted two straight lines, a yellow line that measures the ratio in the yeast-oriented phase and a blue line that measures the ratio in the sucrose-oriented phase. Interestingly, for both mated AA-challenged females, the yeast-oriented phase has a P:C ratio around 1:1, while the second sucrose-oriented phase with a P:C ratio around 1:4, which surprisingly matches the ratio previously reported by (Lee et al. 2008). Virgins, on the other hand, have a strong carbohydrate drive, with P:C ratios around 1:8 that are kept more or less constant throughout the assay (Figure 4.22B and D).

4.3.1 Do flies go back to the fully-fed state after 2 hours of exposure to yeast?

We showed in section 2.3.7 that flies can dynamically modulate their exploitation and exploration patterns as they satiate. We also showed that the parameters related to eagerness revert back to the values of fully-fed flies after the 2 hours of the assay (Figure 4.23A-C).

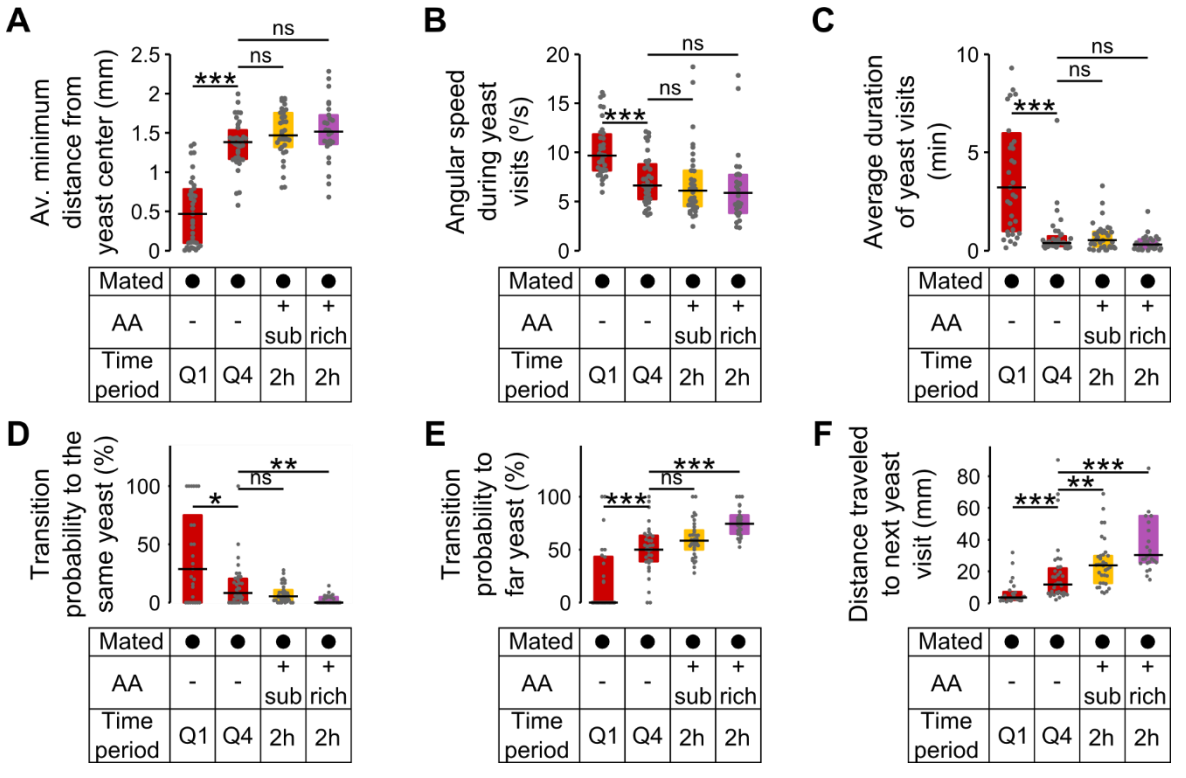

Figure 4.23 – Exploration parameters do not revert to fully fed state after 2 hours

(A-C) Exploitation parameters from first yeast quartile (Q1) and fourth yeast quartile (Q4) of AA-deprived mated females compared to the values observed in flies pre-fed a rich and a suboptimal diet along the 2 hours of the video tracking assay. (A) Average minimum distance of the head to the center of the yeast patch, (B) angular speed, during yeast visits. (C) Average duration of yeast visits. (D-E) Exploration parameters. (D) Probability of returning to the same yeast patch, (E) Probability of transitioning to a far yeast patch (F) Average distance covered during transitions to yeast visits. *ns*, not significant ($p \geq 0.05$), ***$p < 0.001$, significance was tested by Wilcoxon rank-sum test with Bonferroni correction.

What about the exploration parameters? Parameters such as the probability of transitioning to a far yeast patch, the probability of returning to the same yeast patch and the distance traveled between yeast visits do not revert back to the values of fully-fed flies (Figure 4.23D-F). If we assume these parameters are reporting the internal state of the fly, given that they do change in the direction expected of more satiated flies, this result suggests that 2 hours is not enough to reconstitute the full physiological state of a fly that has been fed an AA+ rich diet.

4.4 The role of sensory perception and octopamine in yeast-related foraging behavior

4.4.1 Is olfactory perception modulated by AA deprivation?

Testing *Orco* mutant flies in our tracking setup demonstrated that OR-mediated olfaction is key to recognize yeast *efficiently* as an appropriate food source after AA deprivation. Given this important role in yeast recognition, one can hypothesize that olfactory perception might be modulated by AA deprivation. Indeed, we did observe a decrease in the time elapsed until flies engage in a yeast-intensive period after AA-deprivation (Figure 4.24A) and we have shown that this latency period is severely affected in flies with impaired olfaction (Figure 2.7C).

We also tested antennectomized flies to evaluate the role of the antennae, the main olfactory organ of the fly, in the response to AA deprivation (Figure 4.24B). The results were inconclusive as half of the tested flies behaved as the AA deprived controls with a very short latency, while the other half behaved like the *Orco* mutant flies with latency values over 5 min yielding no statistical difference between flies lacking both antennae and the handling controls (Figure 4.24C). Still, these results could suggest a role of the maxillary palps, the second olfactory organ in mediating the efficiency of yeast recognition.

The decrease in latency observed in *Canton S* (wild type) flies is not due to increased locomotor activity: AA-deprived flies moved as much, moved as fast and encountered yeast at the same rate as non-deprived flies during the latency period (Figure 4.24D). Yet, it can be attributed to a higher visual saliency of yeast patches as these experiments were performed with white light making the creamy yeast patches clearly distinguishable from the transparent sucrose patches.

The approach to yeast spots, as measured by the rate of yeast encounters, is also greatly increased in AA-deprived flies (Figure 4.24E), but this increase might be due to the high rate of returning to the same patch that these flies display (Figure 4.24F). Therefore, to correct for this effect, we merged the encounters that were due to revisits into the same encounter and looked at the yeast preference index (YPI) of the food encounters:

$$YPI_{encounters} = \frac{Nº\ yeast\ encounters - Nº\ sucrose\ encounters}{Nº\ yeast\ encounter + Nº\ sucrose\ encounters}$$

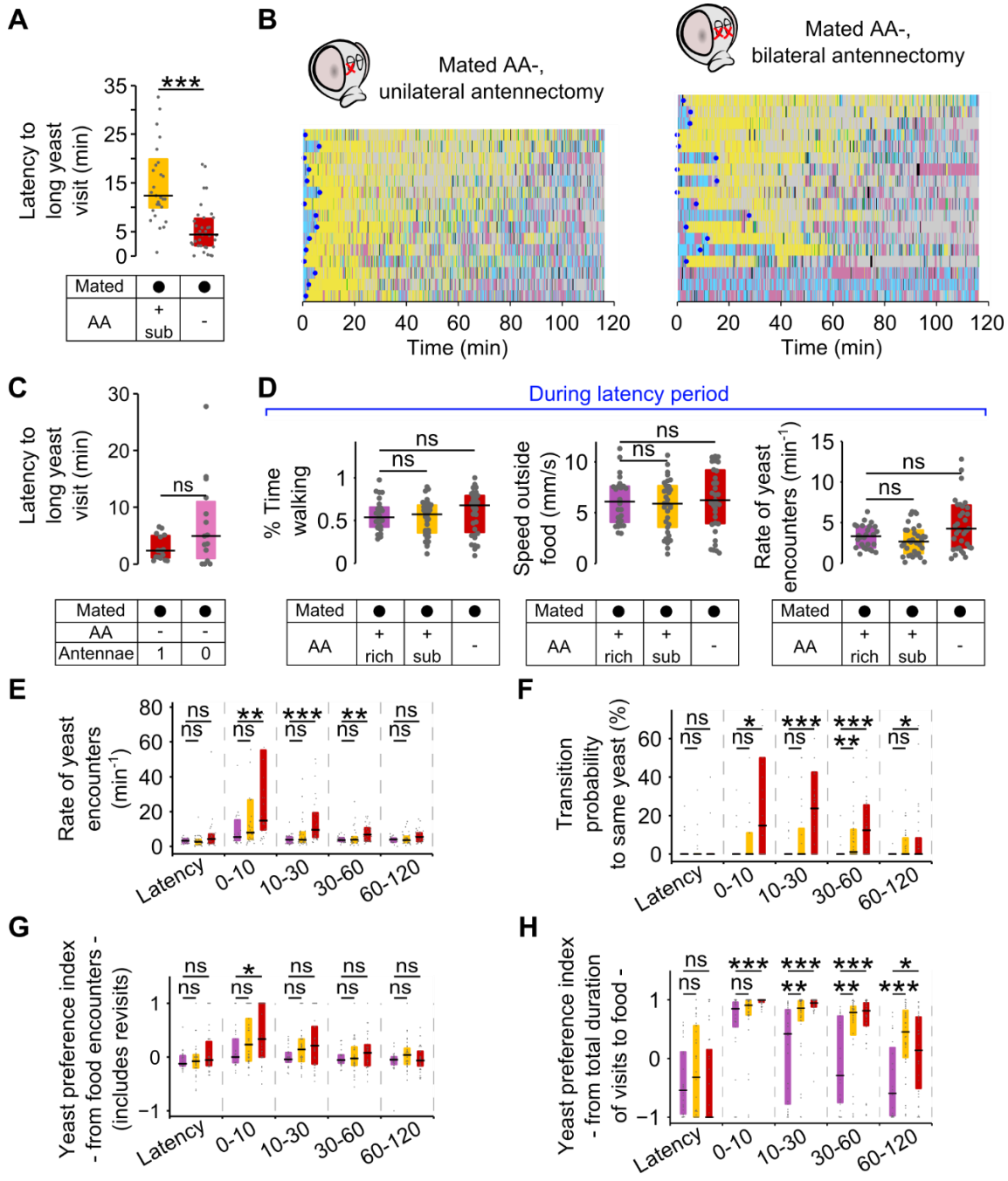

Figure 4.24 – Olfaction might be modulated by AA deprivation

(A) Effect of AA deprivation on the time elapsed until the fly engages in the first "long" (≥ 30 s) yeast visit. (B) Behaviors displayed by flies with unilateral or bilateral antennectomy, along the 120 minutes of the assay. Each row represents the ethogram of a single fly. The third antennal segments were removed 24h before the assay using ice as anesthetic. Yellow: yeast micromovements. Black: sucrose micromovements. Pink: micromovements outside the food patches. Blue: walking bouts. Gray: resting bouts. Green: sharp turns. Blue circles indicate the latency (see C) of each fly. (C) Effect of antenna removal on the time elapsed until the fly engages in the first "long" yeast visit. (D) Locomotor activity of mated flies during the latency period. (E) Effect of internal state on the decision to approach a yeast patch quantified as the number of yeast encounters per minute of walking outside the food patches (rate of yeast encounters). Flies from different internal state conditions were compared in different time segments counting from the latency of each fly. (F) Effect of internal state on the probability of returning to the same patch for different time segments aligned to the latency of each fly. (G) Effect of internal state on the yeast preference index (YPI) based on food encounters, for different time segments aligned to the latency of each fly. (H) Effect of internal state on the YPI based on duration of food patch visits, for different time segments aligned to the latency of each fly. The box plots in C-F correspond to the same internal state conditions labeled in B.

This metric quantifies the preference in approach to either yeast or sucrose. Surprisingly, the values for this preference index were close to zero for mated flies pre-fed a rich diet during the first 10 minutes after the latency period (Figure 4.24G, focus on the 0-10 min segment). YPI = 0 means no preference to approach either yeast or sucrose, even when in this particular time segment these flies prefer to spend, in proportion, more than 90% of the time on yeast rather than on sucrose, as shown by an alternative quantification of the YPI based on food visit durations:

$$YPI_{duration\ of\ food\ visits} = \frac{Total\ duration\ of\ yeast\ visits - Total\ duration\ of\ sucrose\ visits}{Total\ time\ spent\ visiting\ food}$$

This YPI based on durations is almost 1 for these flies (Figure 4.24H). The differences between these two measurements of yeast preference speak in favor of a modulation of the sensory perception (visual or olfactory) of the yeast resource after deprivation, as the high yeast preference observed fully-fed flies during this time period is not mediated by an increased yeast approach or attraction at distance. In support of this hypothesis, AA-deprived flies show a slightly higher YPI based on encounters, which means that these flies are biasing their approach towards yeast patches in a higher proportion than full-fed flies during the same time segment (Figure 4.24G).

These results suggest that although the visual component cannot be ruled out at the moment, the slight increase in approach preference towards yeast in AA-deprived mated females could be due to an enhanced olfactory response to yeast volatiles.

4.4.2 Gustatory stimuli is necessary to sustain interest for yeast after AA deprivation

To investigate the role of gustatory stimuli in resource exploration and exploitation we used the Gal4-UAS system (Brand and Perrimon 1993) to suppress synaptic transmission in neurons that express the *Pox neuro* (*Poxn*) gene, by expressing tetanus toxin (TNT) under the control of the *Poxn* promoter. TNT is a protease that specifically cleaves synaptobrevin, an integral membrane protein of small synaptic vesicles (Schiavo et al. 1992). *Poxn* is a gene involved in the appropriate development of gustatory bristles on wings, legs and labellum and in specifying the connectivity of the corresponding chemosensory neurons (Nottebohm, Dambly-Chaudière, and Ghysen 1992).

The behavior of the Gal4 and UAS controls was clearly different from the previously described *Canton S* mated females. Boll and Noll (2002) developed a *Poxn-Gal4* line to gain additional information about the spatial and temporal expression patterns of Poxn. The *Poxn-Gal4 (*herein after *Poxn* >) control flies showed very low interest for yeast when pre-fed a suboptimal diet but showed a robust increase in the total duration of yeast micromovements (Figure 4.25 left panels) and visits (Figure 4.26A) after AA deprivation. On the other hand, the *UAS-TNT* (or simply *TNT*) control flies showed an expected high interest on yeast when pre-fed suboptimal diet but failed to show a robust increase in the total duration of yeast visits after AA deprivation (Figure 4.26A). Despite these differences, both control flies showed a clear decrease in the latency to engage in the first long (> 30s) yeast visit (Figure 4.26I). *Poxn >TNT* flies showed a significant decrease in the total duration of the yeast visits when compared to control flies after AA deprivation but not after being pre-fed a suboptimal diet (Figure 4.26A).

A look into the dynamics of yeast visits highlights the fact that after AA deprivation the control flies sustain yeast visits for a shorter period of time than the corresponding *Canton S* flies (Figure 4.26B). Yet, *Poxn>TNT* flies have an even shorter high-yeast period.

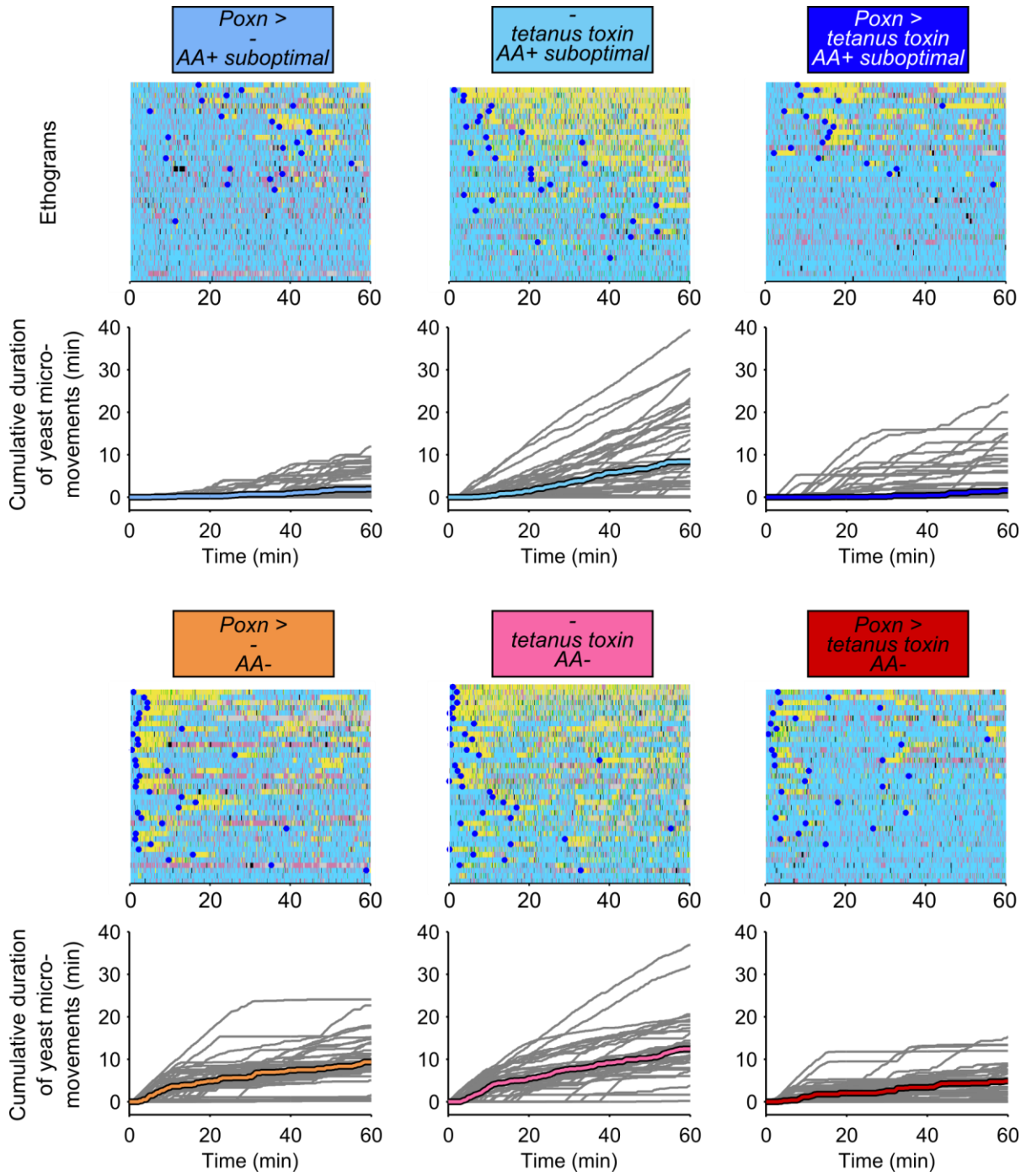

Figure 4.25 – Effect of AA deprivation on the behavior of *Poxn > TNT* flies and corresponding control flies

Behaviors displayed by single flies in which *Poxn-Gal4 (Poxn>)* is driving the expression of tetanus toxin (TNT) and the respective driver and UAS control flies, for two metabolic conditions: flies pre-fed suboptimal diet and AA-deprived flies (n=37-38). In the ethograms each row represents a single fly, with the following color code: Yellow: yeast micromovements. Black: sucrose micromovements. Pink: micromovements outside the food patches. Blue: walking bouts. Gray: resting bouts. Green: sharp turns. In the cumulative duration of yeast micromovements, the gray lines correspond to single flies and the thick colored lines indicate median.

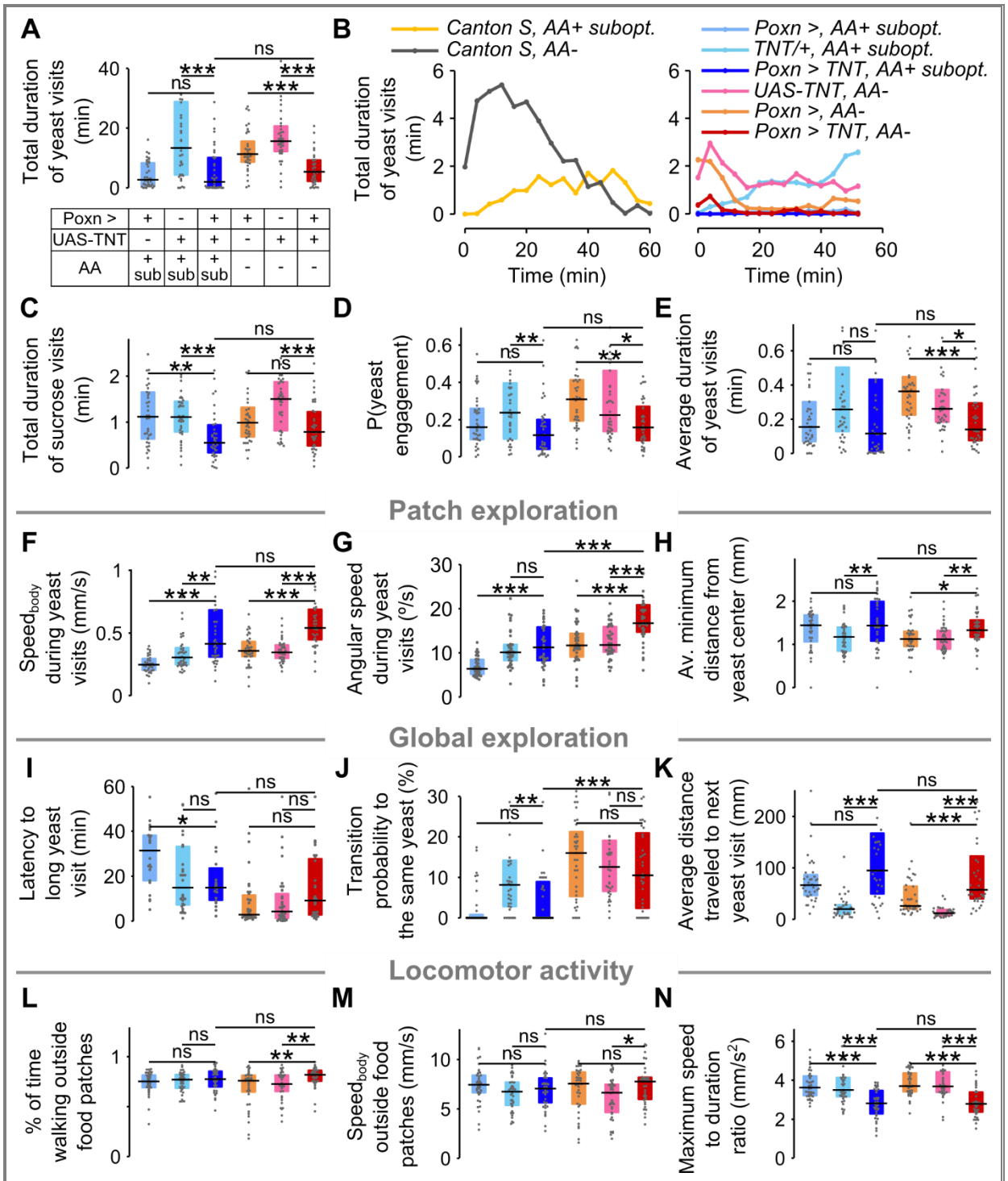

Figure 4.26 – *Poxn*+ neurons are necessary to sustain interest for yeast after AA deprivation

(A, C-N) Effect of AA deprivation on the indicated parameter for flies in which *Poxn-Gal4 (Poxn>)* is driving the expression of tetanus toxin (UAS-TNT or simply TNT) and for the respective driver and UAS control flies. The legend of the metabolic state and genotype is as shown for panel A. (B) Rolling median of the total duration of yeast visits using a 5 minute window and a step of 4 minutes for the indicated conditions.

The total duration of sucrose visits is reduced in the *Poxn>TNT* flies after being pre-fed a suboptimal diet but not after AA deprivation (Figure 4.26C).

The observed decrease in the total duration of yeast visits in the *Poxn>TNT* flies after AA deprivation is due to a decrease in both the decision to engage (Figure 4.26D) and the decision to stay in the yeast patches (Figure 4.26E). Interestingly, these flies showed higher locomotor activity at the yeast patches than the controls (Figure 4.26F and G), typically observed in wild type flies that are eager to eat from yeast (Figure 2.4). However, *Poxn>TNT* AA-deprived flies showed a higher distance to the center of the yeast patches (Figure 4.26H) and did not show shorter latency than the control flies (Figure 4.26I). These four parameters where shown to be associated to full AA deprivation in *Canton S* flies (Figure 2.4) and these results might indicate that different mechanisms mediate different aspects (local exploration on one hand and increased activity on the other hand) of the eagerness-related phenotypes observed after AA deprivation.

A closer look into the raw data (Figure 4.25 right panels) shows that most of the *Poxn>TNT* AA-deprived flies do not even show a clear high-yeast period and there is a higher proportion of yeast non-eaters, which might suggest that external taste stimuli is important for the initiation of yeast-intense periods. Together with the results obtained with the *Orco* mutant flies, this results indicate that the integration of both taste and olfactory stimuli is necessary for the efficient recognition of the yeast patches as appropriate food sources. In terms of global exploration, *Poxn>TNT* AA-deprived flies showed no increased rate of returns to the same yeast patch (Figure 4.26J) but showed increased distances when moving from one yeast visit to the next (Figure 4.26K). This last result is consistent with the observed increase in activity outside of the food patches when compared to controls (Figure 4.26L and N). These flies kept a similar speed than that of controls (Figure 4.26M) but showed a different walking pattern as reported by a lower maximum-speed-to-duration ration (Figure 4.26N).

Importantly, although *Poxn* mutant flies are not completely taste-blind as they have functional internal sense organs in the pharynx (LeDue et al. 2015), *Poxn>TNT* flies might be as the *Poxn-Gal4* driver was reported to express in neurons innervating the labral sense organ in the pharynx (Boll and Noll 2002). Internal sense organs play a critical role in the robust consumption of sugar in the absence of external gustatory stimuli (LeDue et al. 2015; Yapici et al. 2016). It is possible that *Poxn>TNT* flies cannot sustain longer yeast visits after engagement because the neurons innervating the internal sense organs are silenced. Acute manipulations of the different gustatory organs in a *Poxn* mutant background using the flyPAD technology (Itskov et al. 2014) could shed more light into the different roles of the external and internal gustatory organs in the initiation of feeding and in the continuation of feeding after initiation.

4.4.3 Octopamine is required for postmating yeast appetite

Octopamine regulates important aspects of female reproductive physiology such as ovulation, egg laying and female receptivity after copulation (M Monastirioti, Linn, and White 1996; Maria Monastirioti 2003; Cole et al. 2005; Rezával et al. 2014). We tested the effect of depleting octopamine in the feeding behavior of mutants for the gene encoding Tyramine β-hydroxylase (TβH), an enzyme

required for the biosynthesis of octopamine. We found that AA-deprived mated flies lacking octopamine behaved like wild type virgin flies: They showed similar total number of yeast sips (Figure 4.27A) with the same feeding microstructure with longer inter-burst-intervals (Figure 4.27B) and lower sips per burst (Figure 4.27B) than those observed for mated *Canton S* (wild type) females. These results demonstrate that octopamine is required for the postmating increase in yeast feeding. This finding was published in (Walker, Corrales-Carvajal, and Ribeiro 2015).

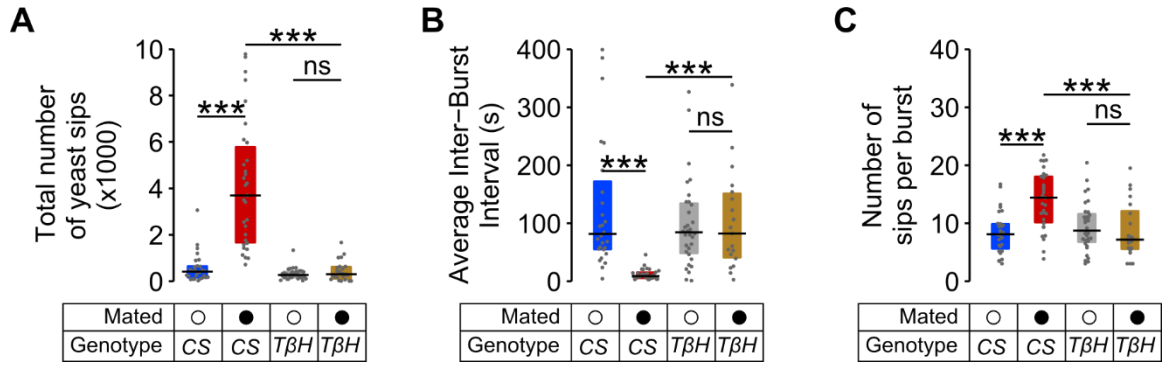

Figure 4.27 – Octopamine is required for postmating yeast appetite

(A-C) Effect of *TβH* mutation on the postmating yeast appetite and feeding microstructure. (A) Total number of yeast sips, (B) Average inter-feeding burst-interval, (C) Number of sips per feeding burst for AA-deprived *Canton S* and $T\beta h^{nM18}$ females, using the flyPAD assay. *ns*, not significant ($p \geq 0.05$), ***p <0.001, significance was tested by Wilcoxon rank-sum test with Bonferroni correction.

Chapter 5. General discussion

During this project we built a machine-vision setup that tracks the position and orientation of single flies as they walk in a foraging arena containing several food patches of different quality. We performed a detailed characterization of the exploration patterns and nutrient decisions taken by the flies and evaluated how internal state and sensory perception modulated the fly's behavior. We demonstrated that our automated system can be used to study the underlying neuronal and molecular mechanisms of nutrient choice.

In this chapter I discuss some insights obtained from this work, I speculate about the implications of some of the findings and few proposals for future work.

5.1 The role of sensory perception in different aspects of nutrient choice

We found that pre-feeding flies a diet that had an imbalanced amino acid (AA) ratio and yet the same amount of biologically available nitrogen, was enough to elicit a change in the decisions to stop at and leave the yeast patch, as well as a change in the yeast exploration patterns, decreasing the probability of transition to far patches and increasing the probability of returning to the same patch. Flies that were completely deprived from AAs did not change the decision to stop at and leave the yeast patches, but continued to narrow their exploration showing an even higher rate of returns to the same patch. They also showed a higher rate of approach to yeast and a higher eagerness to exploit it, demonstrated by the reduced latency to engage yeast at the beginning of the assay and a higher locomotor activity on the patch, coupled with higher number of yeast sips.

I would like to propose that there are at least two mechanisms underlying the observed behaviors, and that they are executed in parallel and are both dependent on the internal level of limiting AAs in the fly: The first mechanism regulates the degree of exploration of the relevant resources, in this case the proteinaceous patches. It does so in a continuous/dosage-dependent manner: the more AA-deprived the fly is, the more conservative the exploration will be. This mechanism seems to be independent of sensory perception, as flies do not need olfaction or gustation to maintain a high rate of returns to the same patch when they are AA-deprived (Figure 2.7I and Figure 4.26J). The second mechanism controls the way in which the resource is exploited, and it could do so by controlling 3 modules: the first module could modulate the decisions to stop at and leave the yeast patch; the second module the feeding motor pattern once feeding is initiated and the third module could control approach and latency to engage for the first time on yeast.

Mild AA-deprivation or imbalance could activate the first module, which could act through a modulation of gustatory perception, as flies with impaired gustatory perception (*Poxn>TNT* flies) displayed lower probability of engagement and shorter visit durations (Figure 4.26D and E). There is evidence of

neuronal mechanisms that promote feeding initiation while inhibiting locomotion, which could be the way in which the brain implements the decision to engage/stop at the food patch. A pair of interneurons in the ventral nerve cord was identified to control the switch between feeding initiation and locomotion (Mann, Gordon, and Scott 2013). Another study also identified two distinct sugar-sensory neurons in the legs, one type sent projections to the brain and was involved in feeding initiation, while the second type sent projections to the thoracic ganglia played a role in sugar-dependent suppression of locomotion (Thoma et al. 2016).

The second and third modules could be activated only after severe AA deprivation. The feeding motor pattern could be directly regulated by internal AA levels, while the decision to approach could be modified via a modulation of the middle-range olfactory perception, based on the observed increase in yeast approach rate (Figure 2.3B) and in the increased latency to engage yeast in olfaction-impaired flies (Figure 2.7C).

5.1.1 Future work

With a combination of the flyPAD and the tracking in the same setup, it could be possible to perform an acute neuronal activation or inactivation screen to evaluate which neurons could be responsible for a yeast-dependent suppression of locomotion, by comparing the elicited stops outside the food patches and the ones happening specifically after a yeast encounter (leg touch). To evaluate if olfactory perception is modulated by AA deprivation, experiments in the dark or with obstacles could be performed. An assay with a single yeast patch in the middle that measures the latency to find it, in the dark, similar to the one used in (Root et al. 2011), would be easy to perform in the current tracking setup. A more definite assay, would be to measure if the preference of flies to stay a yeast odorized quadrant (Beshel and Zhong 2013) is increased after AA-deprivation.

5.2 The cost of leaving a food patch

One of the common questions I was asked when I was presenting my work was: Is there any cost associated with leaving a food patch in these assay? Because the food patches are really close to each other, it gives the impression that there is no cost associated with leaving the patch. However, AA-deprived flies tended to keep a conservative exploration around yeast patches, which was gradually expanding as they reached satiation. This might suggest that there is a hard-wired mechanism that pushes for the higher exploitation of a resource that satisfies the current needs even when there is virtually no cost of leaving it. On the other hand, the highest median value for the probability of returning was about 20% in the initial minutes of the assay when flies were most deprived (data not shown), which means that even when they had been AA-deprived for 3 days and all yeast patches were the same, they still explored continuously all the patches and this exploration only increased over time, even when the environment was not changing. This suggests that there must be an intrinsic need to explore the environment probably with the goal of finding an even better food source, especially in an environment where leaving the patch implied no risks.

5.2.1 Future work

We could easily test what is the role of the patch quality in the decision of return by putting patches with different yeast concentrations in the same arena. We could also modify the cost of leaving by increasing the distance between the patches.

An experiment with multiple food concentrations would also give us more information about the factors that control the decision to leave or to explore or to tune how "conservative" the exploration around the food patch is.

Varying distances could also be another way to increase costs of leaving. In fact, together with Pawel Bujalski, a rotation student in our lab, we designed a new arena intended to introduce some cost in the access to a yeast patch by having to follow a "long" access tunnel to get to it (Figure 5.1A). However, preliminary results indicated that flies tend to spend more time in that chamber when compared to a chamber with easier access containing the same type and quality of resource. This could imply that by making this chamber more difficult to access, we also made it more difficult to leave. Another caveat is that although this new chamber was bigger, it seemed that there was no cost on covering the whole arena several times. Actually, the challenge of increasing cost by increasing distance becomes evident when we look at the total distances covered by the flies during 2 hours in the current tracking assay (Figure 4.2A): most flies covered more than 20 meters and some of them even covered more than 60 meters. I therefore suggest that a better way to increase cost would be to use obstacles or to increase agarose concentration, so the food is harder to consume.

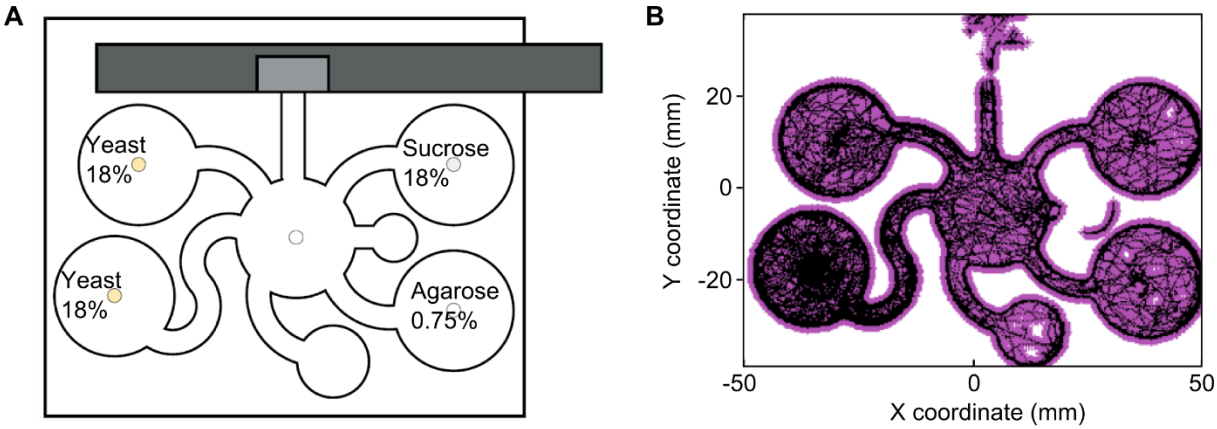

Figure 5.1 – New arena design

Prototype of a new foraging arena, manufactured and tested by Pawel Bujalski. (A) The new arena contains 5 chambers: one intended to have a more difficult access by having a longer access tunnel, 3 symmetrical chambers containing different types of food patches, one empty chamber and one small chamber where a male would be place to interact with the female being tested. (B) Representative trajectory of an AA-deprived mated fly in the arena.

Maybe a more realistic setup would be one with a big open space where the flies could fly and stay as long as they prefer and then have a small chamber with food to which the fly enters by crossing a small tunnel with a beam that when crossed triggers a camera that can track the movements around the food. In this way, we could have a controlled, but more naturalistic environment, in which it would

be possible to quantify global foraging strategies, such as rate of arrival and return to the food chamber, decision to leave the chamber and so on.

5.3 Individual variability

The great variability observed in mated females in their response to yeast opens innumerable possibilities to study the different mechanisms that control yeast intake.

5.3.1 Future work

Because we have access to the information of single individuals that could be genetically identical, we could explore correlations between number of eggs laid, amount of food consumed before the assay, levels of locomotor activity in the absence of food and time on yeast during the assay. There are a number of tests that could also be performed after the assay to each individual such as amount of Sex Peptide in the reproductive tract, metabolite levels and even TOR signaling. If non-invasive tests are performed after the assay, individuals could be re-tested and after a second test, imaging of sensory neurons could be performed so the neural activity responses could be directly associated to the behavior of that individual, bypassing the challenge that the huge yeast response variability poses for conclusions about neuronal recordings.

5.4 Hierarchical structure of feeding and foraging behavior

I like to think that the foraging behaviors I've described follow a hierarchical organization in which the basic unit is the *sip* (Figure 5.2). Sips are then grouped into *feeding bursts* that in turn happen inside *food micromovements*. Several food micromovements constitute *food patch visits*. Long visits and a high rate of returns to the same patch could be seen as an *explotatory period* while short visits to multiple patches would constitute an *exploratory period*. As I mentioned in section 5.1, AA deprivation turns exploration more conservative narrowing the spatial scale at which exploration happens and favoring exploitation, therefore, exploration and exploitation do not necessarily have to be seen as mutually exclusive: increased exploitation in this case is just exploration changing spatial scale (see representative trajectories from 3 to 1 in Figure 5.2).

5.5 Other proposed experiments

5.5.1 Multi-sensory integration

The fact that flies with impaired OR-mediated olfaction had a delayed latency to engage in yeast but still managed to spend the same time on yeast as the wildtype controls, raises the question: what happens at that moment in which the flies engage actively on yeast for the first time? Maybe occasionally tasting yeast with their legs at every encounter has an associated probability of spontaneously extending the proboscis, this probability might be enhanced by the presence of the

yeast odor at short-range, suggesting, as we had mentioned before, a role of olfaction in increasing the efficiency of yeast recognition. Indeed, it has been reported that flies can extend their proboscis in response to tarsal stimulation with yeast (Masek and Keene 2013). This assay, therefore, opens the opportunity to study how taste and olfactory perception of the yeast substrate are integrated in the fly brain to achieve protein homeostasis.

A future experiment to test if tarsal taste is indeed the first gate to yeast engagement would be to test tarsal taste-impaired flies in an *Orco*$^{1/1}$ background. It would also be interesting if we could pinpoint the chemosensory receptor responsible for the effect observed in the *Orco* mutants. One way to start that search would be to test if the absence of maxillary palps alone has a similar effect to the one observed in *Orco* mutants. A positive result would be interesting as the role of maxillary palps in nutrient choice is poorly understood. This experiment would yield even more information if it was performed in a flyPAD-Tracking combined setup, to be able to distinguish leg touches on the food from sips using the proboscis.

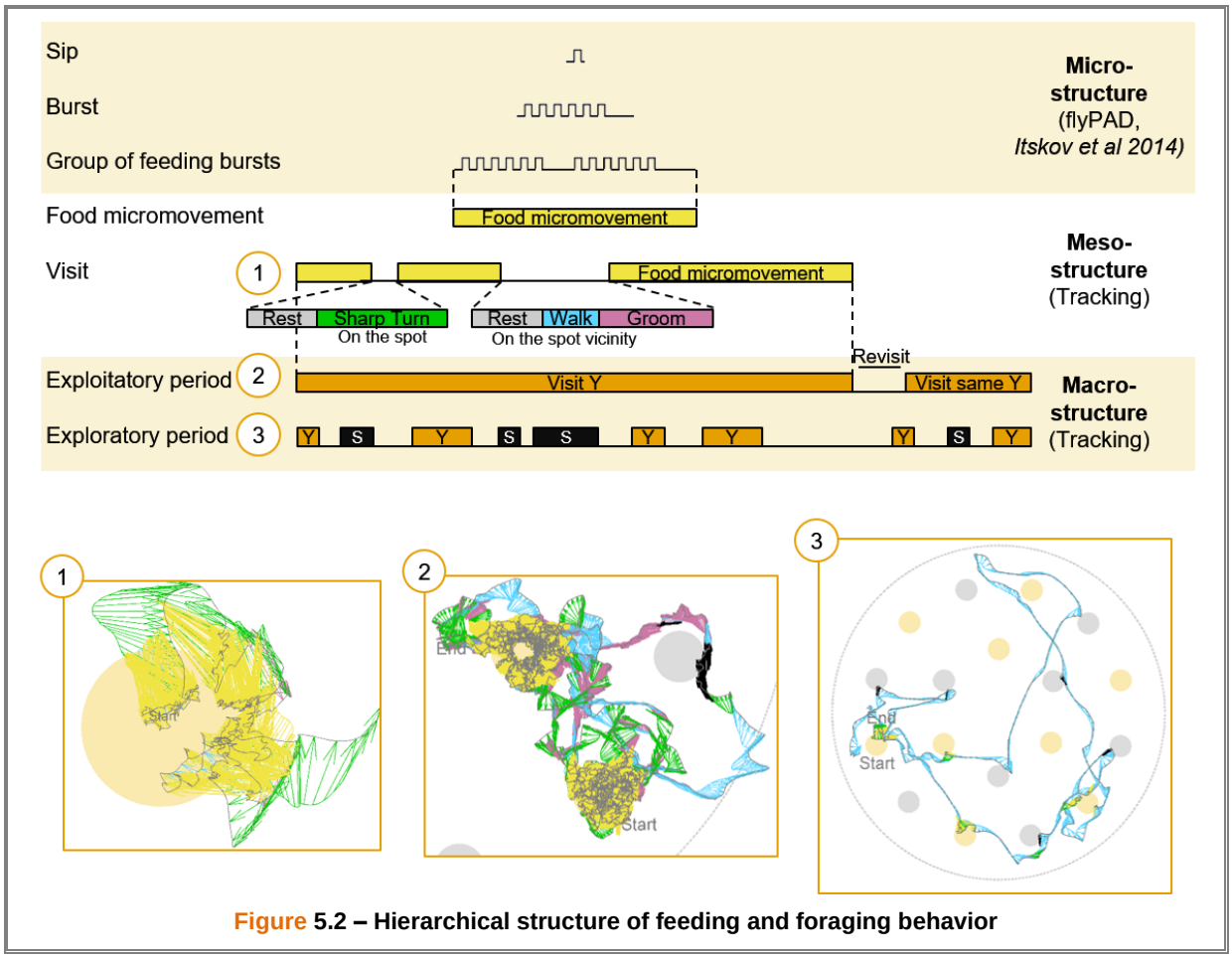

Figure 5.2 – Hierarchical structure of feeding and foraging behavior

5.5.2 *Is locomotor activity modulated by AA-deprivation and if so, is this effect mediated by octopamine?*

It has been reported that octopamine mediates the starvation-induced increase in locomotor activity in flies (Z. Yang et al. 2015). A very simple experiment comparing the locomotor activity in the absence of food for flies fed in AA+ rich diet versus those AA-deprived would answer the first part of that question. If there is AA-deprivation-induced hyperactivity and given the availability of the genetic and neuronal manipulation tools in *Drosophila*, it should be straight forward to test the involvement of octopamine in such process.

5.5.3 *Where in the brain (if in the brain) is octopamine acting to modulate the postmating-induced increase in yeast feeding?*

We showed that octopamine mediates the postmating-induced increase in yeast feeding (Figure 4.27). A group of nine *Tdc2/dsx*$^{+}$ neurons in the female abdominal ganglion mediate postmating responses such as receptivity and egg-laying (Rezával et al. 2014). However, it has been proposed that as these neurons innervate the reproductive tract, they might play a role in SP release. SP signal is carried to the brain through the SAG neurons (Feng et al. 2014), which have already been shown to mediate postmating increase in yeast feeding (Walker, Corrales-Carvajal, and Ribeiro 2015). Therefore, the current model suggests that the role of octopamine in postmating yeast feeding responses is played upstream of SP signaling, at the reproductive tract, not in the brain. An experiment to test this hypothesis would be to directly inject SP in the abdomen of *Tβh* virgin mutants and see if they increase yeast feeding. This experiment was performed by Yapici (2008) and resulted in unreceptive females, suggesting that indeed octopamine signaling is upstream of SP signaling, but it remains to be tested if yeast feeding responses follow the same mechanism.

5.5.4 *Long-term dynamics of behavioral changes to achieve protein homeostasis*

The current tracking setup and analysis of the different exploration and exploitation parameters, could be used in a re-feeding protocol across several days to investigate the long-term dynamics of the hungry-to-fed phenotype. Previous re-feeding experiments in the lab showed that flies need 3 days to restore the fully-fed low preference for yeast in a two-color assay (data not shown). It would be interesting to know, in the long-term, which strategies stop being implemented as the fly gets closer to protein homeostasis. During this project we learned, for example, that after two hours in an arena with yeast patches, flies display the same behavior at the patch (locomotor activity and distance to the center of the patch) than fully-fed flies, but they still have more conservative exploration patterns than fully-fed flies (Figure 4.23).

5.5.5 *Testing path integration in flies*

Although all of the returns to the same patch quantified in this project were by definition a consequence of the fly constraining its exploration to the vicinity of the patch, it should be rather

simple to test if the probability to visit a given patch increases if that patch was visited before. Preliminary results showed that the flies tend to return to the same patch after a full lap walking on the edge of the arena (Figure 4.7), indicating that they somehow mark or remember the last visited patch, independently of its quality (as this behavior was observed in agarose patches as well). I'd say that designing an arena with a simple labyrinth hiding the yeast spots in different locations would be a cool way to test if flies remember the way back to a nutritious patch. A recent study suggests that *Drosophila* can learn efficient paths to a sugar source (Navawongse et al. 2016).

5.5.6 Social effects

This assay could also be used to test how nutrient choice is affected by the choice of other flies present in the same arena.

5.6 Closing remarks

The present study opens the possibility for many other exciting studies that can help us understanding better how animals modulate behavioral choices according to their internal state.

Chapter 6. Publications

6.1 Papers

Corrales-Carvajal, V. M., Faisal, A. A., Ribeiro, C. (2016). Internal states drive nutrient homeostasis by modulating exploration-exploitation trade-off. *eLife.* doi: 10.7554/eLife.19920.

Walker, S. J., Corrales-Carvajal, V. M., & Ribeiro, C. (2015). Postmating Circuitry Modulates Salt Taste Processing to Increase Reproductive Output in Drosophila. *Current Biology*, 1–10. doi:10.1016/j.cub.2015.08.043.

6.2 Conferences and Posters

2014 Measuring Behavior 2014. 9th International Conference on Methods and Techniques in Behavioral Research. Wageningen, The Netherlands. Oral presentation.

2014 Advanced Behaviour Technology Course. Champalimaud Center for the Unknown. Lisbon, Portugal. Attendant.

2014 VII European Conference on Behavioural Biology. Prague, Czech Republic. Oral presentation.

2014 Systems neuroscience of *Drosophila:* From genes to circuits to behaviours. Center de Regulació Genòmica. Barcelona, Spain. FLiACT workshop. Attendant.

2014 4th MIT Portugal Program Conference - New Frontiers for a Sustainable Prosperity. Poster presentation.

2013 10º National Congress of Ethology. Champalimaud Center for the Unknown. Lisbon, Portugal. Oral presentation.

2013 Neurobiology of *Drosophila.* Cold Spring Harbor Laboratory. New York, United States. Oral presentation.

2013 Champalimaud Neuroscience Symposium. Champalimaud Center for the Unknown. Lisbon, Portugal. Poster presentation.

2012 Champalimaud Neuroscience Symposium. Champalimaud Center for the Unknown. Lisbon, Portugal. Poster presentation.

Chapter 7. References

Agresti, Alan, and Brent A Coull. 1998. “Approximate Is Better Than ‘exact’ for Interval Estimation of Binomial Proportions.” *The American Statistician* 52 (2): 119–26. doi:10.2307/2685469.

Anderson, David J. J, and Pietro Perona. 2014. “Toward a Science of Computational Ethology.” *Neuron* 84 (1): 18–31. doi:10.1016/j.neuron.2014.09.005.

Asahina, Kenta, Kiichi Watanabe, Brian J. Duistermars, Eric Hoopfer, Carlos Roberto González, Eyrún Arna Eyjólfsdóttir, Pietro Perona, and David J. Anderson. 2014. “Tachykinin-Expressing Neurons Control Male-Specific Aggressive Arousal in Drosophila.” *Cell* 156 (1–2): 221–35. doi:10.1016/j.cell.2013.11.045.

Ayroles, Julien F., Sean M. Buchanan, Chelsea O’Leary, Kyobi Skutt-Kakaria, Jennifer K. Grenier, Andrew G. Clark, Daniel L. Hartl, and Benjamin L. de Bivort. 2015. “Behavioral Idiosyncrasy Reveals Genetic Control of Phenotypic Variability.” *Proceedings of the National Academy of Sciences* 112 (21): 201503830. doi:10.1073/pnas.1503830112.

Barabási, Albert-László. 2005. “The Origin of Bursts and Heavy Tails in Human Dynamics.” *Nature* 435 (7039): 207–11. doi:10.1038/nature03459.

Barron, Andrew B, Kevin N Gurney, Lianne F S Meah, Eleni Vasilaki, and James A R Marshall. 2015. “Decision-Making and Action Selection in Insects: Inspiration from Vertebrate-Based Theories.” *Frontiers in Behavioral Neuroscience* 9 (August): 216. doi:10.3389/fnbeh.2015.00216.

Barrozo, Romina B, Christophe Gadenne, and Sylvia Anton. 2010. “Switching Attraction to Inhibition: Mating-Induced Reversed Role of Sex Pheromone in an Insect.” *The Journal of Experimental Biology* 213 (Pt 17): 2933–39. doi:10.1242/jeb.043430.

Bath, Daniel E, John R Stowers, Dorothea Hörmann, Andreas Poehlmann, Barry J Dickson, and Andrew D Straw. 2014. “FlyMAD: Rapid Thermogenetic Control of Neuronal Activity in Freely Walking Drosophila.” *Nature Methods* 11 (7): 756–62. doi:10.1038/nmeth.2973.

Becher, Paul G., Marie Bengtsson, Bill S. Hansson, and Peter Witzgall. 2010. “Flying the Fly: Long-Range Flight Behavior of Drosophila Melanogaster to Attractive Odors.” *Journal of Chemical Ecology* 36 (6): 599–607. doi:10.1007/s10886-010-9794-2.

Becher, Paul G., Gerhard Flick, Elżbieta Rozpędowska, Alexandra Schmidt, Arne Hagman, Sébastien Lebreton, Mattias C. Larsson, et al. 2012. “Yeast, Not Fruit Volatiles Mediate Drosophila Melanogaster Attraction, Oviposition and Development.” Edited by Ken Thompson. *Functional Ecology* 26 (4): 822–28. doi:10.1111/j.1365-2435.2012.02006.x.

Beck, Jeffrey M., Wei Ji Ma, Xaq Pitkow, Peter E. Latham, and Alexandre Pouget. 2012. “Not Noisy, Just Wrong: The Role of Suboptimal Inference in Behavioral Variability.” *Neuron* 74 (1). Elsevier Inc.: 30–39. doi:10.1016/j.neuron.2012.03.016.

Benjamini, Yoav, Dina Lipkind, Guy Horev, Ehud Fonio, Neri Kafkafi, and Ilan Golani. 2010. “Ten Ways to Improve the Quality of Descriptions of Whole-Animal Movement.” *Neuroscience and Biobehavioral Reviews* 34 (8). Elsevier Ltd: 1351–65. doi:10.1016/j.neubiorev.2010.04.004.

Berman, Gordon J, William Bialek, and Joshua W Shaevitz. 2016. “Predictability and Hierarchy in Drosophila Behavior.” *BioRxiv*. doi:http://dx.doi.org/10.1101/052928.

Berman, Gordon J, Daniel M Choi, William Bialek, and Joshua W Shaevitz. 2014. “Mapping the Stereotyped Behaviour of Freely Moving Fruit Flies.” *Journal of The Royal Society Interface* 11 (August). doi:10.1098/rsif.2014.0672.

Beshel, Jennifer, and Yi Zhong. 2013. “Graded Encoding of Food Odor Value in the Drosophila Brain.”

The Journal of Neuroscience 33 (40): 15693–704. doi:10.1523/JNEUROSCI.2605-13.2013.

Bidaye, Salil S, Christian Machacek, Yang Wu, and Barry J Dickson. 2014. "Neuronal Control of Drosophila Walking Direction." *Science* 344 (6179): 97–101. doi:10.1126/science.1249964.

Bjordal, Marianne, Nathalie Arquier, Julie Kniazeff, Jean Philippe Pin, and Pierre Léopold. 2014. "Sensing of Amino Acids in a Dopaminergic Circuitry Promotes Rejection of an Incomplete Diet in Drosophila." *Cell* 156 (3): 510–21. doi:10.1016/j.cell.2013.12.024.

Boll, Werner, and Markus Noll. 2002. "The Drosophila Pox Neuro Gene: Control of Male Courtship Behavior and Fertility as Revealed by a Complete Dissection of All Enhancers." *Development (Cambridge, England)* 129 (24): 5667–81. doi:10.1242/dev.00157.

Brand, a H, and Norbert Perrimon. 1993. "Targeted Gene Expression as a Means of Altering Cell Fates and Generating Dominant Phenotypes." *Development (Cambridge, England)* 118 (2): 401–15. http://www.ncbi.nlm.nih.gov/pubmed/8223268.

Branson, Kristin, Alice A Robie, John Bender, Pietro Perona, and Michael H Dickinson. 2009. "High-Throughput Ethomics in Large Groups of Drosophila." Journal Article. *Nature Methods* 6 (6): 451–57. doi:10.1038/nmeth.1328.

Brembs, Björn. 2011. "Towards a Scientific Concept of Free Will as a Biological Trait: Spontaneous Actions and Decision-Making in Invertebrates." *Proceedings of the Royal Society B: Biological Sciences* 278 (1707): 930–39. doi:10.1098/rspb.2010.2325.

Briggman, K L, and H D I Abarbanel. 2005. "Optical Imaging of Neuronal Populations During." *Science* 307 (265): 896–902. doi:10.1126/science.1103736.

Broderick, Nichole A, and Bruno Lemaitre. 2012. "Gut-Associated Microbes of Drosophila Melanogaster." *Gut Microbes* 3 (4): 307–21. doi:10.4161/gmic.19896.

Brown, André E X, Eviatar I Yemini, Laura J Grundy, Tadas Jucikas, and William R Schafer. 2013. "A Dictionary of Behavioral Motifs Reveals Clusters of Genes Affecting Caenorhabditis Elegans Locomotion." *Proceedings of the National Academy of Sciences* 110 (2): 791–96. doi:10.1073/pnas.1211447110.

Buchanan, Sean M., Jamey S. Kain, Benjamin L De Bivort, and Benjamin L. de Bivort. 2015. "Neuronal Control of Locomotor Handedness in Drosophila." *Proceedings of the National Academy of Sciences* 112 (21): 201500804. doi:10.1073/pnas.1500804112.

Calhoun, Adam J, Sreekanth H Chalasani, and Tatyana O Sharpee. 2014. "Maximally Informative Foraging by Caenorhabditis Elegans." *eLife* 3: 1–13. doi:10.7554/eLife.04220.

Chantranupong, Lynne, Rachel L. Wolfson, and David M. Sabatini. 2015. "Nutrient-Sensing Mechanisms across Evolution." *Cell* 161 (1): 67–83. doi:10.1016/j.cell.2015.02.041.

Chen, P.S., E. Stumm-Zollinger, T. Aigaki, J. Balmer, M. Bienz, P. Böhlen, P.C. Andrews, et al. 1988. "A Male Accessory Gland Peptide That Regulates Reproductive Behavior of Female D. Melanogaster." *Cell* 54 (3): 291–98. doi:10.1016/0092-8674(88)90192-4.

Chiappe, M. Eugenia, Johannes D. Seelig, Michael B. Reiser, and Vivek Jayaraman. 2010. "Walking Modulates Speed Sensitivity in Drosophila Motion Vision." *Current Biology* 20 (16). Elsevier Ltd: 1470–75. doi:10.1016/j.cub.2010.06.072.

Christiaens, Joaquin F., Luis M. Franco, Tanne L. Cools, Luc de Meester, Jan Michiels, Tom Wenseleers, Bassem A. Hassan, Emre Yaksi, and Kevin J. Verstrepen. 2014. "The Fungal Aroma Gene ATF1 Promotes Dispersal of Yeast Cells through Insect Vectors." *Cell Reports* 9 (2): 425–32. doi:10.1016/j.celrep.2014.09.009.

Clauset, Aaron, Cosma Rohilla Shalizi, and M. E. J. Newman. 2009. "Power-Law Distributions in Empirical Data." *SIAM Review* 51 (4): 661–703. doi:10.1137/070710111.

Clyne, P J, C G Warr, M R Freeman, D Lessing, J Kim, and J R Carlson. 1999. "A Novel Family of

Divergent Seven-Transmembrane Proteins: Candidate Odorant Receptors in Drosophila." *Neuron* 22 (2): 327–38. doi:10.1016/S0896-6273(00)81093-4.

Coen, Philip, Jan Clemens, Andrew J Weinstein, Diego a Pacheco, Yi Deng, and Mala Murthy. 2014. "Dynamic Sensory Cues Shape Song Structure in Drosophila." *Nature* 507 (7491). Nature Publishing Group: 233–37. doi:10.1038/nature13131.

Coen, Philip, Marjorie Xie, Jan Clemens, and Mala Murthy. 2016. "Sensorimotor Transformations Underlying Variability in Song Intensity during Drosophila Courtship." *Neuron* 89 (3): 629–44. doi:10.1016/j.neuron.2015.12.035.

Cohn, Raphael, Ianessa Morantte, and Vanessa Ruta. 2015. "Coordinated and Compartmentalized Neuromodulation Shapes Sensory Processing in Drosophila." *Cell* 163 (7): 1742–55. doi:10.1016/j.cell.2015.11.019.

Cole, Shannon H., Ginger E. Carney, Colleen A. McClung, Stacey S. Willard, Barbara J. Taylor, and Jay Hirsh. 2005. "Two Functional but Noncomplementing Drosophila Tyrosine Decarboxylase Genes: Distinct Roles for Neural Tyramine and Octopamine in Female Fertility." *Journal of Biological Chemistry* 280 (15): 14948–55. doi:10.1074/jbc.M414197200.

Dankert, Heiko, Liming Wang, Eric D Hoopfer, David J Anderson, and Pietro Perona. 2009. "Automated Monitoring and Analysis of Social Behavior in Drosophila." *Nature Methods* 6 (4): 297–303. doi:10.1038/nmeth.1310.

Davis, John D., and Gerard P. Smith. 1992. "Analysis of the Microstructure of the Rhythmic Tongue Movements of Rats Ingesting Maltose and Sucrose Solutions." *Behavioral Neuroscience* 106 (1): 217–28. doi:10.1037/0735-7044.106.1.217.

Dawkins, Richard. 1976. "Hierarchical Organisation: A Candidate Principle for Ethology." In *Growing Points in Ethology*, edited by P. P. G. Bateson and R. A. Hinde, 7–54. Cambridge University Press.

de Ruyter van Steveninck, R. R., Geoffrey D. Lewen, Steven P. Strong, Roland Koberle, and William Bialek. 1997. "Reproducibility and Variability in Neural Spike Trains." *Science* 275 (5307): 1805–8. doi:10.1126/science.275.5307.1805.

Dell, Anthony I., John a. Bender, Kristin Branson, Iain D. Couzin, Gonzalo G. de Polavieja, Lucas P.J.J. Noldus, Alfonso Pérez-Escudero, et al. 2014. "Automated Image-Based Tracking and Its Application in Ecology." *Trends in Ecology & Evolution* 29 (7): 417–28. doi:10.1016/j.tree.2014.05.004.

Demir, Ebru, and Barry J. Dickson. 2005. "Fruitless Splicing Specifies Male Courtship Behavior in Drosophila." *Cell* 121 (5): 785–94. doi:10.1016/j.cell.2005.04.027.

Dethier, Vincent G. 1976. *The Hungry Fly: A Physiological Study of the Behavior Associated with Feeding*. Cambridge, MA: Harvard University Press.

Dingemanse, Niels J., Anahita J N Kazem, Denis Réale, and Jonathan Wright. 2010. "Behavioural Reaction Norms: Animal Personality Meets Individual Plasticity." *Trends in Ecology and Evolution* 25 (2): 81–89. doi:10.1016/j.tree.2009.07.013.

Domenici, Paolo, David Booth, Jonathan M. Blagburn, and Jonathan P. Bacon. 2008. "Cockroaches Keep Predators Guessing by Using Preferred Escape Trajectories." *Current Biology* 18 (22). Elsevier Ltd: 1792–96. doi:10.1016/j.cub.2008.09.062.

Dominici, Nadia, Yuri P Ivanenko, Germana Cappellini, Andrea d'Avella, Vito Mondì, Marika Cicchese, Adele Fabiano, et al. 2011. "Locomotor Primitives in Newborn Babies and Their Development." *Science* 334 (6058): 997–99. doi:10.1126/science.1210617.

Dweck, Hany K. M., Markus Knaden, and Bill S. Hansson. 2015. "Functional Loss of Yeast Detectors Parallels Transition to Herbivory." *Proceedings of the National Academy of Sciences* 112 (November): 1–2. doi:10.1073/pnas.1501319112.

Dweck, Hany K M, Shimaa A M Ebrahim, Abu Farhan, Bill S. Hansson, and Marcus C. Stensmyr. 2015. “Olfactory Proxy Detection of Dietary Antioxidants in Drosophila.” *Current Biology* 25 (4): 455–66. doi:10.1016/j.cub.2014.11.062.

Egnor, S.E. Roian, and Kristin Branson. 2016. “Computational Analysis of Behavior.” *Annual Review of Neuroscience* 39 (1): 217–36. doi:10.1146/annurev-neuro-070815-013845.

Faisal, a Aldo, Luc P J Selen, and Daniel M Wolpert. 2008. “Noise in the Nervous System.” *Nature Reviews. Neuroscience* 9 (4): 292–303. doi:10.1038/nrn2258.

Feng, Kai, Mark T Palfreyman, Martin Häsemeyer, Aaron Talsma, and Barry J Dickson. 2014. “Ascending SAG Neurons Control Sexual Receptivity of Drosophila Females.” *Neuron* 83 (1): 135–48. doi:10.1016/j.neuron.2014.05.017.

Fontana, Luigi, and Linda Partridge. 2015. “Promoting Health and Longevity through Diet: From Model Organisms to Humans.” *Cell* 161 (1): 106–18. doi:10.1016/j.cell.2015.02.020.

Gaudry, Quentin, and William B Kristan. 2009. “Behavioral Choice by Presynaptic Inhibition of Tactile Sensory Terminals.” *Nature Neuroscience* 12 (11): 1450–57. doi:10.1038/nn.2400.

Gibson, G., and S. J. Torr. 1999. “Visual and Olfactory Responses of Haematophagous Diptera to Host Stimuli.” *Medical and Veterinary Entomology* 13 (1): 2–23. doi:10.1046/j.1365-2915.1999.00163.x.

Gilestro, Giorgio F. 2012. “Video Tracking and Analysis of Sleep in Drosophila Melanogaster.” *Nature Protocols* 7 (5). Nature Publishing Group: 995–1007. doi:10.1038/nprot.2012.041.

Golani, Ilan. 1992. “A Mobility Gradient in the Organization of Vertebrate Movement: The Perception of Movement through Symbolic Language.” *Behavioral and Brain Sciences* 15 (2): 249–66. doi:10.1017/S0140525X00068539.

Gold, Joshua I, and Michael N Shadlen. 2007. “The Neural Basis of Decision Making.” Journal Article. *Annual Review of Neuroscience* 30 (1): 535–74. doi:doi:10.1146/annurev.neuro.29.051605.113038.

Gomez-Marin, Alex, Efrat Oron, Anna Gakamsky, Dan Valente, Yoav Benjamini, and Ilan Golani. 2016. “Generative Rules of Drosophila Locomotor Behavior as a Candidate Homology across Phyla.” *Scientific Reports* 6 (May). Nature Publishing Group: 27555. doi:10.1038/srep27555.

Gomez-Marin, Alex, Joseph J Paton, Adam R Kampff, Rui M Costa, and Zachary F Mainen. 2014. “Big Behavioral Data: Psychology, Ethology and the Foundations of Neuroscience.” *Nature Neuroscience* 17 (11): 1455–62. doi:10.1038/nn.3812.

Gomez-Marin, Alex, Greg J Stephens, and André E X Brown. 2016. “Hierarchical Compression of Caenorhabditis Elegans Locomotion Reveals Phenotypic Differences in the Organization of Behaviour.” *Journal of The Royal Society Interface* 13 (121): 20160466. doi:10.1098/rsif.2016.0466.

Gomez-Marin, Alex, Greg J Stephens, and Matthieu Louis. 2011. “Active Sampling and Decision Making in Drosophila Chemotaxis.” *Nature Communications* 2 (January). Nature Publishing Group: 441. doi:10.1038/ncomms1455.

Gorter, Jenke A, Samyukta Jagadeesh, Christoph Gahr, Jelle J Boonekamp, Joel D Levine, and Jean-Christophe Billeter. 2016. “The Nutritional and Hedonic Value of Food Modulate Sexual Receptivity in Drosophila Melanogaster Females.” *Scientific Reports* 6 (January). Nature Publishing Group: 19441. doi:10.1038/srep19441.

Grandison, Richard C, Matthew D W Piper, and Linda Partridge. 2009. “Amino-Acid Imbalance Explains Extension of Lifespan by Dietary Restriction in Drosophila.” *Nature* 462 (7276). Nature Publishing Group: 1061–64. doi:10.1038/nature08619.

Griffioen-Roose, Sanne, Monica Mars, Els Siebelink, Graham Finlayson, Daniel Tomé, and Cees de

Graaf. 2012. “Protein Status Elicits Compensatory Changes in Food Intake and Food Preferences.” *The American Journal of Clinical Nutrition* 95 (1): 32–38. doi:10.3945/ajcn.111.020503.

Haberkern, Hannah, and Vivek Jayaraman. 2016. “Studying Small Brains to Understand the Building Blocks of Cognition.” *Current Opinion in Neurobiology* 37. Elsevier Ltd: 59–65. doi:10.1016/j.conb.2016.01.007.

Hassell, M. P., and T. R. E. Shouthwood. 1978. “Foraging Strategies of Insects.” *Annual Review of Ecology and Systematics* 9: 75–98.

Heisenberg, Martin. 2015. “Outcome Learning, Outcome Expectations, and Intentionality in Drosophila.” *Learning & Memory (Cold Spring Harbor, N.Y.)* 22: 294–98. doi:10.1101/lm.037481.114.

Hills, Thomas T., Peter M. Todd, David Lazer, A. David Redish, Iain D. Couzin, Melissa Bateson, Roshan Cools, et al. 2015. “Exploration versus Exploitation in Space, Mind, and Society.” *Trends in Cognitive Sciences* 19 (1): 46–54. doi:10.1016/j.tics.2014.10.004.

Hogan, Jerry A. 2015. “A Framework for the Study of Behavior.” *Behavioural Processes* 117 (August). Elsevier B.V.: 105–13. doi:10.1016/j.beproc.2014.05.003.

Hoopfer, Eric D, Yonil Jung, Hidehiko K Inagaki, Gerald M Rubin, and David J Anderson. 2015. “P1 Interneurons Promote a Persistent Internal State That Enhances Inter-Male Aggression in Drosophila.” *eLife* 1 (December): 1689–99. doi:10.1017/CBO9781107415324.004.

Huang, Kuo-Hua, Misha B Ahrens, Timothy W Dunn, and Florian Engert. 2013. “Spinal Projection Neurons Control Turning Behaviors in Zebrafish.” *Current Biology* 23 (16): 1566–73. doi:10.1016/j.cub.2013.06.044.

Hussain, Ashiq, Habibe K Üçpunar, Mo Zhang, Laura F Loschek, and Ilona C Grunwald Kadow. 2016. “Neuropeptides Modulate Female Chemosensory Processing upon Mating in Drosophila.” *PLoS Biology* 14 (5): e1002455. doi:10.1371/journal.pbio.1002455.

Hussain, Ashiq, Mo Zhang, Habibe K Üçpunar, Thomas Svensson, Elsa Quillery, Nicolas Gompel, Rickard Ignell, and Ilona C Grunwald Kadow. 2016. “Ionotropic Chemosensory Receptors Mediate the Taste and Smell of Polyamines.” *PLoS Biology* 14 (5): e1002454. doi:10.1371/journal.pbio.1002454.

Inagaki, Hidehiko K., Ketaki M. Panse, and David J Anderson. 2014. “Independent, Reciprocal Neuromodulatory Control of Sweet and Bitter Taste Sensitivity during Starvation in Drosophila.” *Neuron* 84 (4): 806–20. doi:10.1016/j.neuron.2014.09.032.

Ito, Kei, Kazunori Shinomiya, Masayoshi Ito, J. Douglas Armstrong, George Boyan, Volker Hartenstein, Steffen Harzsch, et al. 2014. “A Systematic Nomenclature for the Insect Brain.” *Neuron* 81 (4): 755–65. doi:10.1016/j.neuron.2013.12.017.

Itskov, Pavel M, José-maria Moreira, Ekaterina Vinnik, Gonçalo Lopes, Steve Safarik, Michael H Dickinson, and Carlos Ribeiro. 2014. “Automated Monitoring and Quantitative Analysis of Feeding Behaviour in Drosophila.” *Nature Communications* 5 (August). doi:10.1038/ncomms5560.

Itskov, Pavel M, and Carlos Ribeiro. 2013. “The Dilemmas of the Gourmet Fly: The Molecular and Neuronal Mechanisms of Feeding and Nutrient Decision Making in Drosophila.” *Frontiers in Neuroscience* 7 (January): 12. doi:10.3389/fnins.2013.00012.

Jin, Dezhe Z., and Alexay A. Kozhevnikov. 2011. “A Compact Statistical Model of the Song Syntax in Bengalese Finch.” *PLoS Computational Biology* 7 (3). doi:10.1371/journal.pcbi.1001108.

Jones, Walton D, Pelin Cayirlioglu, Ilona Grunwald Kadow, and Leslie B Vosshall. 2007. “Two Chemosensory Receptors Together Mediate Carbon Dioxide Detection in Drosophila.” *Nature* 445 (7123): 86–90. doi:10.1038/nature05466.

Joseph, Ryan M, Anita V Devineni, Ian F G King, and Ulrike Heberlein. 2009. “Oviposition Preference for and Positional Avoidance of Acetic Acid Provide a Model for Competing Behavioral Drives in Drosophila.” Journal Article. *Proceedings of the National Academy of Sciences* 106 (27): 11352–57. doi:10.1073/pnas.0901419106.

Jung, Kanghoon, Hyeran Jang, Jerald D Kralik, and Jaeseung Jeong. 2014. “Bursts and Heavy Tails in Temporal and Sequential Dynamics of Foraging Decisions.” *PLoS Computational Biology* 10 (8): e1003759. doi:10.1371/journal.pcbi.1003759.

Kabra, Mayank, Alice A Robie, Marta Rivera-Alba, Steven Branson, and Kristin Branson. 2013. “JAABA: Interactive Machine Learning for Automatic Annotation of Animal Behavior.” *Nature Methods* 10 (1): 64–67. doi:10.1038/nmeth.2281.

Kacelnik, Alex, and Claire El Mouden. 2013. “Triumphs and Trials of the Risk Paradigm.” *Animal Behaviour* 86 (6): 1117–29. doi:10.1016/j.anbehav.2013.09.034.

Kain, Jamey S, Chris Stokes, and Benjamin L de Bivort. 2012. “Phototactic Personality in Fruit Flies and Its Suppression by Serotonin and White.” *Proceedings of the National Academy of Sciences* 109 (48): 19834–39. doi:10.1073/pnas.1211988109.

Kain, Jamey, Chris Stokes, Quentin Gaudry, Xiangzhi Song, James Foley, Rachel Wilson, and Benjamin de Bivort. 2013. “Leg-Tracking and Automated Behavioural Classification in Drosophila.” *Nature Communications* 4 (May). Nature Publishing Group: 1910. doi:10.1038/ncomms2908.

Kato, Saul, Harris S. Kaplan, Tina Schrödel, Susanne Skora, Theodore H. Lindsay, Eviatar Yemini, Shawn Lockery, and Manuel Zimmer. 2015. “Global Brain Dynamics Embed the Motor Command Sequence of Caenorhabditis Elegans.” *Cell* 163 (3): 656–69. doi:10.1016/j.cell.2015.09.034.

Keene, Alex C, and Scott Waddell. 2007. “Drosophila Olfactory Memory: Single Genes to Complex Neural Circuits.” *Nature Reviews. Neuroscience* 8 (5): 341–54. doi:10.1038/nrn2098.

Kiehn, Ole. 2016. “Decoding the Organization of Spinal Circuits That Control Locomotion.” *Nature Reviews. Neuroscience* 17 (4): 224–38. doi:10.1038/nrn.2016.9.

Koganezawa, Masayuki, Hiroaki Hara, Yoshinori Hayakawa, and Ichiro Shimada. 2009. “Memory Effects on Scale-Free Dynamics in Foraging Drosophila.” *Journal of Theoretical Biology* 260 (3). Elsevier: 353–58. doi:10.1016/j.jtbi.2009.06.018.

Konopka, R J, and S Benzer. 1971. “Clock Mutants of Drosophila Melanogaster.” *Proceedings of the National Academy of Sciences of the United States of America* 68 (9): 2112–16. doi:10.1073/pnas.68.9.2112.

Krashes, Michael J., Shamik DasGupta, Andrew Vreede, Benjamin White, J. Douglas Armstrong, and Scott Waddell. 2009. “A Neural Circuit Mechanism Integrating Motivational State with Memory Expression in Drosophila.” *Cell* 139 (2): 416–27. doi:10.1016/j.cell.2009.08.035.

Kubli, E. 2003. “Sex-Peptides: Seminal Peptides of the Drosophila Male.” *Cellular and Molecular Life Sciences : CMLS* 60 (8): 1689–1704. doi:10.1007/s00018-003-3052.

Larsson, Mattias C., Ana I. Domingos, Walton D. Jones, M. Eugenia Chiappe, Hubert Amrein, and Leslie B. Vosshall. 2004. “Or83b Encodes a Broadly Expressed Odorant Receptor Essential for Drosophila Olfaction.” *Neuron* 43 (5): 703–14. doi:10.1016/j.neuron.2004.08.019.

LeDue, Emily E., Yu-Chieh Chen, Aera Y. Jung, Anupama Dahanukar, and Michael D. Gordon. 2015. “Pharyngeal Sense Organs Drive Robust Sugar Consumption in Drosophila.” *Nature Communications* 6. Nature Publishing Group: 6667. doi:10.1038/ncomms7667.

Lee, Kwang Pum, Stephen J. Simpson, Fiona J Clissold, Robert Brooks, J William O Ballard, Phil W Taylor, Nazaneen Soran, and David Raubenheimer. 2008. “Lifespan and Reproduction in Drosophila: New Insights from Nutritional Geometry.” Journal Article. *Proceedings of the National*

Academy of Sciences 105 (7): 2498–2503. doi:10.1073/pnas.0710787105.

Leitão-gonçalves, Ricardo, and Carlos Ribeiro. 2014. “Using Neuron Specific RNAi in Drosophila for Understanding the Molecular and Neuronal Basis of Behavior.” In *Behavioral Genetics of the Fly (Drosophila Melanogaster)*, edited by Josh Dubnau, 202–2016. Cambridge University Press.

Levine, Morgan E, Jorge a Suarez, Sebastian Brandhorst, Priya Balasubramanian, Chia-Wei Cheng, Federica Madia, Luigi Fontana, et al. 2014. “Low Protein Intake Is Associated with a Major Reduction in IGF-1, Cancer, and Overall Mortality in the 65 and Younger but Not Older Population.” *Cell Metabolism* 19 (3): 407–17. doi:10.1016/j.cmet.2014.02.006.

Levitis, Daniel A., William Z. Lidicker, and Glenn Freund. 2009. “Behavioural Biologists Do Not Agree on What Constitutes Behaviour.” *Animal Behaviour* 78 (1). Elsevier Ltd: 103–10. doi:10.1016/j.anbehav.2009.03.018.

Libert, Sergiy, Jessica Zwiener, Xiaowen Chu, Wayne Vanvoorhies, Gregg Roman, and Scott D Pletcher. 2007. “Regulation of Drosophila Life Span by Olfaction and Food-Dervied Odors.” *Science* 315 (February): 1133–37. doi:10.1126/science.1136610.

Lihoreau, Mathieu, Laure-Anne Poissonnier, Guillaume Isabel, and Audrey Dussutour. 2016. “*Drosophila* Females Trade off Good Nutrition with High Quality Oviposition Sites When Choosing Foods.” *The Journal of Experimental Biology*, no. June: jeb.142257. doi:10.1242/jeb.142257.

Lisman, John. 2015. “The Challenge of Understanding the Brain: Where We Stand in 2015.” *Neuron* 86 (4): 864–82. doi:10.1016/j.neuron.2015.03.032.

Liu, Huanfa, and Eric Kubli. 2003. “Sex-Peptide Is the Molecular Basis of the Sperm Effect in Drosophila Melanogaster.” *Proceedings of the National Academy of Sciences* 100 (17): 9929–33. doi:10.1073/pnas.1631700100.

London, M., A. Roth, L. Beeren, M. Häusser, and P. E. Latham. 2010. “Sensitivity to Perturbations in Vivo Implies High Noise and Suggests Rate Coding in Cortex.” *Nature* 466 (7302): 123–27. doi:10.1038/nature09086.

Lopes, Gonçalo, Niccolò Bonacchi, João Frazao, Joana P. Neto, Bassam V. Atallah, Sofia Soares, Luís Moreira, et al. 2015. “Bonsai: An Event-Based Framework for Processing and Controlling Data Streams.” *Frontiers in Neuroinformatics* 9 (April): 7. doi:10.3389/fninf.2015.00007.

Lorenz, Konrad Z. 1958. “The Evolution of Behavior.” *Scientific American* 199 (6): 67–78. doi:10.1038/scientificamerican1258-67.

Luo, Liqun, Edward M. Callaway, and Karel Svoboda. 2008. “Genetic Dissection of Neural Circuits.” *Neuron* 57 (5): 634–60. doi:10.1016/j.neuron.2008.01.002.

Maesani, Andrea, Pavan Ramdya, Steeve Cruchet, Kyle Gustafson, Richard Benton, and Dario Floreano. 2015. “Fluctuation-Driven Neural Dynamics Reproduce Drosophila Locomotor Patterns.” *PLoS Computational Biology* 11 (11): 1–24. doi:10.1371/journal.pcbi.1004577.

Mahler, Stephen V, David E Moorman, Rachel J Smith, Morgan H James, and Gary Aston-Jones. 2014. “Motivational Activation: A Unifying Hypothesis of Orexin/hypocretin Function.” *Nature Neuroscience* 17 (10). Nature Publishing Group: 1298–1303. doi:10.1038/nn.3810.

Maimon, Gaby, Andrew D Straw, and Michael H Dickinson. 2010. “Active Flight Increases the Gain of Visual Motion Processing in Drosophila.” *Nature Neuroscience* 13 (3). Nature Publishing Group: 393–99. doi:10.1038/nn.2492.

Mann, Kevin, Michael D. Gordon, and Kristin Scott. 2013. “A Pair of Interneurons Influences the Choice between Feeding and Locomotion in Drosophila.” *Neuron* 79 (4). Elsevier Inc.: 754–65. doi:10.1016/j.neuron.2013.06.018.

Marella, Sunanda, Walter Fischler, Priscilla Kong, Sam Asgarian, Erroll Rueckert, and Kristin Scott.

2006. “Imaging Taste Responses in the Fly Brain Reveals a Functional Map of Taste Category and Behavior.” *Neuron* 49 (2): 285–95. doi:10.1016/j.neuron.2005.11.037.

Martin, J, P Faure, and R Ernst. 2001. “The Power Law Distribution for Walking-Time Intervals Correlates with the Ellipsoid-Body in Drosophila.” *Journal of Neurogenetics* 15 (3–4): 205–19. http://www.ncbi.nlm.nih.gov/pubmed/12092904.

Martin, Jean-René. 2004. “A Portrait of Locomotor Behaviour in Drosophila Determined by a Video-Tracking Paradigm.” *Behavioural Processes* 67 (2): 207–19. doi:10.1016/j.beproc.2004.04.003.

Masek, Pavel, and Alex C Keene. 2013. “Drosophila Fatty Acid Taste Signals through the PLC Pathway in Sugar-Sensing Neurons.” *PLoS Genetics* 9 (9): e1003710. doi:10.1371/journal.pgen.1003710.

Maye, Alexander, Chih-Hao Hsieh, George Sugihara, and Björn Brembs. 2007. “Order in Spontaneous Behavior.” *PloS One* 2 (5): e443. doi:10.1371/journal.pone.0000443.

McMeniman, Conor J., Román A. Corfas, Benjamin J. Matthews, Scott A. Ritchie, and Leslie B. Vosshall. 2014. “Multimodal Integration of Carbon Dioxide and Other Sensory Cues Drives Mosquito Attraction to Humans.” *Cell* 156 (5): 1060–71. doi:10.1016/j.cell.2013.12.044.

Mendes, César S, Imre Bartos, Turgay Akay, Szabolcs Márka, and Richard S Mann. 2013. “Quantification of Gait Parameters in Freely Walking Wild Type and Sensory Deprived Drosophila Melanogaster.” *eLife* 2 (January): e00231. doi:10.7554/eLife.00231.

Miller, Paige M, Julia B Saltz, Veronica A Cochrane, Caitlin M Marcinkowski, Raisa Mobin, and Thomas L Turner. 2011. “Natural Variation in Decision-Making Behavior in Drosophila Melanogaster.” Journal Article. *PLoS ONE* 6 (1). Public Library of Science: e16436. http://dx.doi.org/10.1371/journal.pone.0016436.

Miranda, Jason A, and Walter Wilczynski. 2009. “Female Reproductive State Influences the Auditory Midbrain Response.” *Journal of Comparative Physiology. A, Neuroethology, Sensory, Neural, and Behavioral Physiology* 195 (4): 341–49. doi:10.1007/s00359-008-0410-7.

Monastirioti, M, C E Linn, and K White. 1996. “Characterization of Drosophila Tyramine Beta-Hydroxylase Gene and Isolation of Mutant Flies Lacking Octopamine.” *The Journal of Neuroscience* 16 (12): 3900–3911.

Monastirioti, Maria. 2003. “Distinct Octopamine Cell Population Residing in the CNS Abdominal Ganglion Controls Ovulation in Drosophila Melanogaster.” *Developmental Biology* 264 (1): 38–49. doi:10.1016/j.ydbio.2003.07.019.

Morrison, Christopher D, and Thomas Laeger. 2015. “Protein-Dependent Regulation of Feeding and Metabolism.” *Trends in Endocrinology and Metabolism: TEM* 26 (5): 256–62. doi:10.1016/j.tem.2015.02.008.

Muijres, Florian T, Michael J Elzinga, Johan M Melis, and Michael H Dickinson. 2014. “Flies Evade Looming Targets by Executing Rapid Visually Directed Banked Turns.” *Science* 344 (6180): 172–77. doi:10.1126/science.1248955.

Navawongse, Rapeechai, Deepak Choudhury, Marlena Raczkowska, James Charles Stewart, Terrence Lim, Mashiur Rahman, Alicia Guek Geok Toh, Zhiping Wang, and Adam Claridge-Chang. 2016. “Drosophila Learn Efficient Paths to a Food Source.” *Neurobiology of Learning and Memory* 131. Elsevier Inc.: 176–81. doi:10.1016/j.nlm.2016.03.019.

Nottebohm, Eugénie, Christine Dambly-Chaudière, and Alain Ghysen. 1992. “Connectivity of Chemosensory Neurons Is Controlled by the Gene Poxn in Drosophila.” *Nature* 359: 829–32.

Ofstad, Tyler a, Charles S Zuker, and Michael B Reiser. 2011. “Visual Place Learning in Drosophila Melanogaster.” *Nature* 474 (7350). Nature Publishing Group: 204–7. doi:10.1038/nature10131.

Ohyama, Tomoko, Casey M Schneider-Mizell, Richard D Fetter, Javier Valdes Aleman, Romain

Franconville, Marta Rivera-Alba, Brett D Mensh, et al. 2015. “A Multilevel Multimodal Circuit Enhances Action Selection in Drosophila.” *Nature* 520. doi:10.1038/nature14297.

Olsen, Shawn R., and Rachel I. Wilson. 2008. “Cracking Neural Circuits in a Tiny Brain: New Approaches for Understanding the Neural Circuitry of Drosophila.” *Trends in Neurosciences* 31 (10): 512–20. doi:10.1016/j.tins.2008.07.006.

Öst, Anita, Adelheid Lempradl, Eduard Casas, Melanie Weigert, Theodor Tiko, Merdin Deniz, Lorena Pantano, et al. 2014. “Paternal Diet Defines Offspring Chromatin State and Intergenerational Obesity.” *Cell* 159 (6): 1352–64. doi:10.1016/j.cell.2014.11.005.

Palmer, Chris R., and William B. Kristan. 2011. “Contextual Modulation of Behavioral Choice.” *Current Opinion in Neurobiology* 21 (4): 520–26. doi:10.1016/j.conb.2011.05.003.

Pérez-Escudero, Alfonso, Julián Vicente-Page, Robert C Hinz, Sara Arganda, and Gonzalo G de Polavieja. 2014. “idTracker: Tracking Individuals in a Group by Automatic Identification of Unmarked Animals.” *Nature Methods* 11 (7): 743–48. doi:10.1038/nmeth.2994.

Pfeiffenberger, Cory, Bridget C. Lear, Kevin P. Keegan, and Ravi Allada. 2010. “Locomotor Activity Level Monitoring Using the Drosophila Activity Monitoring (DAM) System.” *Cold Spring Harbor Protocols* 5 (11). doi:10.1101/pdb.prot5518.

Piper, Matthew D W, Eric Blanc, Ricardo Leitão-Gonçalves, Mingyao Yang, Xiaoli He, Nancy J Linford, Matthew P Hoddinott, et al. 2014. “A Holidic Medium for Drosophila Melanogaster.” *Nature Methods* 11 (1): 100–105. doi:10.1038/nmeth.2731.

Ramdya, Pavan, Pawel Lichocki, Steeve Cruchet, Lukas Frisch, Winnie Tse, Dario Floreano, and Richard Benton. 2014. “Mechanosensory Interactions Drive Collective Behaviour in Drosophila.” *Nature*, December. doi:10.1038/nature14024.

Renart, Alfonso, and Christian K. Machens. 2014. “Variability in Neural Activity and Behavior.” *Current Opinion in Neurobiology* 25. Elsevier Ltd: 211–20. doi:10.1016/j.conb.2014.02.013.

Rezával, Carolina, Tetsuya Nojima, Megan C Neville, Andrew C Lin, and Stephen F Goodwin. 2014. “Sexually Dimorphic Octopaminergic Neurons Modulate Female Postmating Behaviors in Drosophila.” *Current Biology* 24 (March): 725–30. doi:10.1016/j.cub.2013.12.051.

Ribeiro, Carlos, and Barry J Dickson. 2010. “Sex Peptide Receptor and Neuronal TOR/S6K Signaling Modulate Nutrient Balancing in Drosophila.” Journal Article. *Current Biology* 20 (11). Cell Press: 1000–1005. doi:10.1016/j.cub.2010.03.061.

Rind, F Claire, Roger D Santer, and Geraldine A Wright. 2008. “Arousal Facilitates Collision Avoidance Mediated by a Looming Sensitive Visual Neuron in a Flying Locust.” *Journal of Neurophysiology* 100 (2): 670–80. doi:10.1152/jn.01055.2007.

Ro, Jennifer, Zachary M. Harvanek, and Scott D. Pletcher. 2014. “FLIC: High-Throughput, Continuous Analysis of Feeding Behaviors in Drosophila.” *PLoS ONE* 9 (6). doi:10.1371/journal.pone.0101107.

Roberts, Seth, and Afshin Gharib. 2006. “Variation of Bar-Press Duration: Where Do New Responses Come From?” *Behavioural Processes* 72 (3): 215–23. doi:10.1016/j.beproc.2006.03.003.

Robie, Alice a, Andrew D Straw, and Michael H Dickinson. 2010. “Object Preference by Walking Fruit Flies, Drosophila Melanogaster, Is Mediated by Vision and Graviperception.” *The Journal of Experimental Biology* 213 (Pt 14): 2494–2506. doi:10.1242/jeb.041749.

Root, Cory M M, Kang I I Ko, Amir Jafari, and Jing W W Wang. 2011. “Presynaptic Facilitation by Neuropeptide Signaling Mediates Odor-Driven Food Search.” Journal Article. *Cell* 145 (1): 133–44. doi:10.1016/j.cell.2011.02.008.

Rytz, Raphael, Vincent Croset, and Richard Benton. 2013. “Ionotropic Receptors (IRs): Chemosensory Ionotropic Glutamate Receptors in Drosophila and beyond.” *Insect Biochemistry*

and Molecular Biology 43 (9). Elsevier Ltd: 888–97. doi:10.1016/j.ibmb.2013.02.007.

Santos, Fernando J., Rodrigo F. Oliveira, Xin Jin, and Rui M. Costa. 2015. “Corticostriatal Dynamics Encode the Refinement of Specific Behavioral Variability during Skill Learning.” *eLife* 4 (September): 1–19. doi:10.7554/eLife.09423.

Scheidler, Nicole H, Cheng Liu, Kelly A Hamby, Frank G Zalom, and Zainulabeuddin Syed. 2015. “Volatile Codes: Correlation of Olfactory Signals and Reception in Drosophila-Yeast Chemical Communication.” *Scientific Reports* 5 (January). Nature Publishing Group: 14059. doi:10.1038/srep14059.

Schiavo, Giampietro, Fabio Benfenati, Patrizia Polveino de Laureto, Bibhuti R DasGupta, and Cesare Montecucco. 1992. “Tetanus and Botulinum-B Neurotoxins Block Neurotransmitter Release by Proteolytic Cleavage of Synaptobrevin.” *Nature* 359: 832–35.

Schneider, Jonathan, Michael H Dickinson, and Joel D Levine. 2012. “Social Structures Depend on Innate Determinants and Chemosensory Processing in Drosophila.” *Proceedings of the National Academy of Sciences* 109 (2): 17174–79. doi:10.1073/pnas.1121252109.

Scott, K, R Brady, a Cravchik, P Morozov, a Rzhetsky, C Zuker, and R Axel. 2001. “A Chemosensory Gene Family Encoding Candidate Gustatory and Olfactory Receptors in Drosophila.” *Cell* 104 (5): 661–73. http://www.ncbi.nlm.nih.gov/pubmed/11257221.

Seeds, Andrew M, Primoz Ravbar, Phuong Chung, Stefanie Hampel, Frank M Midgley, Brett D Mensh, and Julie H. Simpson. 2014. “A Suppression Hierarchy among Competing Motor Programs Drives Sequential Grooming in Drosophila.” *eLife* 3 (August): 1–23. doi:10.7554/eLife.02951.

Seelig, Johannes D., and Vivek Jayaraman. 2015. “Neural Dynamics for Landmark Orientation and Angular Path Integration.” *Nature* 521 (7551): 186–91. doi:10.1038/nature14446.

Seelig, Johannes D, M Eugenia Chiappe, Gus K Lott, Anirban Dutta, Jason E Osborne, Michael B Reiser, and Vivek Jayaraman. 2010. “Two-Photon Calcium Imaging from Head-Fixed Drosophila during Optomotor Walking Behavior.” *Nature Methods* 7 (7): 535–40. doi:10.1038/nmeth0211-184b.

Semmelhack, Julia L, and Jing W Wang. 2009. “Select Drosophila Glomeruli Mediate Innate Olfactory Attraction and Aversion.” *Nature* 459 (7244). Nature Publishing Group: 218–23. doi:10.1038/nature07983.

Serguera, Che, Viviana Triaca, Jakki Kelly-Barrett, Mumna Al Banchaabouchi, and Liliana Minichiello. 2008. “Increased Dopamine after Mating Impairs Olfaction and Prevents Odor Interference with Pregnancy.” *Nature Neuroscience* 11 (8). Nature Publishing Group: 949–56. doi:10.1038/nn.2154.

Shimada, Ichiro, Yoshiyuki Kawazoe, and Hiroaki Hara. 1993. “A Temporal Model of Animal Behavior Based on a Fractality in the Feeding of Drosophila Melanogaster.” *Biological Cybernetics* 68: 477–81.

Silbering, a. F., R. Rytz, Y. Grosjean, L. Abuin, P. Ramdya, G. S. X. E. Jefferis, and R. Benton. 2011. “Complementary Function and Integrated Wiring of the Evolutionarily Distinct Drosophila Olfactory Subsystems.” *Journal of Neuroscience* 31 (38): 13357–75. doi:10.1523/JNEUROSCI.2360-11.2011.

Simon, Jasper C, and Michael H Dickinson. 2010. “A New Chamber for Studying the Behavior of Drosophila.” *PloS One* 5 (1): e8793. doi:10.1371/journal.pone.0008793.

Simpson, Stephen J., David G. Le Couteur, and David Raubenheimer. 2015. “Putting the Balance Back in Diet.” *Cell* 161 (1): 18–23. doi:10.1016/j.cell.2015.02.033.

Simpson, Stephen J., and David Raubenheimer. 2005. “Obesity: The Protein Leverage Hypothesis.” *Obesity Reviews : An Official Journal of the International Association for the Study of Obesity* 6

(2): 133–42. doi:10.1111/j.1467-789X.2005.00178.x.

Simpson, Stephen J, and David Raubenheimer. 2012. *The Nature of Nutrition: A Unifying Framework from Animal Adaptation to Human Obesity*. Princeton University Press.

Skorupa, Danielle A, Azra Dervisefendic, Jessica Zwiener, and Scott D Pletcher. 2008. “Dietary Composition Specifies Consumption, Obesity, and Lifespan in Drosophila Melanogaster.” *Aging Cell* 7 (4): 478–90. doi:10.1111/j.1474-9726.2008.00400.x.

Sokolowski, M B. 2001. “Drosophila: Genetics Meets Behaviour.” *Nature Reviews. Genetics* 2 (11): 879–90. doi:10.1038/35098592.

Solon-Biet, Samantha M, Aisling C McMahon, J William O Ballard, Kari Ruohonen, Lindsay E Wu, Victoria C Cogger, Alessandra Warren, et al. 2014. “The Ratio of Macronutrients, Not Caloric Intake, Dictates Cardiometabolic Health, Aging, and Longevity in Ad Libitum-Fed Mice.” *Cell Metabolism* 19 (3): 418–30. doi:10.1016/j.cmet.2014.02.009.

Solon-Biet, Samantha M, Kirsty A Walters, Ulla K Simanainen, Aisling C McMahon, Kari Ruohonen, John William O Ballard, David Raubenheimer, David J Handelsman, David G Le Couteur, and Stephen J Simpson. 2015. “Macronutrient Balance, Reproductive Function, and Lifespan in Aging Mice.” *Proceedings of the National Academy of Sciences* 112 (11): 3481–86. doi:10.1073/pnas.1422041112.

Sørensen, Allan, David Mayntz, David Raubenheimer, and Stephen J. Simpson. 2008. “Protein-Leverage in Mice: The Geometry of Macronutrient Balancing and Consequences for Fat Deposition.” *Obesity (Silver Spring, Md.)* 16 (3): 566–71. doi:10.1038/oby.2007.58.

Sorribes, Amanda, Beatriz G Armendariz, Diego Lopez-Pigozzi, Cristina Murga, and Gonzalo G de Polavieja. 2011. “The Origin of Behavioral Bursts in Decision-Making Circuitry.” Journal Article. *PLoS Computational Biology* 7 (6). Public Library of Science: e1002075. doi:10.1371/journal.pcbi.1002075.

Stephens, Greg J, Bethany Johnson-Kerner, William Bialek, and William S Ryu. 2008. “Dimensionality and Dynamics in the Behavior of C. Elegans.” *PLoS Computational Biology* 4 (4): e1000028. doi:10.1371/journal.pcbi.1000028.

Sternson, Scott M. 2013. “Hypothalamic Survival Circuits: Blueprints for Purposive Behaviors.” *Neuron* 77 (5): 810–24. doi:10.1016/j.neuron.2013.02.018.

Stökl, Johannes, Antonia Strutz, Amots Dafni, Ales Svatos, Jan Doubsky, Markus Knaden, Silke Sachse, Bill S. Hansson, and Marcus C. Stensmyr. 2010. “A Deceptive Pollination System Targeting Drosophilids through Olfactory Mimicry of Yeast.” *Current Biology* 20 (20): 1846–52. doi:10.1016/j.cub.2010.09.033.

Stone, James V. 2013. “An Introduction to Bayes’ Rule.” In *Bayes’ Rule: A Tutorial Introduction to Bayesian Analysis*, First edit, 1–13. Sheffield: Sebtel Press.

Straw, Andrew D, Kristin Branson, Titus R Neumann, and Michael H Dickinson. 2011. “Multi-Camera Real-Time Three-Dimensional Tracking of Multiple Flying Animals.” Journal Article. *Journal of The Royal Society Interface* 8 (56): 395–409. doi:10.1098/rsif.2010.0230.

Taghert, Paul H, and Michael N Nitabach. 2012. “Peptide Neuromodulation in Invertebrate Model Systems.” *Neuron* 76 (1): 82–97. doi:10.1016/j.neuron.2012.08.035.

Tang, S, and a Guo. 2001. “Choice Behavior of Drosophila Facing Contradictory Visual Cues.” *Science* 294 (5546): 1543–47. doi:10.1126/science.1058237.

Tervo, Dougal G.R., Mikhail Proskurin, Maxim Manakov, Mayank Kabra, Alison Vollmer, Kristin Branson, and Alla Y. Karpova. 2014. “Behavioral Variability through Stochastic Choice and Its Gating by Anterior Cingulate Cortex.” *Cell* 159 (1). Elsevier Inc.: 21–32. doi:10.1016/j.cell.2014.08.037.

Thoma, Vladimiros, Stephan Knapek, Shogo Arai, Marion Hartl, Hiroshi Kohsaka, Pudith Sirigrivatanawong, Ayako Abe, Koichi Hashimoto, and Hiromu Tanimoto. 2016. “Functional Dissociation in Sweet Taste Receptor Neurons between and within Taste Organs of Drosophila.” *Nature Communications* 7. Nature Publishing Group: 10678. doi:10.1038/ncomms10678.

Thorne, Natasha, Caroline Chromey, Steve Bray, and Hubert Amrein. 2004. “Taste Perception and Coding in Drosophila.” *Current Biology* 14 (12): 1065–79. doi:10.1016/j.cub.2004.05.019.

Tinbergen, Niko. 1951. *The Study of Instinct*. New York, NY: Clarendon Press/Oxford University Press.

Todd, Jeremy G, Jamey S Kain, and Benjamin L de Bivort. 2016. “Systematic Exploration of Unsupervised Methods for Mapping Behavior.” *BioRxiv* 51300. doi:http://dx.doi.org/10.1101/051300.

Ugur, Berrak, Kuchuan Chen, and Hugo J Bellen. 2016. “Drosophila Tools and Assays for the Study of Human Diseases.” *Disease Models & Mechanisms* 9 (3): 235–44. doi:10.1242/dmm.023762.

van Breugel, Floris, Jeff Riffell, Adrienne Fairhall, and Michael H. Dickinson. 2015. “Mosquitoes Use Vision to Associate Odor Plumes with Thermal Targets.” *Current Biology* 25 (16). Elsevier Ltd: 2123–29. doi:10.1016/j.cub.2015.06.046.

van Breugel, Floris, and Michael H Dickinson. 2014. “Plume-Tracking Behavior of Flying Drosophila Emerges from a Set of Distinct Sensory-Motor Reflexes.” *Current Biology* 24 (3): 274–86. doi:10.1016/j.cub.2013.12.023.

Van Der Maaten, L, and G Hinton. 2008. “Visualizing Data Using T-SNE.” *Journal of Machine Learning Research* 9: 2579–2605. doi:10.1007/s10479-011-0841-3.

Vargas, Misha a, Ningguang Luo, Atsushi Yamaguchi, and Pankaj Kapahi. 2010. “A Role for S6 Kinase and Serotonin in Postmating Dietary Switch and Balance of Nutrients in D. Melanogaster.” *Current Biology* 20 (11): 1006–11. doi:10.1016/j.cub.2010.04.009.

Verhagen, Justus V., and Lina Engelen. 2006. “The Neurocognitive Bases of Human Multimodal Food Perception: Sensory Integration.” *Neuroscience and Biobehavioral Reviews* 30: 271–86. doi:10.1016/j.neubiorev.2005.11.003.

Vogelstein, Joshua T, Youngser Park, Tomoko Ohyama, Rex a Kerr, James W Truman, Carey E Priebe, and Marta Zlatic. 2014. “Discovery of Brainwide Neural-Behavioral Maps via Multiscale Unsupervised Structure Learning.” *Science* 344 (386): 386–92. doi:10.1126/science.1250298.

von Philipsborn, Anne C., Tianxiao Liu, Jai Y. Yu, Christopher Masser, Salil S. Bidaye, and Barry J. Dickson. 2011. “Neuronal Control of Drosophila Courtship Song.” *Neuron* 69 (3). Elsevier Inc.: 509–22. doi:10.1016/j.neuron.2011.01.011.

Vosshall, Leslie B. 2007. “Into the Mind of a Fly.” Journal Article. *Nature* 450 (7167). Nature Publishing Group: 193–97. doi:10.1038/nature06335.

Vosshall, Leslie B, and Reinhard F Stocker. 2007. “Molecular Architecture of Smell and Taste in Drosophila.” *Annual Review of Neuroscience* 30: 505–33. doi:10.1146/annurev.neuro.30.051606.094306.

Walker, Samuel James, Verónica María Corrales-Carvajal, and Carlos Ribeiro. 2015. “Postmating Circuitry Modulates Salt Taste Processing to Increase Reproductive Output in Drosophila.” *Current Biology*, 1–10. doi:10.1016/j.cub.2015.08.043.

Wiersma, C.A.G., and K. Ikeda. 1964. “Interneurons Commanding Swimmeret Movements in the Crayfish, Procambarus Clarki (Girard).” *Comparative Biochemistry and Physiology* 12 (4): 509–25. doi:10.1016/0010-406X(64)90153-7.

Wilmers, Christopher C., Barry Nickel, Caleb M. Bryce, Justine A. Smith, Rachel E. Wheat, Veronica Yovovich, and M. Hebblewhite. 2015. “The Golden Age of Bio-Logging: How Animal-Borne

Sensors Are Advancing the Frontiers of Ecology." *Ecology* 96 (7): 1741–53. doi:10.1890/14-1401.1.

Wiltschko, Alexander B., Matthew J. Johnson, Giuliano Iurilli, Ralph E. Peterson, Jesse M. Katon, Stan L. Pashkovski, Victoria E. Abraira, Ryan P. Adams, and Sandeep Robert Datta. 2015. "Mapping Sub-Second Structure in Mouse Behavior." *Neuron* 88 (6). Elsevier Inc.: 1121–35. doi:10.1016/j.neuron.2015.11.031.

Wolf, Reinhard, and Martin Heisenberg. 1991. "Basic Organization of Operant Behavior as Revealed in Drosophila Flight Orientation." *Journal of Comparative Physiology A* 169 (6): 699–705. doi:10.1007/BF00194898.

Yang, Chung-Hui, Priyanka Belawat, Ernst Hafen, Lily Y Jan, and Yuh-Nung Jan. 2008. "Drosophila Egg-Laying Site Selection as a System to Study Simple Decision-Making Processes." Journal Article. *Science* 319 (5870): 1679–83. doi:10.1126/science.1151842.

Yang, Zhe, Yue Yu, Vivian Zhang, Yinjun Tian, Wei Qi, and Liming Wang. 2015. "Octopamine Mediates Starvation-Induced Hyperactivity in Adult Drosophila." *Proceedings of the National Academy of Sciences*, 201417838. doi:10.1073/pnas.1417838112.

Yapici, Nilay. 2008. "Molecular and Genetic Analysis of Drosophila Melanogaster Female Reproductive Behaviours." PhD thesis: University of Vienna.

Yapici, Nilay, Raphael Cohn, Christian Schusterreiter, Vanessa Ruta, and Leslie B Vosshall. 2016. "A Taste Circuit That Regulates Ingestion by Integrating Food and Hunger Signals." *Cell* 165 (March). doi:10.1016/j.cell.2016.02.061.

Yapici, Nilay, Young-Joon Kim, Carlos Ribeiro, and Barry J Dickson. 2008. "A Receptor That Mediates the Post-Mating Switch in Drosophila Reproductive Behaviour." *Nature* 451 (7174): 33–37. doi:10.1038/nature06483.

Yin, Yan, Nannan Chen, Shixing Zhang, and Aike Guo. 2009. "Choice Strategies in Drosophila Are Based on Competition between Olfactory Memories." Journal Article. *European Journal of Neuroscience* 30 (2). Blackwell Publishing Ltd: 279–88. doi:10.1111/j.1460-9568.2009.06821.x.

Zeevi, David, Tal Korem, Niv Zmora, David Israeli, Daphna Rothschild, Adina Weinberger, Orly Ben-Yacov, et al. 2015. "Personalized Nutrition by Prediction of Glycemic Responses." *Cell* 163 (5): 1079–95. doi:10.1016/j.cell.2015.11.001.

Zhang, Ke, Jian Zeng Guo, Yueqing Peng, Wang Xi, and Aike Guo. 2007. "Dopamine-Mushroom Body Circuit Regulates Saliency-Based Decision-Making in Drosophila." Journal Article. *Science* 316 (5833): 1901–4. doi:10.1126/science.1137357.

Zou, Sige, Pablo Liedo, Leopoldo Altamirano-Robles, Janeth Cruz-Enriquez, Amy Morice, Donald K Ingram, Kevin Kaub, Nikos Papadopoulos, and James R Carey. 2011. "Recording Lifetime Behavior and Movement in an Invertebrate Model." *PloS One* 6 (4): e18151. doi:10.1371/journal.pone.0018151.

Chapter 8. Appendix

8.1 How to use the tracking setup – step by step

1) Connect the lights of each chamber. Cam 03 and 04 are connected to the same power source.
2) Check that the computers are working fine:
   a. To switch between computers: Press twice ScrLk and then Enter.
   b. Connect one camera on each computer.
   c. Open the Virtual Dub program.
   d. Confirm that the camera is working: To acquire image click: *File → Capture avi…* If it does not work, try disconnecting the camera and connecting again or restarting the computer. If this does not work check section 8.2, step 9 (*Configure DALSA Network*), to check that each camera is being recognized by an independent PCI card.
   e. Connect the second camera on each computer and open the second Virtual Dub window. Acquire image: *File → Capture avi…* if the screen is black, go to *Video → Capture Pin… → Source* and select the other camera.
   f. Confirm that the back light illumination is working.
3) Set the name for the video: *File → Set Capture File…* following format in Table 3.2:

   For *Canton S* experiment, the video filename should look as following:

   0003C01R01Cam01P0WT-CantonS → Run 1, Cam 1, Repetition 1 (day 1)

   0003C02R03Cam04P0WT-CantonS → Run 2, Cam 4, Repetition 3 (day 3)

4) Confirm properties of the recording (Figure 8.1), going to *Video → Capture Pin…*

   a. Format tab: Packet Size = 1500
   b. Format tab: Frame Rate = 50
   c. Analog tab is different for each camera. Cam01: 7000, Cam02: 5500, Cam03: 7500, Cam04: 7500.

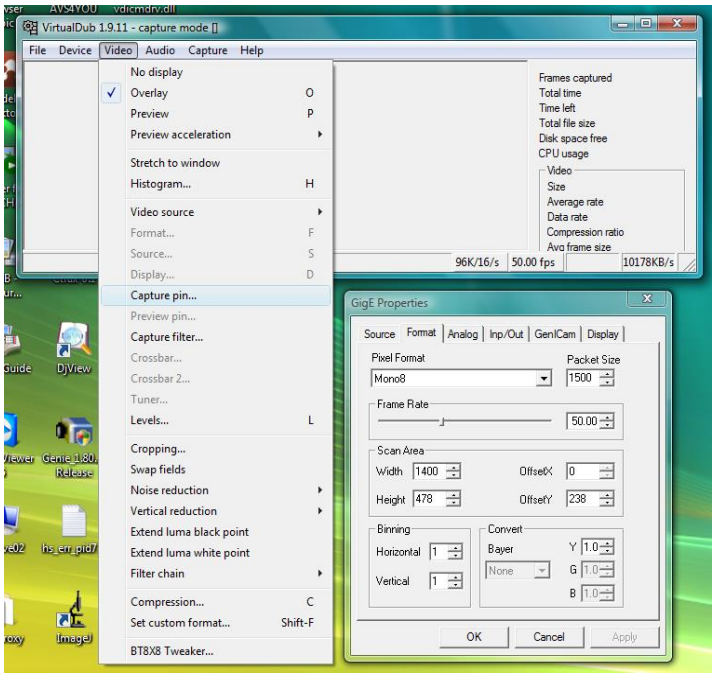

Figure 8.1 – Properties of video acquisition

5) Wash and dry the arenas with pressurized air inside the behavior room.
6) Place yeast and sucrose spots following the geometry depicted in Figure 3.2.
7) Clean the glass with pressurized air to remove fibers. Distribute flies in the arenas according to Table 8.1. Make sure to match the Camera (= box), the arena side (Left, Center or Right) and the run.

Table 8.1 – Experiment schedule during the day

Cam	Start Time	Food Deprivation	Mating	Born Date	Deprivation Times Date:	Recording Times and Date:
1	10h40	AA+ suboptimal	Mated		Run 1 (~ 11h00)	
2	10h40	AA+ suboptimal	Virgin			
3	11h20	AA-	Mated			
4	11h20	AA-	Virgin			
1	14h00	AA+ suboptimal	Virgin		Run 2 (~ 14h20)	
2	14h00	AA-	Mated			
3	14h40	AA-	Virgin			
4	14h40	AA+ suboptimal	Mated			
1	16h40	AA-	Mated		Run 3 (~17h00)	
2	16h40	AA-	Virgin			
3	17h20	AA+ suboptimal	Mated			
4	17h20	AA+ suboptimal	Virgin			

8) **Check that the flies are in focus.** To adjust focus, screw or un-screw the lens of the camera, very carefully.
   a. Check that each camera has the right visual field: The corners of the visual field should match with the marks. If they do not match, you can adjust the angle of the camera buy screwing or un-screwing the screws that are attached directly to the camera, **not the ones on the top of the box**.
9) Check that the name of the video is correct and start recording: *Capture → Capture Video*.
10) Stop the recording when 2h2min have passed. *Capture → Stop Capture*
11) Set Calibration file (this is a short video with low exposure to facilitate yeast spot detection described in section 3.2.
   a. *File → Set Capture File…* → Add a space and "Calib" to the name of the video → Save.
   b. *Video → Capture pin → Analog*: 4000 → OK
   c. Check again that the name of the video is "video Calib" in the top of the window, and that no "[FILE EXISTS]" appears.
   d. Capture → Capture video
   e. Let run for 1 second
   f. *Capture → Stop Capture*.
12) Set the name of the next video, by changing the run number:

a. *File → Set Capture File…* → Change the run number
b. *Video → Capture pin…* → Analog: write the value in step 3

13) Wash the arenas, put the spots and the flies. The approximate timing of each of these steps is shown in Figure 8.2.

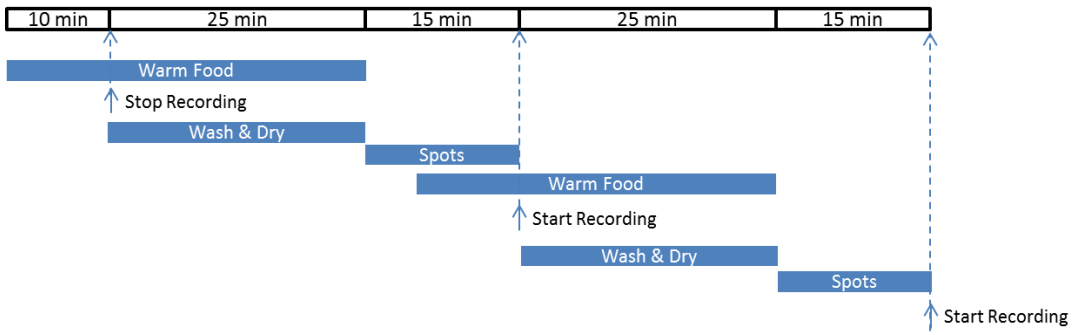

Figure 8.2 – Timeline of arena preparation for tracking experiments

The timeline for the preparation of 6 arenas (2 cameras) simultaneously is described.

14) Capture the video: *Capture → Capture Video*
15) Disconnect the cameras and the lights
16) Input the information of the experimental conditions used in the excel file described in section 3.4.

8.2 Installing and Starting Genie cameras

1. From DALSA-Genie CD-ROM, Install: Genie Framework Version 1.70.00.0256 and CamExpert version 7.00.00.0912 which includes Sapera LT Run-Time (Free version, not the 60-days trial).
2. Connect the camera to the power supply
3. Connect camera's Ethernet cable to a Gigabit PCI card (Currently, the cameras are connected to the built-in Gigabit PCIs in the MotherBoard).
4. Update Genie firmware: Start →Programs→DALSA→Genie→ Firmware Update. If update is required, click on "automatic" button. Wait until "Device reset complete".
5. Download codec ffdshow. Check for k-lite codec pack in Programs(x86).
6. For MATLAB Acquisition, go to GenIcam downloads website and download: GenICam GenApi Reference Implementation v.2.0.1, for 64-bit (application file: GenICam_VC80_Win64_x64_v2_0).
7. For VirtualDub acquisition (maybe also required for MATLAB), Install "ActiveGigE" from a-b Software. Then Install GigE Vision Filter from Active GigE package.
8. Configure PCI Network card (Figure 8.3):

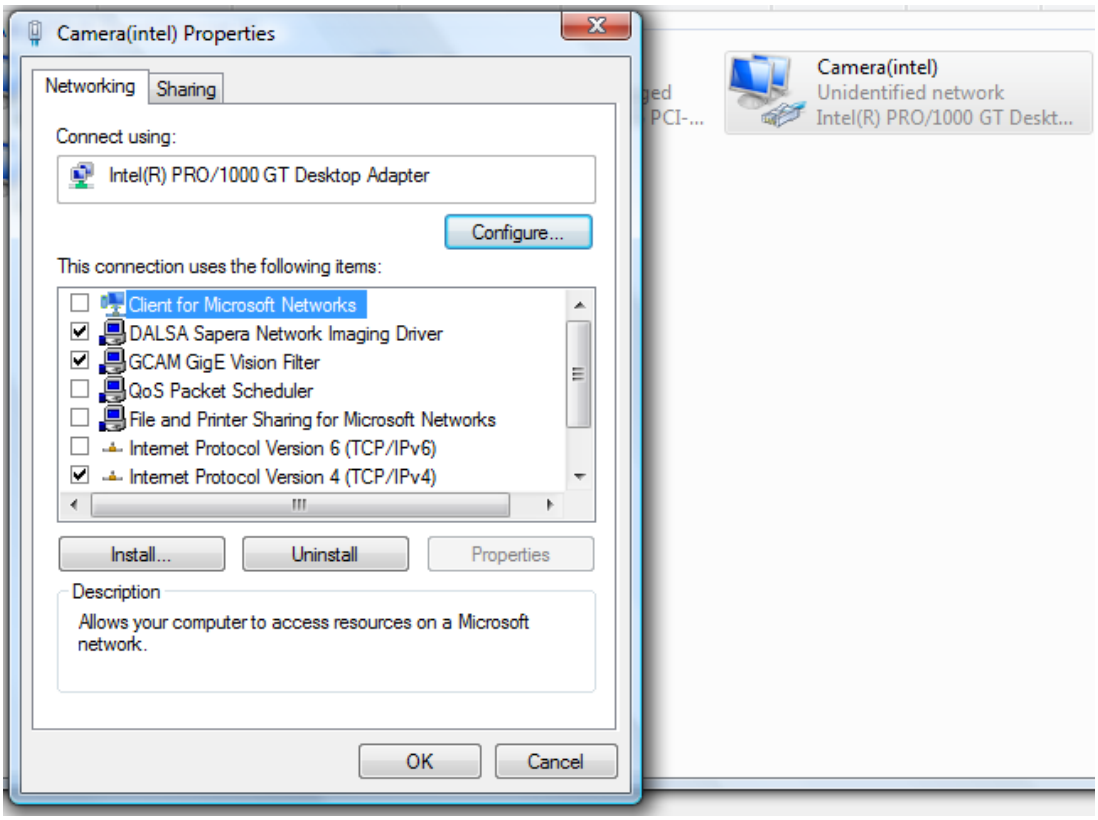

Figure 8.3 – Configuration of PCI network card

a. Control Panel → Network and Sharing Center → Manage Network Connection → Right clic in PCI card where Genie is connected → Properties→ Select: DALSA Sapera Network Imaging Driver, GCAM GigE Vision Filter, Internet Protocol version 4.
b. If GCAM GigE Vision Filter does not appear in the list (go to Active GigE User Guide for more details):
    i. Open Local Area Connection Properties dialog for your GigE adapter and click the Install... button. The Select Network Component Type dialog will appear. Select Service and click Add...
    ii. The Select Network Service dialog will appear. Click Have Disk... and provide the path to ActiveDcam Driver folder where GcamFilter.inf is located typically C:\Program Files\ActiveGige\Driver).Click OK
    iii. In the Select Network Service dialog highlight GCAM GigE Vision Filter and click OK (Ignore several warning messages from Microsoft. Confirm the presence of the filter driver in the Local Area Connection Properties list.)
c. Click in Configure... → Advanced. Set:
    i. Jumbo packet (frames): 9014 Bytes
    ii. Receive descriptors (buffers): 2048 (max)
    iii. Interrupt moderation rate: minimal

9. Configure DALSA Network (Figure 8.4): Programs →DALSA → Sapera Network Imaging Package → DALSA Network Configuration TooL →
    a. Click in the PCI card → NIC Configuration → Select Enable DALSA DHCP Server on this adapter and the Automatic IP (DHCP). If there is a second camera, it should have persistent IP mode. → Apply.

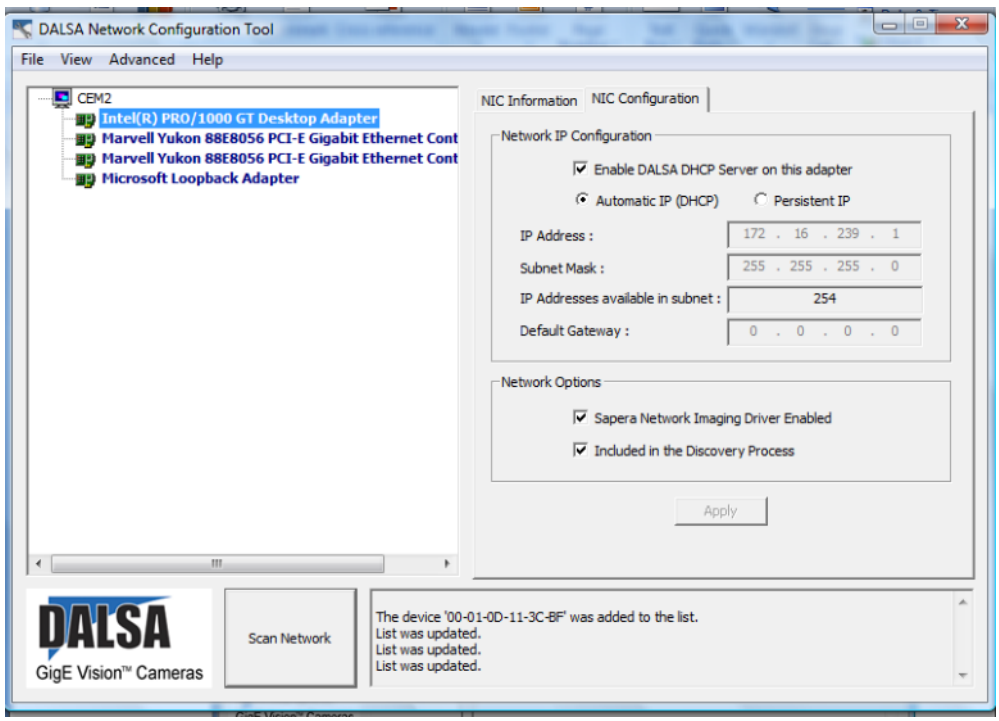

Figure 8.4 – Network configuration – step 1

b. Click in the camera (Figure 8.5): S4405728 → Device IP Configuration → Check if DHCP/LLA Mode is active. The second camera must not be LLA mode, but Persistent IP Mode!

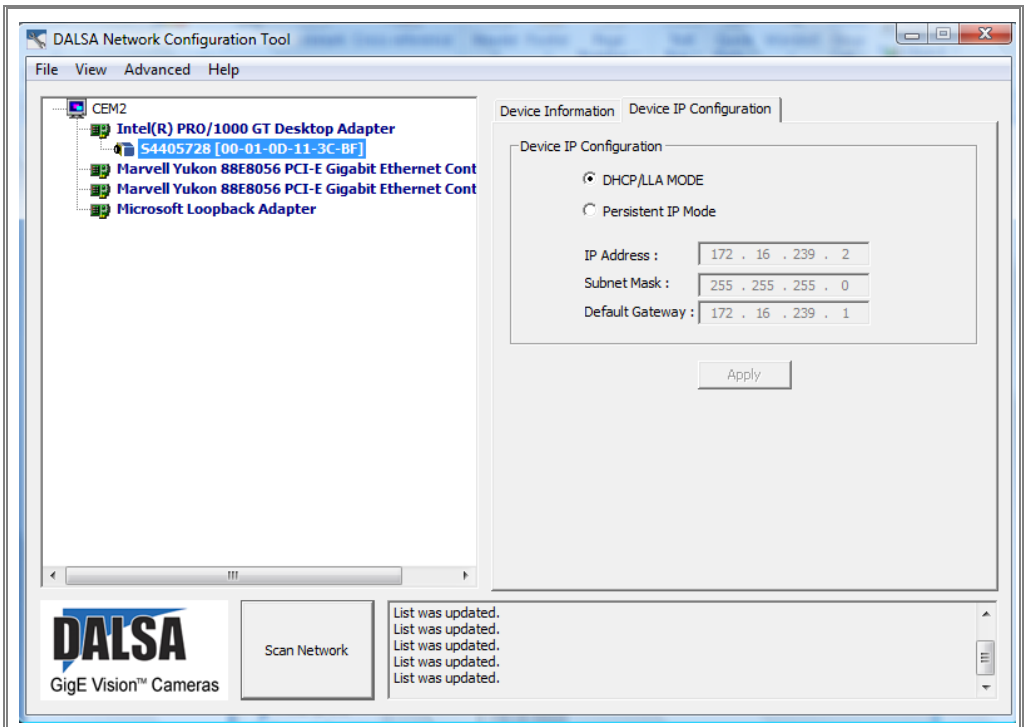

Figure 8.5 – Network configuration – step 2

Ana's note: Always check if the codec that is install in the Computer that is used to aquire the movies is the same in the Computer that is used to run the matlab code (ffdshow_beta7_rev3154_20091209).

10. Download VirtualDub. Open VirtualDub: *File* → *Capture avi...*
11. Configure Video Acquisition Parameters in Virtual Dub (Table 8.2): *Video* → *Capture pin...*

Table 8.2 – Video acquisition parameters

Width	1400	**Height**	478	**Offset Y**	238
Frame Rate	50 fps	**Packet Size**	1500	**Pixel Format**	Mono8
Palette	grey	**Zoom**	1	**Background..frames**	8

12. Compression Configuration (Figure 8.6): *Video* → *Compression…* → Xvid MPEG-4 Codec → *Configure* → Quality (Target quantizer): 1 → *Other options…* → Number of threads: 4 to 8.

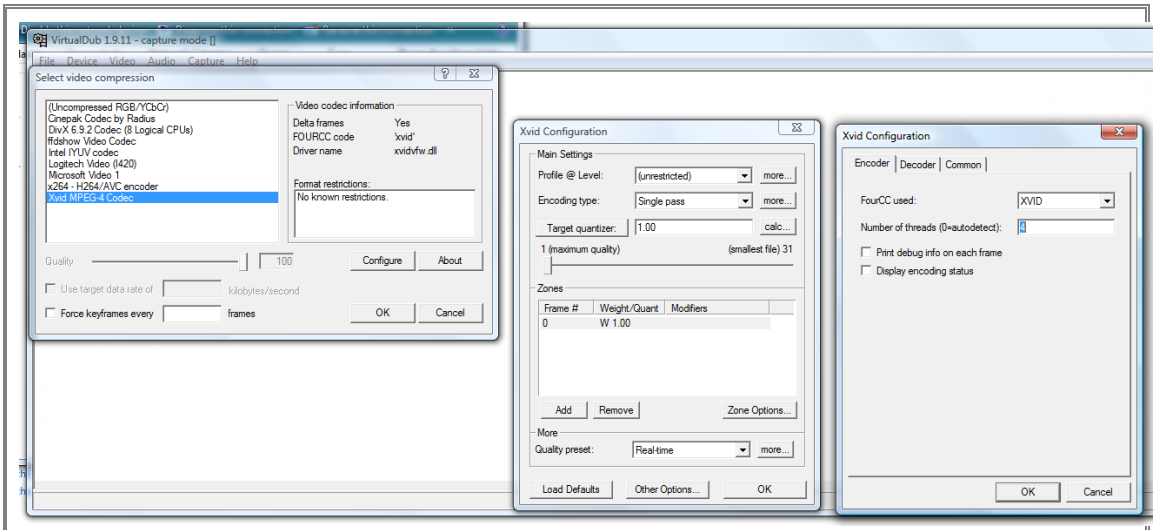

Figure 8.6 – Video compression configuration